TRANSMISSIVITY OF GEONETS IN SECONDARY LEACHATE COLLECTION SYSTEMS OF WASTE CONTAINMENT FACILITIES

by

Harvey Wayne Choy

B.A.Sc. The University of British Columbia, 1986
M.A.Sc. The University of British Columbia, 1993

A THESIS SUBMITTED IN PARTIAL FULFILLMENT OF

THE REQUIREMENTS FOR THE DEGREE OF

MASTER OF APPLIED SCIENCE

in

THE FACULTY OF GRADUATE STUDIES

Department of Civil Engineering

Geotechnical Engineering

We accept this thesis as conforming
to the required standard

THE UNIVERSITY OF BRITISH COLUMBIA

DECEMBER 1993

In presenting this thesis in partial fulfilment of the requirements for an advanced degree at the University of British Columbia, I agree that the Library shall make it freely available for reference and study. I further agree that permission for extensive copying of this thesis for scholarly purposes may be granted by the head of my department or by his or her representatives. It is understood that copying or publication of this thesis for financial gain shall not be allowed without my written permission.

(Signature)

Department of Civil Engineering

The University of British Columbia
Vancouver, Canada

Date December 22, 1993

ABSTRACT

The leak detection system of a waste containment facility may comprise of a geonet between two geomembranes. One of the main design parameters for such a system is the in-plane flow capacity or transmissivity. Test devices with stress-controlled boundaries were specially designed and constructed to determine the flow capacity of such geosynthetic leak detection systems under different operating conditions.

Two separate testing programs were performed. The Series W tests were performed over a period of 5 days at hydraulic gradients of 0.02, 0.04, 0.06, 0.08, and 0.10, and confining stresses of 25, 100, 200, 300, and 400 kPa; in addition, sedimentation tests were performed. This series of tests were performed to determine the influence that material properties, hydraulic gradient, and confining stress had on the transmissivity. Series WLC tests were performed at a constant hydraulic gradient of 0.02 and confining stress of 300 kPa for a period of 5 or 10 days and were intended to examine the long-term flow capacity.

The series W test results indicate that increasing the hydraulic gradient increased the flow capacity, but not in a direct relationship because the flow regime in the geonet was semi-turbulent to turbulent. Increasing the confining stress decreased the flow capacity as a result of geomembrane intrusion into the apertures of the geonet and compression of the geonet. Stiffer geomembranes showed less tendency to intrude into the pore space of a geonet, and geonets with narrower flow channels were less susceptible to intrusion from geomembanes. Geonets made of high density polyethylene, have high compressive strengths and tend to compress less.

Extrapolation of the series WLC test results indicate that the flow capacity will decrease by 30% to 67% after a period of 28.5 years; a factor of safety for creep and intrusion of 1.75-3.0 may be appropriate, depending on material properties, for a performance period of about 30 years. Comparison of the data to granular soils indicate the geonets are approximately equivalent to 1/2 inch to 3/4 inch gravel and have a flow capacity equivalent to a 0.75 m thick layer of gravel possessing a hydraulic conductivity of 0.05-0.10 m/s.

The results have some implications for materials testing; it is recommended that seating periods and orientation of test specimens be standardized. Boundaries of the test device should simulate field conditions, and be flexible to allow intrusion of adjacent construction materials into the geonet. A hydraulic gradient of 0.02 should be the minimum used in testing.

TABLE OF CONTENTS

TABLE OF CONTENTS (cont.)

LIST OF TABLES

LIST OF FIGURES

LIST OF FIGURES (cont.)

LIST OF FIGURES (cont.)

ACKNOWLEDGMENTS

I would like to thank the B.C. Science Council for funding this research project and also, the following persons for their contributions towards this research project. Dr. J. Fannin for his direct supervision and Professor J. Atwater for co-supervising; Dr. Y. Vaid for his contribution to the design of the test devices and manufacturing of latex bladders.

I would also like to thank the following persons for their assistance in preparation of the test equipment: Fred Zirkirchen for construction of the test devices and flow meters. Art Brookes, Harold Shremmp, Guy Kirsch and Dick Postgate for additional technical help. Susan Harper and Paula Parkinson for supplying materials and laboratory space for manufacturing latex bladders; John Wong and Ron Dolling for design and construction of the data acquisition system.

Again, I would like to thank the persons mentioned above; this research project would not have been possible without their contributions.

1. INTRODUCTION

In the last decade, the use of geosynthetics in civil engineering applications has grown rapidly. Some of the applications include railway construction, road construction, retaining walls, and waste containment. Considering waste containment specifically, geosynthetics have been used for waste containment applications which include municipal solid waste landfills, hazardous waste landfills and impoundments, secondary containment of petroleum products, and heap leach pads in the mining sector. Some of the applications above require primary and secondary leachate collection systems; the latter is the focus of this study. Geosynthetics are often used for secondary leachate collection (or leak detection systems); unfortunately, little is known about the flow capacity of such systems in the field. This presents the engineer with the difficult task of designing secondary leachate collection systems with few performance data. Presently, the flow capacity of the materials used for these systems is obtained from laboratory tests, but not under simulated field conditions. Therefore, the data cannot be directly used for design purposes. Hence, **the objective of this thesis is to determine the flow capacity of geosynthetic leak detection systems under different operating conditions, and through interpretation of the results, to better understand the factors influencing the flow capacity.**

Geosynthetics are polymers in sheet form that are used in geotechnical and environmental projects. Several types of geosynthetics are recognized in the Canadian Foundation Engineering Manual (Canadian Geotechnical Society, 1992): geotextiles, geogrids, geonets, geocells, geomembranes, and geocomposites. Geotextiles are continuous sheets of woven, non-woven or knitted fibers; they are flexible, permeable, have the appearance of a fabric and are used for separation, filtration, drainage, and reinforcement. Geogrids are thin, open grid-like sheets that are used primarily for reinforcement of soil. Geonets are open grid-like materials formed by two sets of coarse, parallel, extruded strands of material intersecting at constant angles; the network forms a thick sheet with porosity that promotes the in-plane flow of fluid. Geocells are relatively thick, three-dimensional networks constructed from strips of polymeric material; the strips are joined together to form interconnected cells that are infilled with soil. Geomembranes are continuous sheets of low permeability which are used for fluid containment and as vapour

barriers. Geocomposites are geosynthetics made from two or more types of geosynthetic to obtain properties from each of the individual components in a single unit.

Variables in the types of geomembrane include polymer type, thickness, textured or smooth sheets, and reinforced or non-reinforced. Typically, geomembranes are made from chlorinated polyethylene (CPE), chlorosulfinated polyethylene (CSPE), high-density polyethylene (HDPE), very low density polyethylene (VLDPE), polyvinyl chloride (PVC), and polypropylene (PP). Presently, HDPE is the most widely used, likely due to its perceived resistance to a wide range of chemicals. Very low density polyethylene and PVC appear to be popular choices for cover liners. Polypropylene is a relatively new material used in the manufacture of geomembranes. Thicknesses of geomembranes range from 0.5 mm to 2.5 mm. Smooth sheets are the standard choice with textured sheets being used when greater interface friction angles are required, which is usually the case on steep slopes. Most geomembranes are non-reinforced; reinforced geomembranes have the polymer laminated to a scrim which is made of a woven fabric and is intended to provide better tensile strength. Geonets are made from HDPE, MDPE, LDPE, and inter polymer alloys. The strands are either solid or of air-entrained material (the strands of a geonet form the skeleton structure and are governed by the manufacturing technique).

Geosynthetics from several of the categories listed above are being used in conjunction with natural materials in waste containment facilities. Consider the four main components of a double-lined solid waste landfill: a low permeability barrier or liner (primary and secondary), a primary leachate collection system, a secondary leachate collection system (also known as a leak detection system), and a cover system (Fig. 1.1). The low permeability barrier (primary and secondary) and cover liner may include a geomembrane, and the leachate collection and leak detection systems may be geonets.

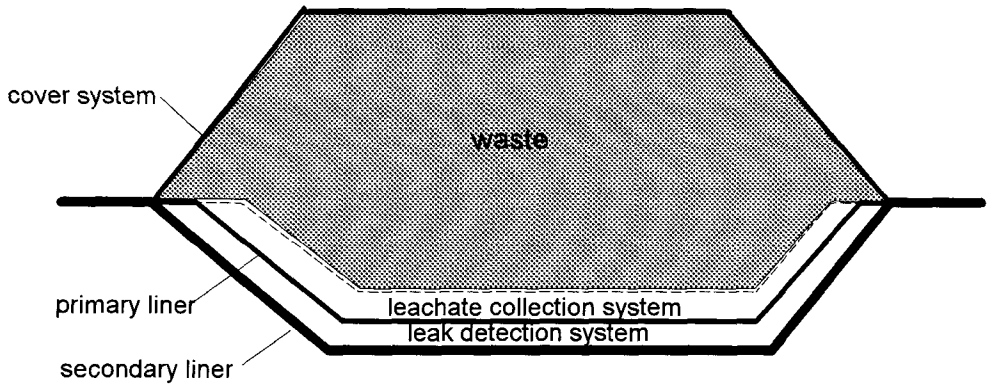

Figure 1.1 Schematic of Hazardous Waste Landfill

Geotextiles are often used in the cover system for venting methane gas produced by the waste (Koerner and Richardson, 19??) and as filters between differently graded soils, and may be used as the filter layer above the leachate collection system (Landreth, 1990). The increased use of geomembranes has arisen from changes in legislation governing the "minimum technology". The United States Environmental Protection Agency (U.S. E.P.A.) requires synthetic liners be used in secure landfills. These regulations, Canadian national regulations, and the provincial regulations of British Columbian are examined in Chapter 2.

The leachate collection system is located above the primary liner, and the secondary leachate collection system or leak detection system is located beneath the primary liner. The leak detection system is installed for two purposes; first, if there is a defect in the primary liner, any leachate (liquid that has percolated through the waste and absorbed some of the constituents of the waste) passing through the primary liner will be collected and removed by the leak detection system. The rate at which leachate enters the leak detection system acts as a warning signal that the primary liner may be failing and remedial action may be necessary. Second, in the event of a failure of the primary leachate collection system, the leak detection system then becomes the primary leachate collection system. Therefore, the leak detection system must have a flow capacity equivalent to the primary leachate collection system.

The last component of a waste containment facility is the engineered cover which is used for the following reasons:

1. to separate potentially harmful contaminants from the environment;

2. to control surface water infiltration (to reduce leachate generation);

3. to collect any possible gases generated from the landfill;

4. to sustain vegetation growth and provide an aesthetically pleasing finished appearance.

The four components of a waste containment facility offer many challenges in design, but it is the leak detection component that is of interest here. In order to properly design a geosynthetic leak detection system (geomembrane/geonet/ geomembrane), it is necessary to have knowledge of the flow capacity or transmissivity (defined by the American Society for Testing and Materials (ASTM) as the volumetric flow rate of water per unit width of specimen per unit gradient in a direction parallel to the plane of the specimen) under operating conditions. There are two sources of uncertainty in design regarding flow capacity. First, few data are published on the in-plane flow capacity or transmissivity of geonets. Available data are provided by manufacturers from index tests: index tests are typically used to compare the material properties of different products, but do not provide adequate information on in-service or field behavior. A performance test is best suited to the provision of the property of a material under simulated field conditions. Second, very little is known about the governing factors which influence the transmissivity of a geosynthetic leak detection system. Recall that the objective of this thesis is to determine the flow capacity of geosynthetic leak detection systems under different operating conditions, and through interpretation of the results, to better understand the factors influencing the flow capacity. These objectives will be addressed by observing the transmissivity of geomembrane/geonet/geomembrane systems under simulated field conditions.

The testing is preceded with a review of the literature, followed by a description of the test equipment. Results of the transmissivity tests are then presented with the interpretation of the results following. Finally, conclusions and recommendations are presented.

2. LITERATURE REVIEW

This review addresses Canadian national, and provincial, and American federal regulations. Test standards, results of previous transmissivity tests, and design of waste containment facilities are examined.

2.1 REGULATIONS

2.1.1 National Guidelines

The National Guidelines for the Landfilling of Hazardous Waste (Canadian Council of Ministers of the Environment, 1991) were developed in consultation with the provinces to avoid any conflicts with provincial guidelines, and explicitly recognize the use of geosynthetics or natural materials.

A containment facility contains four main components: a liner, a leachate collection system, a leak detection system, and a cover system. The liner of a waste containment facility is a very low permeable barrier that is intended to severely restrict the seepage of contaminants into the environment. Some of the choices for liner material listed in the guidelines include: geomembranes or flexible membrane liners (FML), soil liner (clay), bentonite and bentonite mixtures, soil cement, and asphalt. There is no specification for a single liner or a double liner system. A single liner system is a facility that only has one low permeability liner with a leachate collection system above. A double liner system has two low permeability liners with a leachate collection system above the primary liner and a leak detection system between the two liners (see Fig. 1.1). The first two choices for liner material are the most common; in fact, geomembranes and soil liners are often combined to make a composite liner. A composite liner is a liner composed of two or more of the lining materials listed above. The guidelines also specify several considerations for design such as chemical compatibility with waste and leachate, resistance to physical damage, quality assurance, and long term performance and service life of the liner.

A leachate collection system (LCS) is required to control contaminant migration from the site by collecting and treating any leachate produced; the guidelines also recognize leak detection and removal systems (LDRS) as a secondary means of leachate removal. However, the

guidelines do not explicitly specify a requirement for a leak detection and removal system; it is left to the engineer to design a facility that controls contaminant migration which may require only a LCS or both LCS and LDRS. The guidelines allow the choice of conventional granular materials and pipes, or geonets and/or geotextiles to be used for leachate collection, but do not address any minimum performance standards for the materials used for leachate collection.

In regards to the cover system, the guidelines require that the four functions presented in section 1 are implemented for any cover system .

In short, these guidelines specify a requirement for three of the four main components of a hazardous waste facility; there is no specification for a leak detection system. It is possible that the use of a leak detection system is regarded as a optional feature that the engineer will implement as needed on a site specific basis. The geosynthetic material choice for liners includes geomembranes and the material choice for leachate collection (primary and secondary) includes geonets and/or geotextiles. There is no performance specification for the liner(s) or the leachate collection system(s).

2.1.2 Provincial Guidelines

The provincial guidelines are described in The Waste Management Act - Special Waste Regulations (Ministry of Environment, Parks, and Land, 1988) and require the owner of the secure landfill comply with performance standards.

Special waste is defined by the Transport of Danagerous Goods material listing - designated materials and/or by its leachate characteristics. Regulations specify a dual liner system to prevent any migration of special waste leachate out of the landfill to the adjacent subsurface soil or ground water during the operating life and after closure. Design considerations are as follows:

-each liner to have a maximum permeability of $1x10^{-9}$m/s under 0.305 m hydraulic head and minimum thickness of 1 mm (geomembrane) and 0.5m (soil);

-both liners should have appropriate chemical properties, strength and thickness to prevent failure;

-lining system to be placed on subgrade material that will not fail due to compression, uplift or settlement

For leachate collection, the guidelines specify that the minimum standards are:

-a leachate collection system:

*installed immediately above the upper liner at a slope greater than 2% and have a permeability greater than 1.0×10^{-5} m/s with a minimum thickness of 0.75 m

*constructed of materials that are:

a)chemically resistant to the waste and the leachate

b)sufficiently strong to prevent failure due to overlying loads of the landfill.

*designed and constructed to prevent clogging over the life of the facility

-a leak detection and removal system between the two liners.

For the final cover, the Act specifies that the final cover of the landfill should meet the following minimum characteristics:

-be designed and constructed to function with minimum maintenance;

-have a foundation layer of soil compacted to maximum density at the optimum moisture content and be 0.75 m thick minimum;

-contain an intermediate layer of either impervious soil or clay that is not less than 0.5m or impervious synthetic material not less than 1 mm;

-have a top layer of soil not less than 0.5m thick that does not contain waste, leachate or other material which would contaminate infiltrating water and would provide a suitable long term rooting medium;

-graded and maintained to prevent ponding and have slopes between 3% to 5%.

These guidelines specify a requirement for all four main components of a special waste containment facility. The low permeability barrier must be a dual liner system that may be composed of soil or geomembranes (maximum permeability of 1×10^{-9} m/s); soil liners must be a minimum of 0.5 m thick and geomembranes must be a minimum of 1.0 mm thick. The leachate collection system must be composed of a minimum 0.75 m thick layer of granular material with a

permeability greater than 1.0×10^{-5} m/s at a minimum slope of 2%. The leak detection and removal system between the dual liners has no specification regarding material or performance standard

2.1.3 United States Environmental Protection Agency Guidelines

The United States Environmental Protection Agency (U.S.E.P.A.) regulations (EPA, 1988) are for waste containment and other impoundment facilities. These regulations include a much broader range of waste containment than the previous two regulations; for example, a municipal solid waste (MSW) landfill would be governed by these regulations. It is perceived that a MSW landfill would not be as environmentally dangerous compared to either hazardous or special waste landfills, therefore, the regulations indicate the prescriptive approach the United States is taking regarding waste containment.

With regard to design of the liner system for hazardous waste, the regulations require it be:

-constructed of materials that have appropriate chemical properties, thickness, and strength to prevent failure due to pressure gradients, chemicals, climatic conditions, and construction and operational stresses;

-placed on a foundation capable of providing support and resist pressure gradients above and below the liner to prevent failure due to settlement, compression or uplift;

-installed to cover all surrounding earth likely to be in contact with the waste or leachate.

The guidelines (EPA, 1988) issue a draft form that require:

-two or more liners with a leachate collection and removal system between the liners. Two options are listed for the minimum double liner system: a FML/composite double liner system or a FML/compacted soil double liner system. The former system is composed of a top FML liner with a FML and compacted clay combined to make up the bottom liner (Fig. 2.1); the latter system has a top FML liner and compacted clay for the bottom liner;

-geomembranes must be a minimum of 0.75 mm (30 mil) thick or 1.14 mm (45 mils) thick if exposed for more than 3 months (note: this is listed as 30 days in EPA, 1989);

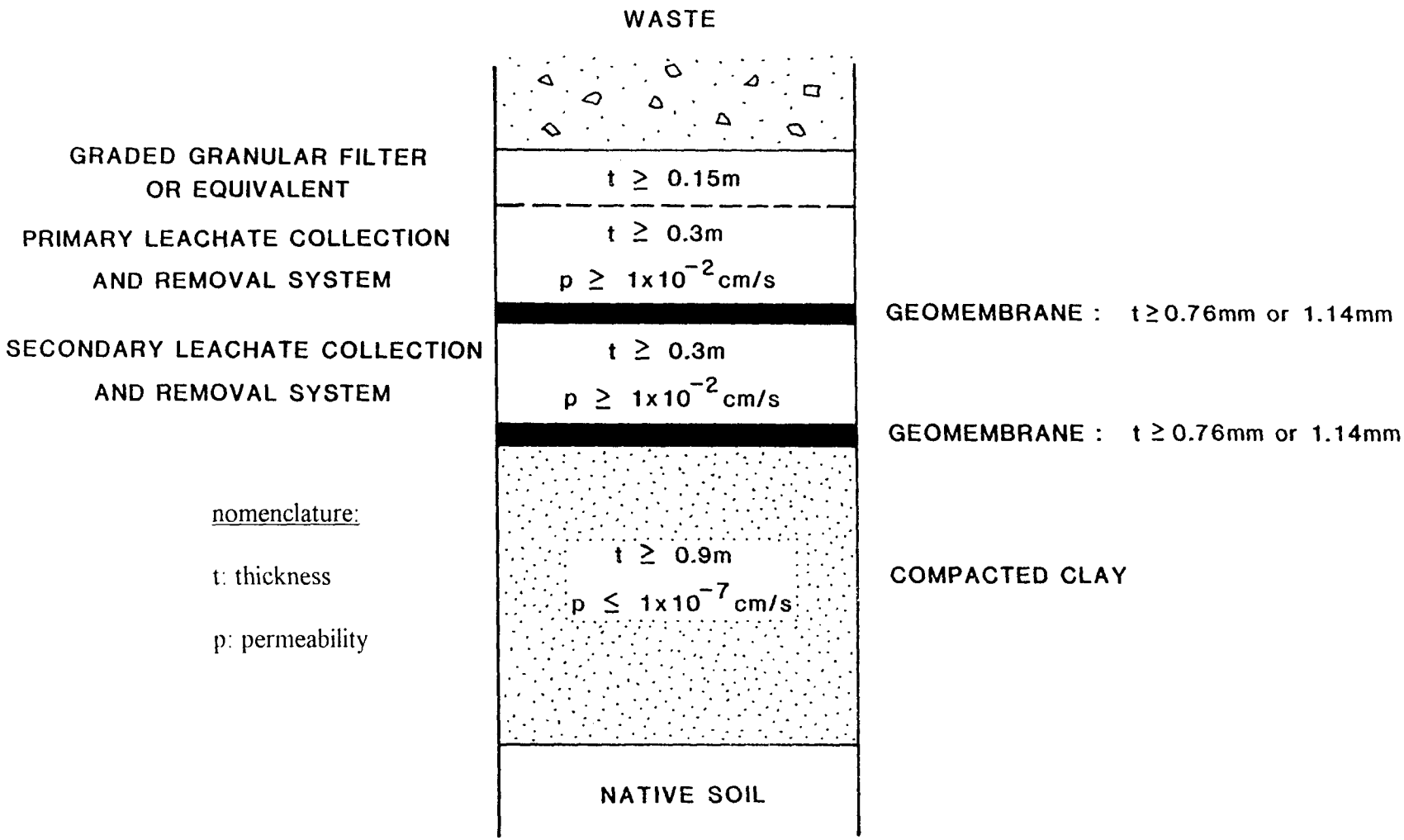

Figure 2.1 U.S.E.P.A. Schematic of FML/Composite Dual Liner System (after Fannin, 1990)

-the clay component of the bottom liner must have a hydraulic conductivity equal or less than 1.0×10^{-9} m/s and be a minimum 0.9 m thick.

The requirements for a leachate collection system are also in draft form; they are as follows:

-a leachate collection system (LCS) above the primary liner and a leak detection and removal system (LDRS) in between the primary and secondary liners which must have a minimum 2% bottom slope;

-the LCS must minimize the hydraulic head of leachate on the primary liner to a maximum level of 0.3 m to the end of the post-closure care period which is assumed to be 30 years;

-if granular soil is used for the LCS, there must be a minimum 150 mm thick graded granular filter or equivalent geotextile above the LCS. The LCS must be a minimum 300 mm thick and have a minimum hydraulic conductivity of 1.0×10^{-4} m/s. Granular soil for the LDRS has the same requirements as the LCS except no filter is needed;

-if a geosynthetic is used for the LDRS, the hydraulic transmissivity must be a minimum of 5.0×10^{-4} m^2/s and if used for the LCS, it must have an equivalent or greater flow capacity than the granular material.

Other design considerations for drainage layers include:

-compressibility of the drainage system with the overburden stress

-mechanical compatibility of the LDRS with the lining system

-chemical compatibility of the LCS and LDRS with the leachate

-methods of monitoring and maintaining performance of the drainage system. The guidelines recognize that the drainage layers may be subject to clogging and may require periodic inspection and flushing by high pressure rinsing.

The last component of a waste containment facility is the cover system or cap; again, these regulations are in draft form and specify a multilayer system consisting of:

-a vegetative layer that has a minimum 0.6 m thick top soil component and a slope between 3%-5% after allowing for subsidence;

-a drainage layer with a minimum thickness of 0.3 m, hydraulic conductivity of

1.0×10^{-4} m/s, and a minimum slope of 2% after allowing for settlement. A synthetic material may be used if it possesses the same or greater flow capacity as a granular layer;

-a low permeability layer which includes a FML with a minimum thickness of 0.5 mm above a compacted clay of minimum 0.6 m thickness and an in-place hydraulic conductivity of 1.0×10^{-9} m/s or less.

In addition to the minimum requirements, other design considerations include:

-a gas venting layer to collect and dissipate any methane gas that may otherwise cause uplifting of the low permeability layer as well as being possibly explosive;

-bedding or protection above and below the FML.

From a design point of view, these guidelines are quite explicit and remove some of the flexibility inherent in engineering design. In the case of the liner system, a dual liner is required with the top or primary liner being a geomembrane with a minimum thickness of 0.75 mm or 1.14 mm depending on exposure time; the bottom liner (for the FML/composite liner system) must be composed of a geomembrane with the same characteristics as the top geomembrane and clay having a permeability less or equal to 1.0×10^{-9} m/s and be a minimum of 0.9 m thick. For leachate collection, the primary system must be a minimum 0.3 m thick with a permeability greater or equal to 1.0×10^{-4} m/s with a minimum slope of 2% after settlement if composed of granular soil; if composed of geosynthetic material, the in-plane flow capacity must be equivalent to the granular soil. In addition, the LCS must limit the hydraulic head of the leachate acting on the primary liner to a maximum of 0.3 m to the end of the post-closure period which is assumed to be 30 years. The requirements of a granular soil for the LDRS are the same as the LCS; if a geosynthetic material is used, the in-plane flow capacity or transmissivity must be equal or greater than 5.0×10^{-4} m^2/s.

2.1.4 Summary of Regulations

Examination of the regulations reveals that the Canadian national guidelines are more general than the provincial guidelines; this is likely the result of the Canadian Council of Ministers of the Environment (CCME) developing its guidelines. The guidelines do not specify any

performance standards and may be described as conceptual. Consequently, the national guidelines are flexible and allow for more design choices that could take advantage of new technology as it becomes available. The B.C. provincial regulations specify some performance standards and may be described as somewhat prescriptive, but there is still some flexibility for design choices. The United States regulations specify performance standards for all of the main components of a waste containment facility and can be described as very prescriptive.

In comparison to the B.C. regulations, the U.S.E.P.A. regulations are generally more stringent with their requirements. This may be illustrated by comparing guidelines for liner systems and leachate collection (primary and secondary). Both require dual liners, but the U.S.E.P.A. currently favours a bottom composite liner, whereas, British Columbia presently only requires a bottom single liner; also, the 0.9 m minimum thickness for the soil component of the U.S.E.P.A. liner is greater than the 0.5 m specified by B.C. Geomembranes must be a minimum 0.75 mm thick or 1.14 mm thick (depending on exposure time) for the U.S.E.P.A. compared to a minimum thickness of 1.0 mm for British Columbia; the two regulations may be considered comparable in this area. These minimum thicknesses of geomembranes are not too rigorous considering that geomembranes are available between 0.5 mm to 2.5 mm. For primary leachate collection, B.C. specifies a minimum 0.75 m thick layer of granular material with a minimum permeability of 1.0×10^{-5} m/s compared to 0.3 m of granular material with a permeability of 1.0×10^{-4} m/s for U.S.E.P.A. or equivalent geosynthetic material. For leak detection and removal, B.C. does not specify any performance standard, whereas, the U.S.E.P.A specifies the same requirement as the primary leachate collection system for granular material and a minimum in-plane flow capacity or transmissivity of 5.0×10^{-4} m^2/s for geosynthetic material.

2.1 TEST STANDARDS

In design and construction, material properties are characterized by standard test methods. Typically, the selected material is tested according to an index or a performance test. Index tests are performed under conditions which are not representative of field conditions and the data are typically used for comparison of materials. Manufacturers index test values are

typically reported in Geotechnical Fabrics Report's annual edition entitled "The Specifier's Guide". Performance tests are done under simulated field conditions and are intended to establish directly, parameters for design. In order to be able to compare results, the test must follow accepted standard methods.

In the case of transmissivity or in-plane flow capacity, the standard is the American Society for Testing and Materials (ASTM, 1987) Standard Test Method for Constant Head Hydraulic Transmissivity (In-Plane Flow) of Geotextiles and Geotextile Related Products, ASTM D4716-87. This test method has been accepted for dual designation by the Canadian General Standards Board (CGSB) as C**/CGSB-148.1 Method 9.2. The geosynthetic used for in-plane drainage is placed between two platens, see Fig. 2.2, which are used to apply a normal stress to the test specimen; adjacent construction materials may be placed between the specimen and the platens to simulate a layered system. The minimum value of applied confining stess is 10 kPa and the maximum value is specified by the user; trials at a minimum of five different stresses within a range of 25 kPa to 250 kPa are required for acceptance testing. The sample is tested under various hydraulic gradients appropriate to the application; a maximum gradient of 0.1 is suggested for tests used to model pressure flow conditions. The test specimen must be a minimum of 100 mm wide, with its length at least twice the width (to a maximum width of 300 mm at which the 2:1 ratio no longer applies). To perform a test, the sample is saturated under the normal stress desired for a seating period of fifteen minutes, after which, the target hydraulic gradient is applied. Once a uniform flow is observed, a minimum volume of 0.0005 m^3 is allowed to pass through the specimen; the time required (to a maximum of fifteen minutes) for the next 0.0005 m^3 of water is recorded and used to calculate the transmissivity or flow rate. The transmissivity is calculated using the following equation:

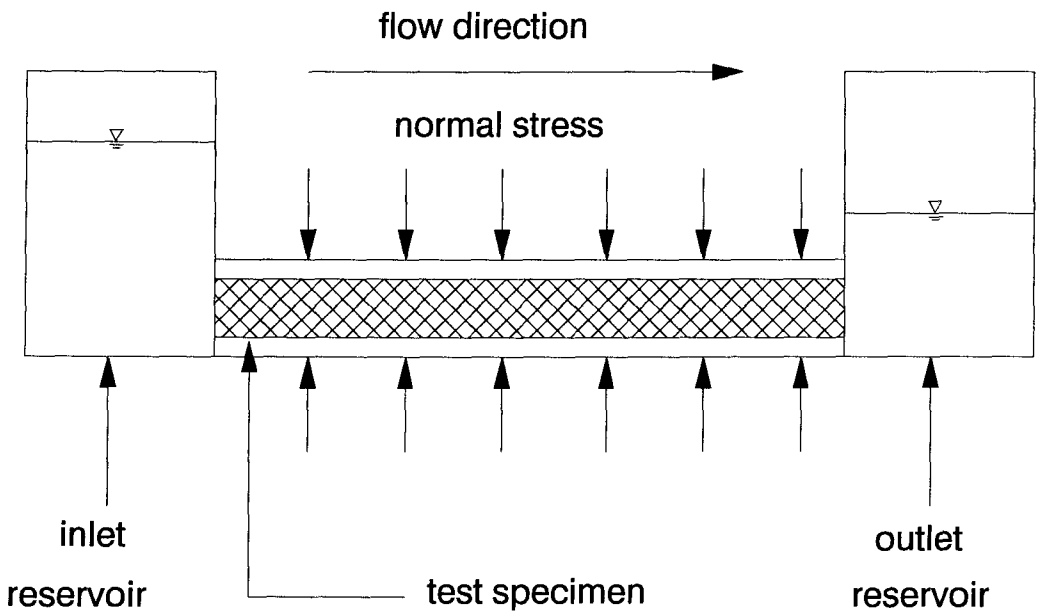

Figure 2.2 Schematic Test Setup for Transmissivity Testing

$$q = QL/WH = Q/Wi \quad (1)$$

where, q = the hydraulic transmissivity (m^2/s)
Q= the average volumetric flow rate (m^3/s)
L = the length of the specimen (m)
W= the width of the specimen (m)
H = the total head drop across the specimen (m)
i = the hydraulic gradient = H/L (dimensionless)

The procedure is repeated until the maximum pressure is reached. The resulting transmissivities are typically plotted against normal stress in presenting the results of the test.

There are three limitations to this test. First, the platens impose rigid boundaries on the geosynthetic specimen. This may be satisfactory for index tests, but is not for performance tests where simulation of flow conditions in a geosynthetic leak detection and removal system requires the geomembrane on either side of the geonet be able to deform. The platens are too stiff and do not intrude into the geonet (or allow adjacent material to intrude), whereas a geomembrane may intrude significantly into a geonet, particularly under high normal stress. The alternative to use closed cell foam rubber (ccfr) to simulate the soil layers is attractive, but rubber may be too compressible.

Second, the maximum normal stress of 250 kPa for acceptance testing may be lower than true field stress levels and cannot be used for performance tests (evidence supporting this is presented in the next section). Third, the test is not adequately standardized with respect to seating period and the specimen size. The seating period is specified as a minimum of fifteen minutes, but no maximum value is specified. Since the specimen may tend to compress under pressure with time, the seating time has a significant influence on the transmissivity values obtained. The only requirements regarding sample size are the minimum width and a minimum length to width ratio. Due to the small size of the samples, boundary effects may be significant, but if samples are not of a constant, fixed size, the magnitude of the boundary effects will be different.

2.3 PREVIOUS TRANSMISSIVITY TESTS

There are not many published papers on transmissivity testing of geonets and fewer on transmissivity testing of geosynthetic leak detection systems. The majority of available literature is on transmissivity testing of geotextiles. However, Hwu et. al. (1990) address the transmissivity of geotextiles in conjunction with geonets, in which the geotextile is placed above the geonet. This combination is often used for either a primary leachate collection system or for a leak detection system in which the primary liner is a composite FML/soil liner; in either case, the geotextile is used as a filter to prevent the geonet from clogging due to soil migration. The results from the tests indicate that intrusion of the geotextile into the geonet is significant and flow rate reductions between 39% to 88% were observed. Creep was investigated from 1000 hr long tests; some materials had constant flow rates while others had slightly decreasing flow rates with time. It was concluded that more tests are required to determine the magnitude and behavior for long-term performance.

There are few data published on the factors governing transmissivity of geonets. Kolbasuk et al. (1992) address many of the more important factors: seating time; water temperature; aspect ratio; permeating fluid; and adjacent soil layers. These variables were examined with respect to a baseline test on a 300 mm x 300 mm sample size geonet under a confining pressure of 718 kPa, a seating time of one hour, a hydraulic gradient of 1.0, and a water temperature of 21 plus/minus 2°C. For the comparison of seating time, periods ranging from 5 minutes to 22 hours were used; it was found that the transmissivity decreased significantly with longer seating periods. This indicates that geonets are subject to short term creep and that a minimum seating time of 15 minutes may not be sufficient for determining long term flow capacity. The water temperature was varied from 7°C to 35°C to determine any effects of temperature. The transmissivity decreased by over a factor of two from 14°C and 28°C, which implies that viscosity corrections cannot make up the difference due to temperatures significantly different than 20°C, and that at service temperatures other than 20°C, a partial factor of safety might be applied. Aspect ratio is defined in the paper as the ratio of the sample length to it width. Tests were performed using aspect ratios of 0.5, 1.0 and 2.0; it was found that the

transmissivity decreased with increasing aspect ratio. Hence, tests should be performed using a standard sample size. Sand, clay, and closed cell foam rubber were placed above the geonet and geotextile to simulate soil layers in field conditions. The results indicated that the materials intruded into the geonet opening by different amounts, but the transmissivity with simulated soil layers were all significantly lower than the other tests. Therefore, it is clear that intrusion in the field can significantly reduce the transmissivity and design values should be obtained from tests simulating adjacent construction materials.

Tests were performed using deaired water and tap water; no differences in transmissivity were observed because the dissolved oxygen content of the tap water was only six parts per million which is considered low. The authors concluded that more studies were required. Halse et al.(1988) have reported observations of flow rate decreasing significantly if the DOC is above six parts per million. At this level of dissolved oxygen, it is likely that air may come out of solution and form bubbles that block flow channels and retard flow rates artificially.

The ASTM D4716-87 designation uses normal stress values from 25 kPa to 250 kPa for modeling pressure flow conditions. There is some guidance in the literature for appropriate stress levels. Gross et al. (1990) estimate the vertical stress at the bottom of a landfill to be between 150 kPa and 300 kPa. Reades et al., (1990), Parker and Salier, (1991), and Hutwelker et al., (1991), report landfill heights between 20-40 m. Typical values of unit weights given in the Caterpillar Performance Handbook are between 3.6 to 8.9 kN/m^3 with the addition of a cover increasing the range to 4.2 to 10.1 kN/m^3. Consequently, stresses between 168 kPa to 404 kPa might be expected. For mining applications, Cincilla and Zagorski (1991) indicate that an average dry unit weight for tailings is 13.3 kN/m^3 which is equivalent to 532 kPa for a 40 m impoundment.

Eith and Koerner (1992) provide some realistic values of normal stress in a field situation. In this paper, the authors describe the transmissivity values of a leak detection system obtained from field tests in which the leak detection system was loaded with a leachate collection system, 13.9 m of solid waste , and 28.3 m of solid waste. These loads represent normal stresses of 12

kPa, 153 kPa, and 311 kPa, respectively; for a unit weight of 11.0 kN/m^3.

They also present several important conclusions from their field study:

- the transmissivity values decreased from 4.52 x 10^{-3} to 4.35 x 10^{-3} to 4.00 x 10^{-3} m^2/s with increasing normal stress and was attributed to elastic intrusion of the geomembrane into the openings of the geonet.
- laboratory tests on the same geonet using the standard test method previously described result in transmissivity values of about one-half of the field value. Hence, it is perceived that laboratory tests provide a conservative or lower bound transmissivity values;
- concerns about scale effects or aspect ratios from laboratory tests are eliminated by a full scale test;
- the transmissivity of the geonet in the field exceeds the referenced regulatory requirement of 5.0 x 10^{-4} m^2/s for natural granular drainage materials.

Feeney and Maxson (1993) report field performance of double liner systems in forty-nine landfills. The observed flow rates (weekly average) of the secondary leachate collection systems or leak detection systems ranged from 0.06-3.53 m^3/hectare/day which is equovalent to 6.9 x 10^{-9} to 4.1 x 10^{-7} m^2/s. These flow rates do not represent maximum flow capacity of the LDRS; they indicate the rate of leachate generation and seepage rates through the liner systems of facilities constructed under strict quality assurance programs.

2.4 DESIGN

There are papers that discuss the principles used in designing geosynthetic leachate collection and leak detection systems. Generally, references to intrusion of the geomembrane into the geonet and creep behavior are made, but no specific data are presented. Koerner (19??) writes "The creep sensitivity of drainage curves varies from nil to enormous. Manufacturers' literature on this subject is weak" . He also writes "The elastic deformation of the material adjacent to the core will cause intrusion, thereby reducing flow. For high stresses and low modulus materials, this reduction can be severe, e.g. up to 50%!". Landreth (1990) writes "Geonets require less space than granular soil for equivalent flow capacity, thus promoting rapid

transmission of fluids. Potential disadvantages over long periods of time and under high compressive loads are creep and intrusion. Again, proper design should minimize the potential for these problems". The general approach to design has been to apply several partial factors of safety for intrusion and creep. Koerner (1990) provides some recommended preliminary Factors of Safety:

for creep of geonet - FS_c = 1.4 to 2.0

for elastic intrusion of geomembrane - FS_i = 1.5 to 2.0

2.5 OBJECTIVES OF RESEARCH

The limitations of the standard test method for transmissivity testing of geonets and the general lack of data regarding intrusion and creep introduce uncertainty to the design of geosynthetic leak detection systems. Hence, the general objectives of the research are to determine the flow capacity of geosynthetic leak detection systems and examine factors influencing it. More specifically, the objectives are:

- a critical evaluation of the standard test method;
- an evaluation of the material properties under simulated performance conditions;
- to establish a practical approach for selection of a factor of safety to be applied to the in-plane flow capacity for long-term design;
- to provide constructive suggestions for leak detection and removal system requirements/ design criteria for updating the provincial regulations.

3. EXPERIMENTATION

3.1 TEST EQUIPMENT

3.1.1 Transmissivity Test Device

Transmissivity test devices were specially designed and constructed for the project. Each has three major sections (Fig. 3.1) separated by a partition wall: an inlet chamber, a chamber for the test specimen and fluid permeant, and an outlet chamber. The test specimen in the center chamber is subjected to a normal confining stress; levels in the inlet and outlet reservoir are adjusted to control the imposed hydraulic gradient across the test specimen. The volume of water flowing through the test specimen as a result of the hydraulic gradient is measured over a period of time to determine the volumetric flow rate.

The transmissivity testing device is made of anodized aluminum plates, 12.5 mm thick for the side and partition walls and 25 mm thick for the base. The end walls are transparent acrylic sheets, 12 mm thick. The overall outside dimensions of the unit are 508 mm long by 152 mm wide by 178 mm deep.

The inflow chamber is 127 mm wide by 102 mm long and is supplied with water from a 25 mm inside diameter tube. The water level is controlled by an adjustable inlet overflow tube. The outflow chamber is similar to the inflow chamber in size: the outlet overflow tube is used to control the water level in this chamber and collect the water flowing through the geonet for measurement. The partition walls incorporate a rubber O-ring cord which makes a water-tight seal with the side walls of the device when assembled. A port in each chamber accommodates a shared differential pressure transducer.

The center chamber contains the composite test specimen, a lower latex bag, a mounting plate, and an upper latex bladder that is used to apply a normal stress to the specimens. The lower latex bag contains fine to medium sand and is placed in a recess measuring 254 mm long x 127 mm wide x 12.5 mm deep in the base plate. It acts as a stress controlled boundary on the test specimen, which is placed above the latex bag and held in place at both ends by the bottom of the partition walls. The mounting plate, which supports the upper latex bladder, rests on top of the geonet/geomembrane system. Normal stress is applied by pressurizing this bladder, see

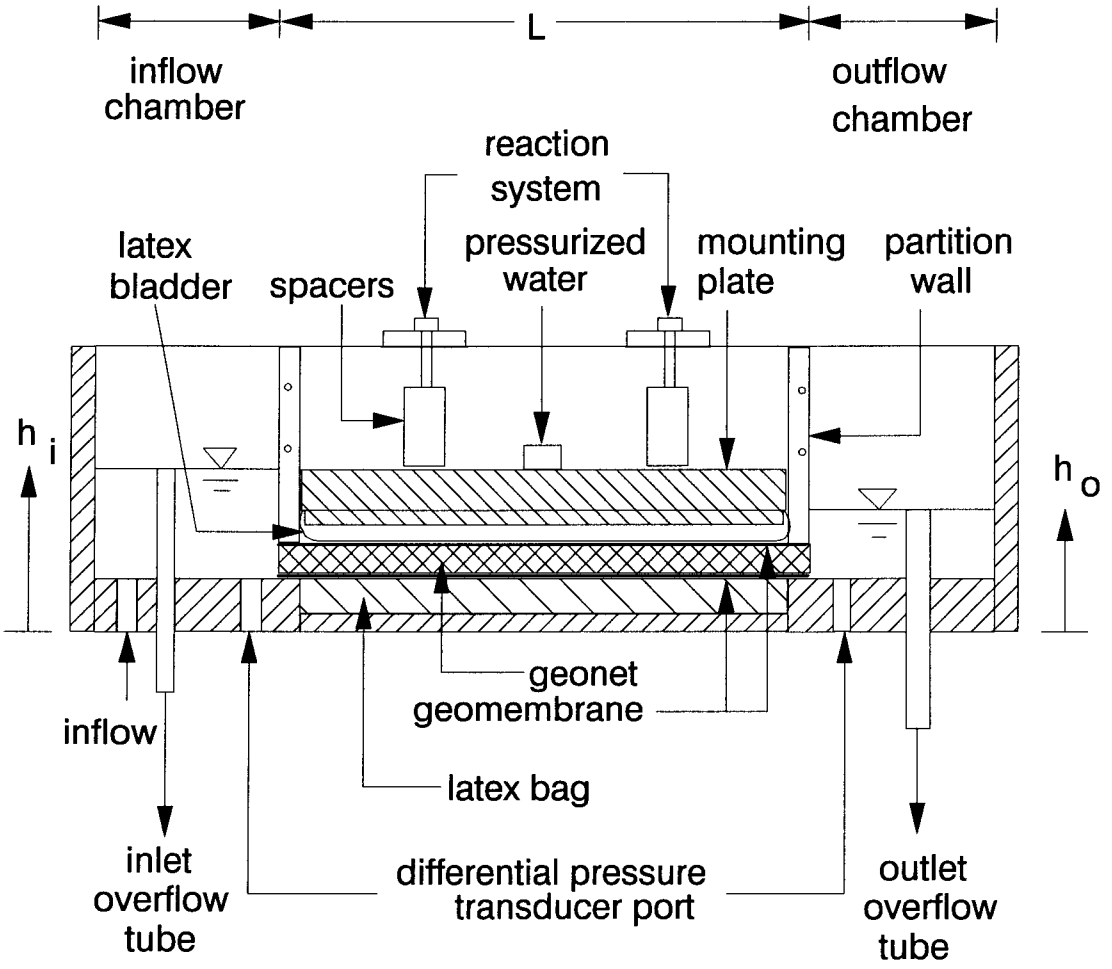

Figure 3.1 Schematic of Transmissivity Test Device

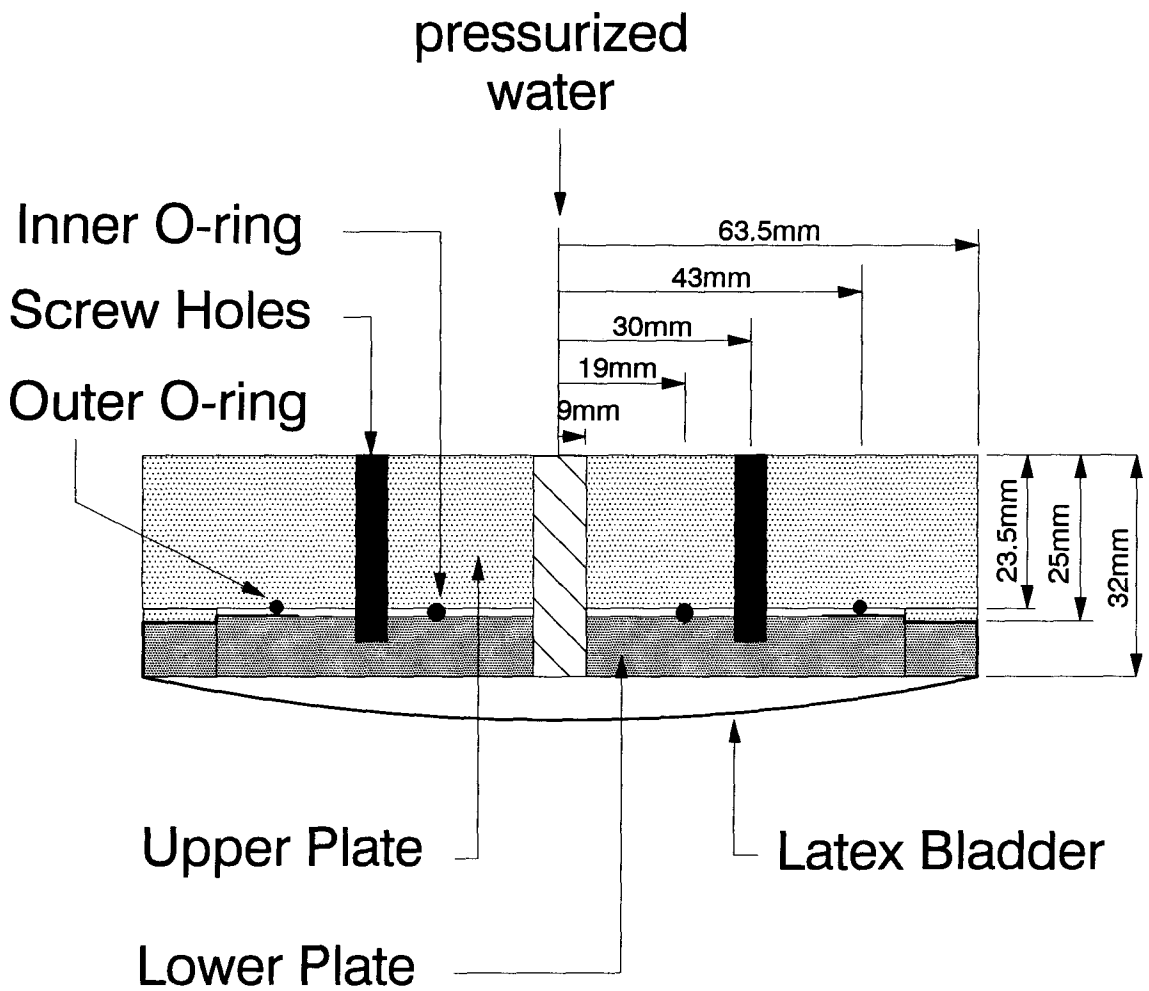

Figure 3.2 Top Mounting Plate

section 3.2.3. The latex bag and bladder are manufactured specifically for these tests developed at the University of British Columbia using a double-dipping technique by Vaid and Campanella (1973). A transverse cross section of the mounting plate is illustrated in Figure 3.2. The O-rings and the recess at the edge of the plates prevent the latex bladder from slipping off the lower plate under pressure. A reaction system (Fig. 3.1) above the mounting plate consists of two cross-braces spacers.

3.1.2 Fluid Circulation System

A schematic drawing of the fluid circulation system is shown on Figure 3.3. The system may also be separated into three components: a supply system; a recharge system; and an overflow system. The supply system consists of the upper reservoirs, the water manifold, and the tubes feeding the testing devices. The recharge system consists of two troughs, a bottom reservoir, and a pump to return the water to the upper reservoirs. The overflow system consists of an overflow tube and a cold water bath. Generally, water is gravity fed to the testing devices via the water manifold which controls the supply rate to the test devices. Water flowing through the test devices is collected by the troughs and fed into the bottom reservoir; the water is then pumped back up into the supply reservoirs at the top. The overflow system prevents the upper reservoirs from overfilling and keeps the water at a constant temperature.

Both test series W and WLC used tap water spiked with a commercially available algaecide, Poly-gard Bioguard, to prevent biological growth observed during preliminary tests. The initial concentration of algaecide added to the water was 13 parts per million; an additional dosage of 5 parts per million was added on a weekly basis to ensure that the water remained free of growth. Chemical precipitation was not a concern because the tap water is soft and relatively free of chemical constituents.

The supply system is gravity controlled. Reservoir number 1 contains approximately 80 litres and reservoir 2 contains approximately 120 litres for a total volume of 200 litres. Water flows from supply reservoir number 2 to the water manifold via a clear vinyl tube with an inside diameter of 25 mm. The hydraulic head from the reservoir to the water manifold is approximately 1.8 metres and can provide more than 16 litres/minute to the manifold. The water

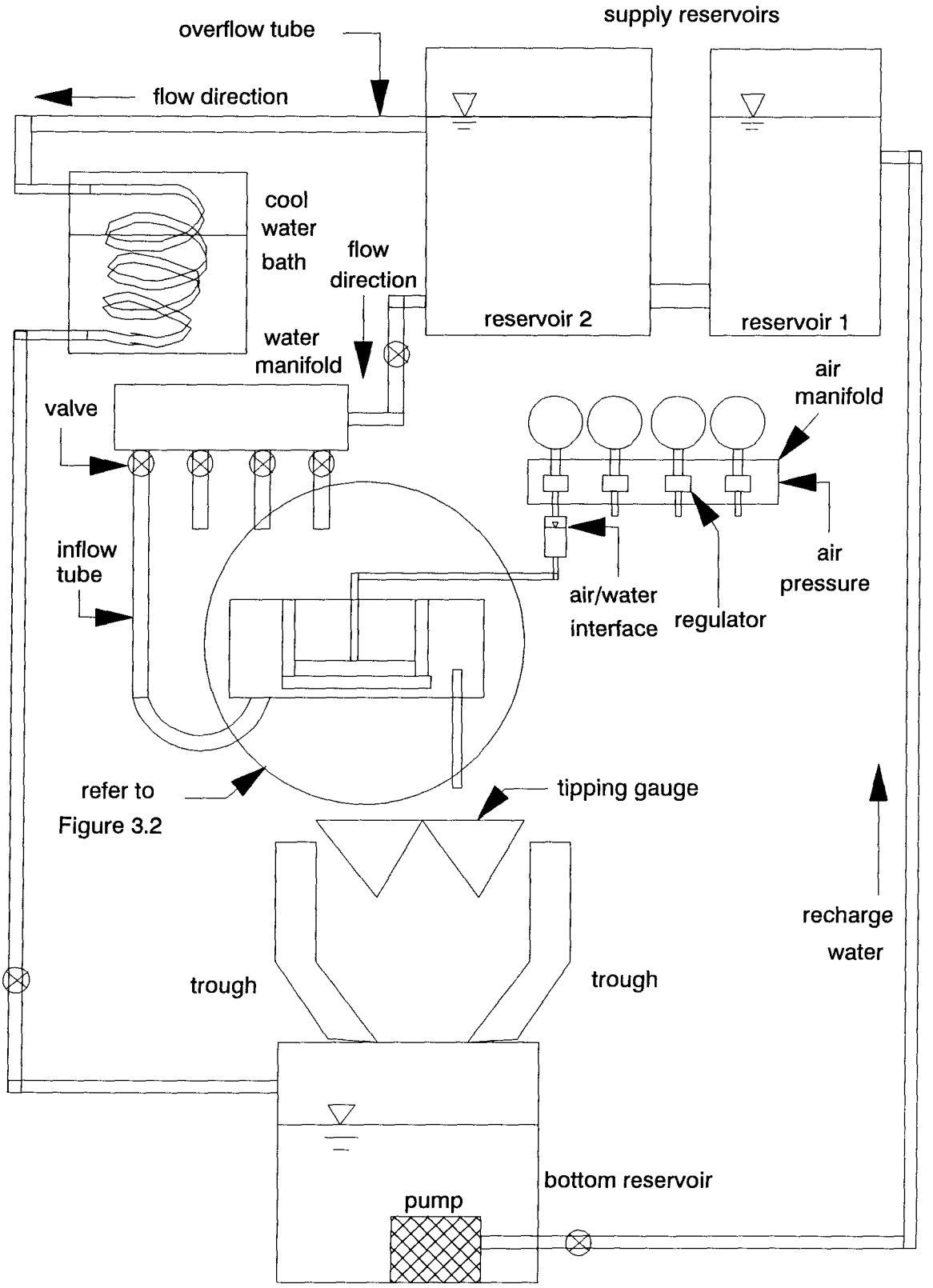

Figure 3.3 Circulation System

manifold is constructed of ABS pipe with an inside diameter of 102 mm and 0.91 m long. Water flows from the manifold to the transmissivity test devices through tubing with a 19 mm inside diameter; the rate is controlled by 19 mm PVC ball valves. After flowing through the test specimen, it and is collected by the outflow tube for measurement by a tipping gauge described in section 3.3.1.

The recharge system comprises of two aluminum collection troughs for the tipping gauges, a bottom reservoir, and a Teel submersible pump. The pump is rated at approximately 50 litres/min when pumping against a hydraulic head of about 2.7 metres (the height between pump and top of water level in supply reservoirs). Since this rate was estimated to be about three times the maximum flow rate through all four test devices combined, a valve was placed between the pump and reservoir number 1 to control the recharge rate.

It was not convenient to keep the combined flow rate of all the test samples and the recharge (pumping) rate at equilibrium, therefore, an overflow system was installed to prevent the supply reservoirs from overflowing. The overflow water flows through a copper coil made of 16 mm outside diameter tubing (approximately 12-13 mm inside diameter) which is submerged in a cold water bath to keep the recirculating fluid at 22°C +/- 1°C. Without the bath, the pump raised the temperature of the recirculating water to 27°C during preliminary testing

Several additions were made to the system during preliminary testing in order to reduce the amount of dissolved oxygen in the recirculating water. It was observed that air bubbles would become trapped in the geonet causing the flow rate to decrease. The behavior was attributed to air coming out of solution in a manner described by Halse et al. (1988). At that time, measurements of the dissolved oxygen content in the water were near saturation at 8 parts per million and efforts were made to reduce this level below saturation. Hence, a second supply reservoir was added to increase the holding time of the water and encourage any oxygen to come out of solution. In addition, measures were made to prevent any splashing of water during collection and recirculation. Some success was achieved, however, the dissolved oxygen content remained near saturation and the air pressure system was modified, described below, to eliminate

the problem.

3.1.3 Air Pressure System

Normal stress on the test samples was provided by an air pressure system, see Fig. 3.4. The laboratory air supply which runs at approximately 650 kPa feeds an air manifold constructed of steel tubing. The air pressure leaving the air manifold is controlled by a Fairchild-Hiller regulator which keeps the air pressure constant at the desired test pressure. The air then enters a clear chamber made of Lucite tubing which is partially filled with water, thus creating an air/water interface. The air pressurizes the water, which in turn, pressurizes the latex bag on the top mounting plate and provides the normal stress for testing. A ball valve at the bottom of the lucite chamber allows the pressure in the water-filled, upper latex bladder to be sealed while water is added to the air/water chamber (if necessary).

Experience during preliminary testing to commission the test devices revealed that, without the air/water interface, defects such as pinholes in the latex bladder allowed air to permeate through it. Considerable efforts were made to eliminate these pinholes, but attempts based on polishing the mold, evacuating the latex, and double-dipping the bladders all proved to be unsuccessful.

3.2 INSTRUMENTATION

3.2.1 Flowmeters

The water flow rate is measured using a tipping gauge comprising of two cells, see Fig. 3.4. Each cell is 200 mm wide and triangular in profile, and the volume of water for each tip (one cell) is approximately 0.6-0.7 litres.

Calibration of the tipping gauges relates the time interval between tips of both cells, termed tip interval, to the flow rate. The calibration was performed by physically measuring the flow rate after it became stable for eight different rates ranging from about 1 ml/s to 75 ml/s, see Fig. 3.5. Each flow rate was measured in three separate trials with the average deviation between trials being less than 1% which indicates excellent agreement. The maximum deviation

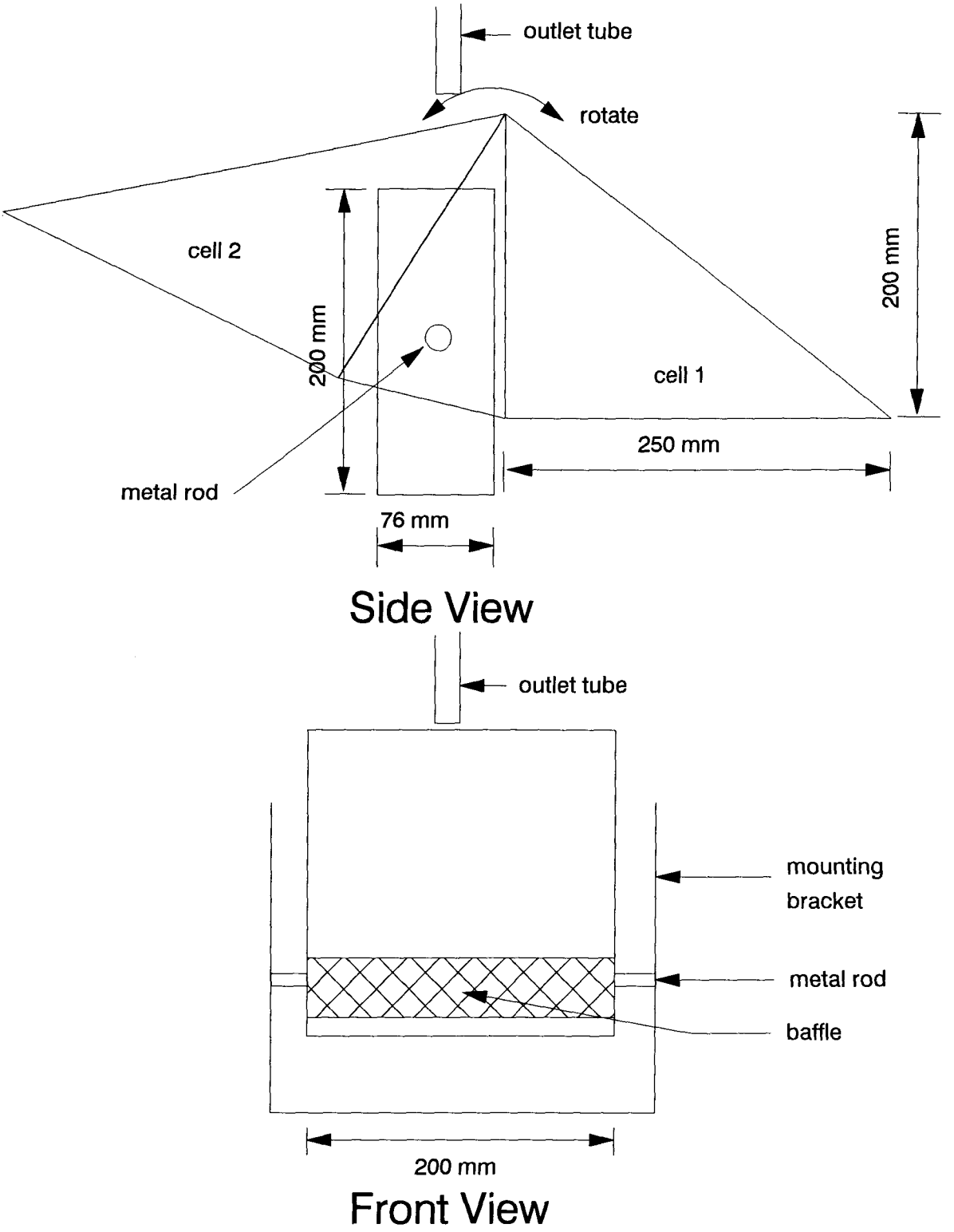

Figure 3.4 Tipping Gauge Details

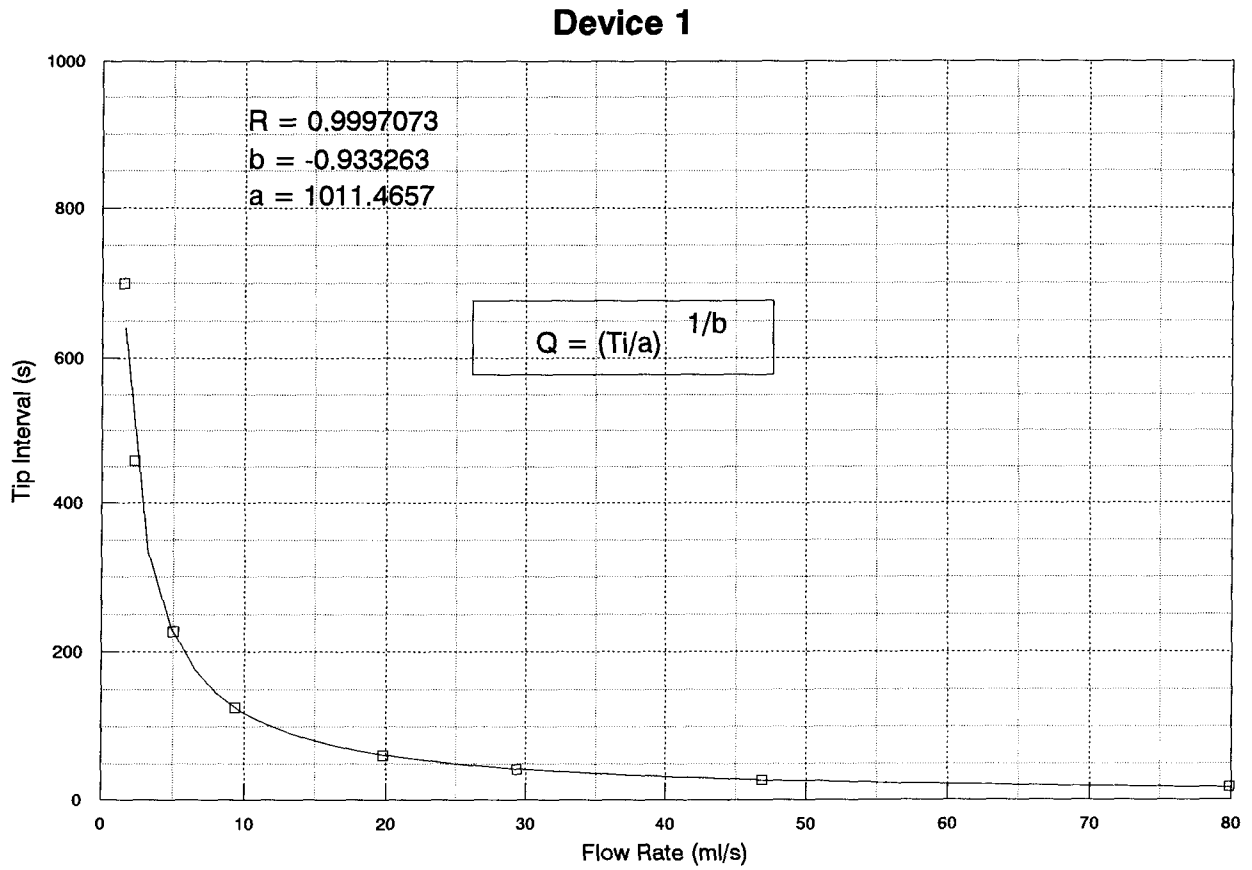

Figure 3.5 Typical Tipping Gauge Calibration

between trials was 2.7% and the minimum deviation was 0.2%. The relationship for the flow rate is determined from equation 2 below:

$$Q = (Ti/a)^{1/b} \qquad (2)$$

where Q = the volumetric flow rate
Ti = the tip interval in seconds
a,b = coefficient to fit curve

The tip interval, Ti, may be manually checked or automatically logged; the coefficients a and b are shown on the calibration curve. A regression analysis was performed for each curve with the regression value, R, also shown on the figure; the excellent curve fit to the data points is exemplified by the regression value very close to 1.0.

3.2.2 Differential Pressure Transducers

Differential pressure transducers were used to measure the difference in the water level between the inlet and outlet chambers (see Fig. 3.1) and therefore, establish the hydraulic gradient. The transducers used for the series W and WLC tests are made by Statham, model PM80TC and have a maximum capacity of 3.45 kPa (0.5psi) differential pressure.

These transducers are very sensitive and extreme care was taken to saturate the cavities with deaired water using a hypodermic syringe, see Fig. 3.6.

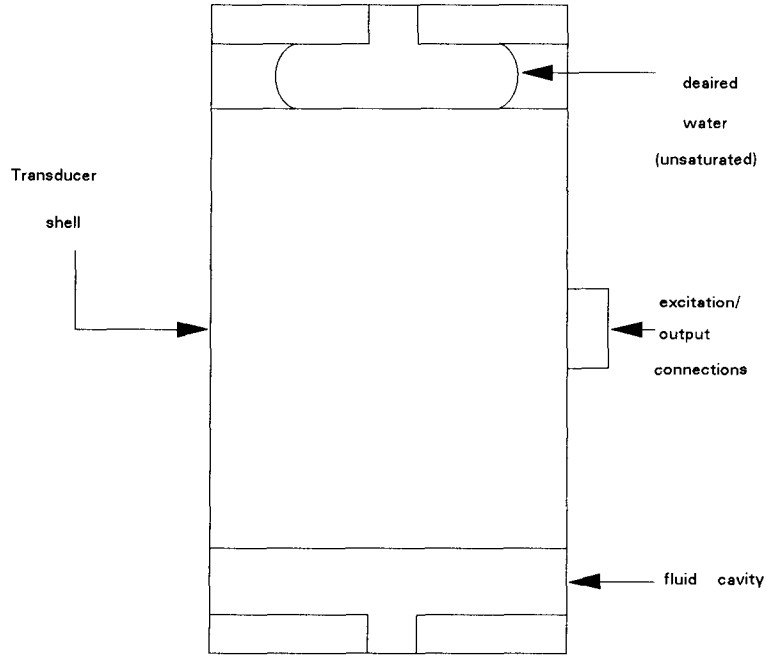

Figure 3.6 Saturation of Transducer Cavity

It was necessary to swirl the transducer in a circular motion in order to overcome surface tension, allowing the deaired water to reach the outer edge of the cavity. The results of a stability check over an 18 hr period are shown on Table 3.2.

Table 3.1 Transducer Stability Check

Elapsed Time (min)	Output (μV)
0	8.090
30	8.103
195	8.094
285	8.080
345	8.088
390	8.082
1018	8.096
1068	8.091

The drift of the output signal is 0.23 microvolts, and is considered negligible compared to the full scale deflection of 5 volts.

The transducers were calibrated for an applied differential pressure between zero and 2.45 kPa, see Fig. 3.7. Pressure was increased and decreased in 0.098 kPa (10 mm of water) intervals, and then cycled to 2.45 kPa two or three times to check any hysteretic behavior of the transducer. The response of each transducer was linear with no significant hysteretic behavior.

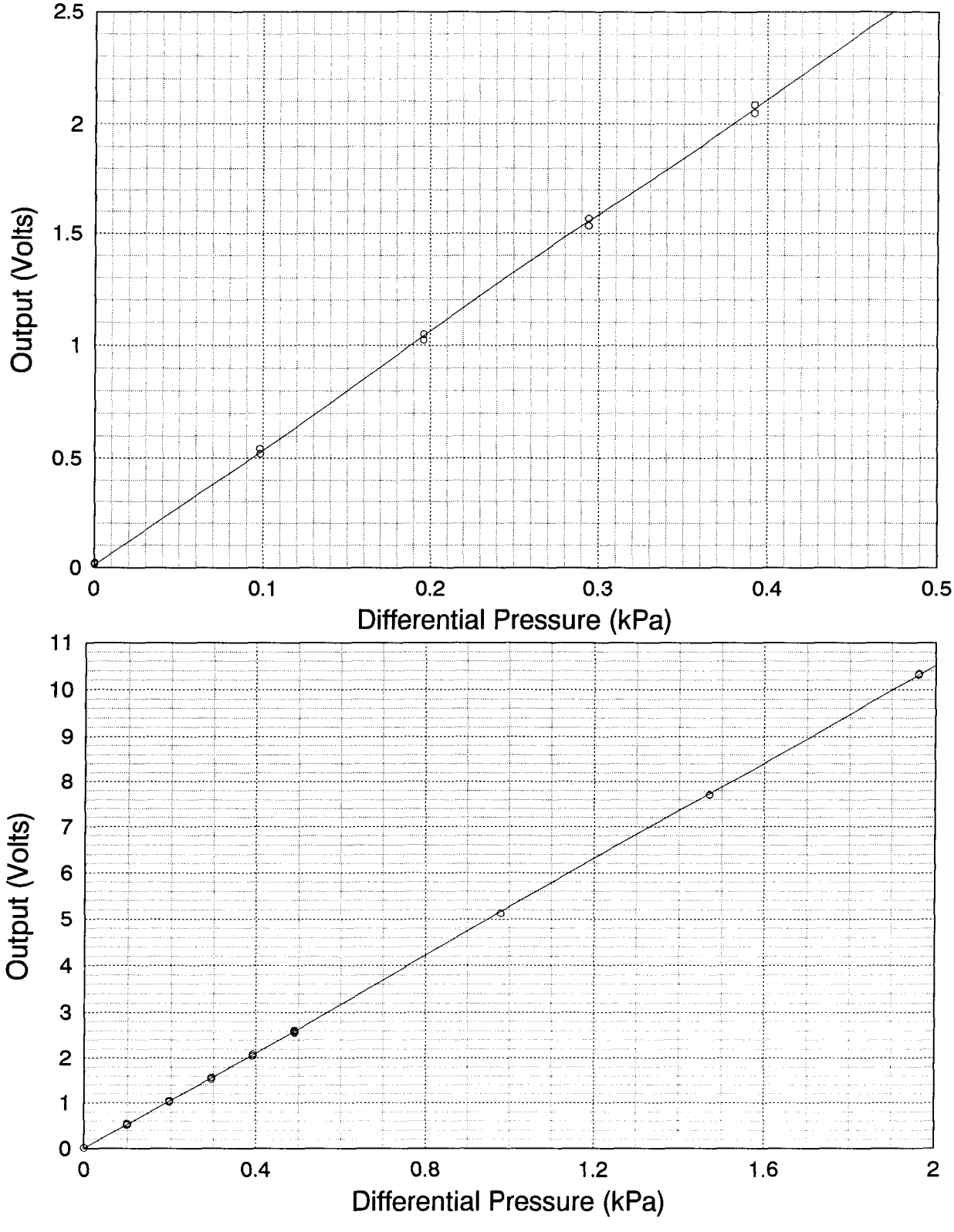

Figure 3.7 Calibration of Differential Pressure Transducer

The differential pressure transducers were used to calculate the hydraulic gradient, given by:

$$i = h_i - h_o / l \qquad (3)$$

where i = the hydraulic gradient
$h_i - h_o$ = the head or pressure loss
l = the length over which the head loss takes place

For these tests, l = the length of the geonet samples (280 mm) and the head loss is the differential pressure (see Fig. 3.1).

Experience has shown the hydraulic gradients calculated from the transducer output were subject to inaccuracy from two sources. First, testing at the higher gradients caused some minor turbulence in the inlet chamber which resulted in minor fluctuations in the water level. These fluctuations were picked up by the transducers, which indicated fluctuating gradients. Second, the calculated gradients occasionally deviated from the set gradient due to an apparent drift of the transducers. The output of the transducer appeared to be drifting because the calculated gradient would change by 1% over a period of a few hours when no changes were made to the gradient. The term apparent was used to describe this difficulty because it may not truly be transducer drift, but rather instability of the electric signal conditioning box (ESCB) which received the transducer output for amplification (1000 times) before being recorded. Since the stability check (see Table 3.1) indicated very little drift in the transducer output, the drift was attributed to the ESCB. Due to the turbulence and apparent transducer drift, the calculated hydraulic gradients using the transducer readings were considered nominal and the true gradient was set by the difference in height of the overflow tubes. Hence, the transducers were only used as a check on the gradient; they were useful because any rapid change in the gradient indicated a problem in the data which were corrected or deleted.

3.2.3 Data Acquisition System

The data acquisition system was incorporated for automated data logging; it comprises of a computer, a software program, an electronic signal conditioning box (ESCB), and relay switches. The computer is an IBM compatible, personal computer with a 386-25Mhz chip, a

100MB hard drive, a 31/2" disk drive and a VGA monitor. The software program is Labtech Notebook. The ESCB is a 16 channel unit that was built for this research project at The University of British Columbia. The relay switches are placed beside each tipping gauge and are triggered when the front cell tips. Whenever the relay switch is triggered, it sends a signal to an electronic counter and to the ESCB which is logged by the computer.

Labtech Notebook is a software program designed with flexible programming options which can be used to optimize the data acquisition system for automated data logging. A separate program was setup for each test device. Data logged for the calculation of the flow rate and gradients were the tip interval of the tipping gauges and the voltage output of the differential pressure transducers. The variation of flow rate with elapsed time was determined knowing the elapsed time. In a parallel subprogram, the voltage output of the differential pressure transducer was also recorded whenever the front cell of the flowmeter tipped. Since, the water level in the inflow chamber varied slightly, a moving average of ten values was recorded over a period of 1 second.

3.3 TEST PROCEDURE

The test procedure may be considered as two phases; the sample preparation and the test method itself. The sample preparation involves preparing the samples and installing them into the test device. The test method includes the procedures followed in measuring the flow rates under several hydraulic gradients and normal stresses for series W tests. The sample preparation for the series WLC tests is the same, but the test procedure is significantly different.

3.3.1 Sample Preparation

The test samples are all cut to the same dimensions, 280 mm x 127 mm, which fit exactly into the center chamber of the test devices. The samples were cut using a metal template as a guide and a sharp razor. The orientation of the geomembranes is of no significance, but the orientation of the geonets is very significant. The geonets have two series of flow channels which cross at different angles, and were cut so that the direct line of flow through the test device would dissect the angle of the flow channels of the sample, as shown in Fig. 3.8. Since

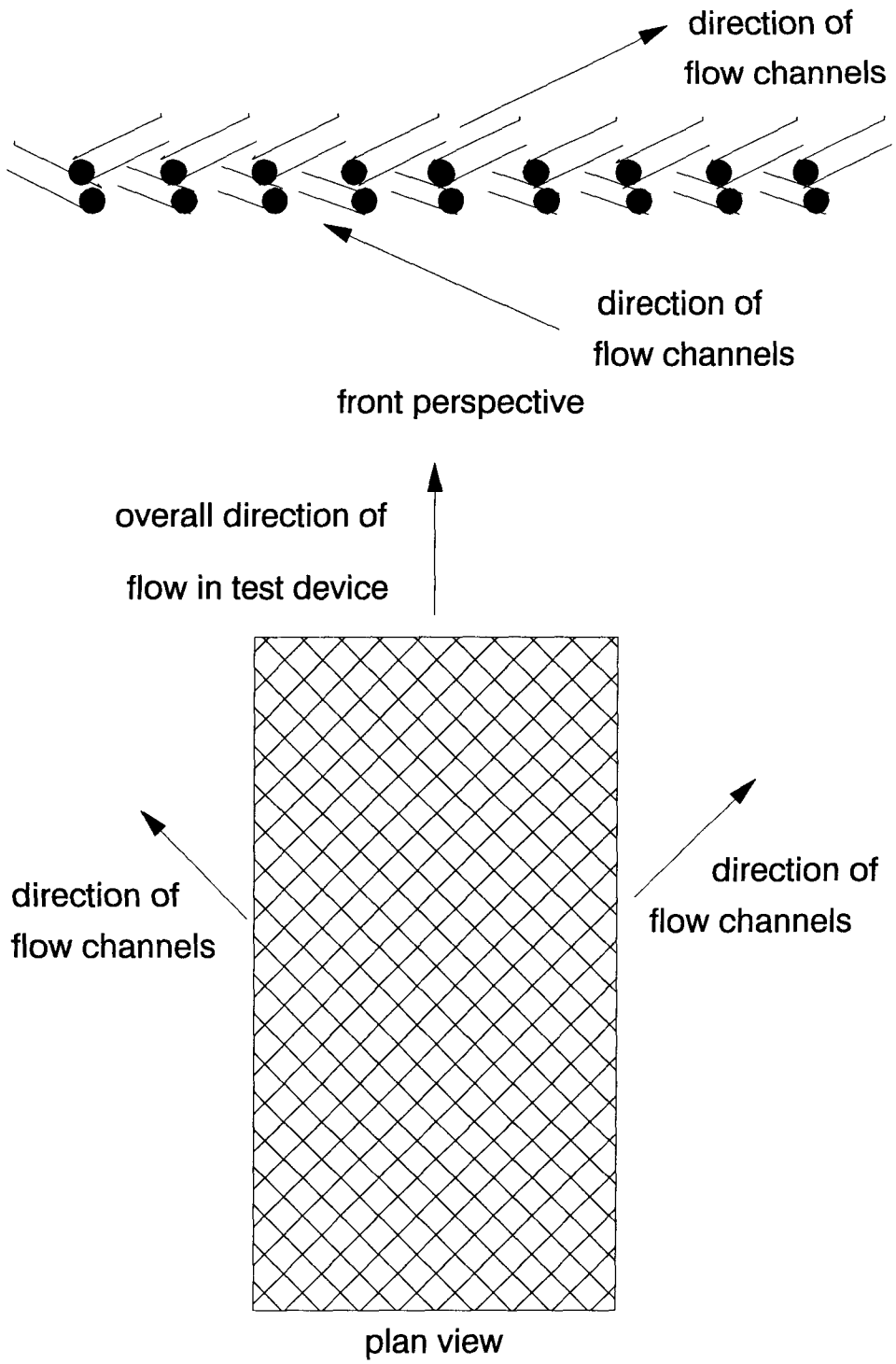

Figure 3.8 Orientation of Geonet Flow Channels

the flow channels did not cross at 90°, this method of cutting results in two possible orientations of the flow channels; the specimens were placed with the flow channels at less than 45° to the flow direction of the test devices., promoting a higher flow rate.

During installation, the bottom latex soil bag was installed first, followed by the rear partition wall (see Fig. 3.1), which was placed, but not securely fastened with the screws. Sufficient water from the manifold was then allowed to enter the device in order to ensure saturation of the geonet by installation underwater. The lower geomembrane was placed first, followed by the geonet and finally the top geomembrane. The mounting plate with the latex bladder filled with water (see next paragraph for description of assembly) was then carefully installed by tipping it upright and slowly lowering one end into the center of the test device. The mounting plate was then turned horizontally while being lowered on top of the test samples. Care was taken not to pinch the latex bladder against the side walls of the test device, which might cause the bladder to puncture. If the bladder did stick to the side wall, the mounting plate was removed and the procedure repeated. Occasionally, the sides of the latex bladder were lubricated with silicone oil when the fit appeared too tight. The other partition wall was placed into the device after centering the mounting plate into place and the screws of both partition walls were hand tightened and then backed off to provide a small amount of slack. The spacers (see Fig. 3.1) were then placed above the mounting plate followed by the cross bars which were fastened on tight.

The top and bottom pieces of the mounting plate are assembled under water along with the latex bladder, see Fig. 3.2. Care is taken to align the pieces together so that the edges of the bladder do not protrude out beyond the edge of the top portion of the mounting plate; otherwise, the mounting plate will not fit into the test device. After the plate is securely tightened and still underwater, the latex bladder is filled with water via a tube and funnel. When the bladder contains sufficient water, the opening of the fitting is either directly connected to the air/water interface chamber or capped until installed into the test device.

3.3.2 Series W

The objective of the series W tests is to examine the influence of material, gradient, and normal stress on the in-plane flow capacity of a leak detection and removal system. Before starting the test, the samples were flushed under a hydraulic gradient of about 0.5 to remove any air bubbles that may have become trapped during the setup. Flushing was performed by setting the front overflow tube to its lowest point, turning on the inflow valves to a high rate and physically blocking the rear overflow tube. Flushing lasted for about 1 minute and then the inflow valves were turned off.

The first normal stress of 25 kPa was applied by turning on the regulators (the air manifold is always connected to the air supply under pressure) and initiating the software program for automatic data logging. The specimens were flushed again to remove any air bubbles that may have pushed through the latex bladder after pressurizing. At this time, there was no flow of water because the inflow valves are still turned off. Therefore, there was no gradient and a zero reading of the differential pressure transducers were taken.

The overflow tubes were then set for the first set of flow readings starting at a 0.02 hydraulic gradient. The tubes were set using gradient bridges made from rectangular aluminum tubing. The height of the bridges was machined so that the height difference between the front and rear overflow tubes corresponds to a gradient of 0.02, 0.04, 0.06, 0.08 or 0.10. The inflow valves were opened to allow water to run into the rear overflow tube, but at a minimal rate so that there was no turbulence. The time from first applying a normal stress to turning on the flow valves for the first set of reading was approximately 12-15 minutes. Flow rate data was recorded 15 minutes after applying a normal stress as indicated by ASTM standards. Flow rate data for each gradient were taken over a period of 15 minutes at which time the hydraulic gradient was increased through 0.04, 0.06, 0.08, and 0.10; when the readings for the 0.10 gradient were completed, the gradient was reset to 0.02.

The next set of gradient readings were taken approximately 2 hours after applying the normal stress, but starting at a gradient of 0.04 because the readings for a 0.02 gradient have been continuous since the 0.10 gradient of the first set. Additional sets of gradient readings were

taken at approximately 7 hours and 24 hours after applying the normal stress in the same fashion. At the end of the 24 hour set of readings, the pressure or normal stress was increased to 100 kPa. The devices were then flushed, zero readings were taken and the inflow valves were turned on to start the first set of gradient readings as before. This procedure was repeated for subsequent stresses of 200 kPa, 300 kPa, and 400 kPa. The test was terminated at the end of the 24 hour reading at a normal stress of 400 kPa.

Two factors govern the resolution of measurement, Firstly, since the gradients were set using bridges, it is important that the devices be completely level. During the setup of the test equipment, the devices were leveled to within 0.3 mm, and the bridges were also manufactured within 0.3 mm of their desired height. Secondly, if the inflow rate (controlled by the inlet valve below the water manifold, see Fig. 3.3.) is a little too high or low, then the drawdown cone at the inlet overflow tube will not match that of the outlet overflow tube and a small variation in gradient occurs. It is estimated that the combined variation in gradient (test apparatus and the inflow rate) could result in deviations of the flow rate of up to 20% for a 0.02 gradient and 14% for a 0.10 gradient.

3.3.3 Series WLC

The objective of the series WLC tests is first, to provide control data for the series L tests and second, to evaluate the creep behavior of the materials. The test procedure is much simpler than the series W tests. Each specimen is subject to a constant normal stress of 300 kPa and a hydraulic gradient of 0.02 throughout the duration of the test. The test duration was 120 hours for most specimens, though four tests were continues for over 240 hours to further examine any effects of creep. The materials for this series of test were chosen for their expected high flow rates. However, the materials used in the extended tests were chosen randomly and does not indicate that creep effects are suspected to be more significant than for the other materials.

Since the tests were performed at constant gradient, the resolution of measurement is only influenced by the inflow rate, as previously described. During testing, it was necessary to occasionally flush the air out of the supply tubes by fully opening the valves (see Fig. 3.3). The valves were then returned to their original position which provided a 0.02 gradient. However, it

was not always possible to return the valve to its *exact* position before flushing and a slightly different inflow rate would result. The different inflow rate would slightly alter the drawdown cone at the inlet overflow tube (see Fig. 3.1), and since the supply tubes required flushing twice a day, it is not unreasonable to expect flow rates to fluctuate by about 10%.

3.4 TEST MATERIALS AND TESTING PROGRAM

3.4.1 Test Materials

The materials tested in this program consisted of four geonets, eight geomembranes, and aluminum plate. Geonets are typically made of high, medium, or low density polyethylene (PE) and one of each type was chosen for testing because of their different compressive strengths. The HDPE geonet has a higher compressive strength than the MDPE geonet which was higher than the LDPE geonet: a second high density geonet was chosen because HDPE is the most common polymer used for geonets. The HDPE and MDPE geonets had solid ribs, whereas the LDPE geonet had foamed ribs. All of the geonets were approximately 5 mm thick and are illustrated in Figure 3.9.

Geomembranes used in testing were textured and smooth, high-density polyethylene (HDPE), smooth very low density polyethylene (VLDPE or LDPE), smooth polyvinyl chloride (PVC), and smooth polypropylene (PP); all geomembranes were non-reinforced. The British Columbia Waste Management Act specifies a minimum thickness of 1.0 mm, hence, test specimens were chosen to meet or exceed this criteria. In addition, the U.S.E.P.A. regulations for municipal solid waste landfills specify a 1.52 mm thickness if the geomembrane is made of HDPE. Therefore, geomembranes 1.52 mm thick were included in the program.

HDPE is classified as a stiff material, whereas LDPE and PVC are classified as flexible materials (Koerner, Halse, and Lord, 1990) with respect to flexural rigidity. However, if LDPE and PVC are compared qualitatively, there is a large difference between them, hence, LDPE was designated to be a semi-flexible material. The polypropylene was also designated to be a semi-flexible category, but it is slightly stiffer than LDPE. The materials were supplied by local manufacturers or distributors and are summarized in Table 3.2.

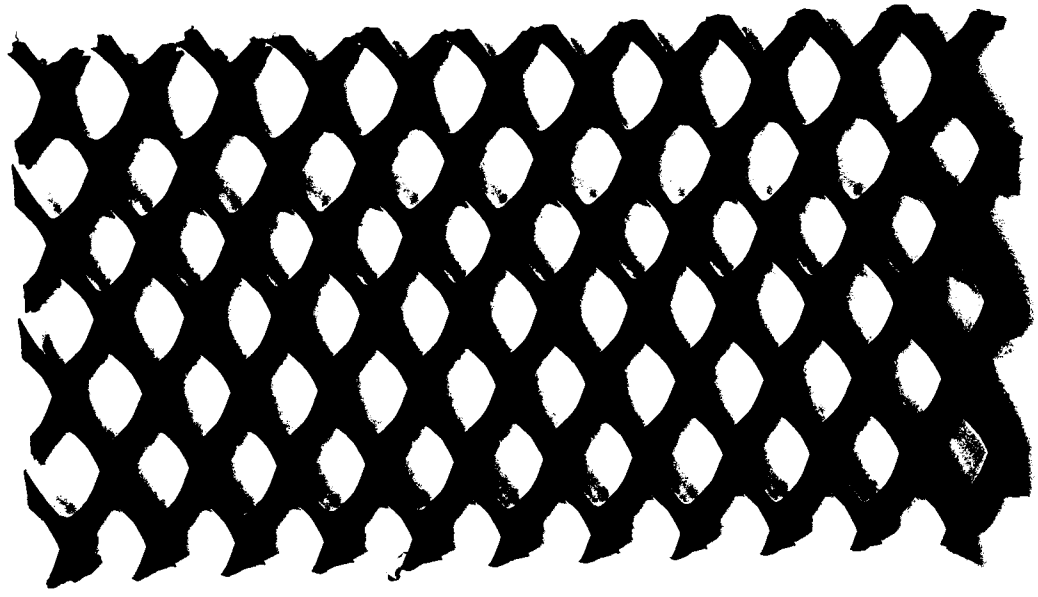

5.1 mm HDPE Geonet

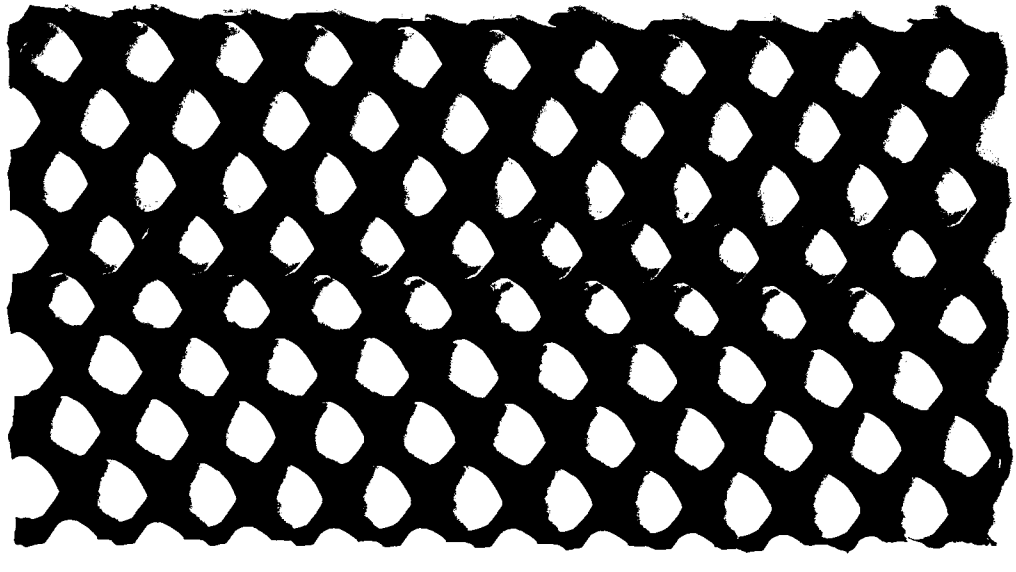

5.2 mm HDPE Geonet

Figure 3.9a Geometry of the Geonets

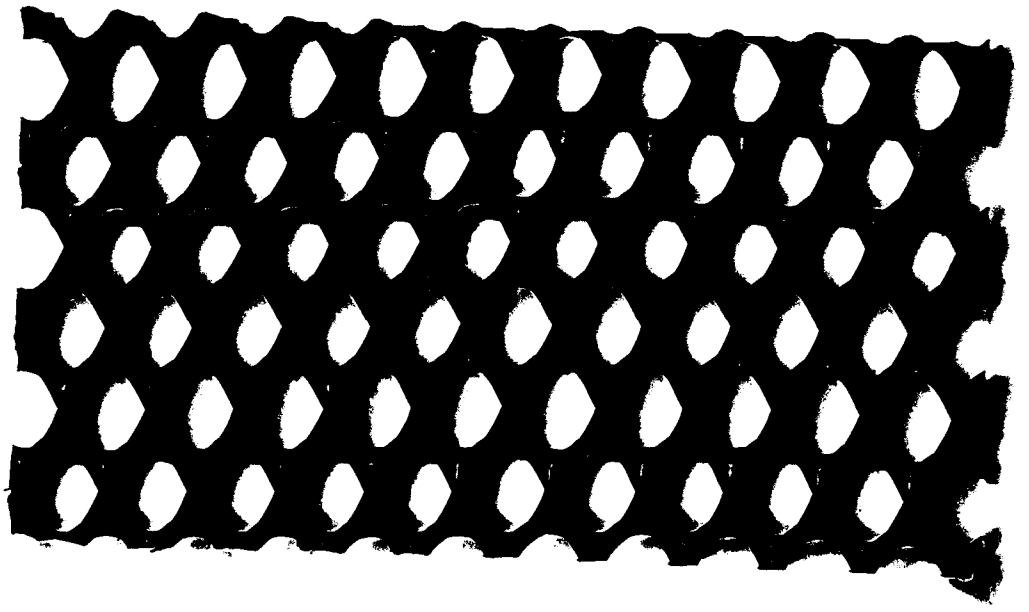

5.2 mm MDPE Geonet

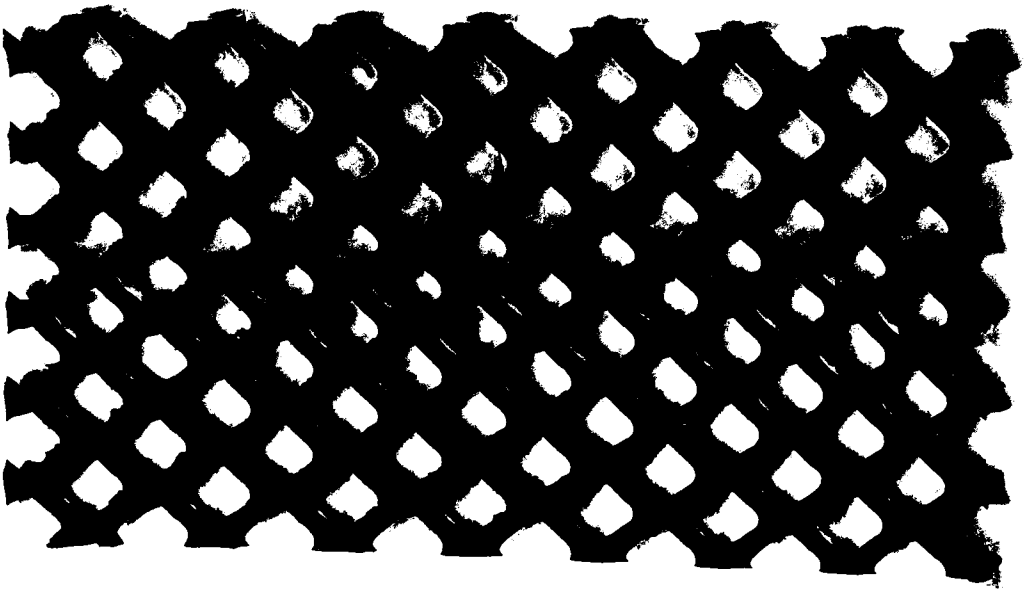

5.6 mm LDPE Geonet

Figure 3.9b Geometry of the Geonets

The aluminum plates were used to perform a test with rigid boundaries as described in ASTM D4716-87; the plates were 1.2 mm thick and had a smooth surface.

3.4.2 Testing Program

The testing program is subdivided in two series; the first is series water or W and the second is series water-leachate control or WLC. Both series of tests were run using regular tap water spiked with an algaecide to prevent growth. The tests were also run concurrently.

Series W constitutes the main body of tests. Each geonet was tested with all eight geomembranes and with the aluminum plates for a total of thirty-two separate geosynthetic combinations and four metal plate control tests. For each test, the normal stress applied to the geonet/geomembrane test specimens was 25 kPa, 100 kPa, 200 kPa, 300 kPa, and 400 kPa for a period of 24 hours at each stress level. Note that 400 kPa is close to the compressive strength of the LDPE geonet. These stress levels were chosen because of the stress levels encountered in the literature review; the maximum expected stress indicated is about 400 kPa. The lower stresses are included because they represent the operating stress. At each stress level, the volumetric flow rate per unit width (Q/w) was measured at hydraulic gradients (i) of 0.02, 0.04, 0.06, 0.08, and 0.10 . The gradient was changed from lowest to highest (termed one gradient cycle) at four separate times during each applied stress level. The cycles were initiated at 0.25 hours, 2 hours, 7 hours and 23 hours after application of the stress increment and required 1 hr to complete. The gradient was reset to 0.02 at the end of each cycle. These gradients were chosen because most landfills have a bottom gradient between 2%-4% (likely to meet minimum regulatory requirements); gradients up to 10% were chosen in the event that higher gradients are used. Hence, the influence of material, normal stress, and hydraulic gradient on the flow rate or in-plane hydraulic conductivity of a geonet may be examined from this series of tests.

Test series WLC was conducted for two purposes; first, it was necessary to provide a control for the companion series L (leachate) tests which were performed to determine the influence of chemical and biological activity on flow rate (Noyon, 1993). The L series of tests were performed at a constant normal stress of 300 kPa and hydraulic gradient of 0.02, using leachate rather than water as the permeant, and continued for 4 to 14 days depending on the flow

Table 3.2a. Properties of the Geonets (after Specifier's Guide, 1992).

Manufacturer	Product Name	Polymer	Rib Structure	Thickness [1] (mm)	Crush Strength[2] (kPa)	Transmiss-ivity[3] (m^2/s)
National Seal Company	Poly-Net PN 3000	HDPE	solid	5.1	Not Available	0.0045
Tensar Corp.	NS 1410	HDPE	solid	5.2	896	0.0048
Tensar Corp.	NS 1405	MDPE	solid	5.2	689	0.0042
Tensar Corp.	NS 1100	LDPE	foamed	5.6	482	0.0045

Table 3.2b. Properties of the Geomembranes (after Specifier's Guide, 1992).

Manufacturer	Product Name	Polymer	Thickness[4] (mm)	Texture	Specific Gravity[5]	Puncture Resistance[6] (kN)
National Seal Company	Friction Seal HD	HDPE	1.52	textured	0.94	0.35
Columbia Geosystems Inc.	HDPE 40 mil	HDPE	1.02	smooth	0.94	0.25
Columbia Geosystems Inc.	HDPE 60 mil	HDPE	1.52	smooth	0.94	0.36
Columbia Geosystems Inc.	40 mil VLDPE	VLDPE	1.02	smooth	0.915	0.23
Columbia Geosystems Inc.	60 mil VLDPE	VLDPE	1.52	smooth	0.915	0.35
Canadian General Tower Ltd.	Geoliner 40	PVC	1.02	smooth	1.45	0.015
Canadian General Tower Ltd.	Geoliner 60	PVC	1.52	smooth	1.45	0.023
Akzo Industrial Systems Co.	Tuff-Ply 3060	PP[7]	1.57	smooth	0.945	0.37

Notes: 1-ASTM D1777, 2-ASTM D1621, 3-ASTM D4716-87 (i=0.1, P=100kPa), 4-ASTM D751, 5-ASTM D792, 6- ASTM 101C, 7-polypropylene alloy.

rates. Therefore, the series WLC tests were performed at the same stress level and gradient and for a period of either 5 days or 12 days. Second, these tests would provide some information on the time dependency or creep behavior of the geonet/geomembrane composite test specimen and its influence on flow rate.

In an attempt to understand some of the physical aspects of flow in the geonet/geomembrane system, two sedimentation tests were incorporated into the series W tests using a fine to medium sand that passed the #60 sieve (0.246 mm) and was retained on the #100 sieve (0.147 mm) (U.S. Bureau of Standards series). These tests were conducted at the conclusion of a series W test using one smooth geomembrane (Tuff-ply 3060) and the textured geomembrane (Friction Seal HD) with all geonets except the LDPE specimen.

4. TEST RESULTS

Results of the series W and WLC are reported with respect to the variation of flow rate with pressure and hydraulic gradient. A description of the results addresses the response of the types of geomembranes and geonets. Initial comments are made on the repeatability of the test devices.

4.1 REPEATABILITY

Preliminary tests were performed at a constant pressure of 150 kPa to check the repeatability of the four test devices using an Amaco DN3 geonet and a 30 mil thick PVC geomembrane as dummy specimens. The geonet samples were randomly cut for the initial trial runs; the measured flow rate of these samples varied by up to 300% because of the orientation of the flow channels. The maximum variation of 300% was for samples cut at right angles; samples cut at other angles varied less. Several tests were then performed using geonet samples cut with the same orientation; this resulted in a more consistent measured flow rate. Hence, it was **necessary to cut the test specimens in the same orientation** and all subsequent specimens were cut using the procedure described in section 3.3.1. Measurements of flow rate were taken for hydraulic gradients of 0.02 to 0.10 and at 0.5, 2, 5, 26, 48, and 96 hrs. after the start of the test.

Results of the tests, see Fig. 4.1, indicate generally good agreement between the devices. All of the curves exhibit the same shape: there is a rapid decrease in flow rate with time during the early part of the test followed by a more gradual decrease thereafter. A variation of 7% from the mean is observed for the initial flow rates at a 0.02 gradient and 11% from the mean at a 0.10 gradient which does not change significantly with time. Variations in flow rate are attributed to calibration of the tipping gauges, geonet specimens not being identical, setting of the gradients, and setting of the pressure and represents the tolerance of repeatability.

In addition to the repeatability tests described above, three repeatability tests were performed on materials of the main test program using series W test conditions (Fig. 4.2 to 4.4) and one test using series WLC test conditions (Fig. 4.5). Typically, the absolute magnitudes of

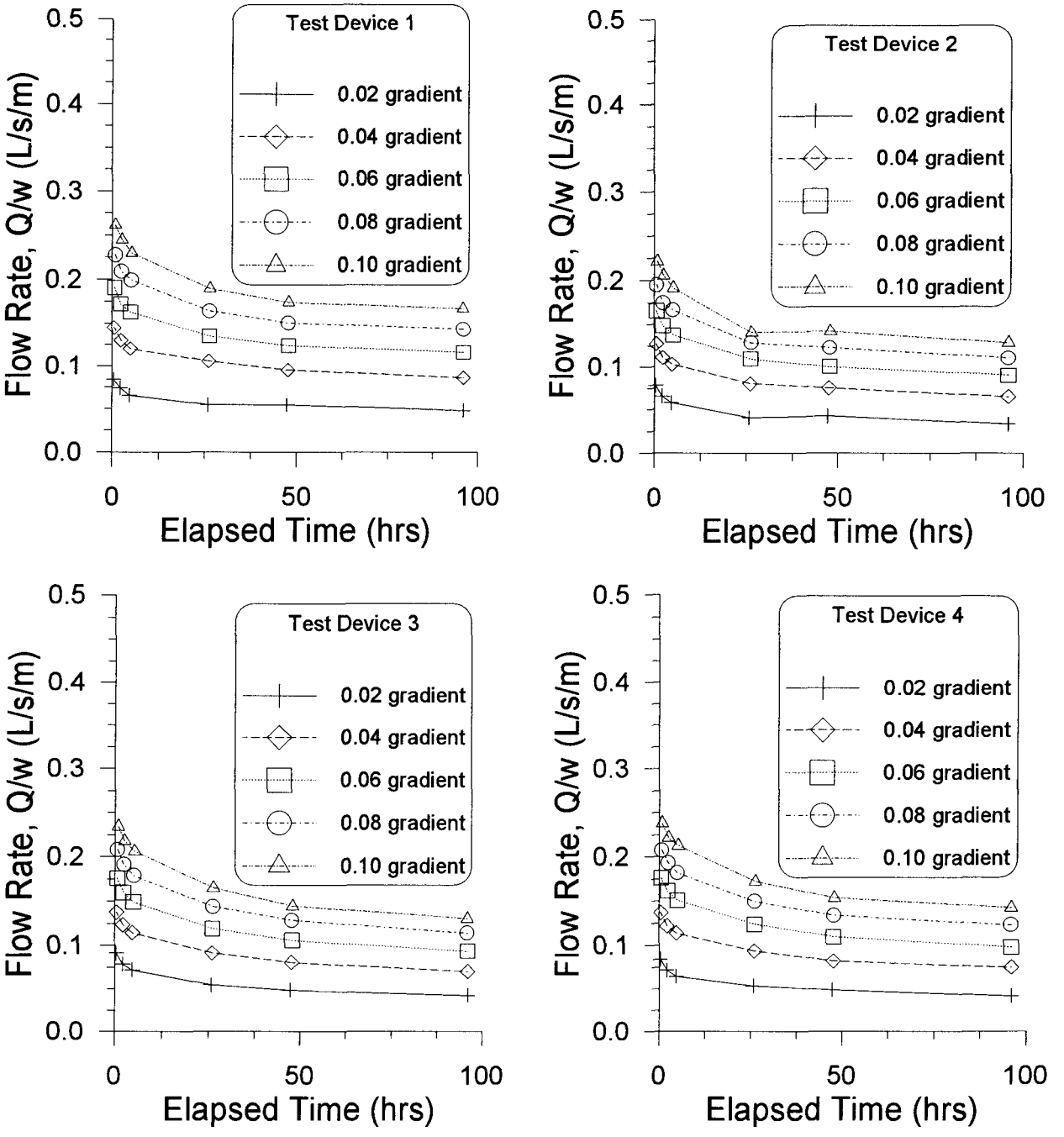

Figure 4.1 Repeatability Tests Using Amaco DN3 Geonet and 30 mil PVC Geomembrane at 150 kPa Pressure

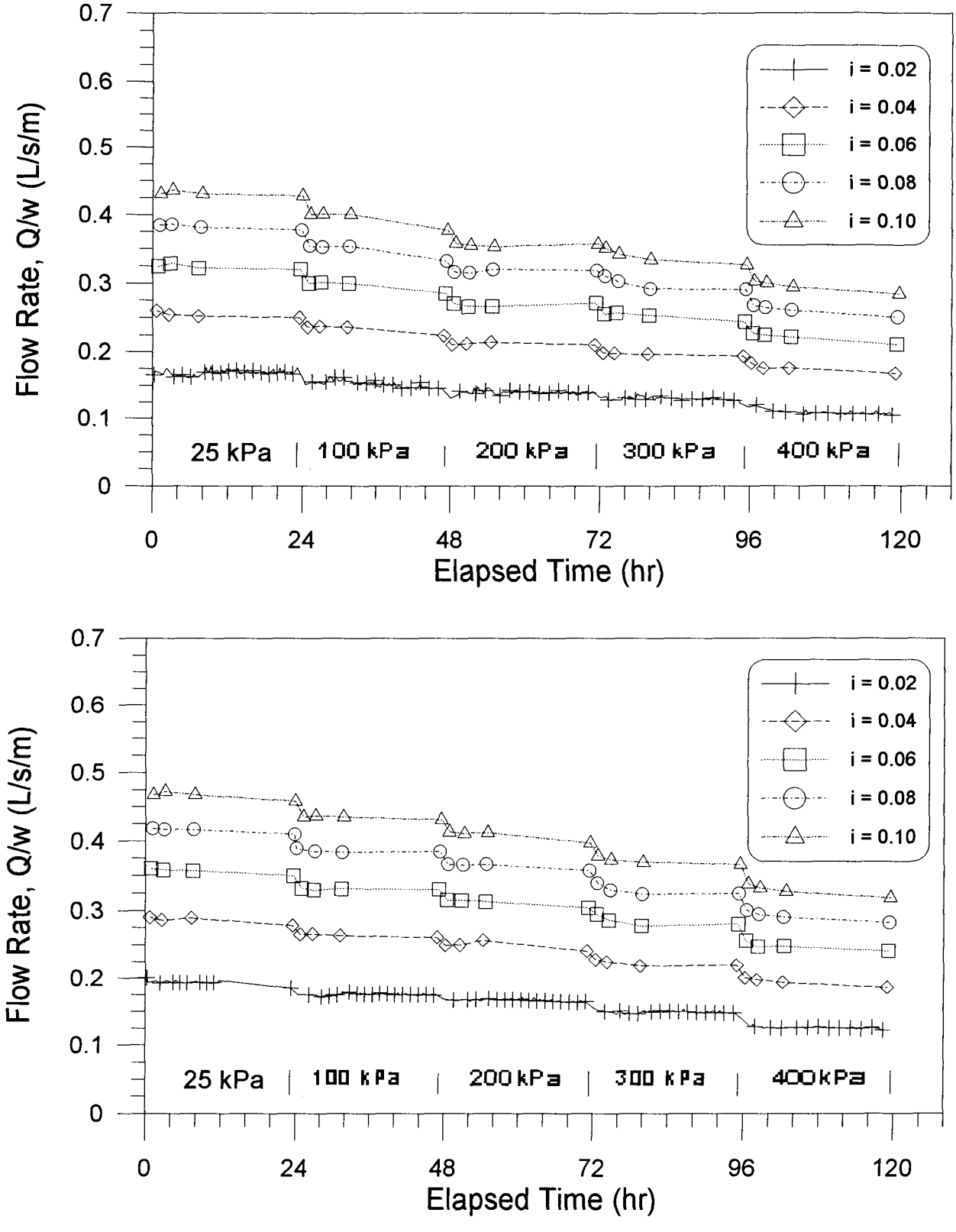

Figure 4.2 Repeatability Test Using Smooth 40 mil HDPE Geomembrane and 5.1 mm HDPE Geonet

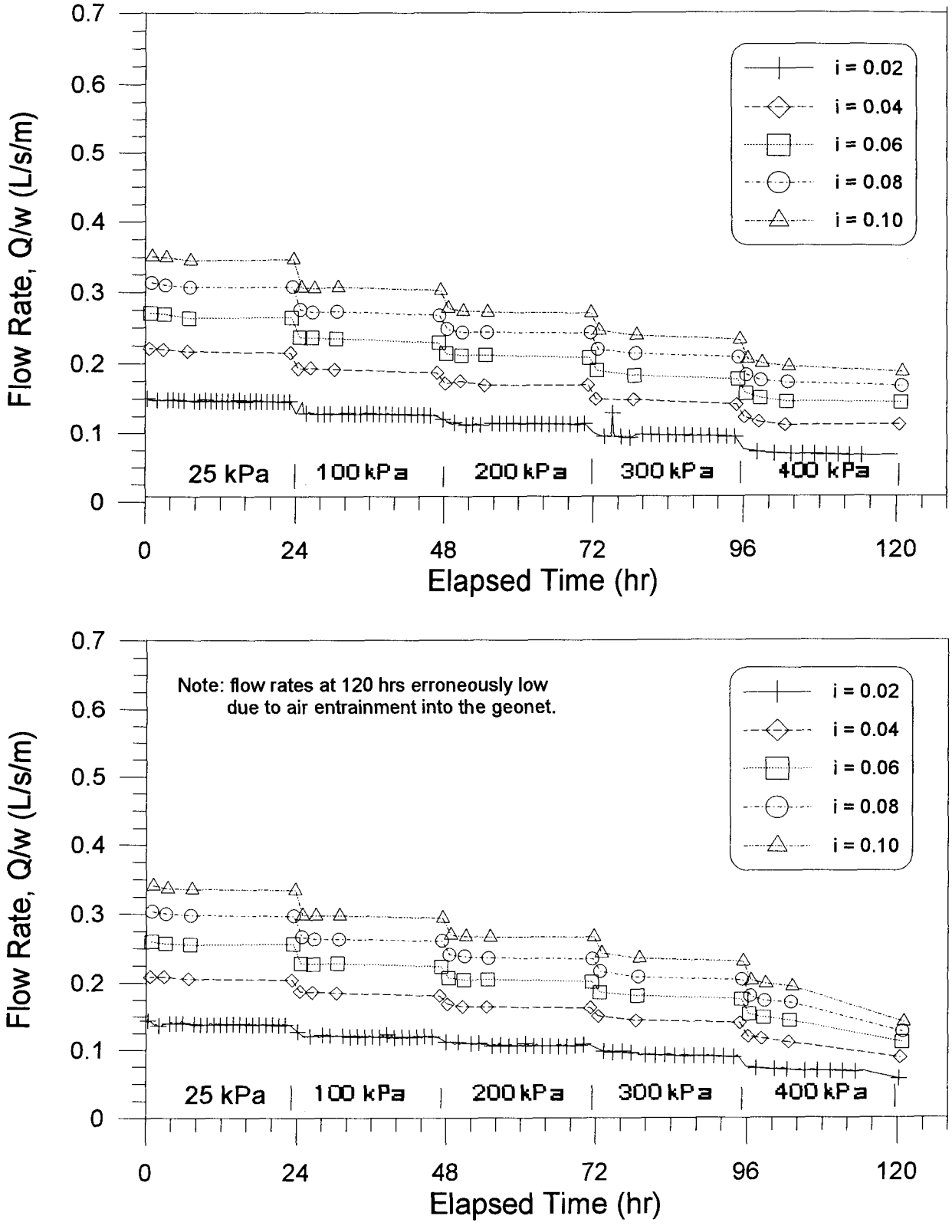

Figue 4.3 Repeatability Test Using Smooth 40 mil LDPE Geomembrane and 5.2 mm HDPE Geonet

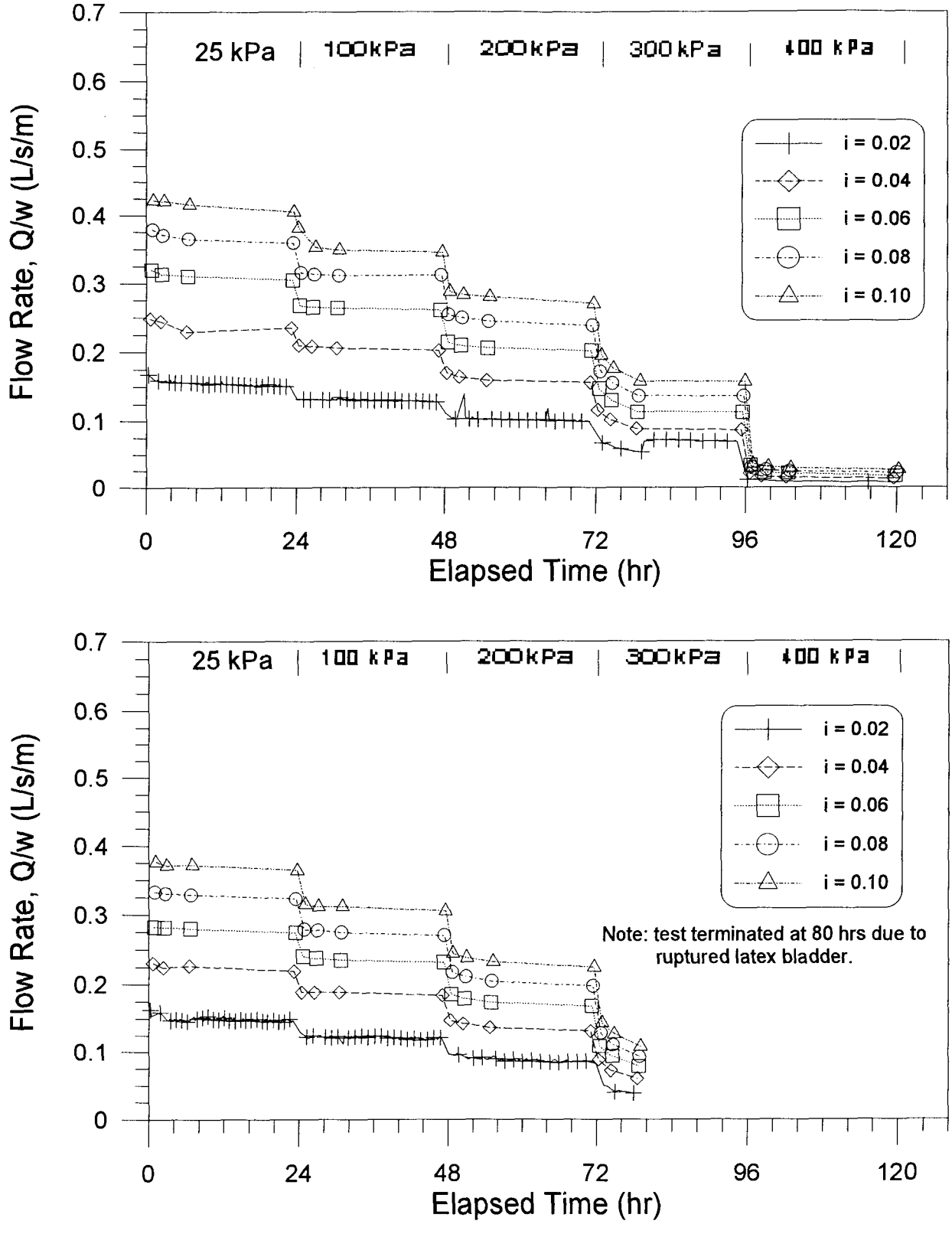

Figure 4.4 Repeatability Test Using Smooth 40 mil HDPE Geomembrane and 5.6 mm LDPE Geonet

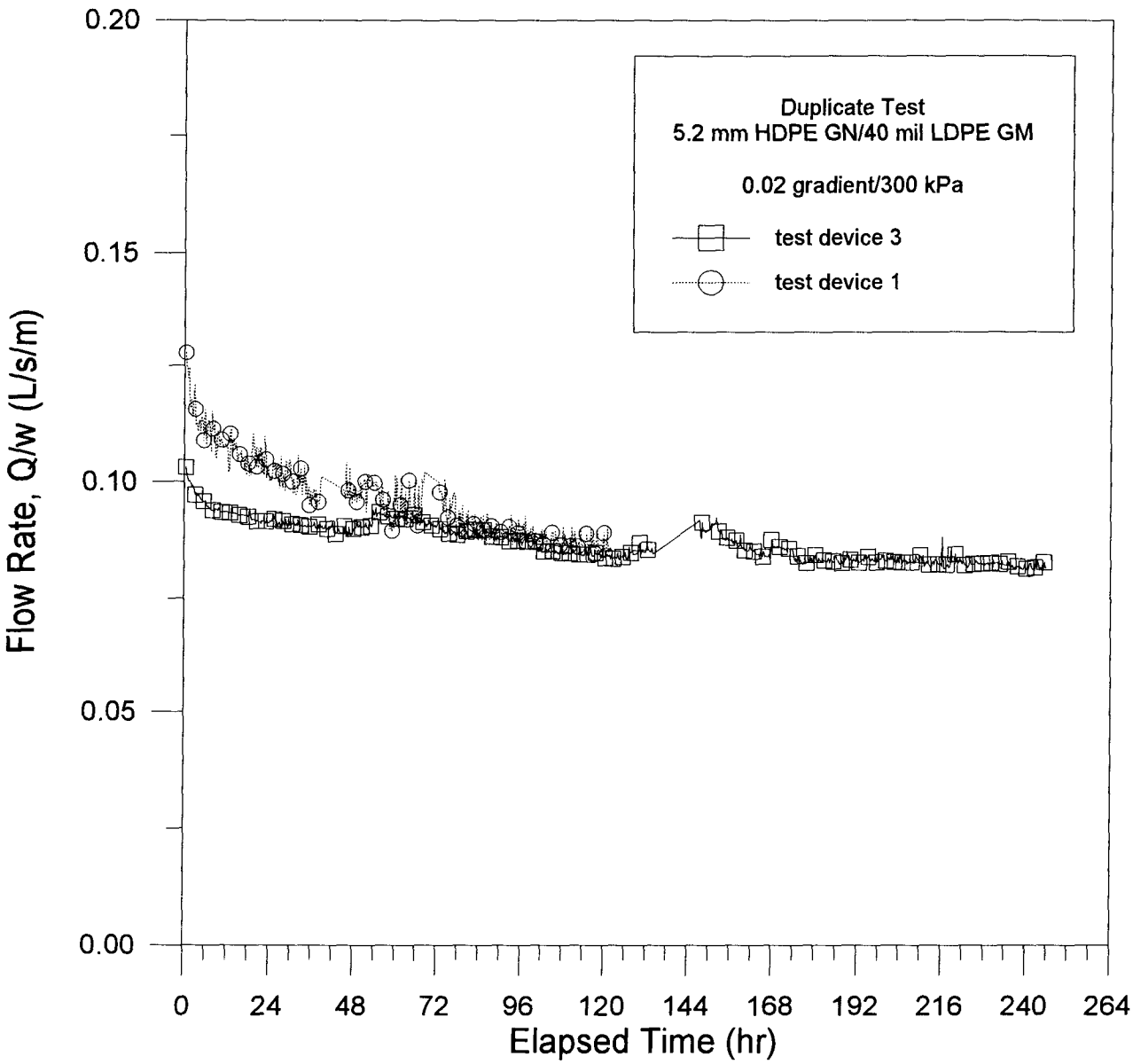

Figure 4.5 Repeatability Test for Series WLC

flow rate in the series W tests vary by less than 5% from the mean which is within the tolerance of repeatability. The relative variation of flow rate with time and pressure shows excellent agreement. Further, there is good repeatability observed in the change of flow rate with increased hydraulic gradient.

The repeatability tests performed using the series WLC test conditions, see Fig. 4.5, were run for a the standard period of 120 hrs and an extended period of 248 hrs. The extended test has a small gap where there are no data as a result of a ruptured latex bladder which had to be replaced. The seating time required before the flow rate returned to the value prior to the rupture was approximately 12 hrs. The initial flow rates (at 0.5 hours) for the two tests vary by approximately 10% from the mean which is within the bounds of repeatability. Even though both tests had different initial flow rates, they reach the same flow rate at about 80 hours after which they are essentially identical. Consequently, the initial difference cannot be attributed to variations in the specimens or imposed pressure; gradient may be a contributing factor because it was periodically reset during testing. It is felt these curves represent reasonable repeatability.

4.2 SERIES W

4.2.1 Smooth Geomembrane Combinations

The smooth geomembrane combinations produced three different relationships between flow rate and time over the range of pressures: termed linear, concave-down and concave-up. A linear response is one in which the decrease in flow rate is the same for each increment of pressure, see Fig. 4.6. A concave-down curve describes larger decreases in flow rate for successive pressure increments (Fig. 4.7) and concave-up describes smaller decreases in the flow rate for successive pressure increases (Fig. 4.8). The fluctuation of the flow rate at a gradient of 0.02 in Fig. 4.7 are attributed to the variation of inflow rate (see section 3.4.3) which indicates the sensitivity of testing at a low gradient of 2%.

Results of the series W tests for the smooth geomembranes and each type of geonet are summarized in Fig. 4.9 to 4.12 with reference to a gradient of 0.06. The response of this gradient is considered to be characteristic and the presentation facilitates comparison of the

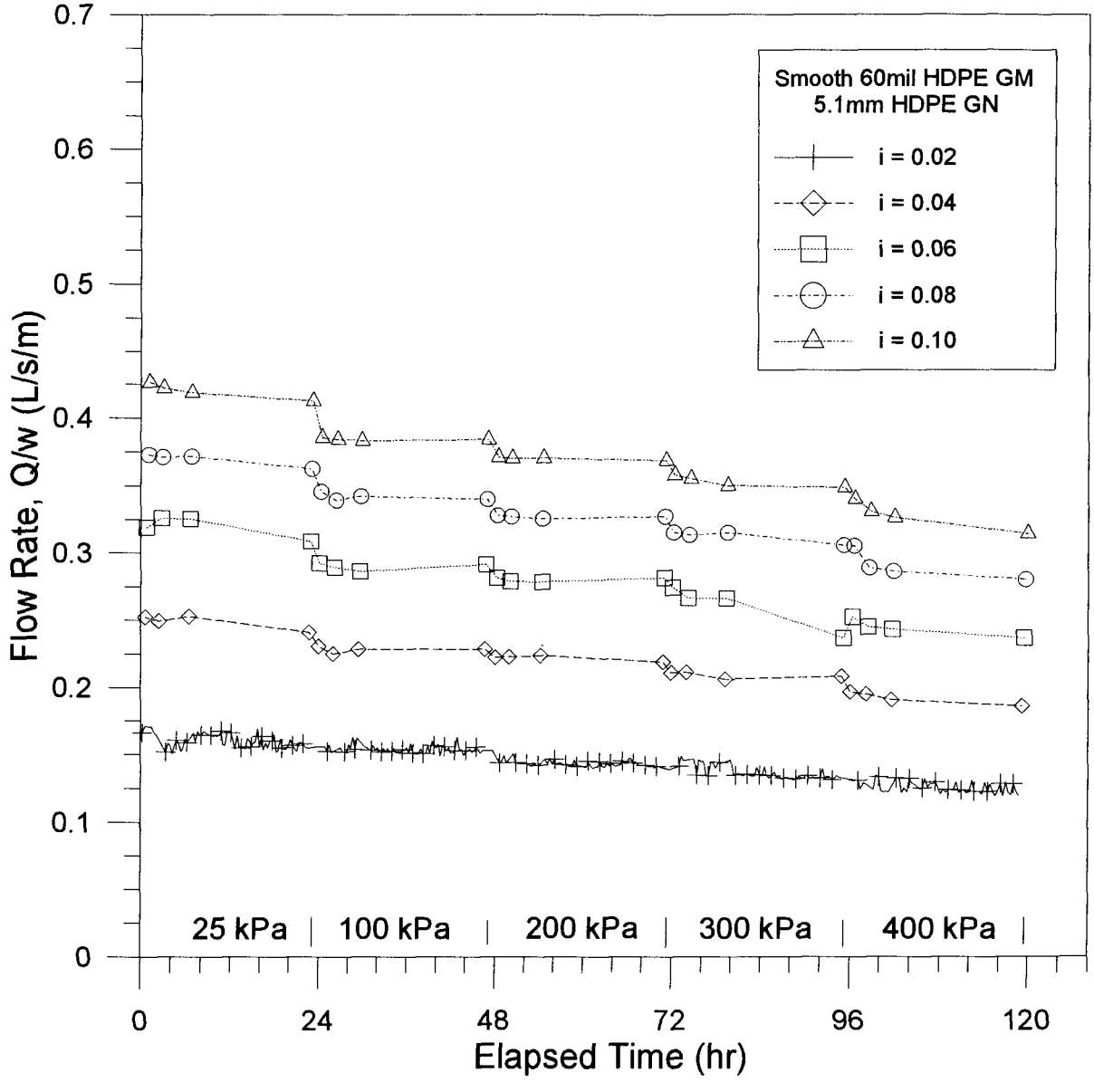

Figure 4.6 Typical Linear Results of Series W Tests

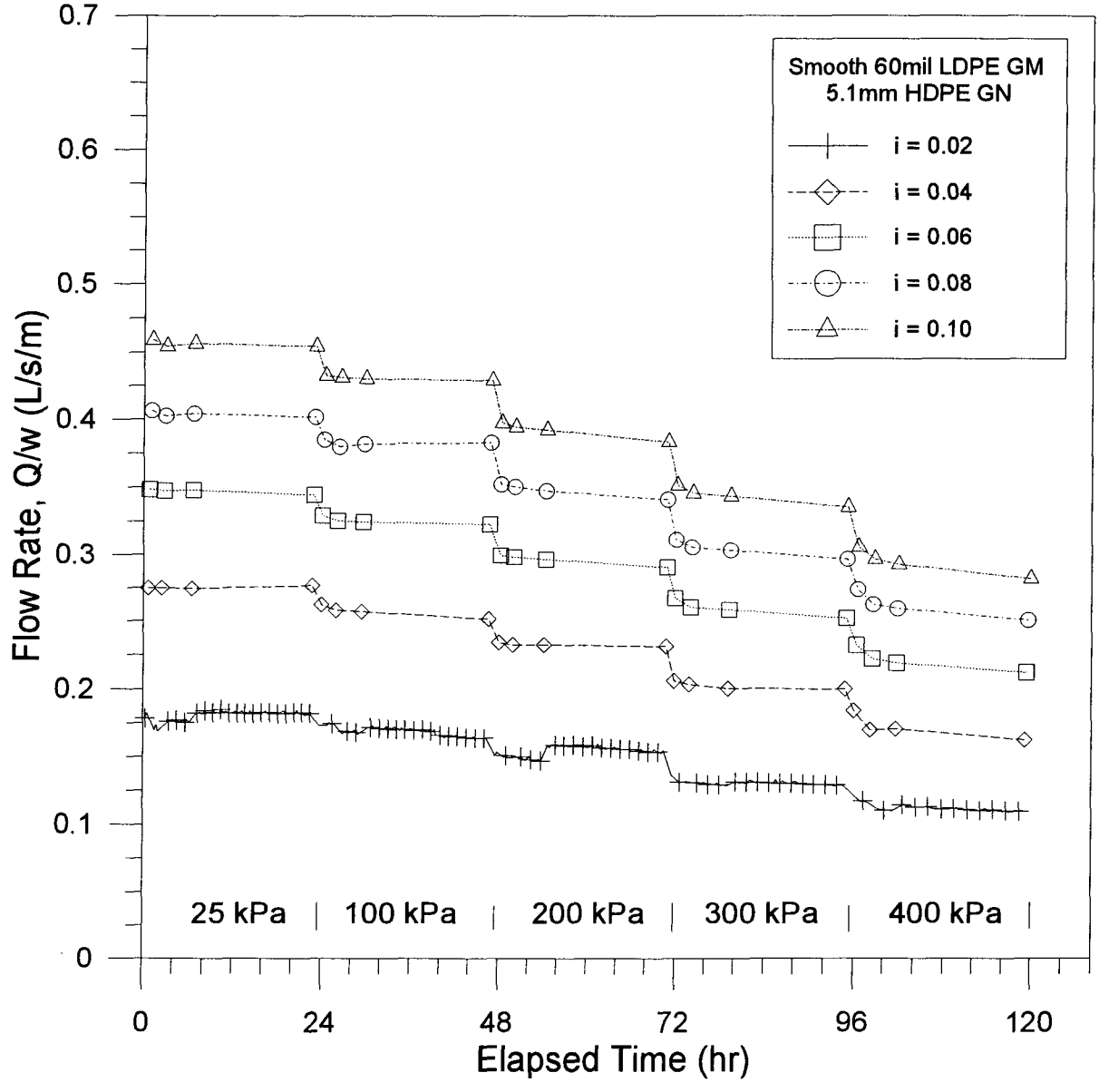

Figure 4.7 Typical Concave-Down Results of Series W Tests

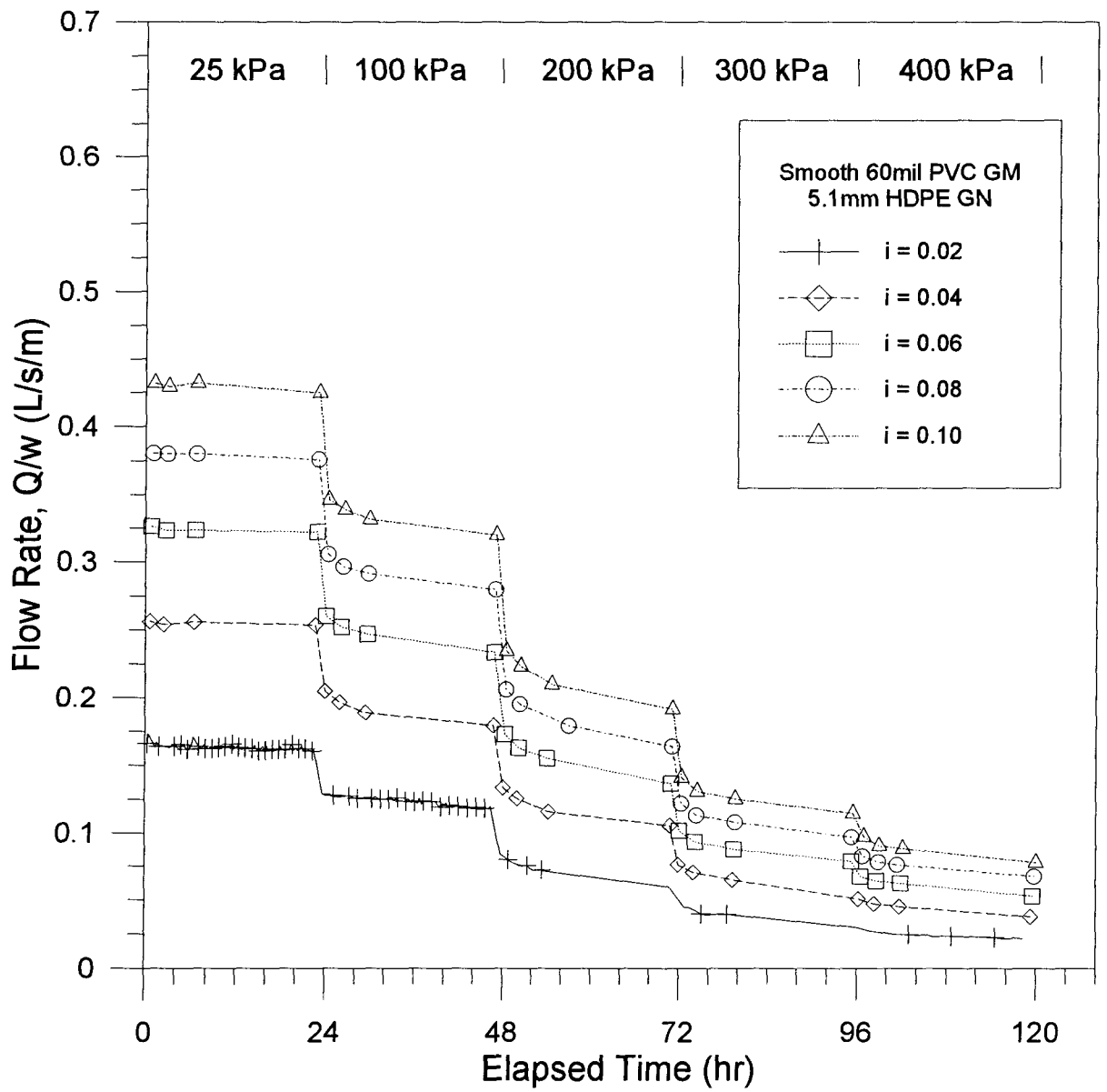

Figure 4.8 Typical Concave-Up Results of Series W Tests

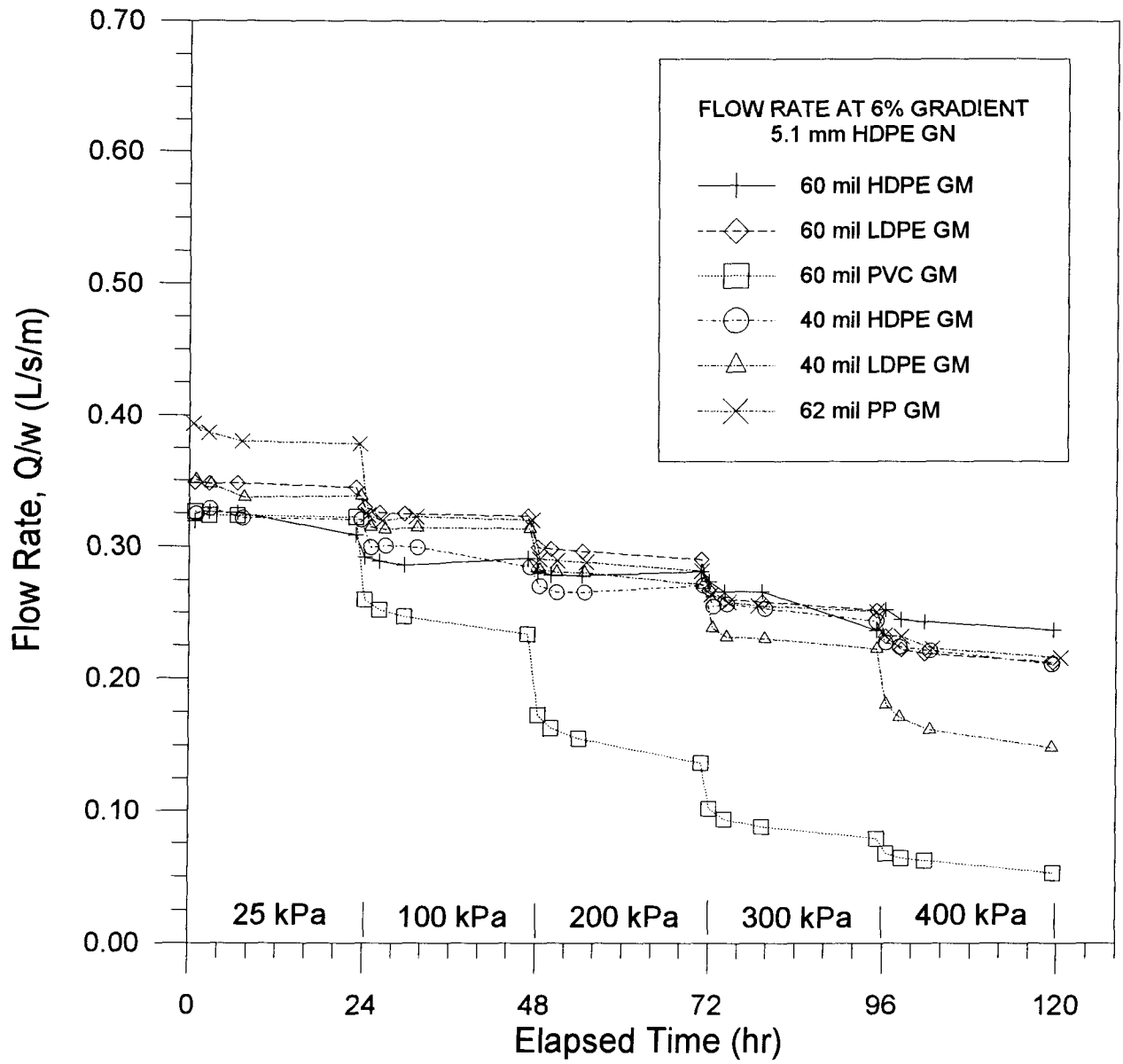

Figure 4.9 Results of 5.1 mm HDPE Geonet Combinations

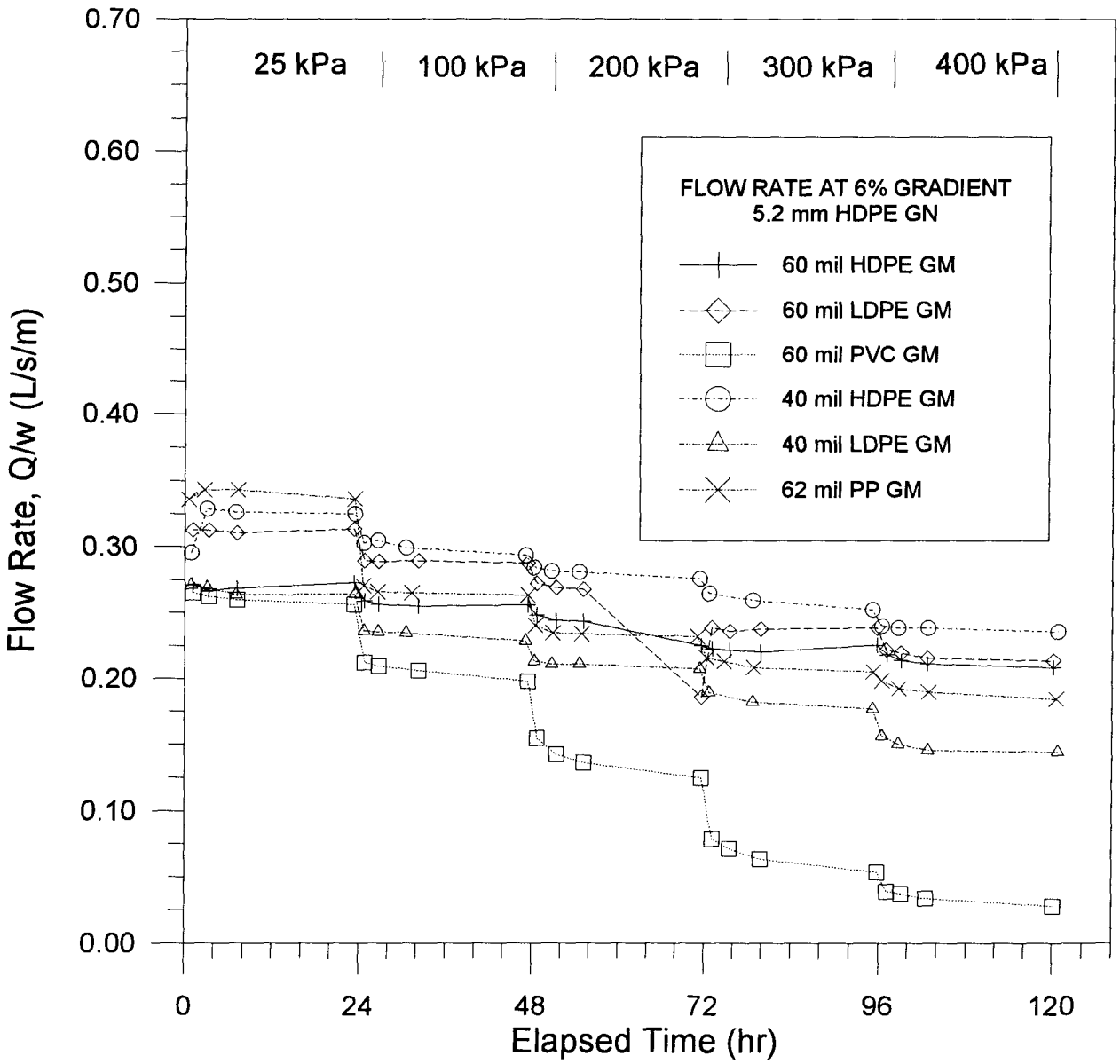

Figure 4.10 Results of 5.2 mm HDPE Geonet Combinations

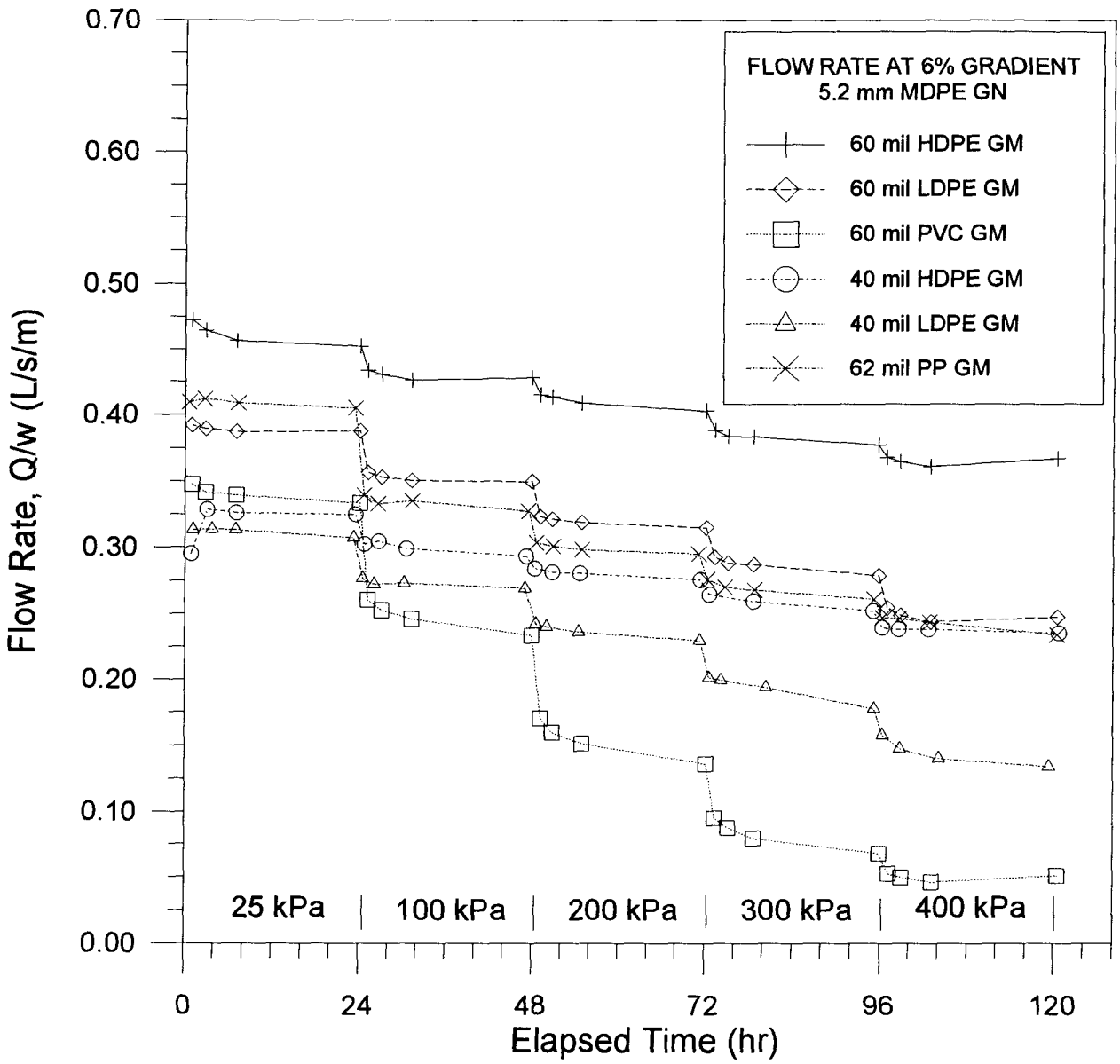

Figure 4.11 Results of 5.2 mm MDPE Geonet Combinations

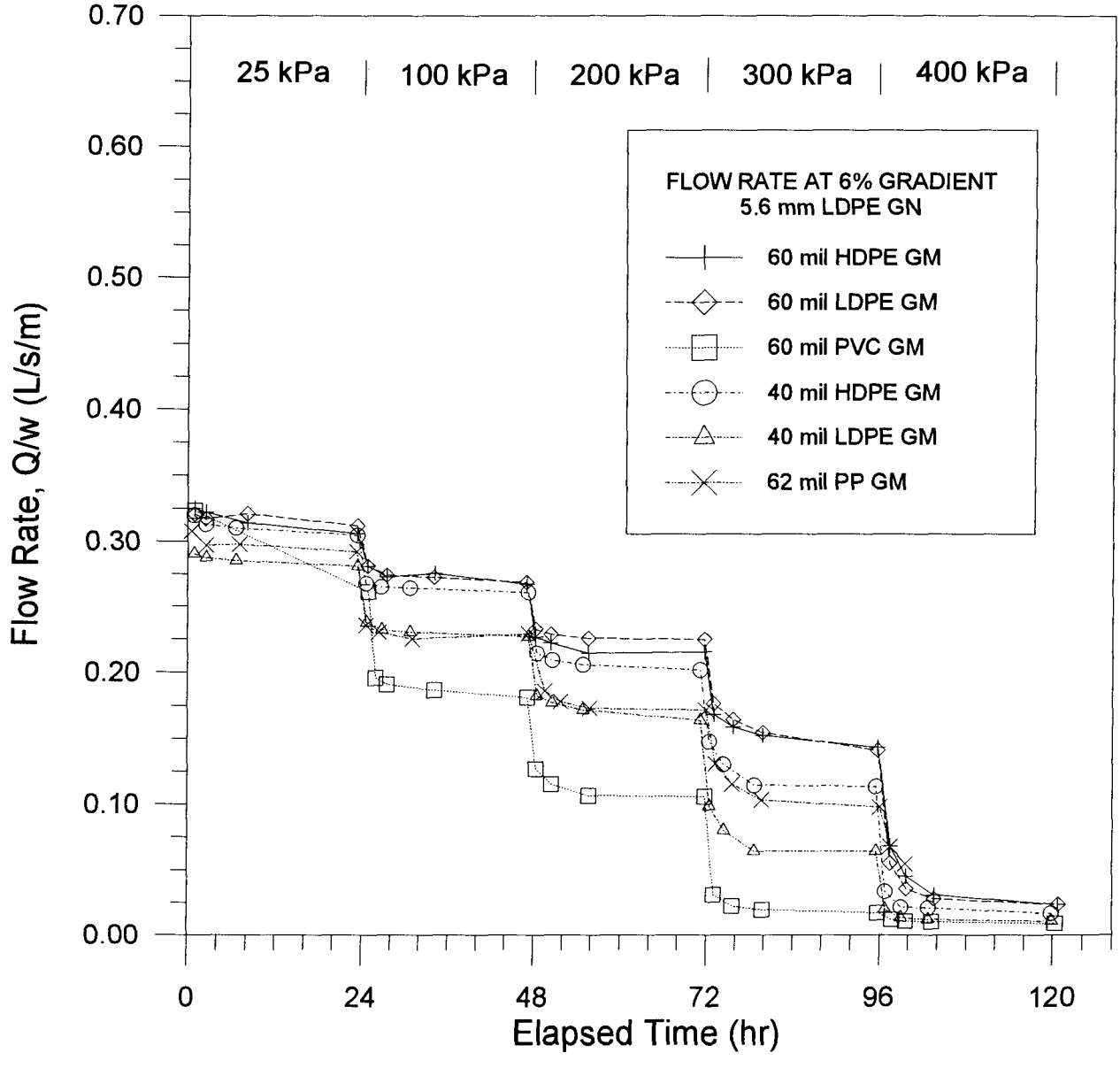

Figure 4.12 Results of 5.6 mm LDPE Geonet Combinations

geomembranes and a cross comparison of the geonet/geomembrane combinations. Generally, the behavior follows the three shapes described above for all of the geomembrane combinations with the linear shape being the most common. A concave-up response is exhibited by the 60 mil PVC geomembrane for all geonets except the 5.6 LDPE geonet and a concave-down response is shown by the 40 mil LDPE geomembrane in combination with the 5.1 mm HDPE and 5.2 mm MDPE geonets. The geomembrane combinations with the 5.6 mm LDPE geonet are generally concave-down; the 40 mil LDPE and 60 mil PVC deviate from a complete concave-down response as the flow rate decreases to near zero. This geonet has a different response compared to the other three geonets which have similar responses; the other three differ by the variation of the absolute magnitudes in flow rate. The 5.6 mm LDPE geonet exhibits larger decreases in flow rate with each pressure increase compared to the other geonets. It is clear that the 5.6 mm LDPE geonet and the 60 mil PVC respond differently than the other geonets and geomembranes, respectively; this different behavior is attributed to the physical properties of the geonets and geomembranes and will be examined in detail in section 5.

4.2.2 Textured Geomembrane Combinations

One textured geomembrane was used in the test program; results for this geomembrane and the four geonets are plotted on Figure 4.13 which can be compared directly with those on Figures 4.9 to 4.12. The curves exhibit the same general shape as the smooth 60 mil HDPE geomembrane, but the magnitude of the flow rates are different. The textured geomembranes typically have a higher initial flow rate and a lower final flow rate than their smooth counterparts which results in larger overall decreases in flow rate. This overall larger decrease in flow rate is attributed to the large drop that occurs when the pressure is increased to 100 kPa; all combinations experience a decease in the flow rate of about 0.75 L/s/m. This decrease in magnitude is not shown by the comparable smooth geomembrane combinations at the onset of 100 kPa pressure, see Figures 4.9 to 4.12, and is attributed to proper seating of the geomembrane. At 100 kPa, the pressure is sufficient to push the small ridges of the textured surface of the geomembrane into the apertures of the geonet which reduces the cross-sectional

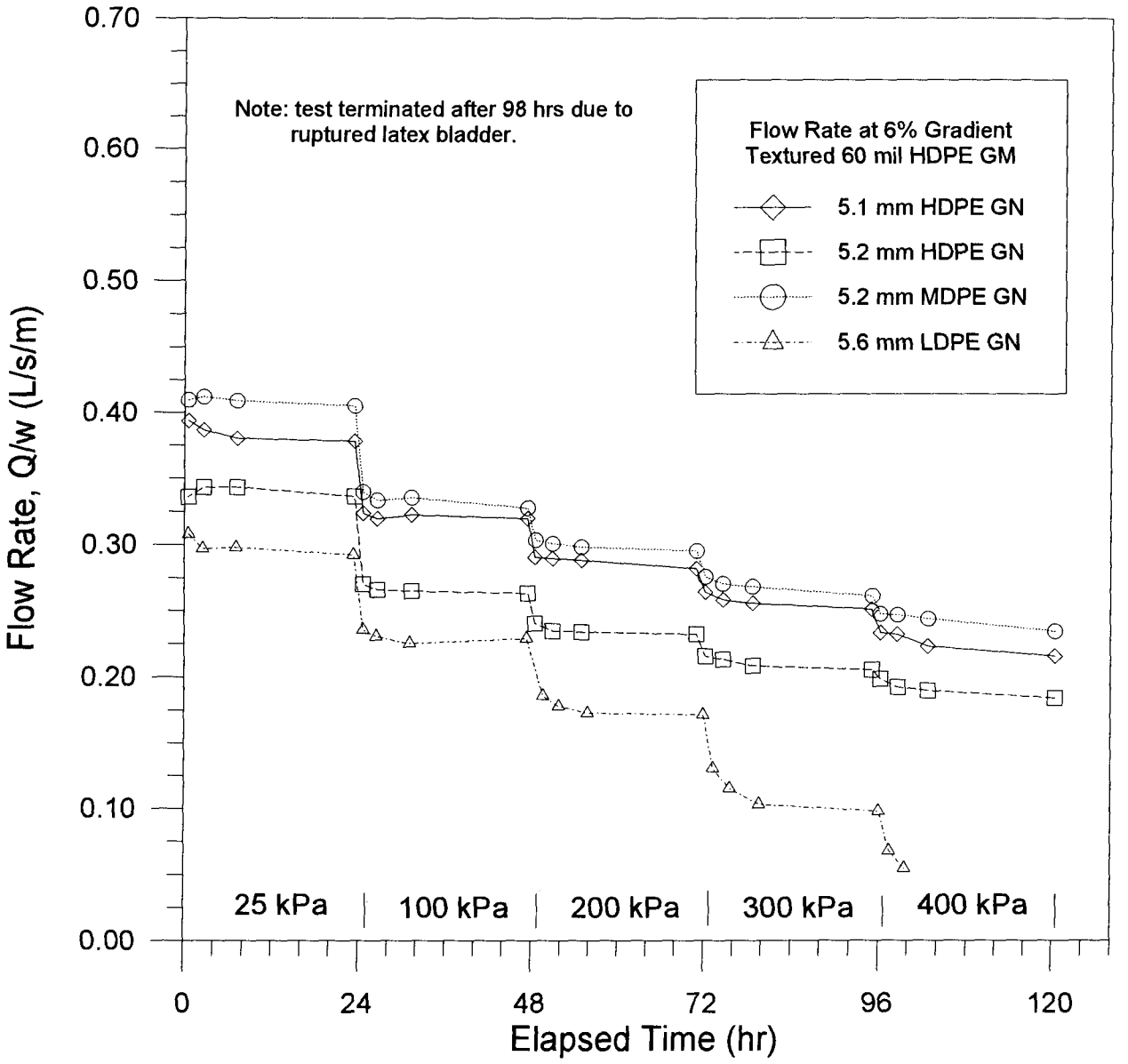

Figure 4.13 Results of Textured 60 mil Geomembrane Combinations

area available for flow.

4.2.3 Metal Plate Combinations

Metal plates were incorporated into the test program to evaluate the relative importance of creep of the geonets and intrusion of the adjacent construction materials. The 1.2 mm thick aluminum plates act as rigid sheets, hence, any reduction in flow rate in these tests can be attributed solely to creep of the geonets.

Three of the curves in Fig. 4.14 have a linear shape while the fourth (5.6 mm LDPE geonet) exhibits a concave-down curve. The general trend of the curves is similar to that of the smooth geomembrane combinations in that the flow rates decrease with time and pressure. However, the magnitude of the decrease in flow rate over each 24 hour period and at the onset of a higher pressure is smaller except for the 5.6 mm LDPE geonet which exhibits a nearly identical decrease in flow rate as the smooth geomembrane combinations. The initial flow rates of the metal plate tests compare favourably with the initial flow rates of the 60 mil HDPE geomembrane (the most rigid of the smooth geomembranes) for the same geonet. These results provide more confidence that very good repeatability is achieved (only the initial flow rates can be compared because the metal plates are rigid and do not intrude into the apertures of the geonet whereas geomembranes can intrude).

Since the boundary conditions of these metal plate tests are similar to those of the standard test method used by manufacturers, it is possible to compare the transmissivity values obtained in this study with those reported in the technical literature. Transmissivity values of the geonets using the ASTM/CGSB standard, see Table 3.2a, are reported for a confining stress of 100 kPa after a seating period of 15 minutes. From Fig. 4.14, the corresponding initial flow rate at 100 kPa for the geonets range from 0.265 L/s/m to 0.410 L/s/m (the earliest measured rate is used to match the short seating period used for the standard test); these volumetric flow rates are converted to transmissivity values by normalizing with respect to the hydraulic gradient of 0.06 (and converting 1 L to 10^{-3} m), see Table 4.1. The transmissivity values from the metal plate tests show reasonable agreement with those reported by the manaufacturers. Generally, the values from the Specifier's Guide are slightly lower and one possible reason is the testing was

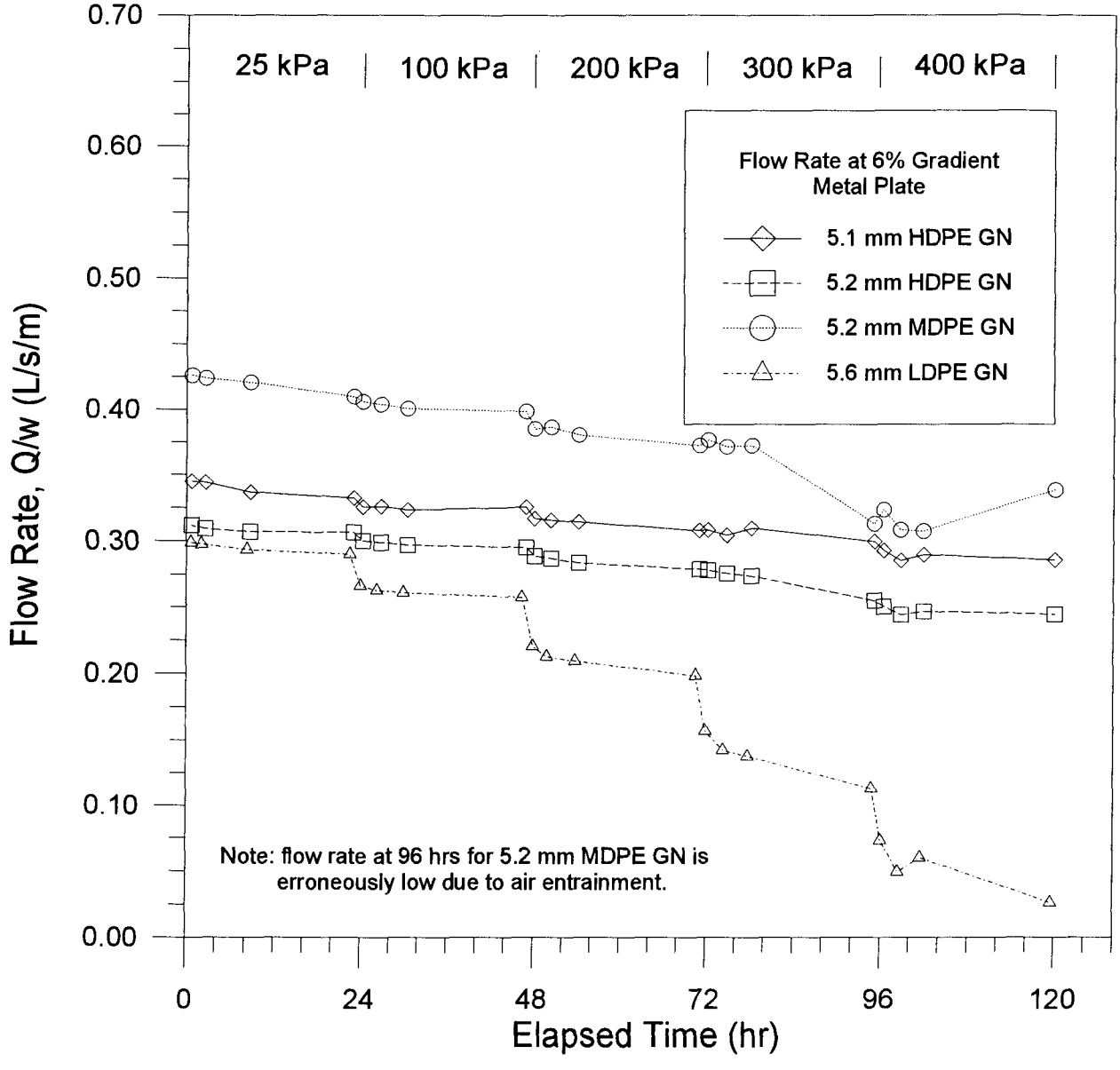

Figure 4.14 Results of Metal Plate Combinations

performed at a hydraulic gradient of 0.10; even though higher gradients result in higher flow rates, transmissivity values may actually decrease when testing is done at high gradients because the flow rate is normalized by the gradient (see equation 1).

Table 4.1 Comparison of Transmissivity Values

	UBC tests with metal plate		Manufacturers' data[1]
	Volumetric Flow Rate	Transmissivity (i =0.06)	Transmissivity (i = 0.10)
Geonet	(L/s/m)	(m2/s)	(m2/s)
5.6 mm LDPE	0.265	0.0044	0.0045
5.2 mm MDPE	0.410	0.0068	0.0042
5.2 mm HDPE	0.308	0.0051	0.0048
5.1 mm HDPE	0.325	0.0054	0.0045

1. from Specifier's Guide, 1992

4.2.4 Sediment Tests

As discussed in section 3.1, a small portion of the series W tests included sediment tests which were performed to examine flushing as a means of restoring flow lost to sediment clogging. The results of these tests will be presented here preceded by a brief description of the test materials and procedure.

Sediment testing was performed at the end of the series W tests with the 62 mil PP and the textured 60 mil HDPE geomembranes in combination with the 5.1 mm HDPE, 5.2 mm HDPE, and 5.2 mm MDPE geonets. The sand used was medium to fine grained, Alouette River Sand; more specifically, the grain size was between 0.25 mm (U.S. Bureau Standard sieve # 60) and 0.149 mm (U.S. Bureau Standard sieve # 100). Approximately 25 cm^3 of this sand was placed into the inlet chamber and agitated to suspend the sand in solution so that the flowing water could carry it into the geonet. The sand then settled into the geonet when it was out of the

agitation zone which simulates escape of sediment through a hole in the primary geomembrane into the geonet underneath or simply sediment clogging in the field. The sediment causes a reduction in the flow rate. Attempts at restoring the flow rate to its original value were made by flushing at 0.06 and 0.10 gradient for a period of approximately 10 minutes at each gradient; after each gradient, the flow rate was measured to check the success of each attempt. The results of the sediment testing are summarized in Table 4.2.

Table 4.2 Results of Sediment Testing (confining pressure = 400 kPa)

	5.1 mm HDPE	5.2 mm HDPE	5.2 mm MDPE
62 mm PP Geomembrane			
Original flow rate @ 0.02 gradient (ml/s)	16.91	13.38	17.07
Sediment reduced flow rate (ml/s)	8.99	8.47	11.87
Percentage of original flow rate	53.2%	63.3%	69.5%
Flow rate after flushing @ 0.06 gradient (ml/s)	12.70	11.05	14.22
Percentage of original flow rate	75.1%	82.6%	83.3%
Flow rate after flushing @ 0.10 gradient (ml/s)	15.85	12.24	16.35
Percentage of original flow rate	93.7%	91.5%	95.8%
textured 60 mil HDPE Geomembrane			
Original flow rate @ 0.02 gradient (ml/s)	14.09	11.30	14.48
Sediment reduced flow rate (ml/s)	9.14	7.49	8.64
Percentage of original flow rate	64.9%	66.3%	59.7%
Flow rate after flushing @ 0.06 gradient (ml/s)	11.94	8.89	10.92
Percentage of original flow rate	84.7%	78.7%	75.4%
Flow rate after flushing @ 0.10 gradient (ml/s)	13.46	10.03	13.08
Percentage of original flow rate	95.5%	88.8%	90.3%

Comparison of the 62 mil PP geomembrane results after flushing at 0.06 gradient indicates similar success; the 5.1 mm HDPE percentage was likely lower only because the reduction due to sediment was greater. The similar success of each is verified from the results of flushing at a 0.10 gradient; the flow rates recovered up to 92%-96% of their original value. Note that the 5.2 mm HDPE geonet had the lowest recovery while the 5.2 mm MDPE geonet had the highest recovery; this is due to the orientation of the flow channels (see Figure 3.15). The 5.2 mm HDPE geonet has the largest angle with respect to straight flow through the sample or test device which makes it the least efficient with regards to flushing in the test device. In contrast, the 5.2 mm MDPE geonet has the smallest angle with respect to flow straight through which makes it the most efficient. Hence, the orientation of the flow channels is reflected in the recovery ratio. At the completion of the testing, the top geomembrane was removed to observe if any sand was still left in the geonet. All three geonets still had a considerable amount of sand trapped against the wall of the test device. The sand was unable to continue moving with the water along the flow channels because of the side walls; this is not a realistic situation in the field and the recovery rate likely should be even higher than the 92%-96% range in a field situation.

The sediment tests with the textured 60 mil HDPE geomembrane have similar results as the 62 mil PP geomembrane except the recovery rates are slightly lower for two of the geonets. After flushing at a 0.06 gradient, the recovery rate is between 75.4% to 84.7%, but two are below 80%. This is about 5% less than the 62 mm PP geomembrane and is attributed to the texturing of the geomembrane. The textured surface causes frictional losses which reduces the driving force of the flowing water. With the higher driving force at a 0.10 gradient, the recovery rate ranges from 88.8% to 95.5% which is only marginally less than the 62 mil PP geomembrane. Hence, the difference between the driving force at a 0.10 gradient between the smooth and textured geomembranes is smaller. Again, the top geomembrane was removed after testing to observe any sand left in the geonet. All three geonets had sand still trapped inside (approximately the same amount as the 62 mm PP geomembrane test), but this time, the sand was spread throughout the geonet. This behavior is different from the 62 mil PP combinations because of the textured surface of the geomembranes; the sand was getting trapped by the tiny

ridges that make the surface textured. The ridges are also likely responsible for changing the recovery rate which is partially controlled by the orientation of the flow channels; the ridges interfere with the regular flow of water through the flow channels and force the water to flow in a more random pattern depending on the placement of the ridges. Hence, the recovery rates for the textured 60 mil HDPE geomembranes do not follow the same order as those from the 62 mil geomembranes. Due to the textured surface of these geomembranes; higher driving forces (gradients) may not result in higher recovery rates because of more turbulence and frictional losses.

Based on these results, it appears that flow rates reduced as a result of physical clogging by sediments can be recovered from a flushing system. Of course, the tests were performed for only one type of soil and with few materials, but there is no reason to suspect much different behavior. These results should be verified by more testing.

4.3 SERIES WLC

The series WLC tests were performed for two purposes. They are control tests for the companion series L tests (Noyon 1993) and they provide information on the creep characteristics of the geonet and geomembrane combinations.

4.3.1 Smooth Geomembrane Combinations

The results of the smooth geomembrane and geonet combinations are presented in Figures 4.15 to 4.17. During testing, some tests did not have a data point recorded until after 0.25 hours; it is important to present the data from the same starting time for comparison; therefore, the time of 0.5 hours was chosen. This may have a considerable effect on the variation of the initial flow rates because the flow rates decrease the most during the early portion of the test as shown by the figures. Even with the variation of the initial flow rates, all of the data exhibit the same general shape; a rapid decrease at the start of the test followed by a more gradual decrease.

The shape of all the geomembranes for the 5.1 mm HDPE geonet, see Fig. 4.15, have nearly identical shapes except the 60 mil LDPE which flattens out earlier than the other three and

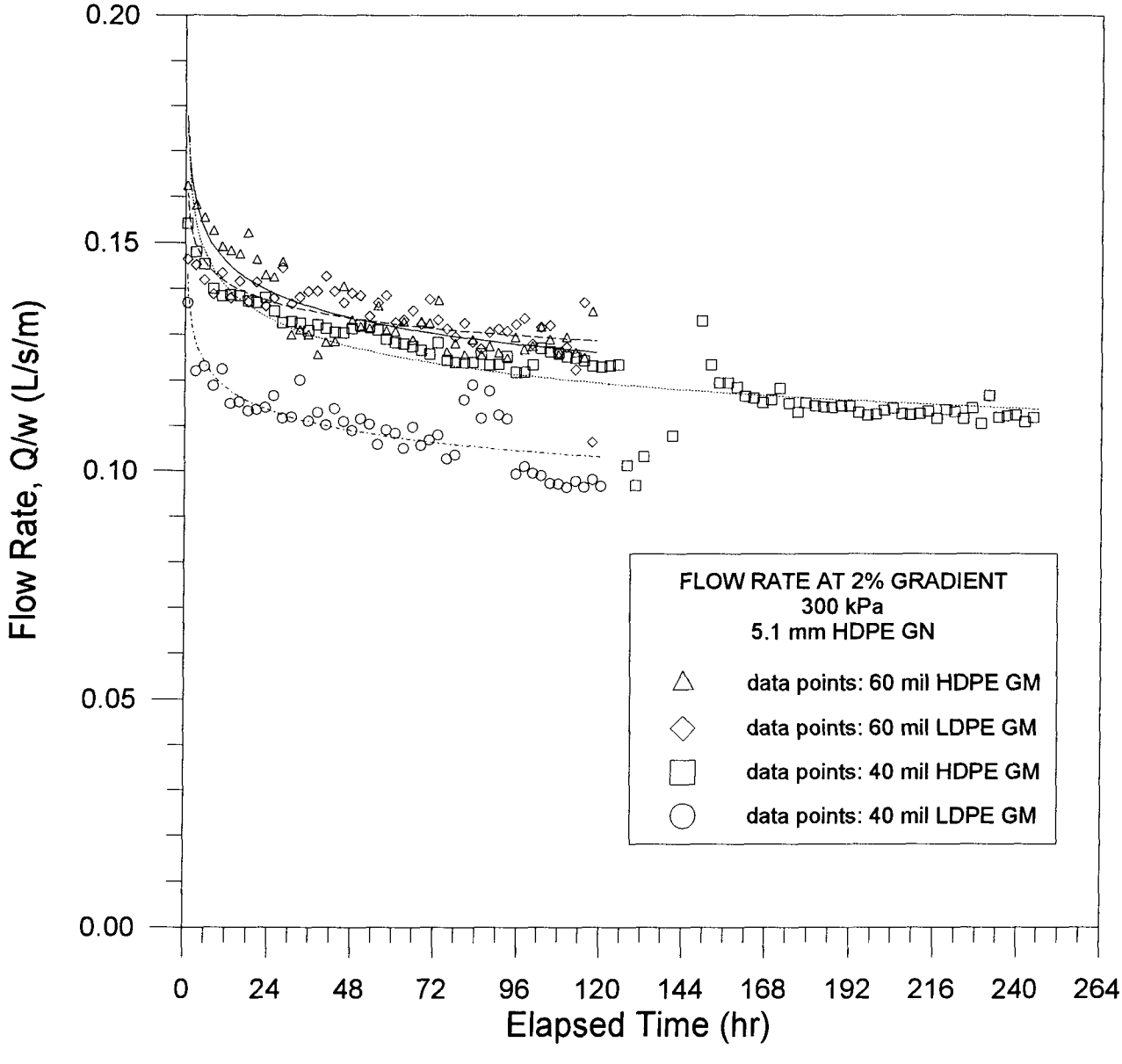

Figure 4.15 Series WLC Test Results of 5.1 mm HDPE Geonet

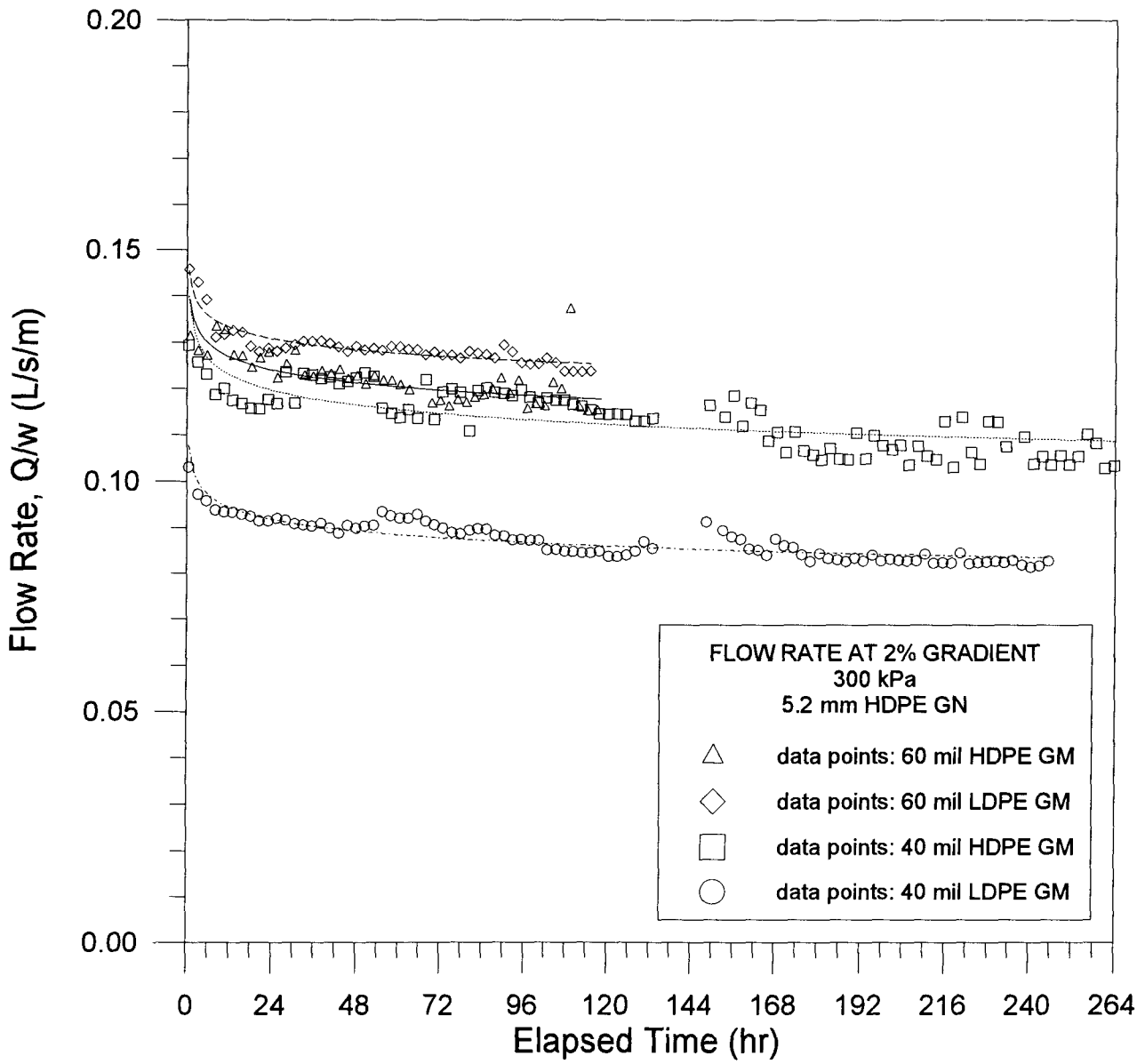

Figure 4.16 Series WLC Test Results of 5.2 mm HDPE Geonet

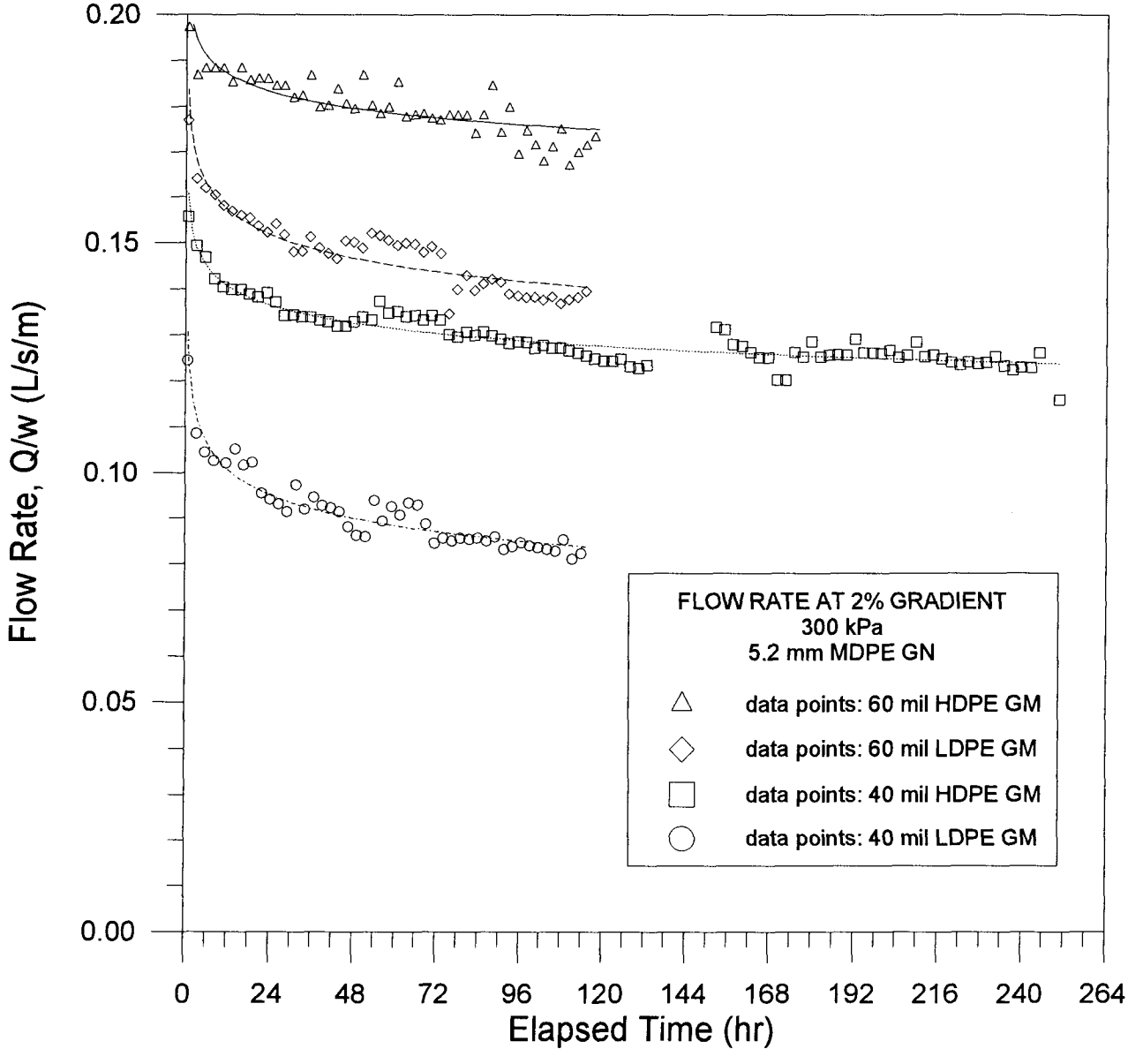

Figure 4.17 Series WLC Test Results of 5.2 mm MDPE Geonet

maintains a shallower slope over the duration of the test. The flow rates of the geomembrane combinations from highest to lowest are 60 mil HDPE, 60 mil LDPE, 40 mil HDPE, and 40 mil LDPE; the 60 mil LDPE eventually overtakes the 60 mil HDPE. The large change at about 128 hours for the 40 mil HDPE geomembrane was a result of a ruptured bladder. The bladder was replaced at about 144 hours, but the flow rate did not return to its previous value before the break until about 150 hours which represents a 6 hour seating period; note that he shape of the curve after replacing the bladder appears to match the shape at the beginning of the test. The ruptured bladder resulted in a pressure loss for all test devices and effected the other extended tests in a similar manner, see Fig. 416 and 4.17.

Results for the 5.2 mm HDPE geonet; Fig. 4.16, are similar to the 5.1 mm HDPE geonet; three of the four curves have nearly identical shapes with the 60 mil LDPE curve being the exception. The two extended tests are identical with the 60 mil HDPE matching the two long tests until its termination. The 60 mil LDPE has a slightly shallower slope than the other three tests. The scatter of data points for the 40 mil HDPE after 144 hrs (after the bladder rupture) is attributed to reseating of the test specimen (from 144 to 168 hrs, also shown by the 40 mil LDPE), periodic resetting of the inflow rate, and the resolution of measurement. The order of the flow rates from these tests by geomembrane combination from highest to lowest is 60 mil LDPE, 60 mil HDPE, 40 mil HDPE, and 40 mil LDPE.

Results for the 5.2 mm MDPE geonet, see Fig. 4.17, are generally the same with three of the four curves matching very well in shape. In this case, the exception is the 40 mil LDPE geomembrane combination; it has a steeper slope than the other three curves. Note that the initial drop between the first and second data points of the LDPE geomembranes is higher than the HDPE geomembranes. The magnitude of the flow rates for this geonet varies much more than the other two geonets and is attributed to the orientation of the flow channels which provides higher flow rates and hence, more chance for variation in magnitude. This is especially true when the initial flow rates presented are at 0.5 hrs which is sufficient to allow the different physical properties of the specimens to react to the 300 kPa pressure. The order of flow rates

from these tests by geomembrane combination from highest to lowest is 60 mil HDPE, 60 mil LDPE, 40 mil HDPE, and 40 mil LDPE.

The following observations are made from comparing all of the geonet and geomembrane combinations.

- The 60 mil geomembrane combinations have higher flow rates than the 40 mil geomembranes.
- The 40 mil LDPE geomembrane always has the lowest flow rate and always has the largest initial decrease.
- The 5.2 mm MDPE geonet has the highest flow rates followed by the 5.1 mm HDPE geonet and the 5.2 mm HDPE geonet.
- The 5.2 mm HDPE geonet exhibits the slowest rate of decrease in flow rate with time.
- The 5.1 mm HDPE geonet and the 5.2 mm MDPE geonet have curves with similar slopes.
- The 5.2 mm HDPE geonet also has the smallest initial decreases in flow rate followed by the 5.1 mm HDPE geonet and the 5.2 mm MDPE geonet having the largest initial decreases (the difference between the latter two geonets is small).
- The shape of the best fit curves of the shorter tests appear to be the same as the longer tests so the behavior over the long term does not depend on the duration of the test.

The previous discussion is concentrated on the patterns apparent in the curves and variation of the magnitude of the flow rates. The patterns in the flow rate are controlled by the amount of intrusion and compression and will be further discussed in section 5.

4.3.2 Textured Geomembrane Combinations

Results of the tests (Fig. 4.18) show the general shape of the curves are the same as the smooth geomembrane combinations, but with some variation. The 5.1 mm HDPE curve has a smaller initial decrease in flow rate and is shallower than its smooth geomembrane counterpart. The 5.2 mm HDPE curves are identical and the 5.2 mm MDPE curves are nearly identical; the initial decrease is slightly smaller and the slope is marginally flatter. Comparison of the three textured geomembrane curves reveals that they are very similar with regard to initial decrease in flow rate and the slope of the curve. The flow rate fluctuations seen in the smooth geomembrane

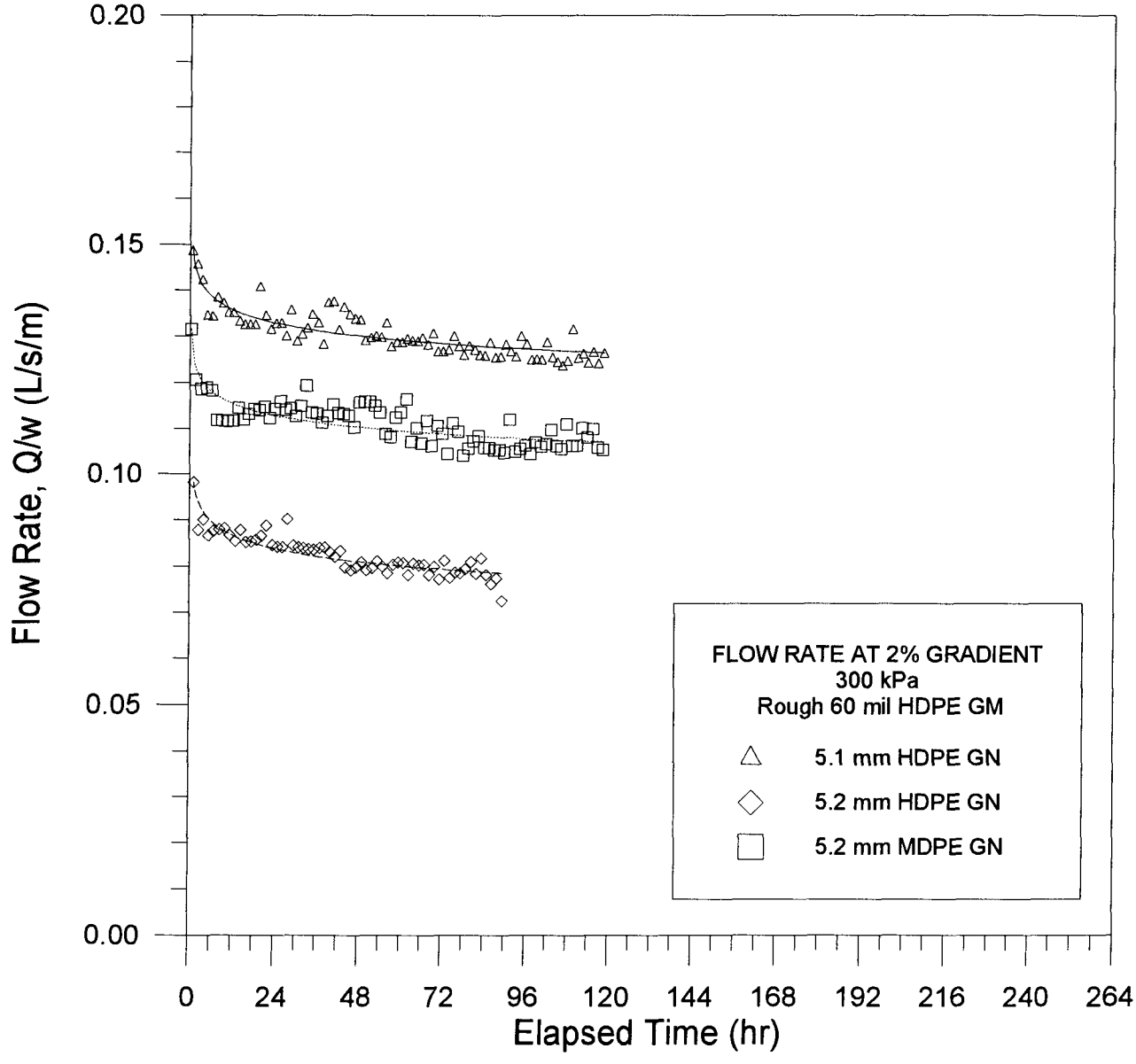

Figure 4.18 Series WLC Test Results of Textured 60 mil HDPE Geomembrane

tests are also present.

The initial flow rate comparisons are not valid for this figure because the geonets are all different. However, this does not preclude comparing the textured 60 mil HDPE geomembrane flow rates from their smooth 60 mil HDPE counterparts which is why the time axis is extended to 264 hours even though the tests only last 120 hours. The resulting comparison reveals that the flow rates of the textured geomembrane are generally lower than the comparable smooth geomembrane at the beginning and the end of the test. The 5.1 mm geonet is about 8% lower while the 5.2 mm HDPE and 5.2 mm MDPE are both 23% lower when compared to the smooth geomembrane combination. As a result, the highest flow rates are exhibited by the 5.1 mm HDPE geonet followed by the 5.2 MDPE geonet and the 5.2 mm HDPE geonet. In comparison, the 5.2 mm MDPE geonet had the highest rates with the smooth geomembranes with the 5.1 mm HDPE geonet second fastest.

5. INTERPRETATION OF RESULTS

The results presented in the previous chapter are examined to determine the factors influencing the flow rate of the geonet and geomembrane combinations. It is clear from the results that the gradient and pressure have a major influence on the flow rate and will be examined in detail.

5.1 INFLUENCE OF HYDRAULIC GRADIENT

The geonets have large interconnecting pores available for flow and may be considered a very porous media much like a uniformly graded gravel. Therefore, the flow through the geonet may be governed by Darcy's law if the flow is laminar. Mathematically, Darcy's law may be described by the following equation:

$$v = kdh/dl = ki \qquad (4)$$

where v = specific discharge of the fluid
k = coefficient of permeability of the media
$dh/dl = i$ = hydraulic gradient

It is often convenient to multiply both sides by the cross-sectional area of flow and write Darcy's law in the form:

$$vA = Q = kiA \qquad (5)$$

where A = cross sectional area of flow
Q = volumetric flow rate

The velocity of flow is directly related to the gradient and the quantity of discharge through porous media are directly proportional to the hydraulic gradient for a constant permeability and cross-sectional area. A geonet, in contrast to a soil, is somewhat more compressible and the cross-sectional area is likely to decrease with increased normal stress. However, the change in cross sectional area is likely to be negligible over short time periods at constant pressure (not immediately after the onset or increase of pressure) and the volumetric flow rate can be considered to be directly related to the hydraulic gradient.

Figures 5.1 to 5.4 were compiled from the series W test results and show the volumetric flow rate plotted against the hydraulic gradient. The data were consolidated to illustrate the

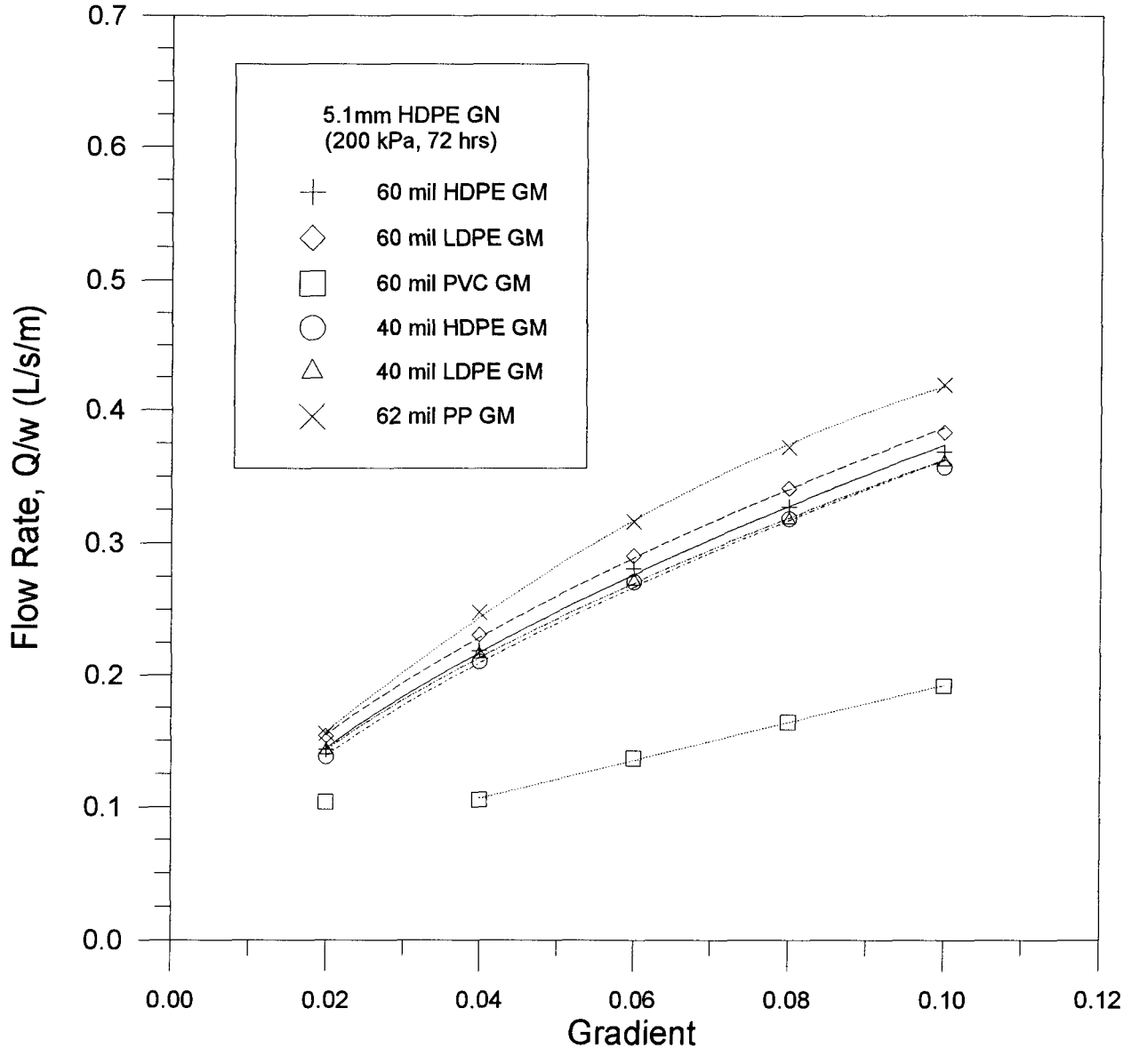

Figure 5.1 Flow Rate vs. Gradient of 5.1 mm HDPE Geonet

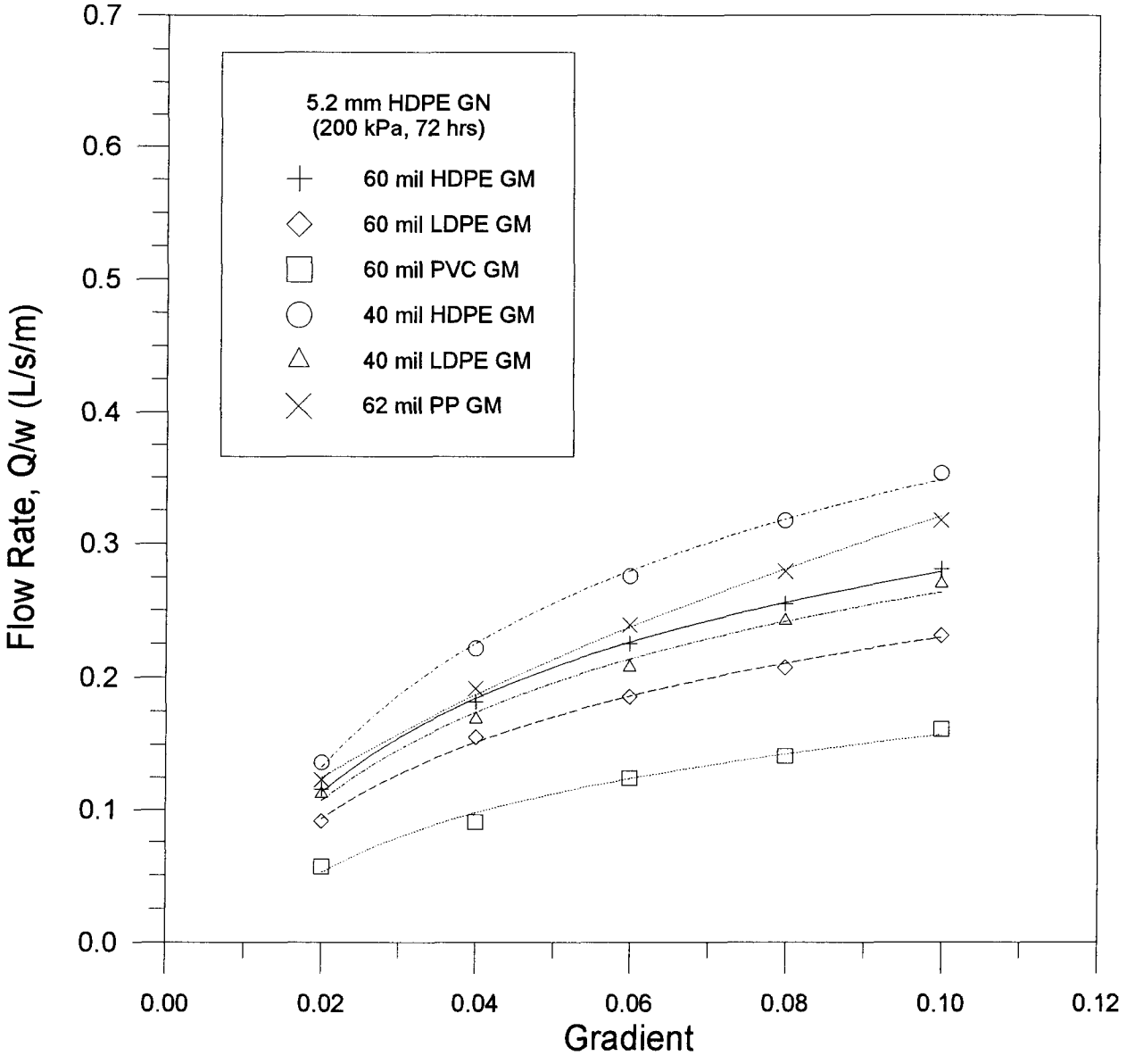

Figure 5.2 Flow Rate vs. Gradient of 5.2 mm HDPE Geonet

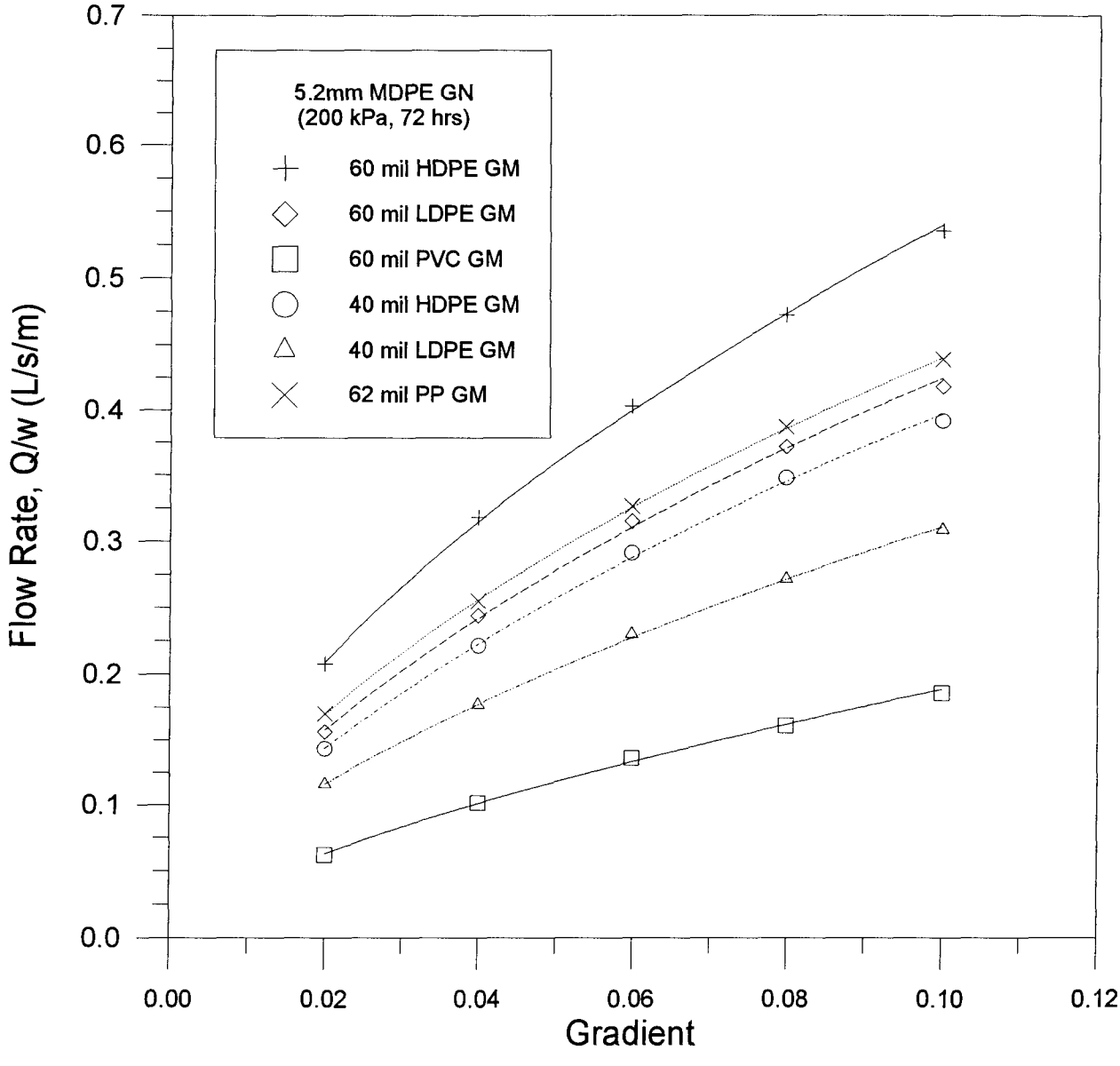

Figure 5.3 Flow Rate vs. Gradient of 5.2 mm MDPE Geonet

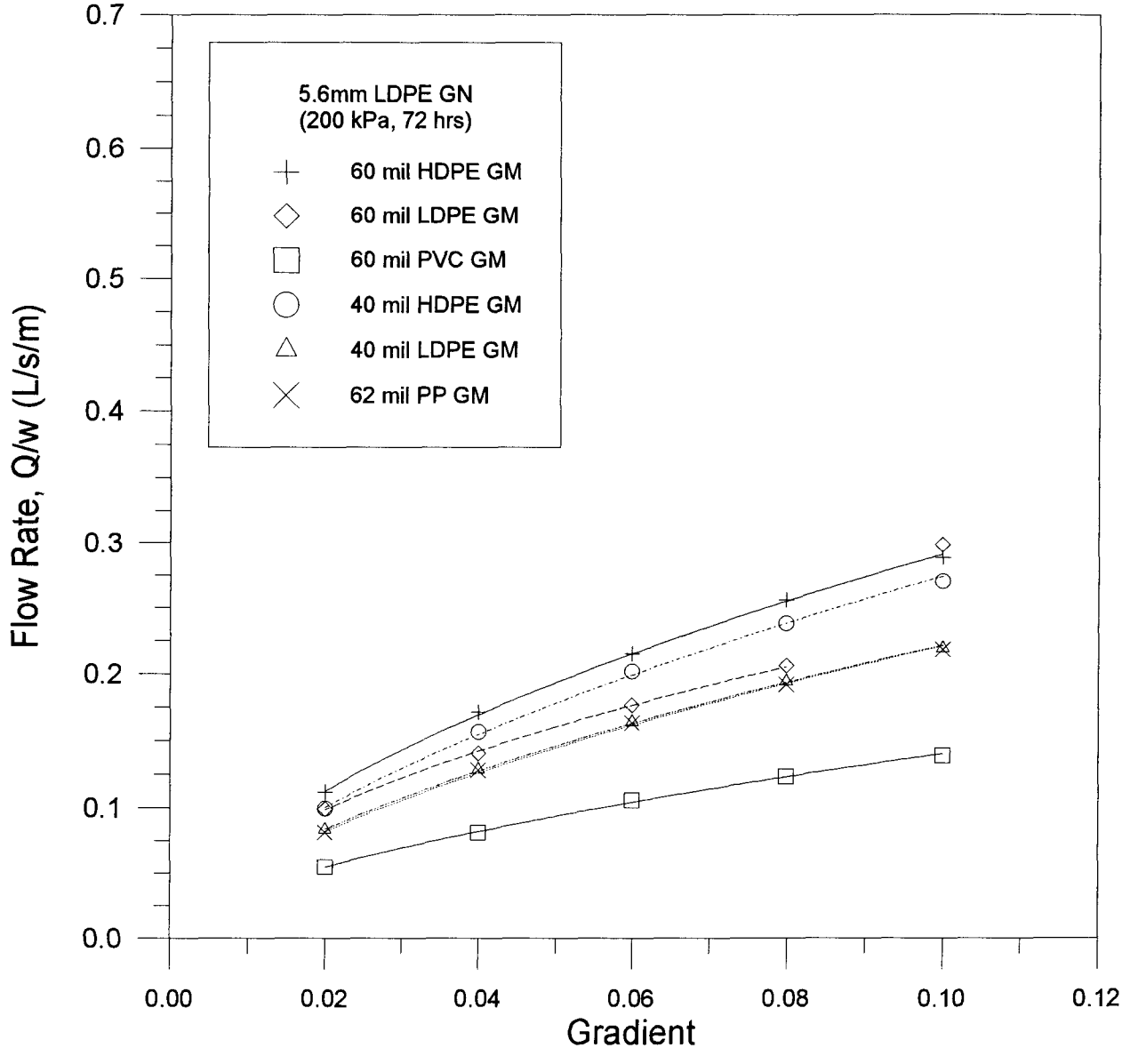

Figure 5.4 Flow Rate vs. Gradient of 5.6 mm LDPE Geonet

results for the various geomembrane combinations for each geonet. The data used were the last set of gradient readings (72 hours from the start of the test) from the 200 kPa pressure stage. The last set of gradient readings for the pressure stage was chosen because any effects of geonet compression are the smallest at the end of the pressure stage. Since the time interval to complete the set of flow readings for the five gradients is only 45 minutes, any geonet compression can be considered negligible and the cross-sectional area for flow is constant (over that time interval). Therefore, the volumetric flow rate will be directly proportional to the hydraulic gradient if Darcy's law is valid.

Best fit lines were drawn through the data points for the 5.1 mm HDPE (Fig. 5.1) geonet for six different geomembrane combinations with the exception of the point at 0.02 gradient of the 60 mil PVC which appears to be inaccurate. Only the 60 mil PVC has a linear fit which indicates a direct relationship, but not Darcian, between the volumetric flow rate and the hydraulic gradient. All of the geomembranes except the 60 mil PVC respond in a similar manner; the best fit lines are curvilinear and are described by a power relationship, indicating that the flow is not laminar. The same general curve shapes are obtained for the 5.2 mm HDPE, 5.2 mm MDPE, and 5.6 mm LDPE geonets, Fig. 5.2 to 5.4. All of the curves are curvilinear, but vary slightly in the degree of curvature. The 60 mil PVC curves are the closest to linear of all the geomembranes.

If comparisons of the flow rates versus gradients are made amongst all of the geonets, the following observations are apparent:

- Extrapolation of the best fit curves to a zero gradient would result in a positive flow rate even when there is no imposed hydraulic gradient.
- The 60 mil PVC geomembrane has a linear or nearly linear curve and it always has the lowest flow rates.
- All of the non-linear data can be described as curvilinear.

Extrapolation of the best fit lines indicates a positive intercept on the flow rate axis of about 0.025 L/s/m which implies flow at zero gradient. Intuitively, this is not realistic because there is no driving force for the water. Furthermore, there was no flow observed when the zero

readings for the differential pressure transducers were taken (performed at zero gradient). This apparent flow at zero gradient is attributed to the resolution of the measurement of the flow rate; see Fig 4.4 or 4.12, these two figures show a near zero flow rate of about 0.025 L/s/m which equates to a drip from the test devices (observed during testing). Therefore, a flow rate of 0.025 L/s/m is the lowest rate of flow measurable.

Darcy's law is valid if the flow is laminar and not valid if the flow is turbulent; the characteristic flow regime is determined by the Reynolds number for flow through a porous media. The Reynolds number is determined from the following equation (Bear, 1972):

$$Re = vd/\mu \qquad (6)$$

where Re = the Reynolds number
v = the specific discharge or velocity (m/s)
d = a characteristic dimension of the porous media (m)
μ = the kinematic viscosity of the fluid (m^2/s)

The flow regime depends on the value of the Reynolds number and the relationship is shown on Table 5.1

Table 5.1 Validity of Darcy's law based on Reynolds number (After Bear, 1972)

Reynolds number	Flow Regime	Comment
0.01 to 1	laminar	Darcy's law valid
between 1 and 100	transition from laminar to turbulent	Darcy's law valid if laminar flow
over 100	turbulent	Darcy's law not valid

The calculation of the Reynolds number requires the velocity of flow which can either be measured or calculated using Darcy's Law which assumes it is valid i.e. laminar flow. In addition, a characteristic dimension must be used in the calculation which may be the diameter of the flow channel or the radius or some other dimension. This approach is somewhat subjective, but the range of values obtained were between 30 and 114 using various characteristic dimensions and flow velocities. Using this approach, the flow may be described as semiturbulent

to turbulent.

The Reynolds number approach for determining the flow regime seems somewhat subjective and an alternate approach is described by Cedergren (1989). The basis of the approach described by Cedergren is a derivative of Darcy's Law shown by equation 7 below:

$$Q/i = k'A = kCA \qquad (7)$$

where Q = volumetric flow rate
i = hydraulic gradient
k'= effective permeability for non-laminar flow
A= cross sectional area
k = permeability
C= relative permeability factor

For laminar flow, Q increases proportionally with i; therefore, Q/i remains constant regardless of hydraulic gradient. For semiturbulent or turbulent flow, Q/i decreases with increasing hydraulic gradient. The flow regime may then be checked quantitatively by simply plotting Q/i vs. i; the flow is laminar if the resulting curve has a zero slope (Q/i = constant) and it is semiturbulent to turbulent if the curve has a slope. Cedergren (1989) results of tests performed on clean American River crushed gravels are shown, Fig. 5.5. In this analysis, it is assumed that laminar flow exists at a 0.01 gradient and the ratio of Q/i is given a value of 1.0 by normalizing by the value of Q/i at a 0.01 gradient, see equation 8 below.

$$C = \frac{\frac{(Q/w)}{i}, i = n}{\frac{(Q/w)}{i}, i = 0.01} \qquad (8)$$

where, C = relative permeability factor
Q/w = volumetric flow rate per unit width
i = gradient

The relative permeability factor, C, is taken as the ratio of Q/i (or (Q/w)/i for volumetric flow rate per unit width) in the figure because k and A are constants which means that Q/i is proportional to C. The upper line on the figure represents 100% laminar flow and the lower

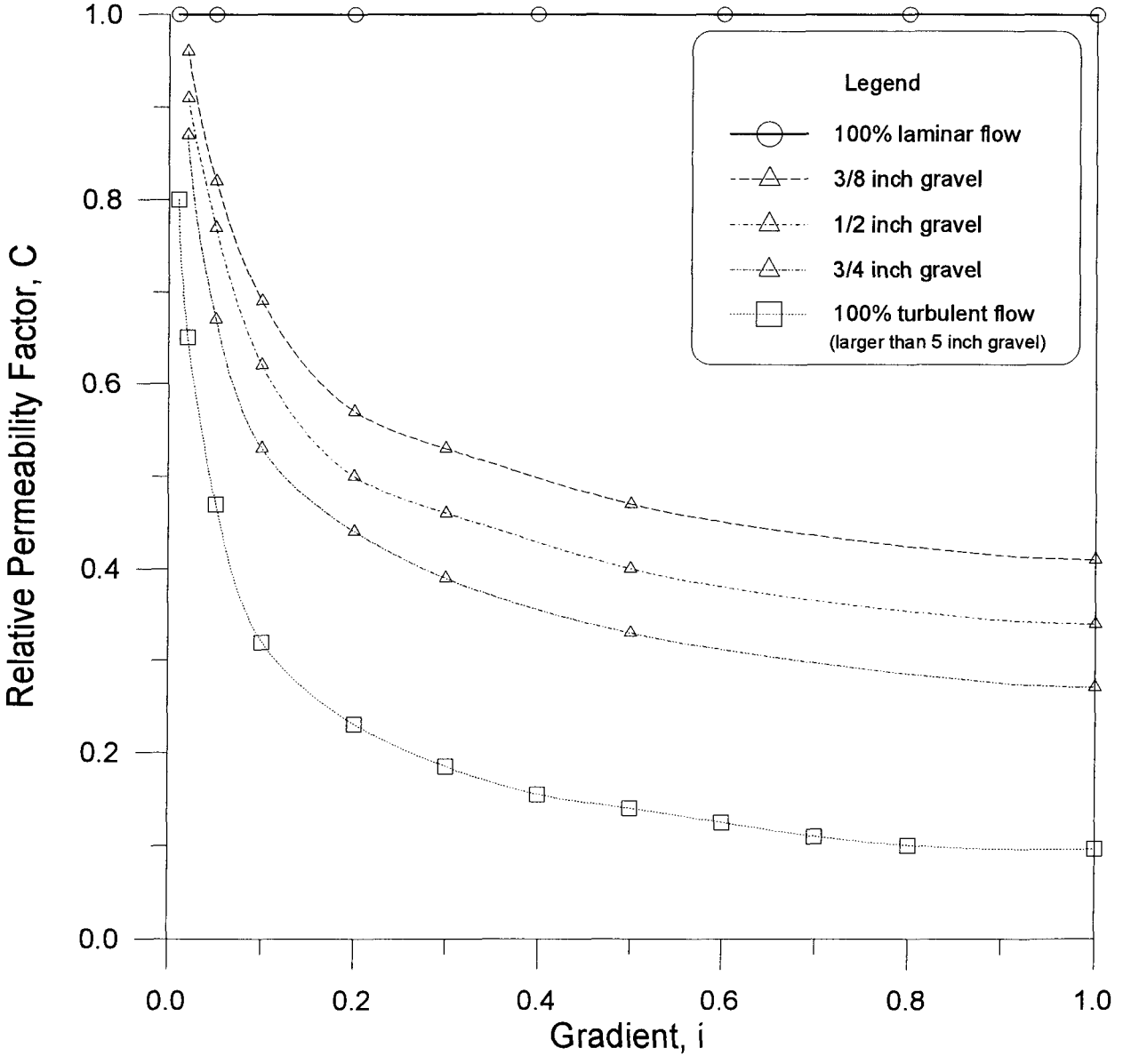

Figure 5.5 Effective Permeability for Laminar to Turbulent Flow (from Cedergren 1989)

curve represents 100% turbulent flow which was obtained from similar tests on other granular soils and represents materials with a grain size over 125 mm in diameter (Cedergren,1989). The curves in between (American River crushed gravel) are used to show where differently graded granular materials fit in the flow regime; the closer to the relative permeability is to 1.0, the closer the flow is to being laminar. The flow regime of the granular materials shown could be described as semiturbulent to turbulent.

Figures 5.6 to 5.9 display similar plots using the data from Figures 5.1 to 5.4; note the horizontal axis only shows the gradients used in testing. The figures display the same lines representing 100% laminar flow and 100% turbulent flow. For simplicity, only the 60 mil PVC and 60 mil HDPE geomembranes are shown; these geomembranes generally represent the lowest and highest flow rates of the various geomembranes used and appear to be equivalent to 1/2 inch to 3/4 inch gravel, see Fig. 5.5. The PVC is generally closer to laminar flow than the HDPE except at the lower gradients for the 5.2 mm HDPE geonet. This means that the relative increase in flow rate (relative permeability) for the HDPE is smaller than the relative increase for the PVC for the same increase in gradient. Interestingly, the 5.6 mm LDPE geonet has both geomembranes with similar flow regimes despite the higher flow rates of the HDPE geomembrane. This indicates that the relative increase in flow rate with increasing gradient for both geomembranes is the same with the 5.6 mm LDPE geonet. Despite the difference between the two geomembranes, the position of the curves relative to the 100% laminar and turbulent flow boundaries indicate that the flow regime is semi-turbulent to turbulent.

It was observed that the majority of the data presented in Figs. 5.1 to 5.4 are curvilinear and are described by a power relationship. It was just shown that the flow regime is semi-turbulent to turbulent. When flow deviates from being laminar, it no longer increases directly with the hydraulic gradient, rather, it increases by some power function related to the degree of turbulence. Hence, the data are consistent with the physical laws governing flow.

In summary, the gradient controls the flow rate when other factors are held constant; the higher the gradient, the higher the flow. If the relationship between the flow rate and the gradient is directly proportional, then the flow regime is laminar and Darcy's law governs the

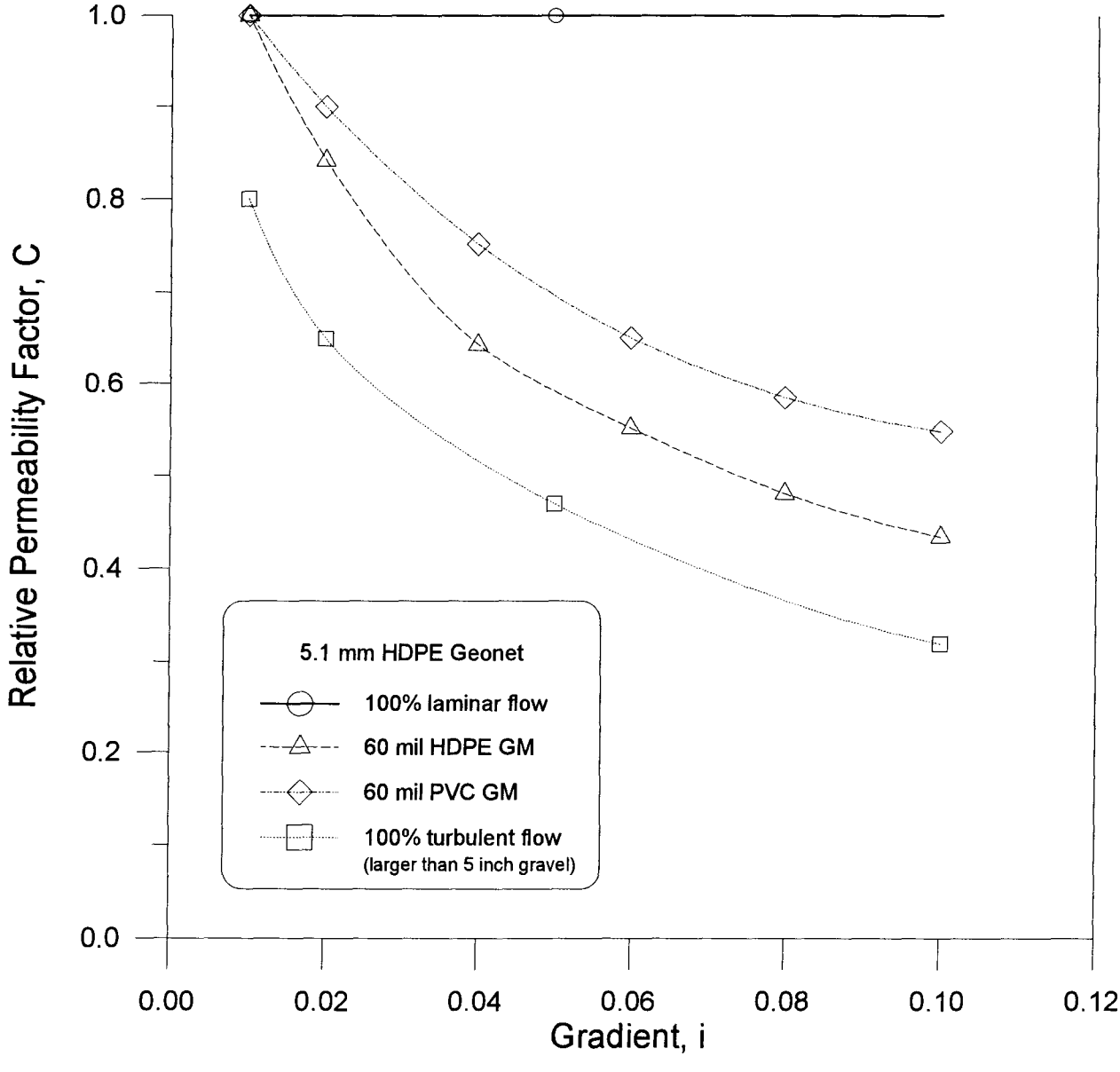

Figure 5.6 Flow Regime of 5.1 mm HDPE Geonet

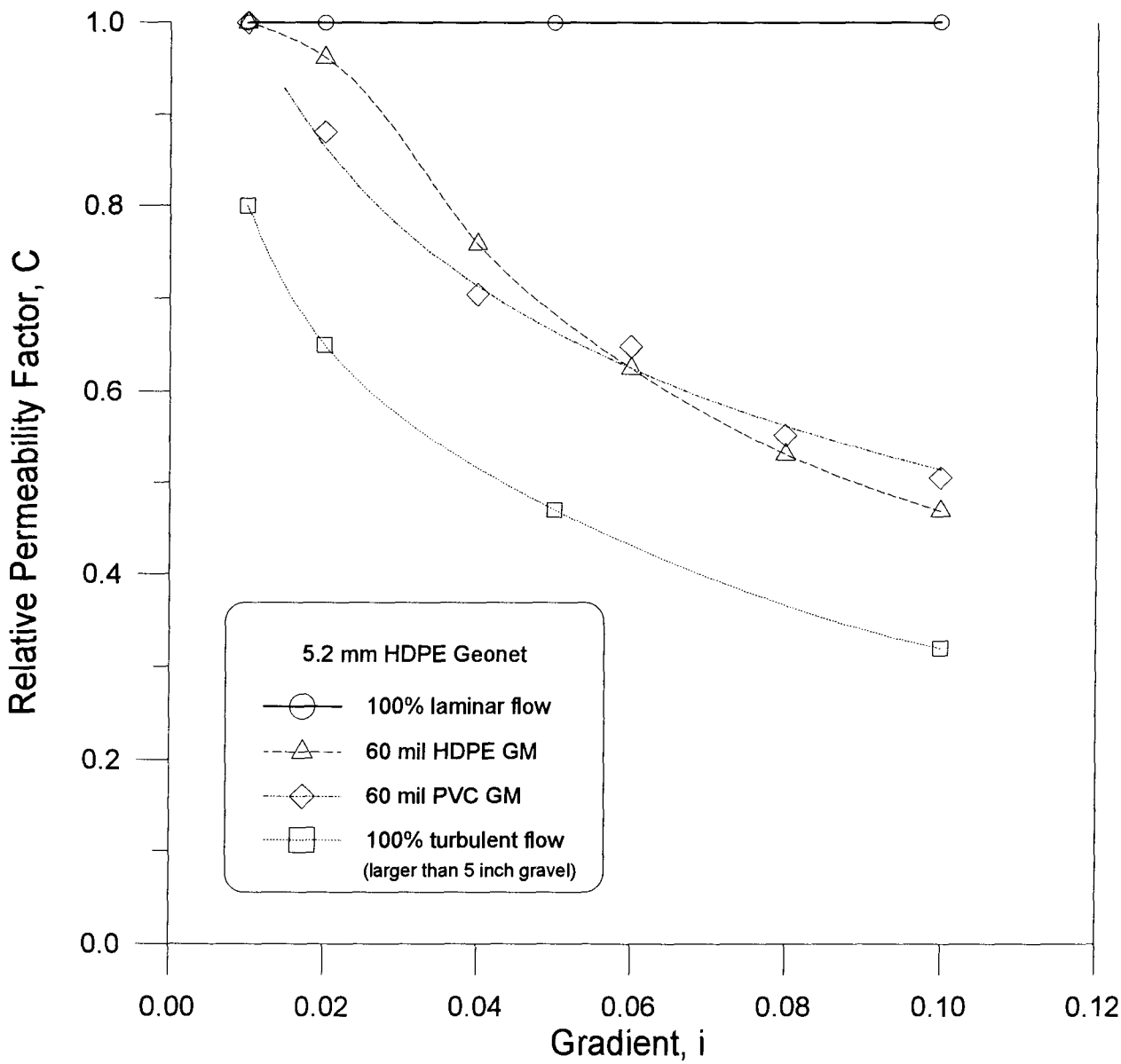

Figure 5.7 Flow Regime of 5.2 mm HDPE Geonet

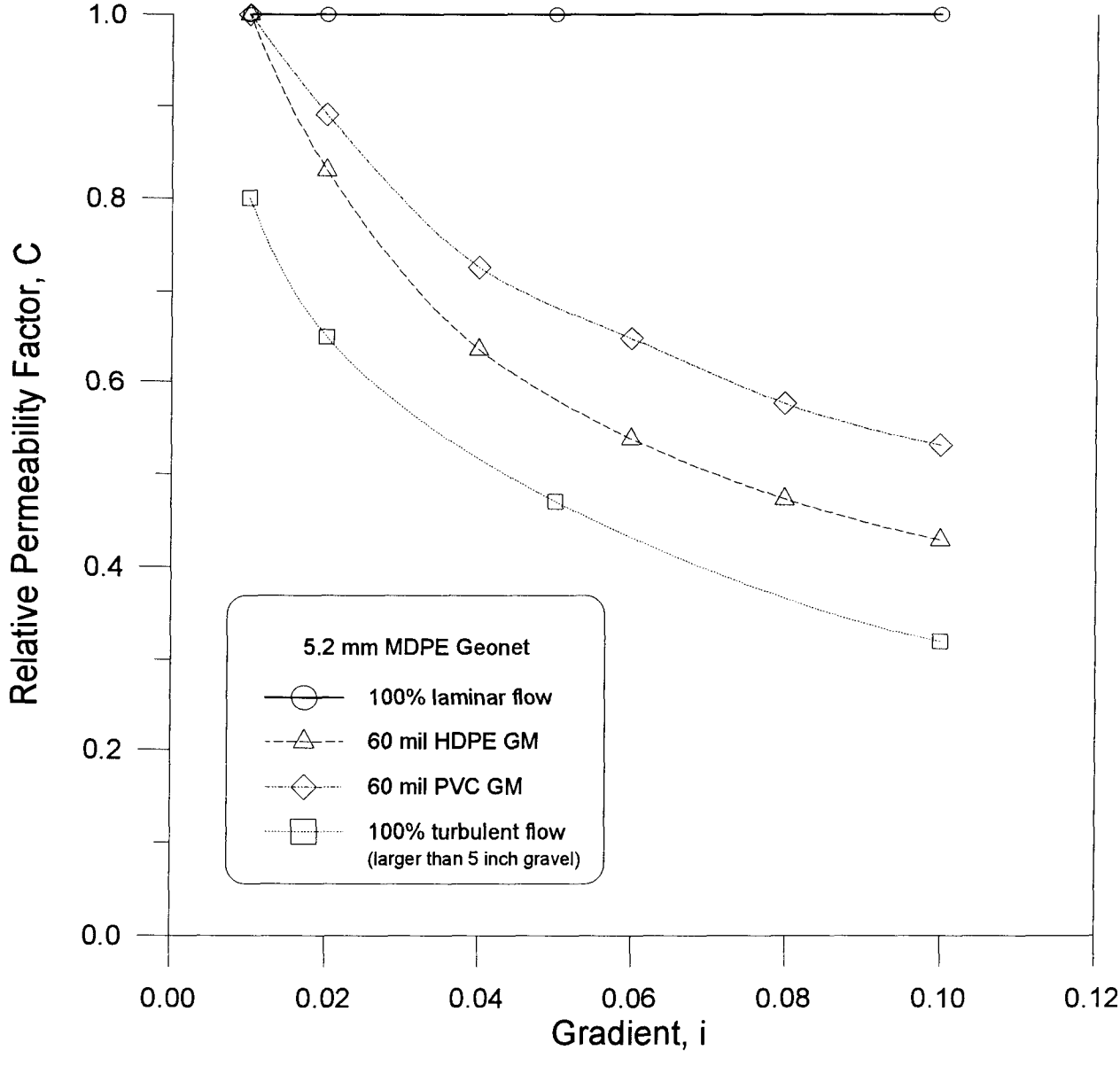

Figure 5.8 Flow Regime of 5.2 mm MDPE Geonet

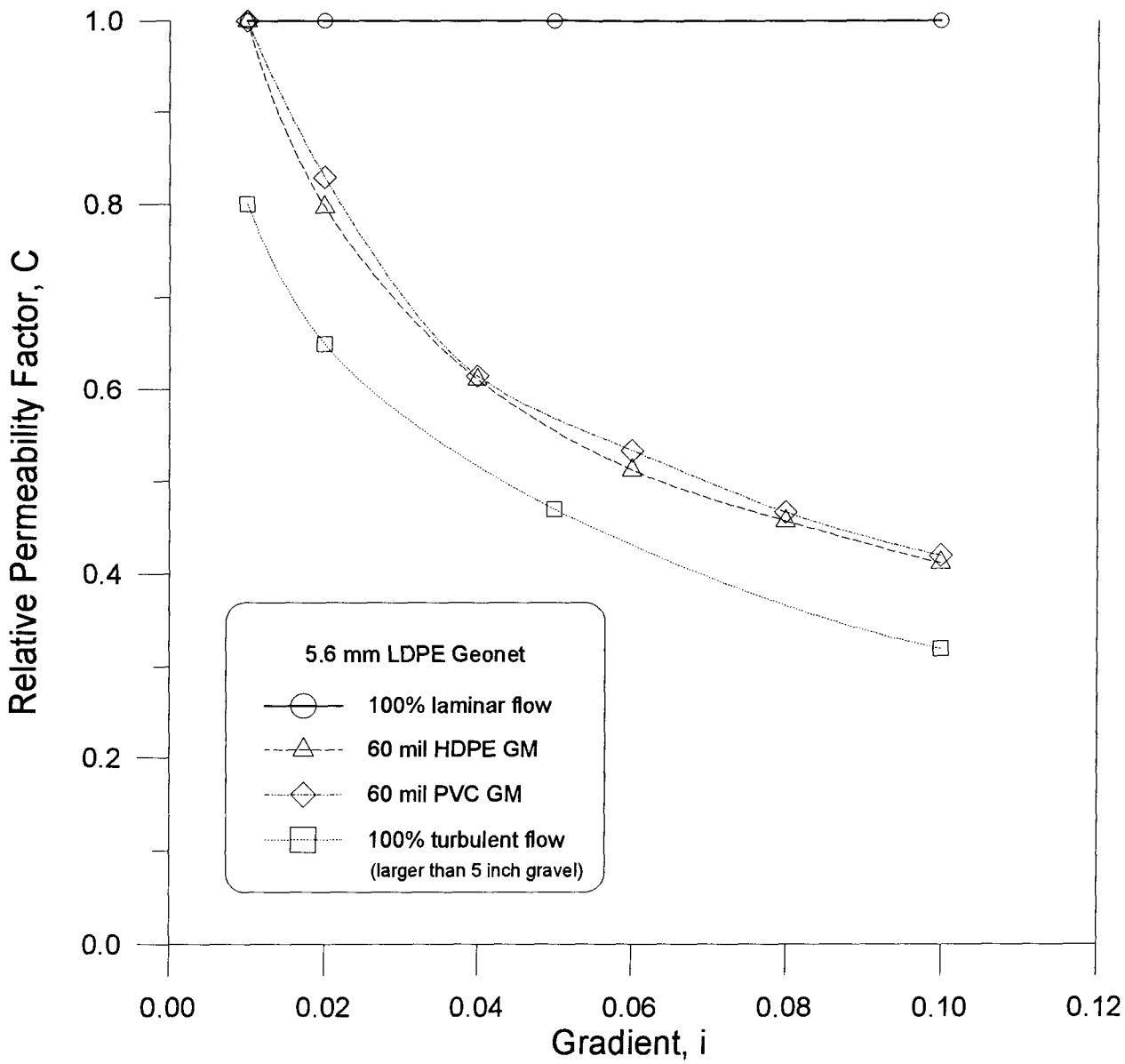

Figure 5.9 Flow Regime of 5.6 mm LDPE Geonet

flow. The Reynolds number is often used to determine whether the flow regime is laminar or turbulent. The Reynolds number indicated that the 60 mil PVC combinations with the geonets had semiturbulent to turbulent flow. These findings were verified by the method described by Cedergren (1989); in fact, the methodology used allowed comparison of flow rates of the geonets to aggregate materials. The geonets tested were equivalent to 1/2 inch to 3/4 inch gravel based on the analyses.

5.2 INFLUENCE OF CONFINING STRESS

The confining stress acting on the composite test specimen results in intrusion of the geomembrane into the pore space of the geonet and creep deformations: a more detailed examination of each action is presented in sections 5.2.1 and 5.2.2. This section addresses these combined effects due to confining stress.

As described in sections 3.1 and 3.4, the test series W was performed using different combinations of geomembranes and geonets under five different values of normal stress. An interpretation of these results of these tests will be presented in the order used in section 4. The results of the smooth geomembrane combinations are summarized on Fig. 5.10 to 5.13; the data points are the last point for each pressure stage and the best fit line is drawn through the points. Note that these best fit curves describe the combined effects of intrusion and creep.

All of the curves for the 5.2 mm HDPE and MDPE geonets (Fig. 5.11 and 5.12) are linear with the exception of the 60 mil PVC curves which are concave-up. The 5.1 mm HDPE geonet (Fig. 5.10) exhibits three concave-down curves, two linear and one concave-up curve which is again, the 60 mil PVC . The 5.6 mm LDPE geonet (Fig. 5.13) exhibit all have concave-down curves except for the 60 mil PVC which is linear. Generally, a concave-up curve indicates that geomembrane intrusion into the geonet is dominant; a concave-down curve indicates that geonet compression is dominant; and a linear curve indicates a balance between intrusion and compression. Note that the last data point for the 60 mil PVC was not used in the best fit because the flow rates had practically reached a minimal value. Including the last point would

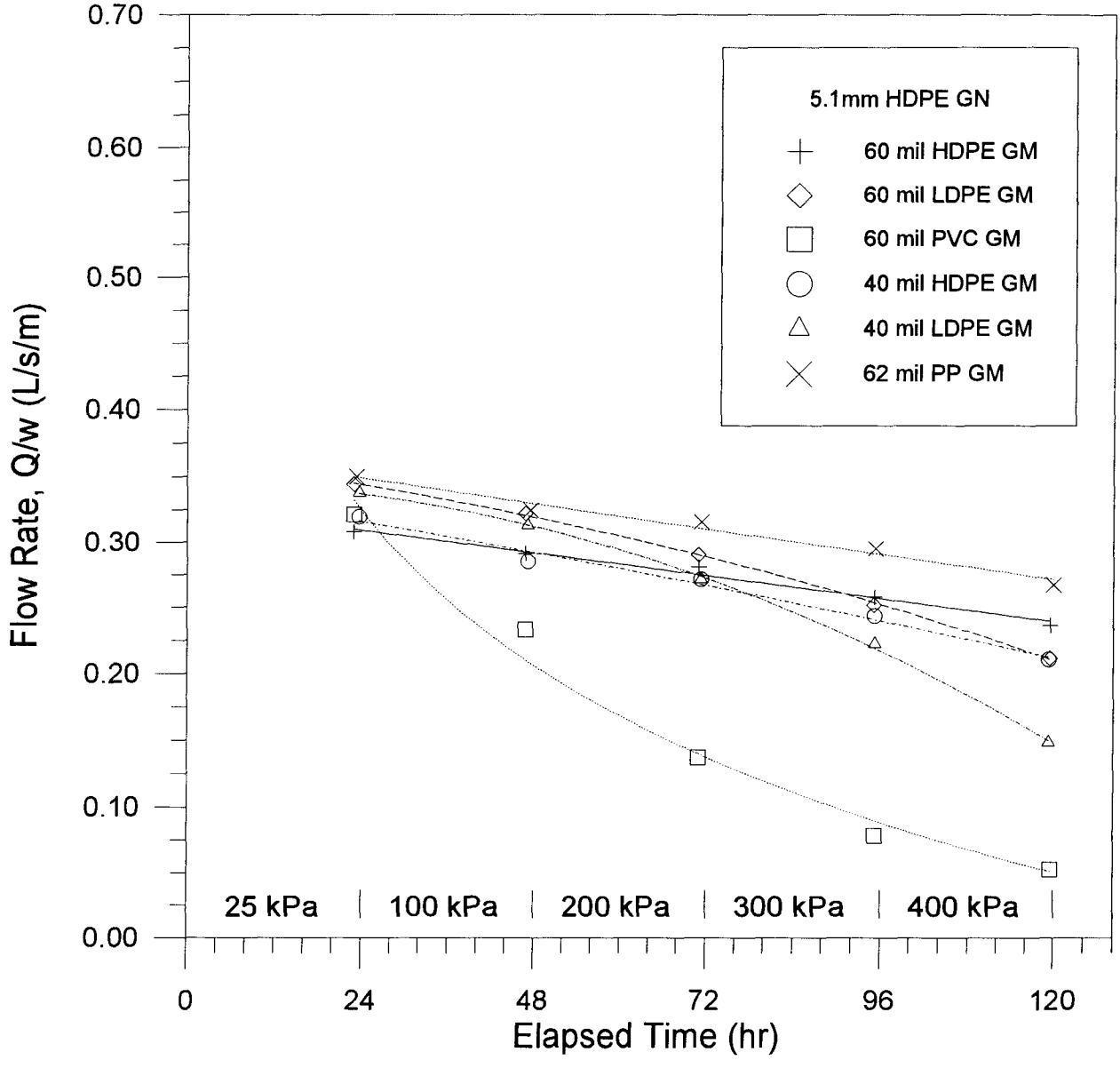

Figure 5.10 Flow Rate of 5.1 mm HDPE Geonet at 0.06 Gradient (24 hour reading at each pressure)

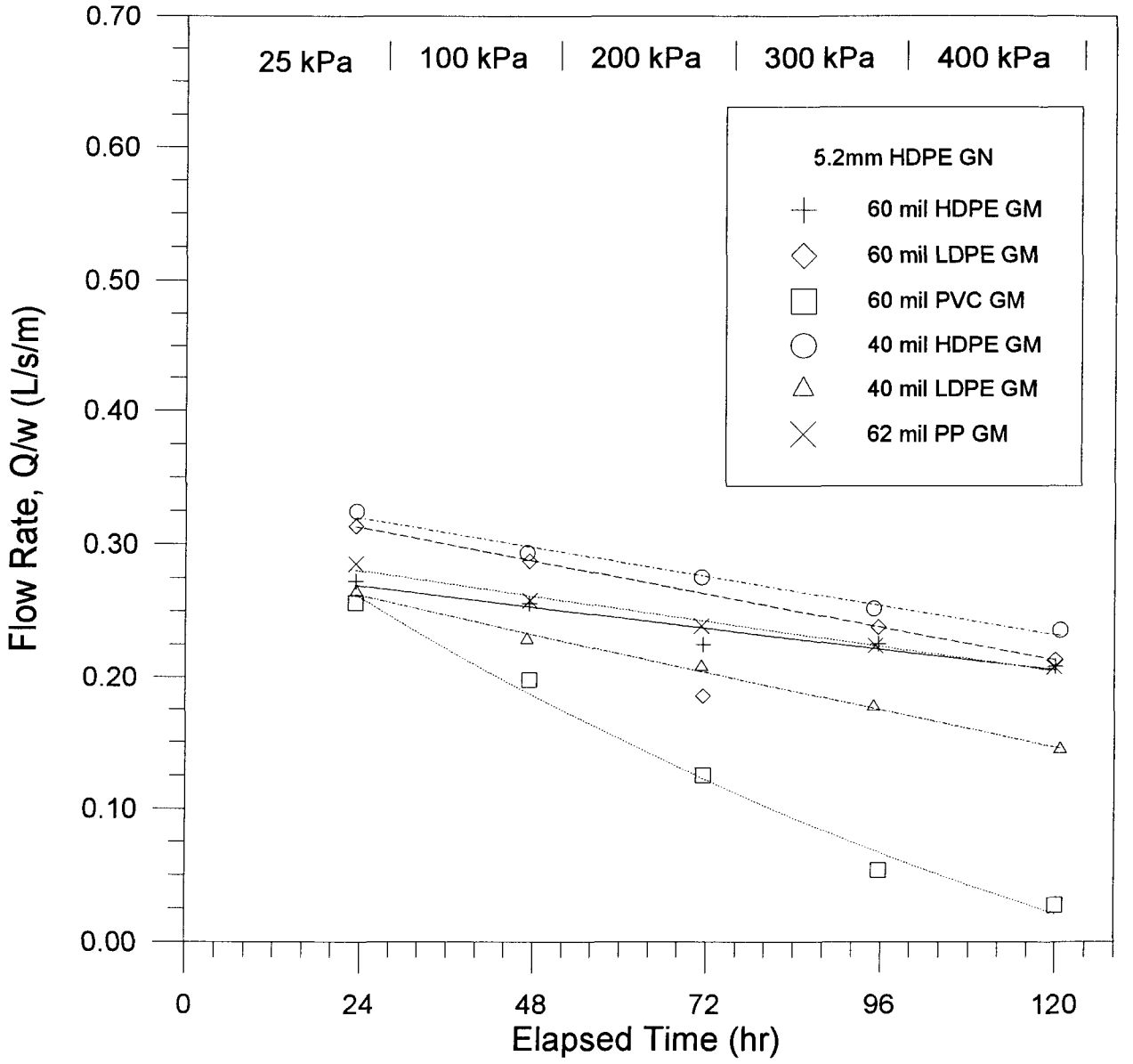

Figure 5.11 Flow Rate of 5.2 mm HDPE Geonet at 0.06 Gradient (24 hour reading at each pressure)

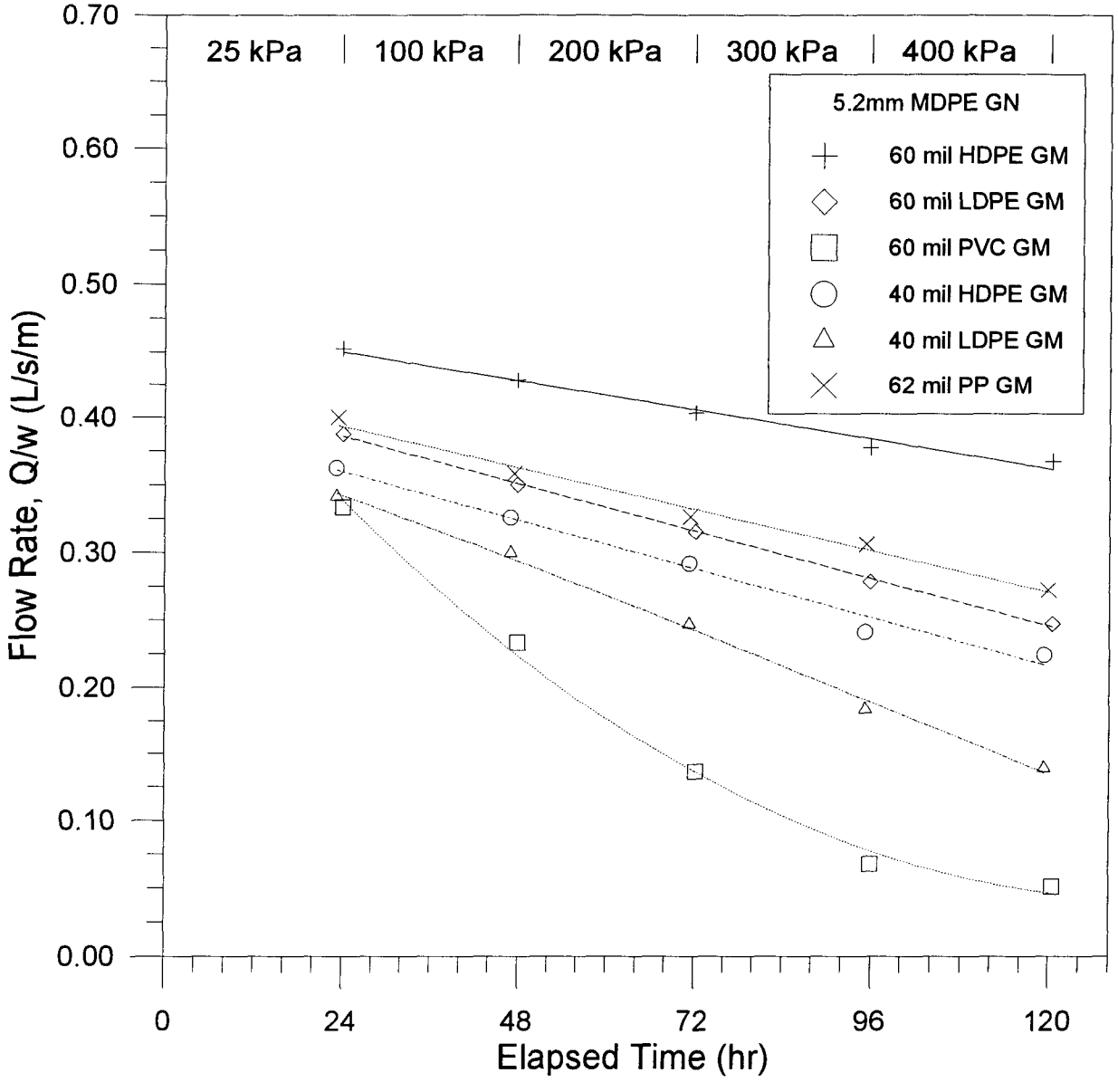

Figure 5.12 Flow Rate of 5.2 mm MDPE Geonet at 0.06 Gradient (24 hour reading at each pressure)

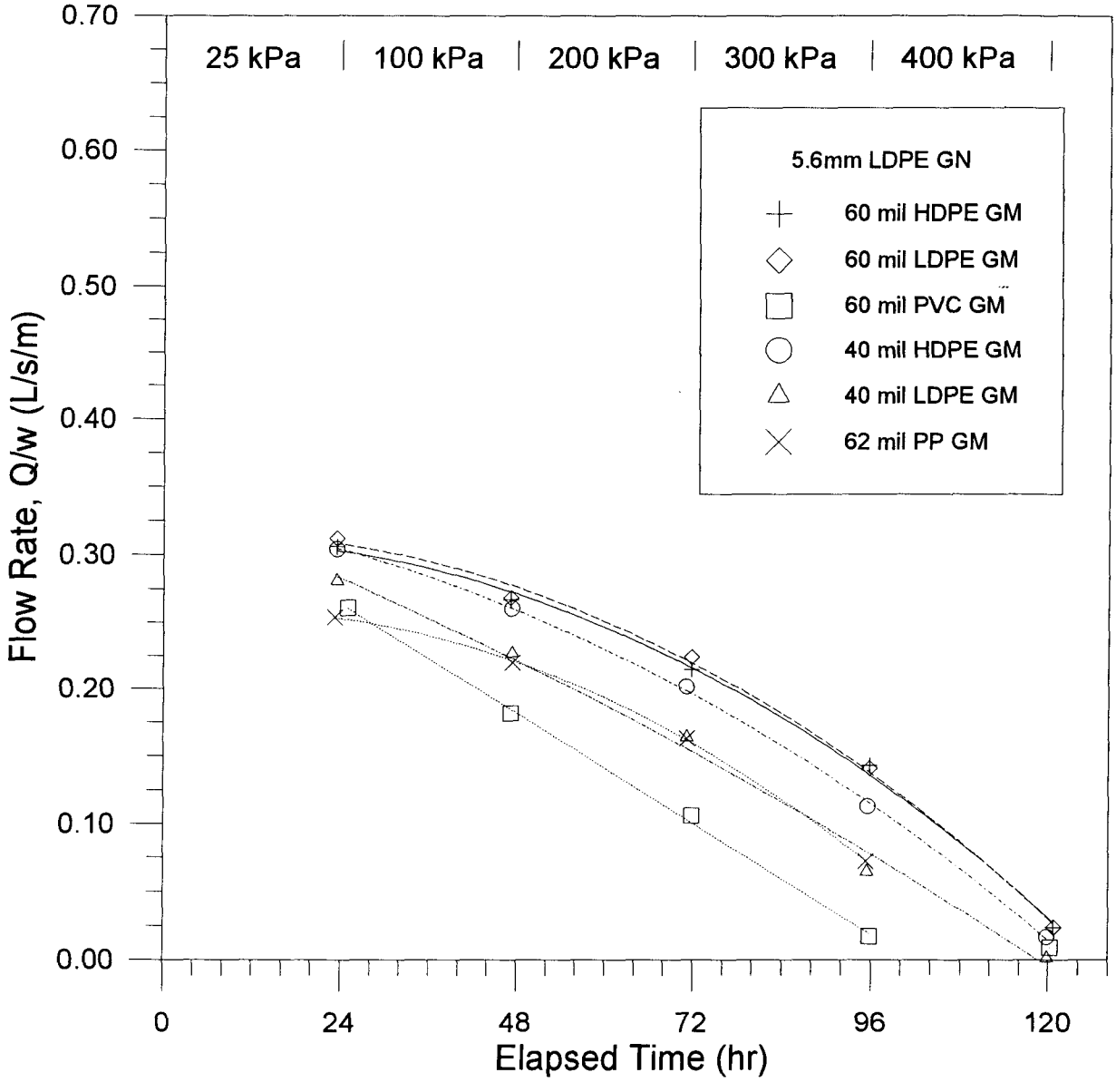

Figure 5.13 Flow Rate of 5.6 mm LDPE Geonet at 0.06 Gradient (24 hour reading at each pressure)

erroneously distort the true best fit. There was no data point for the 62 mm PP at 120 hours due to a ruptured latex bladder which terminated the test.

Comparisons of the geomembrane combinations with all four geonets lead to the following observations:

- The dominant behavior for the 5.2 mm HDPE and 5.2 mm MDPE geonets is linear.
- The 60 mil PVC exhibits a complete loss of flow by intrusion for all geonets.
- The 5.6 LDPE geonet exhibits a complete loss of flow by compression with all geomembrane combinations.
- The 60 mil PVC geomembrane and 5.6 mm LDPE geonet combination exhibits a balance between intrusion and compression, but the complete loss of flow is the fastest.

The dominant linear behavior of the 5.2 mm HDPE and 5.2 mm MDPE geonets make it easy to develop a ranking system among the geomembranes. The slope of the line indicates the rate of decrease in the flow rate and provides a reasonable parameter to use as a ranking system. The 60 mil HDPE geomembrane has the flattest slope which is then followed by the 62 mil PP, 40 mil HDPE, 60 mil LDPE, and the 40 mil LDPE last. The 40 mil HDPE and 60 mil LDPE combinations with the 5.2 mm MDPE geonet have identical slopes, but the higher ranking goes to the 40 mil HDPE because of its flatter slope with the 5.2 mm HDPE geonet. Among the linear curves of the 5.1 mm HDPE geonet, the ordering above holds true as well. In fact, the ranking is independent of the shape of the curve; the concave-down 60 mil and 40 mil LDPE geomembranes (Fig. 5.10) are steeper than the linear curves and follow the 40 mil HDPE in order. The stiffness of the geomembranes is controlling the rate of decrease in the flow rate. The stiffest geomembrane tested (by qualitative standards) is the 60 mil HDPE, followed by the 62 mm PP, the 40 mil HDPE, the 60 mil LDPE, and the 40 mil LDPE.

The 60 mil PVC exhibits concave-down curves with all of the geonets except for the 5.6 mm LDPE geonet because the flow rate approaches zero at 400 kPa. The first three or four points (200 kPa to 300 kPa for all geonets) exhibit linear behavior and would continue if the flow rate did not approach zero. Hence, the shape may be better described as conditionally linear or bi-linear. Regardless of shape, this geomembrane would rank last among the others tested; its

flexibility allows more intrusion than the others which results in larger flow rate decreases.

The 5.6 mm LDPE geonet exhibits concave-down curves with all geomembranes except the 60 mil PVC which is linear. The radius of curvature of all the geomembranes is similar except for the 40 mil LDPE; it was flattened because the flow rate reduced to zero at 120 hours, but should have been reduced to zero at 106 hours (extrapolating the first four points). It should be possible to rank the geomembranes using the slope of the curves as before. Top ranking goes to the 60 mil HDPE followed by the 60 mil LDPE. The 62 mm PP ranks a close third followed by the 40 mil HDPE and 40 mil LDPE. This is the same ranking previously obtained from the other geonets with the exception of the 60 mil LDPE and 62 mm PP switching places. However, given the closeness of those two curves; the ranking is essentially identical.

Examination of the data points for the 5.6 mm LDPE geonet (Fig. 5.10) reveals that the drop in the flow rates is greater at high pressure than at low pressure. The decrease in flow rate increases with each increase in normal stress because of geonet compression until the flow rate is reduced to nearly zero at 400 kPa. This significant loss in flow rate is attributed to near complete compression or collapse of the ribs of the geonet; note that 400 kPa is close to the ultimate compressive strength of the LDPE geonet of 489 kPa (section 3.1.1).

The 5.6 mm LDPE geonet and 60 mil PVC geomembrane experience decreases in flow rate to nearly zero. This large reduction may be considered failure of the drainage system. The 5.6 mm LDPE geonet fails from compression or collapse of the ribs, whereas the 60 mil PVC geomembrane fails by intrusion. The resulting curve shapes for these two failure mechanisms is consistent for each mode: all the 5.6 mm LDPE geonet curves are concave-down and all the 60 mil PVC geomembrane curves are concave-up (except for the 5.6 mm LDPE geonet in combination with the 60 mil PVC). Hence, a concave-down shape may indicate failure or control (if flow rate does not decrease to zero) by compression of the geonet and a concave-up shape may indicate failure or control (if flow rate does not decrease to zero) by intrusion of the geomembrane. The 5.6 mm LDPE geonet and 60 mil PVC combination has a linear curve: in this case, a balance between compression and intrusion is obtained and the resulting curve is linear which is a compromise between concave-down and concave-up.

The geonets may also be ranked using the slope of the curves. As with the geomembranes, the ranking system is independent of the shape of the curve and the following order is obtained: 5.2 mm HDPE, 5.1 mm HDPE , 5.2 mm MDPE , and the 5.6 LDPE geonet last.

Data for the textured geomembrane are reported in Fig. 5.14. There is a dominant concave-up behavior which is exhibited by the 5.1 mm HDPE and 5.2 mm HDPE & MDPE geonets. This appears to be true concave-up because the shape is not caused by an asymptotic approach to zero flow rate. Only the 5.6 mm LDPE geonet has a different curve - it is linear. The reduction in flow rate between 25 kPa and 100 kPa is larger than the other pressure increments which produce nearly equal (linear) decreases in the flow rate. The confining stress of 25 kPa is not sufficient to properly seat the textured geomembrane because of its textured surface, but 100 kPa is sufficient. The 5.6 mm LDPE geonet experiences more compression than the other geonets and shows a linear curve as a result.

As shown by Figure 5.14, the textured geomembrane reacts differently than the smooth geomembrane, but it would be convenient if the textured geomembrane could be ranked with the smooth geomembranes. However, attempts to place the textured geomembrane with the smooth geomembranes produced results that are inconsistent. Therefore, it is concluded that the textured geomembrane should not be ranked with the smooth geomembranes and should only be ranked with other textured geomembranes.

The preceding section concentrated on developing a ranking system for both the geomembranes and the geonets used in testing. The ranking system was based on the relative decrease in flow rate with increasing pressure or normal stress; therefore, higher ranked geomembranes or geonets would experience less reduction in flow than lower ranked geomembranes or geonets when exposed to the same normal stress.

- The ranking of the geomembranes coincides with their relative stiffness as defined by the ASTM Flexural Rigidity Test. The stiffer the geomembrane, the less likely that it will intrude into the geonet openings.

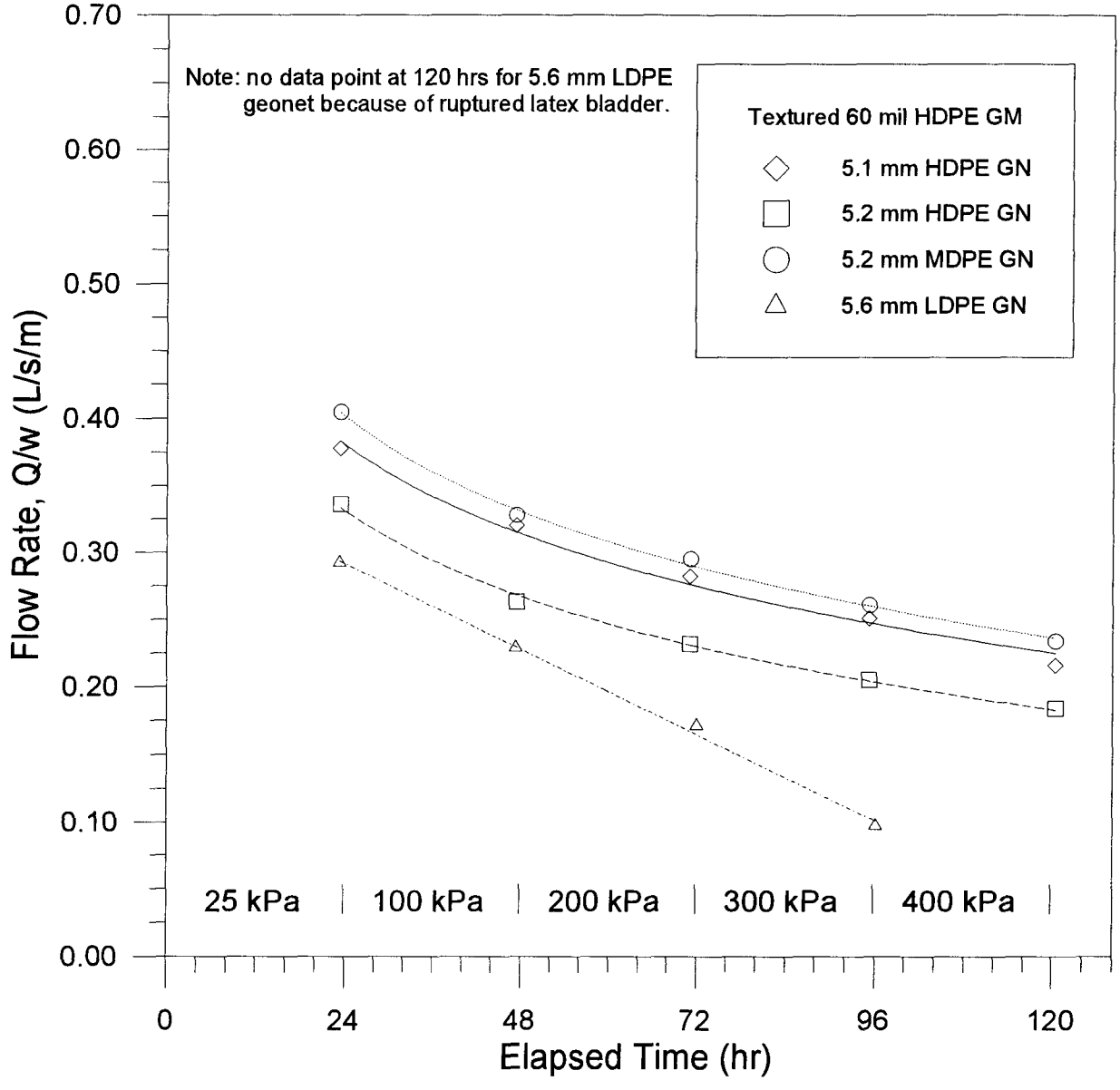

Figure 5.14 Flow Rate of Textured 60 mil Geomembrane at 0.06 Gradient (24 hour reading at each pressure)

- The ranking of the geonets coincides with their polymer density. The higher density geonets have a higher compressive strength which tend to compress or creep less under pressure; therefore, higher density geonets tend to resist flow reduction with increasing pressure because the flow channels stay open.

The test results presented in this section had the effects of both intrusion and creep, but it is possible to separate them. The tests with the metal plates were completed with this purpose in mind; using the data from these tests will allow the effects of intrusion and creep to be examined separately.

5.2.1 Intrusion

Intrusion refers to the action by which a geomembrane is pushed into the apertures or openings of a geonet, see Fig. 5.15, thereby reducing the size of the flow channels and causing a decrease in the flow rate. Typically, the two main factors controlling the amount of intrusion are the imposed normal stress and the stiffness of the geomembrane or adjacent construction material.

In order to examine the effects due to intrusion, it is necessary to isolate the effects of intrusion from the test results. As previously mentioned, the tests with the metal plates, see Fig. 5.16, were done for this purpose. The test was performed for each geonet under the same test procedures used for series W. As before, the data was reduced to facilitate curve fitting; the 96 hour reading for the 5.2 mm MDPE geonet was not included in the curve fit because it is inaccurate. Three of the geonets are linear and have shallower slopes than the tests performed with geomembranes. The 5.6 mm LDPE geonet has a concave-down shape which is nearly identical to those obtained from the tests performed with geomembranes.

The metal plates are rigid and cannot intrude into the flow channels of the geonets; therefore, any reduction in the flow rate is due to compression of the geonet or short term creep (creep will be discussed in the following section). Hence, the reduction in flow rate attributed to intrusion may be obtained from subtracting the results of the metal plate tests (compression only) from the overall test results (intrusion and compression) for each geomembrane combination. The results of the smooth geomembrane are shown on Figures 5.17 to 5.20. The vertical scale

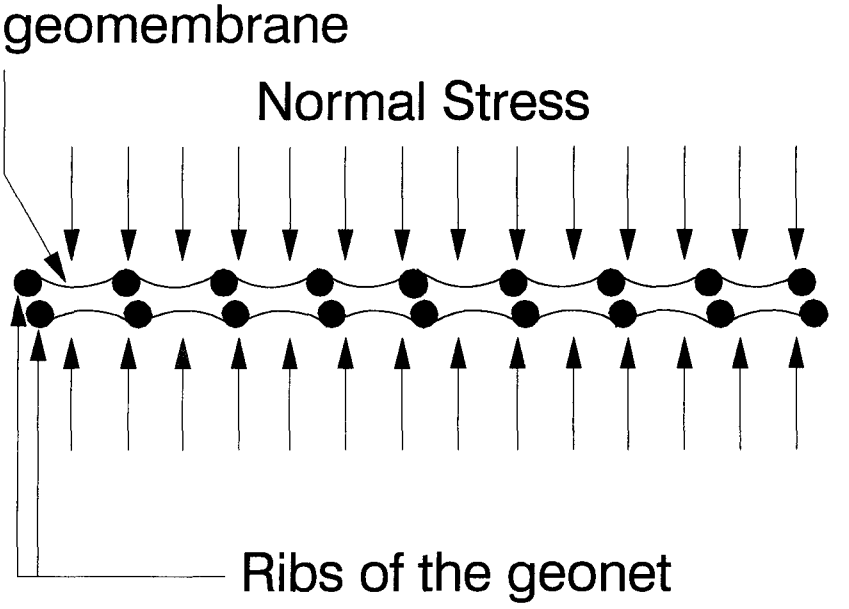

Figure 5.15 Geomembrane Intruding into Flow Channels of a Geonet

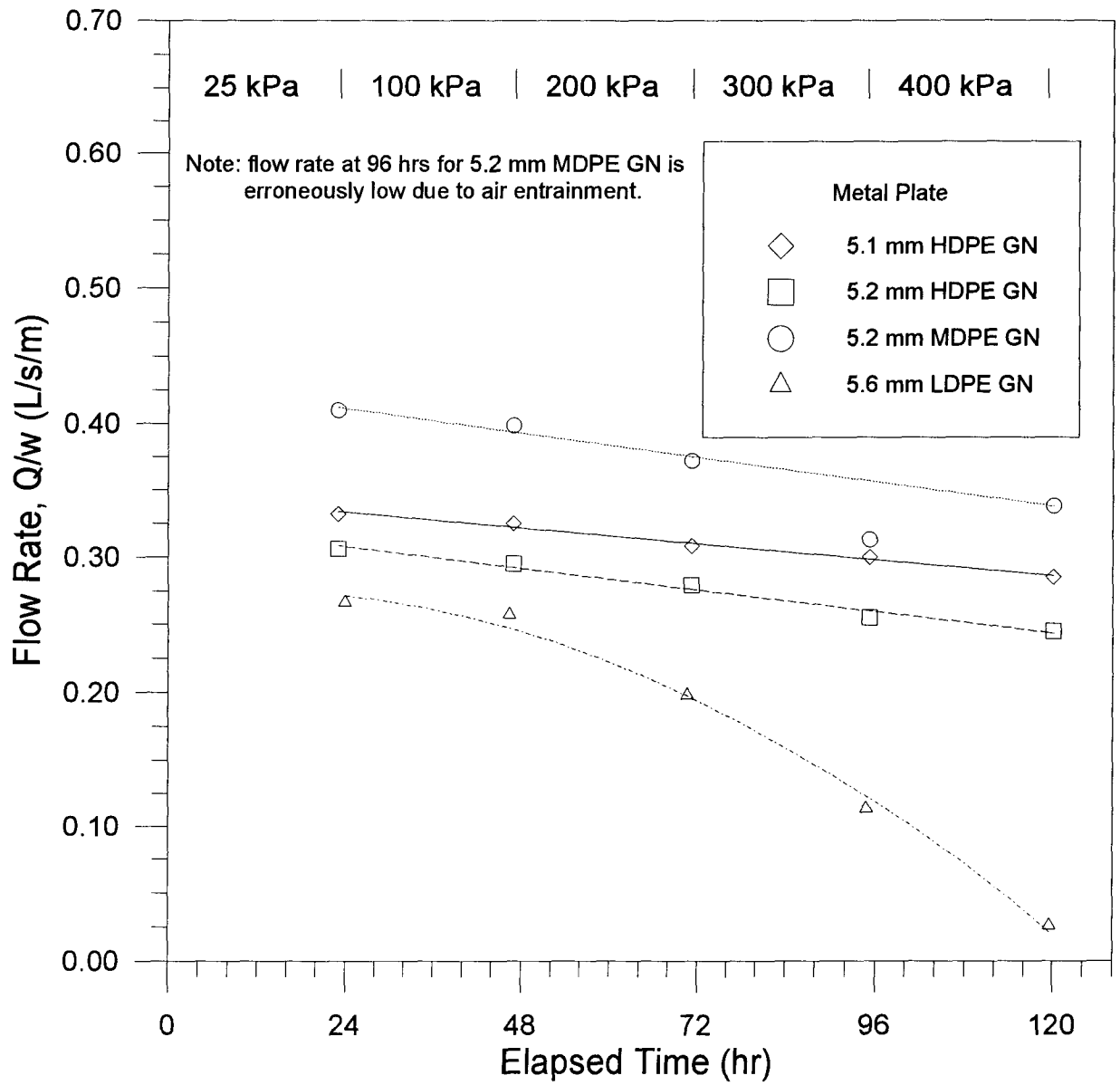

Figure 5.16 Flow Rate of Metal Plate at 0.06 Gradient (24 hour reading at each pressure)

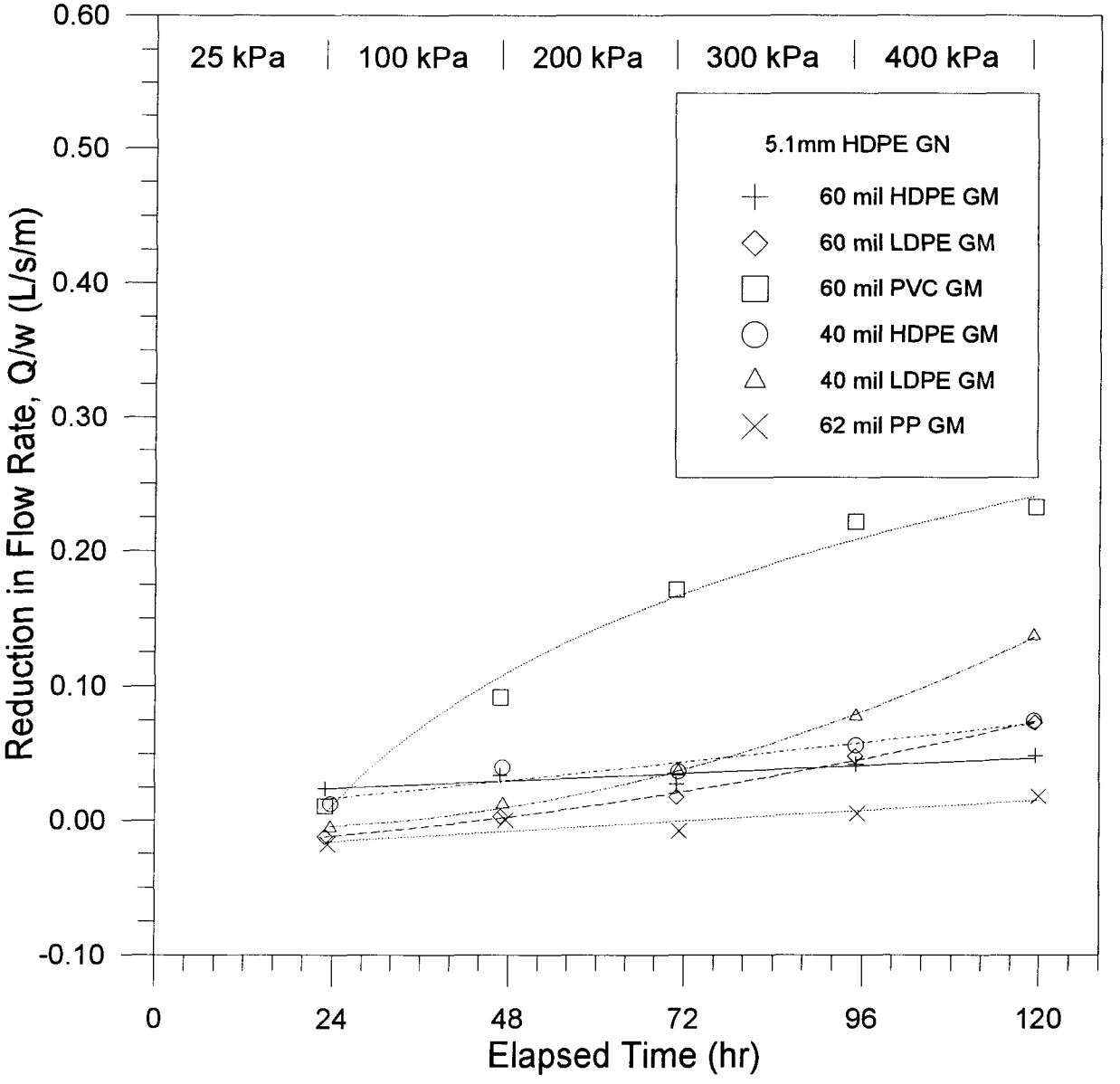

Figure 5.17 Reduction in Flow Rate of 5.1 mm HDPE Geonet at 0.06 Gradient due to Intrusion (24 hour reading at each pressure)

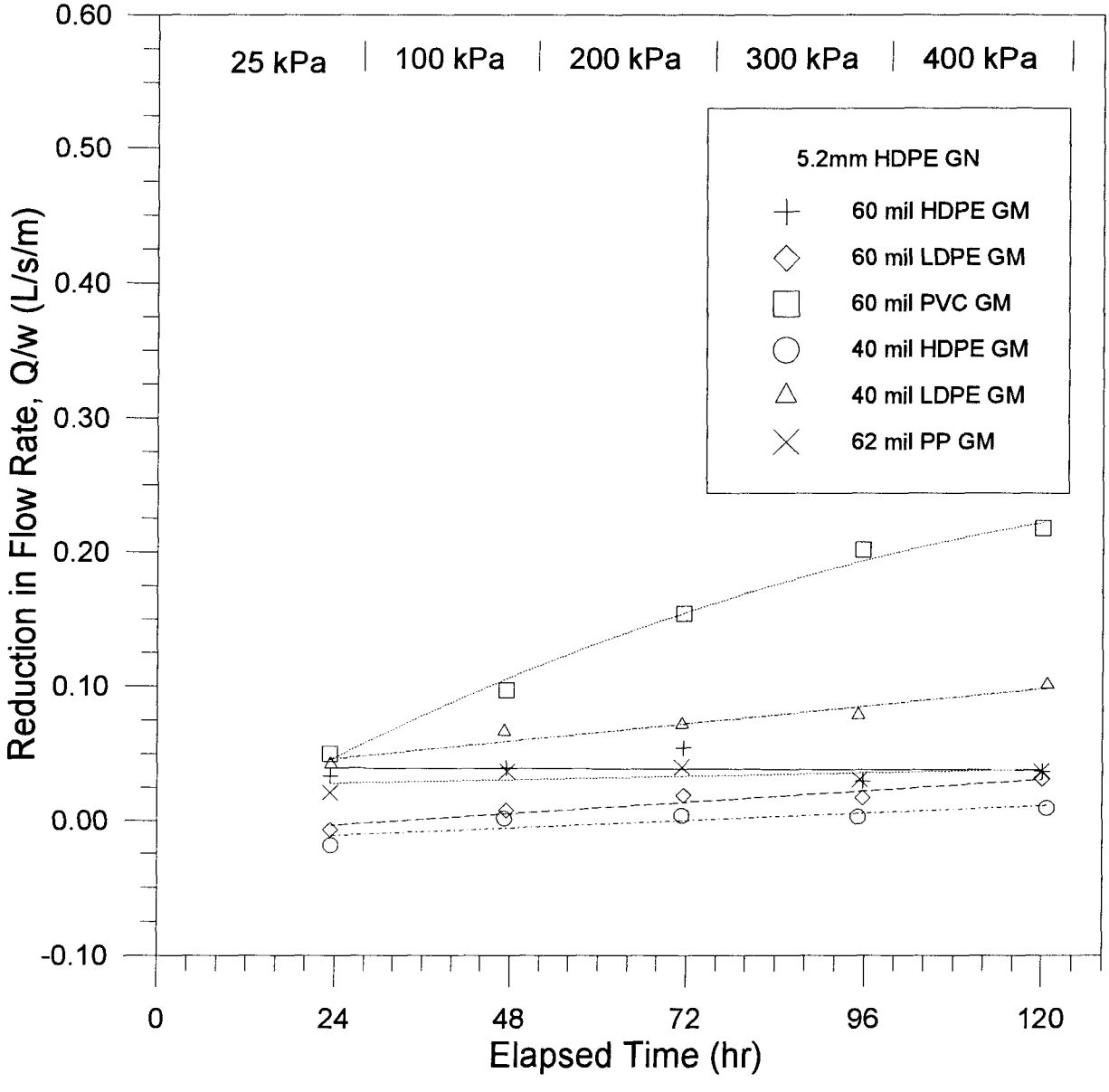

Figure 5.18 Reduction in Flow Rate of 5.2 mm HDPE Geonet at 0.06 Gradient due to Intrusion (24 hour reading at each pressure)

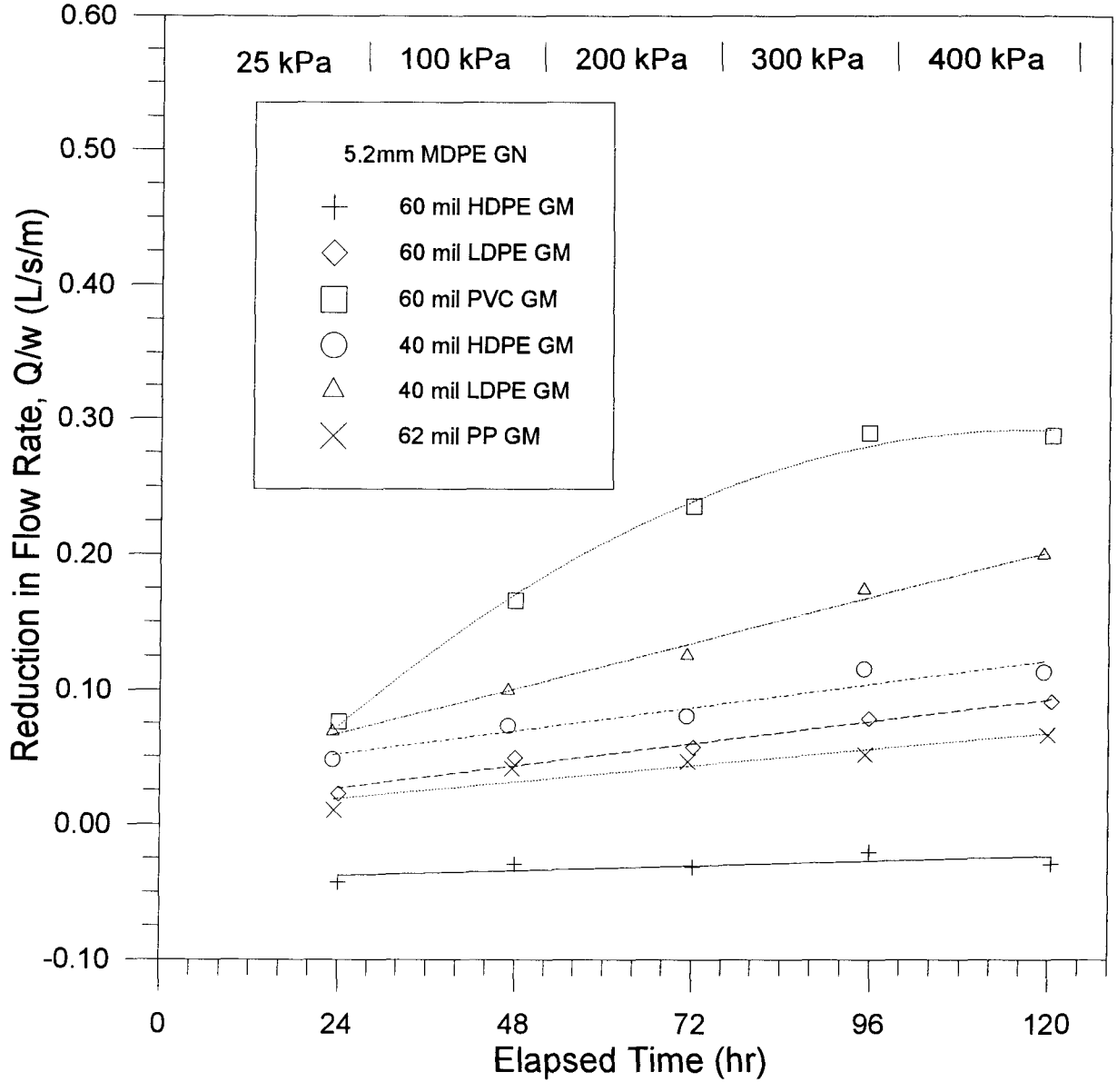

Figure 5.19 Reduction in Flow Rate of 5.2 mm MDPE Geonet at 0.06 Gradient due to Intrusion (24 hour reading at each pressure)

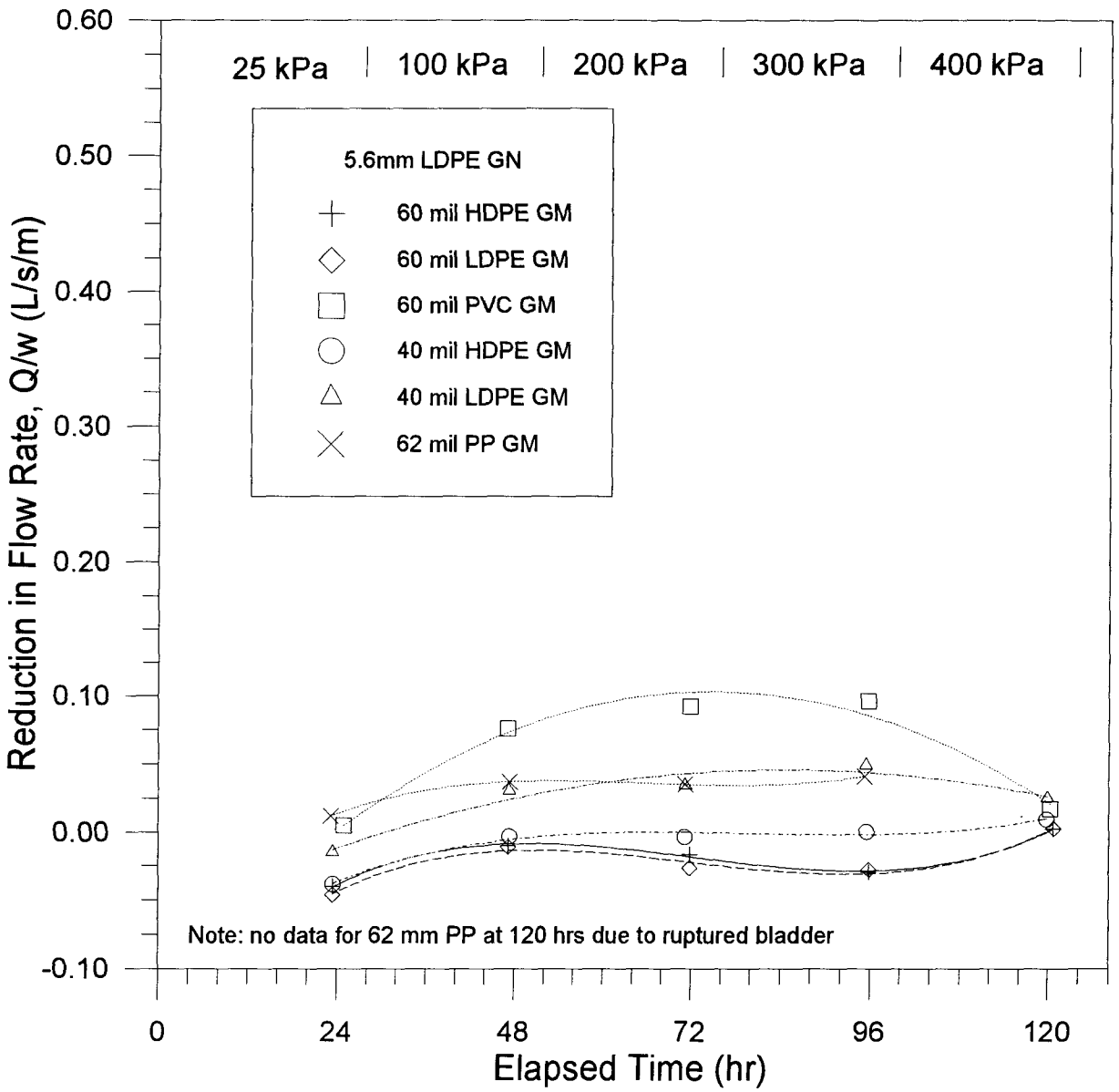

Figure 5.20 Reduction in Flow Rate of 5.6 mm LDPE Geonet at 0.06 Gradient due to Intrusion (24 hour reading at each pressure)

for these figures is the reduction in flow rate due to intrusion. The figures have some points below zero; this an indication of the resolution of measurement. The resolution varies from about 0.025 L/s/m for the 5.1 mm HDPE to about 0.05 L/s/m for the 5.2 mm MDPE geonet. These values represent about 10%-15% of the flow rate which is a within resolution tolerance levels discussed in section 3.4.2.

Figures 5.17 to 5.19 display similar results to those of the combined pressure effects except the slopes are positive instead of negative (due to the convention used for the vertical scale). Hence, it is possible to rank the geomembranes as before, except the ranking is based on the decrease in flow rate due to intrusion only. The order is the same as before: 60 mil HDPE, 62 mm PP, 40 mil HDPE, 60 mil LDPE, 40 mil LDPE, and 60 mil PVC.

The 5.6 mm LDPE geonet combinations, see Fig. 5.20, have all six curves with polynomial shapes; the 60 mil PVC and 40 mil LDPE are 2nd polynomials and the others are 3rd polynomials. As with the overall results, the intrusion results from this geonet do not match the behavior of the other three geonets. Due to the shape of the curves, it is not possible to rank the geomembranes.

The most prominent feature of these results is that all of the data points merge towards zero at 120 hours. This indicates that there is no net reduction in the flow rate at 400 kPa for any of the geomembranes due to intrusion. This does not mean that there is no intrusion; it means that at 400 kPa, the creep or compression of the geonet dominates and most of the flow reduction is due to compression of the geonet. A clearer understanding of the behavior may be obtained from examining the 60 mil PVC curve. After 24 hours at 25 kPa, there is little or no flow reduction due to intrusion, but flow reduction due to intrusion occurs at 100 kPa and increases marginally at 200 kPa and 300 kPa. Then at 400 kPa, the net reduction in the flow rate due to intrusion is zero. This behavior indicates that the geonet is controlling the behavior at the moderate to high pressures. At low pressure, intrusion of the geomembrane into the geonet is significant, but at higher pressures, compression of the geonet dominates the overall reduction in flow rate and intrusion is insignificant.

The amount of intrusion of the same geomembrane is not equal for each of the geonets.

The varying geometry between the geonets, see Fig. 3.9, must control the relative amount of intrusion and is summarized in Table 5.2. (the LDPE geonet is not used in the comparison due to its different behavior).

Table 5.2 Physical Characteristics of the Geonets

	5.1 mm HDPE	5.2 mm HDPE	5.2 mm MDPE
flow channel width [1]	9 mm	8.5 mm	9 mm
orientation of flow channel [2]	31°	35°	26°
shape of ribs [3]	rectangular-trapezoidal	trapezoidal	trapezoidal

1. Measured from inside edges at the top of the ribs forming the channels
2. Measured from line of direct flow through testing device
3. Cross sectional shape of rib

Those geomembranes exhibiting the same shape for all three geonets (60 mil HDPE, 62 mil PP, and 60 mil PVC) should be used for comparison. The resulting ranking (in order of least amount of intrusion) is the 5.2 mm HDPE geonet followed by the 5.2 mm MDPE and the 5.1 mm HDPE. From the data above, the only characteristic consistent with the ranking of the geonets with respect to intrusion is the flow channel width. Note that the flow channel width is measured from the inside edges of the ribs, but at the top of the ribs. Due to the shape of the ribs, the width of the flow channel is different at the bottom of the ribs. If the width is taken from the bottom, then the 5.2 mm HDPE geonet would have a width of 6 mm and the other two geonets would have widths of 7 mm. This is consistent with the previous order of measurements. Intuitively, the width of the flow channel should be a main factor in the anticipating amount of intrusion. The ribs act as fixed supports for the geomembrane which behaves like a bending beam between the ribs; the further apart the supports, the more bending that occurs. Naturally, the shape of the ribs may have an effect on the width of the flow channel, but it appears that the width of the flow channel dominates the behavior with respect to intrusion into geonets.

Figure 5.21 presents the intrusion results for the textured geomembrane combinations with the four geonets. Notice the net reduction in flow due to intrusion for the 5.6 mm LDPE geonet is zero; this supports the conclusion that this geonet is controlling the behavior. The

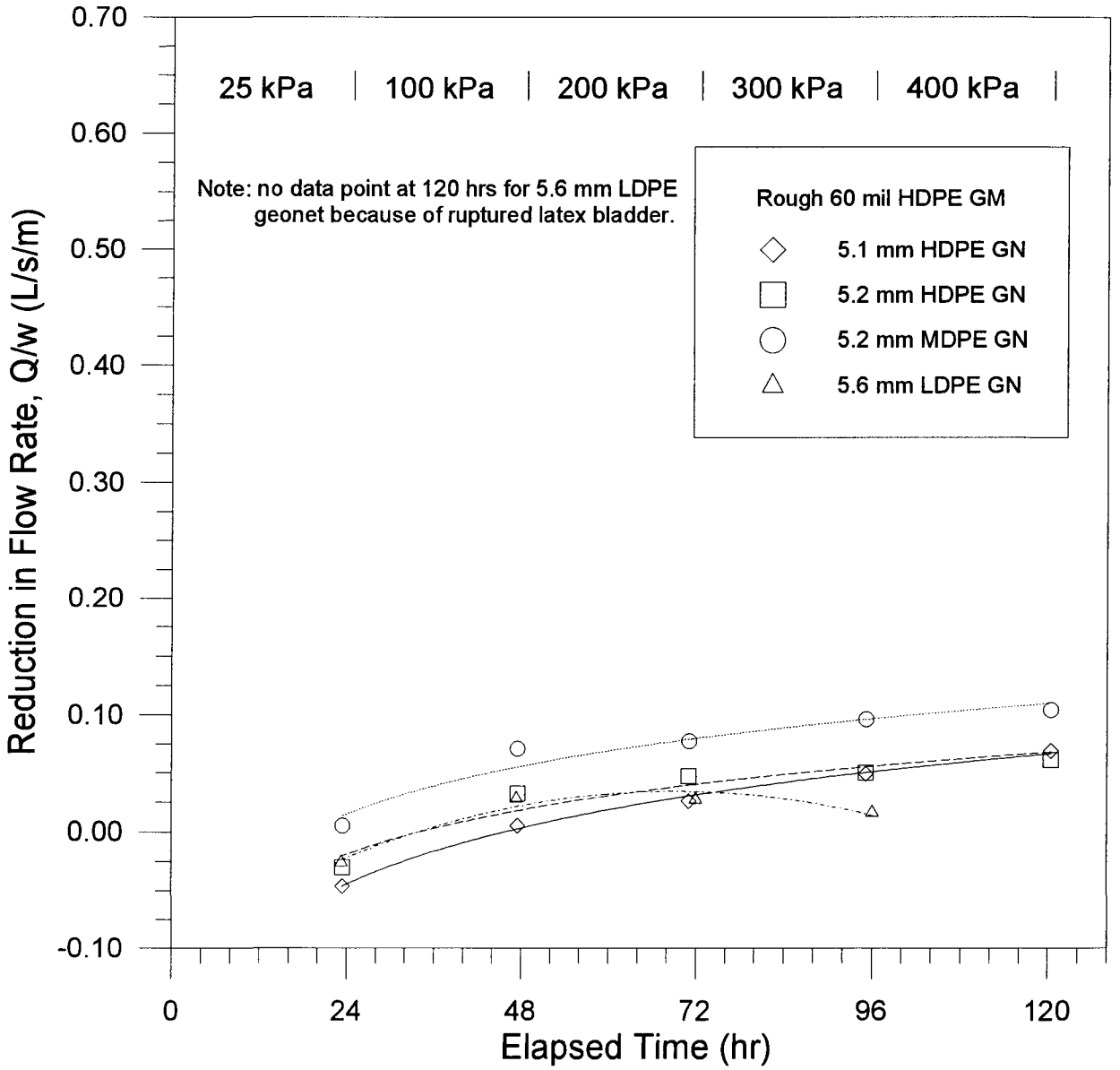

Figure 5.21 Reduction in Flow Rate of Textured 60 mil Geomembrane at 0.06 Gradient due to Intrusion (24 hour reading at each pressure)

other three geonets show higher amounts of intrusion than their smooth geomembrane counterparts which seems intuitive because the extra material used for texturing would block the pore space of the geonets. In addition, the data points for 100 kPa to 400 kPa for the other three geonets lie in a straight line; only the first data point at 25 kPa deviates from linearity because of the relatively large reduction in the flow rate between 25 kPa and 100 kPa (this is the same behavior shown on Figure 5.14 which showed combined effects due to pressure). This large decrease in flow rate was due to seating of the geomembrane at 100 kPa and is attributed to collapse or compression of the textured surface at the ribs of the geonet which allows intrusion of the textured surface into the geonet openings. This means that the reduction in flow rate during the seating period is mostly due to intrusion.

The metal plate tests provided a means of separating the components of intrusion and creep resulting from imposed normal stresses. The resulting analyses on intrusion allows the following conclusions to be drawn:

- The reduction in flow rate of the 5.6 mm LDPE geonet is nearly all due to compression of the geonet.
- The ranking system previously developed for the geomembranes on the basis of flow reductions due to combined effects of intrusion and creep holds true with respect to intrusion only. This fact verifies that the geomembrane stiffness controls the relative amount of intrusion.
- The width of the flow channels governs the relative amount of intrusion for geonets.
- The reduction in flow rate during the seating period is mostly due to intrusion.

5.2.2 Creep

Creep is the continued permanent deformation of a material which occurs at constant stress. Section 5.2.1 addresses intrusion of a geomembrane into the apertures of a geonet which may be partially attributed to creep deformations. The effects of creep on a geomembrane and geonet system are examined in this section using results from the series WLC tests.

Figures 5.22 to 5.25 display the extrapolated lines for the three different geonets and smooth geomembrane combinations and Figure 5.26 displays results of the textured 60 mil

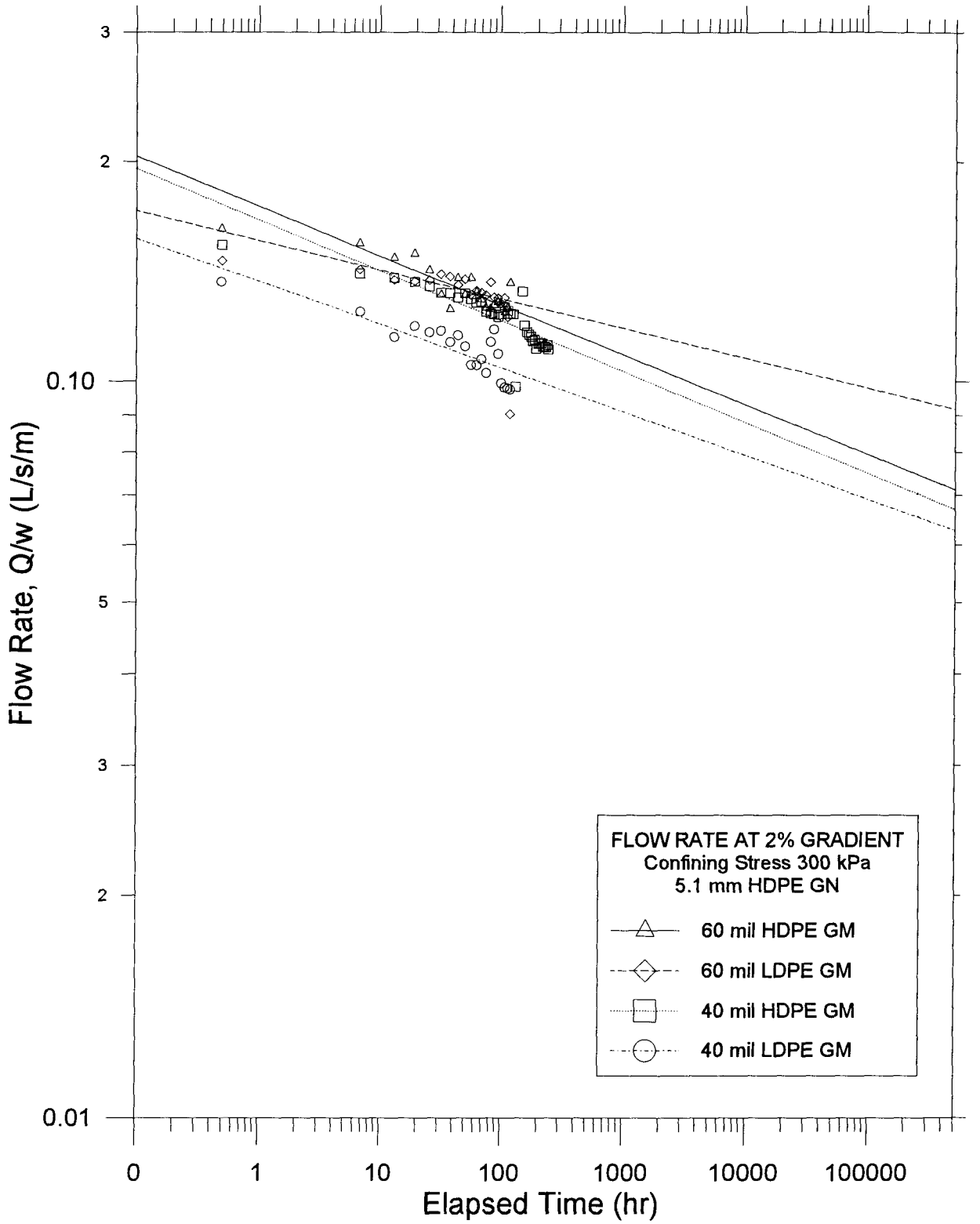

Figure 5.22 Extrapolation of Series WLC Test Results of 5.1 mm HDPE Geonet for Creep Analysis

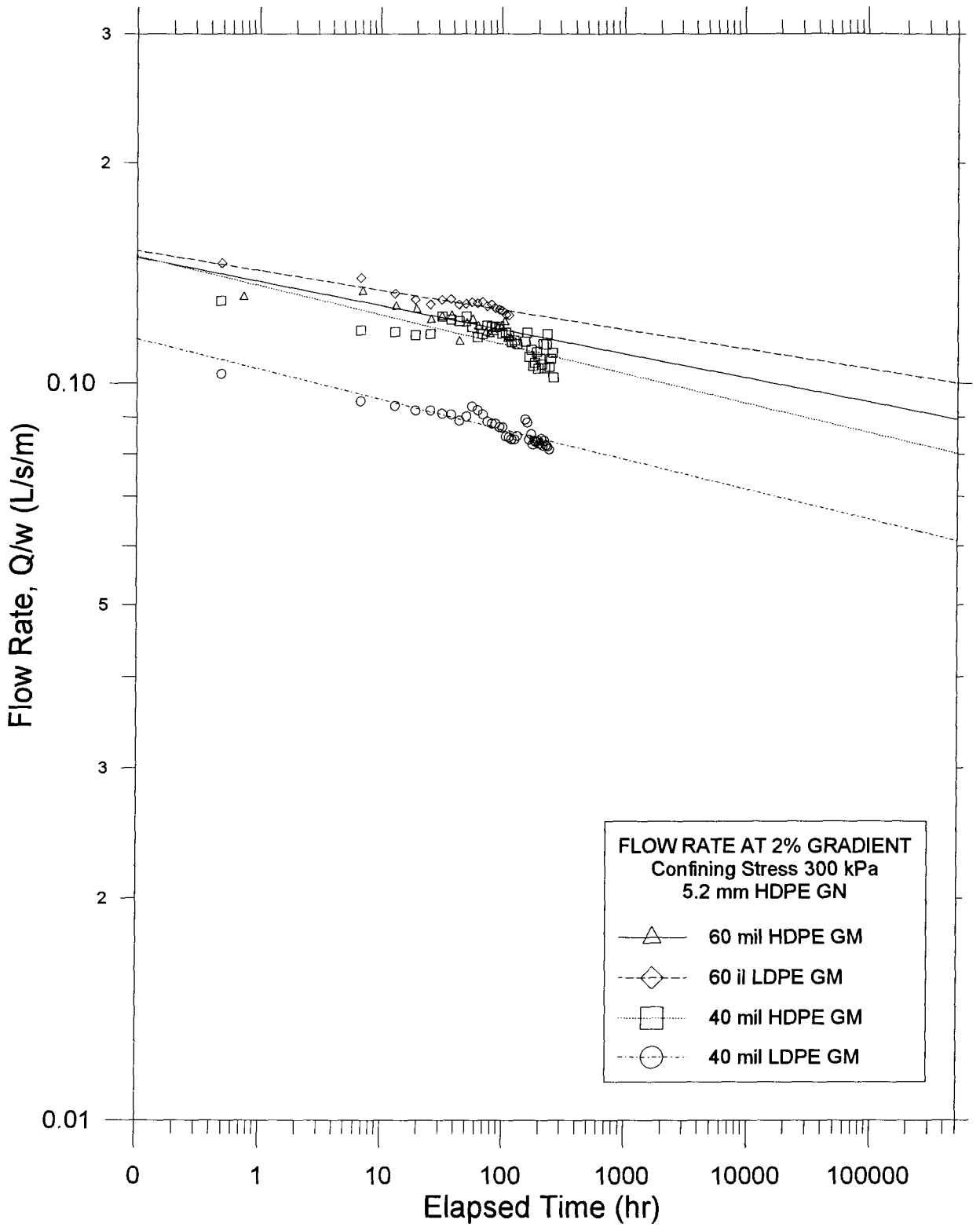

Figure 5.23 Extrapolation of Series WLC Test Results of 5.2 mm HDPE Geonet for Creep Analysis

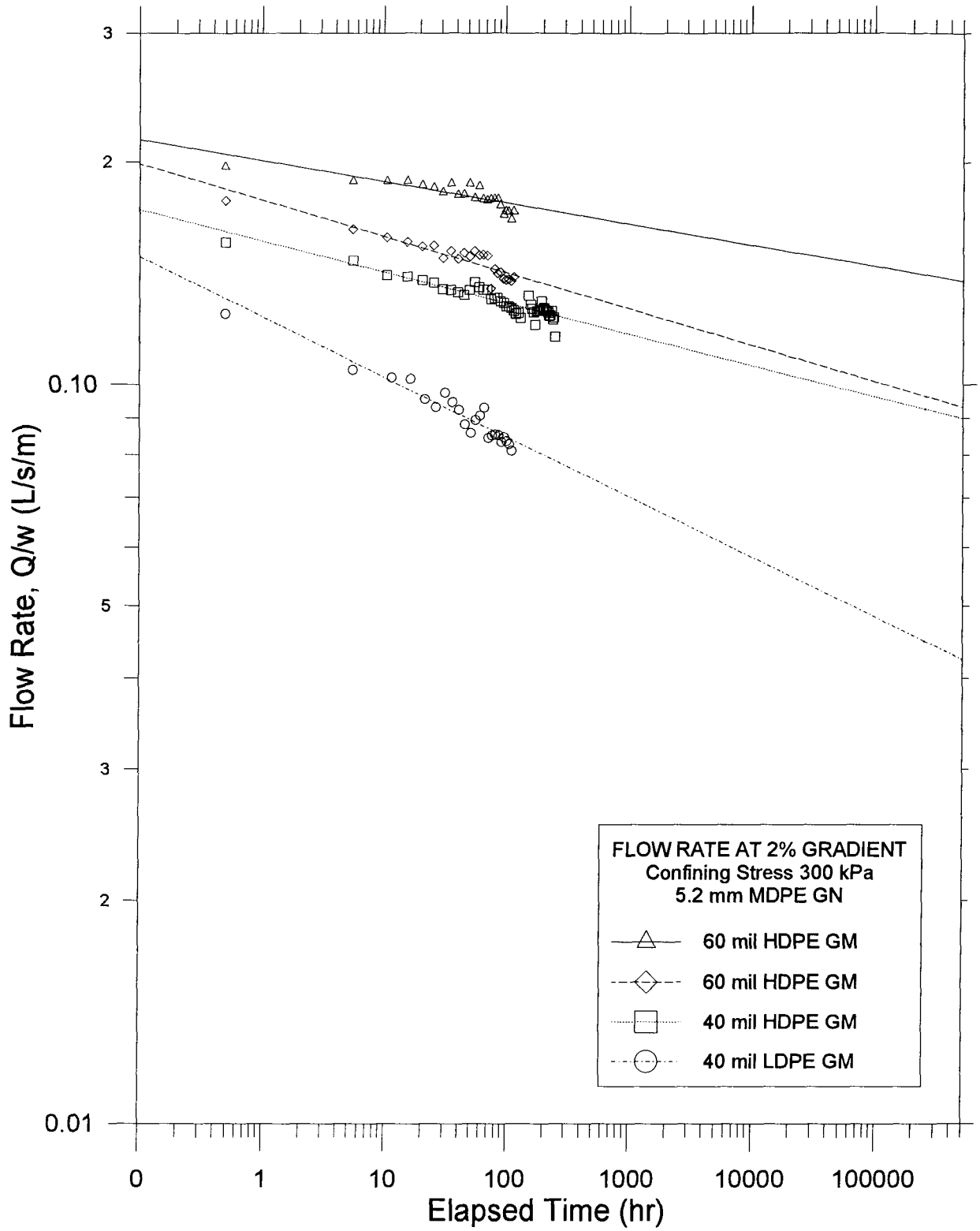

Figure 5.24 Extrapolation of Series WLC Test Results of 5.2 mm MDPE Geonet for Creep Analysis

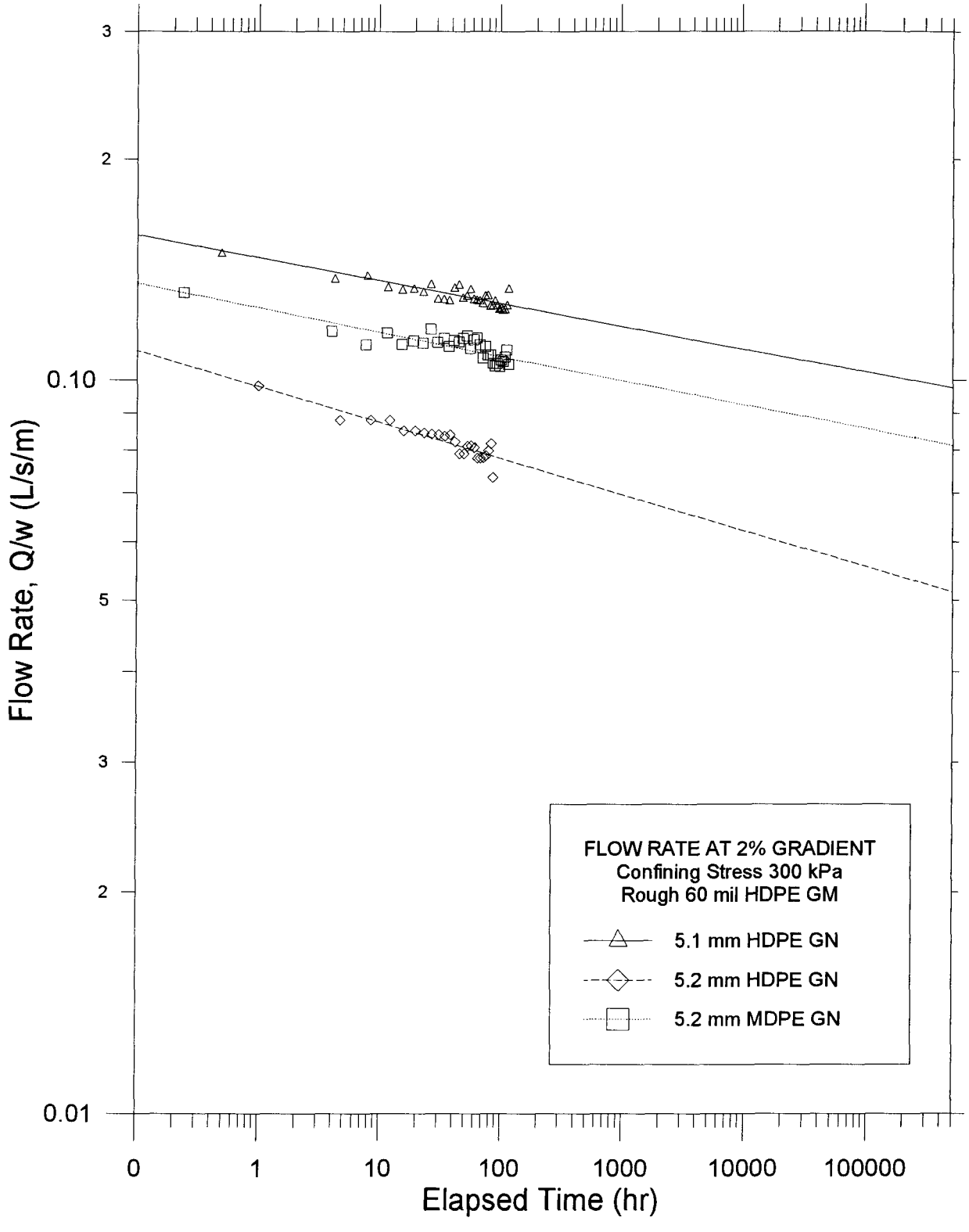

Figure 5.25 Extrapolation of Series WLC Test Results of Textured 60 mil HDPE Geomembrane for Creep Analysis

HDPE geomembrane combinations. Both geomembrane and geonet creep are present in these extrapolations because it is not possible to isolate geomembrane creep from geonet creep in the series WLC tests. Using these extrapolations, the total reduction in flow rate (as a percentage of the initial measured flow rate) due to creep of the geomembrane and geonet can be obtained over an extended period of time; knowledge of this reduction should provide reasonable guidelines for applying a partial factor of safety for creep over the same period. Note that the extrapolations will include the reduction in flow rate over the seating period, but this is not conservative in any way because any geomembrane and geonet combination in the field will also experience a seating period.

These lines may be used to extrapolate the combined creep effects for long term performance. Normally, creep test data may only be extrapolated by one order of magnitude or one log cycle of time; since the longest tests were about 250 hours long, this translates to an extrapolation to 2500 hours or 3.5 months. Unfortunately, this time period is too short to be useful for long-term creep. However, since the data are linear on a log scale, it was assumed that any further extrapolation would also be linear and the data could then be extrapolated by two more log cycles. The extrapolated data would then extend to 250,000 hours or 28.5 years, which is a more realistic time frame for examining long-term creep. The extrapolations were done for both 3.5 months and 28.5 years; the results are shown on Table 5.3. In performing the calculations for the total change in flow rate in percentage, the initial value used was taken from the best fit line and not the first data point because the extrapolations were done using the best fit lines.

The data are grouped in the same manner as the figures for easy comparison and will be examined in the same manner starting with the smooth geomembrane combinations. The 5.1 mm HDPE has 3.5 month flow reductions ranging from 29% to 46% and 43% to 60% at 28.5 years. It is interesting that the total reduction in flow between 3.5 months and 28.5 years is small compared to the first 3.5 months; the latter is two to three times that of the former even though the period is over 28 years longer. It is also interesting that the stiffer geomembrane experiences about the same reduction (in percent) in flow as the semi-stiff geomembrane (40 mil HDPE, 60 &

40 mil LDPE) after only 3.5 months and at 28.5 years (except the 60 mil LDPE). It was expected that the stiffer geomembrane would not creep as much as the semi-stiff geomembranes. The fact that three of these geomembranes experience the same reduction in flow over a sufficient period indicates that the geonet is controlling the creep and that the choice of geomembrane does not matter. This means that the stiff geomembranes have no advantage over the semi-stiff geomembranes in terms of reduction from the initial flow rates. However, the stiff geomembranes generally have higher initial flow rates than the semi-stiff geomembranes.

The 5.2 mm HDPE geonet has total flow reductions ranging from 21% to 32% at 3.5 months and 30% to 43% at 28.5 years. Again, the smallest reductions are experienced by the 60 mil LDPE. The overall reductions for this geonet are less than the 5.1 mm HDPE geonet; this is likely the result of the smaller flow channel width which does not allow as much geomembrane intrusion. Hence, the WLC test data confirm this fact observed from the data of the series W tests (see section 5.2.1 and Table 5.2). Again, the reduction in flow from time zero to 3.5 months is about two to three times as large as the reduction from 3.5 months to 28.5 years.

The 5.2 mm MDPE geonet had flow reductions at 3.5 months ranging from 19% to 52% and at 28.5 years, the range was 36% to 67%. The range in flow reductions for this geonet is the largest of the three at both periods. Part of the reason may be that this geonet always had the highest flow rates so that there was more capacity for reductions and hence, the largest variation. However, it is likely that the geomembranes are partially controlling the behavior; a geomembrane controlled system would likely have a wide range in reductions due to their different degrees of stiffness, whereas, a geonet controlled behavior would produce very similar reductions. The geonet, however, is not without some influence; the very large reduction of 52% and 67% with the 40 mil LDPE geomembrane is likely to be partly caused by the creep of the geonet. Its compressive strength is smaller than its HDPE counterpart and therefore, it is likely to creep more under the same magnitude of stress. This fact is verified by higher total flow reductions with the 5.2 mm MDPE geonet than the 5.2 mm HDPE geonet. Again, the reduction from zero to 3.5 months is larger than from 3.5 months to 28.5 years; however, for this geonet, the ratio ranges from about 1.1 to 3.

Table 5.3 Extrapolation of Measured Flow Rates

		$(Q/w)_{initial}$	$(Q/w)_{lt1}$	$(Q/w)_i$ - lt1/ $(Q/w)_i$	$(Q/w)_{lt2}$	$(Q/w)_i$ - lt2/ $(Q/w)_i$
		Measured Flow Rate at 0.5 hours (L/s/m)	Extrapolated Flow Rate at 2500 hrs (L/s/m)	Relative Change at 2500 hrs (%)	Extrapolated Flow Rate at 250,000 hrs (L/s/m)	Relative Change at 250,000 hrs (%)
51 mm HDPE GN	60 mil HDPE GM	0.178	0.106	-41	0.074	-58
	60 mil LDPE GM	0.161	0.114	-29	0.092	-43
	40 mil HDPE GM	0.175	0.094	-46	0.070	-60
	40 mil LDPE GM	0.145	0.084	-42	0.063	-57
	R 60 mil HDPE GM	0.150	0.114	-24	0.098	-35
52 mm HDPE GN	60 mil HDPE GM	0.140	0.108	-23	0.091	-35
	60 mil LDPE GM	0.145	0.115	-21	0.101	-30
	40 mil HDPE GM	0.140	0.098	-30	0.082	-41
	40 mil LDPE GM	0.108	0.073	-32	0.062	-43
	R 60 mil HDPE GM	0.100	0.063	-37	0.052	-48
52 mm MDPE GN	60 mil HDPE GM	0.203	0.165	-19	0.131	-36
	60 mil LDPE GM	0.185	0.118	-36	0.092	-50
	40 mil HDPE GM	0.161	0.110	-32	0.091	-44
	40 mil LDPE GM	0.131	0.063	-52	0.043	-67
	R 60 mil HDPE GM	0.132	0.094	-29	0.082	-38

The textured geomembrane combinations are considered separately because they behave differently than the smooth geomembranes. The 3.5 month reductions vary from 24% to 37% and the 28.5 year reductions range from 35% to 48%. As with the smooth geomembranes, the reduction from zero to 3.5 months was about twice that from 3.5 months to 28.5 years. Therefore, the textured geomembranes show a similar trend even though the magnitude of total flow reduction is slightly less than the smooth geomembrane counterparts.

From the results of the extrapolations summarized in Table 5.3, it is clear that the majority of the total flow reduction occurs within a short time. Approximately two-thirds of the reduction experienced over 28.5 years is realized by 3.5 months. Of course, a large portion of the reduction in the first 3.5 months is due to the seating period; Figures 4.15 to 4.18 in section 4.3 clearly illustrate this fact. The reduction in flow during the seating period of 24 hrs. is about half of the total reduction over 3.5 months. However, for design purposes, it is necessary to know what the long-term reductions will be, and to account for them using a factor of safety for creep and intrusion, as shown by equation 9 below:

$$(Q/w)_{lt} = \frac{(Q/w)_{initial}}{FS_{ci}} \qquad (9)$$

and

$$FS_{ci} = FS_c \times FS_i \qquad (10)$$

where,

$(Q/w)_{lt}$ = long term flow rate per unit width
$(Q/w)_{initial}$ = initial measured flow rate per unit width
FS_{ci} = factor of safety for creep and intrusion
FS_c = factor of safety for creep
FS_i = factor of safety for intrusion

For the 5.1 mm HDPE, 5.2 mm HDPE, and 5.2 mm MDPE, the factor of safety for creep and intrusion (FS_{ci}) are 2.5, 1.75, and 3.0, respectively (for 300 kPa pressure and 28.5 year period and an initial seating period of 0.50 hrs.). These factors of safety were obtained using the greatest reduction in flow at 28.5 years of the four different smooth geomembranes with each geonet. The initial (0.5 hours after applying confining stress) measured flow capacity of a geonet should be divided by FS_{ci} for long term performance (see equation 9).

These results are based on extrapolations over three log cycles which is a limitation of the results presented and should be verified by creep tests of longer duration. Koerner (1990) discusses 1000 hr creep tests on geonets and states that this is too short a period because extrapolation of trends beyond one log cycle of time is questionable. He further states that a minimum 10,000 hr test would allow extrapolation to 100,000 hrs (11 years) which just begins to get into the framework of life expectancy of these engineered systems. Based on these comments, a facility with a 30 year life expectancy would require creep tests for a minimum of 3 years or 26,300 hours. In addition, the factor of safety for creep and intrusion was obtained using a confining stress between 33% and 44% of the geonets' compressive strength (as reported by the manufacturer). Different ratios of confining stress to geonet compressive strength may result in different factors of safety.

It has been shown that the effect of pressure reduces the flow capacity because of intrusion and creep. These two factors must be taken into consideration when comparing the available flow capacity of synthetic materials to natural material for design purposes. Typically, the velocity of the fluid in a sand is slower than flow through a geonet. Also, natural materials may compress slightly under pressure, but they do not experience the same amount of flow reduction as the geosynthetic materials as a result of pressure. Hence, the factor of safety for creep and intrusion must be applied to the geosynthetic materials before comparing available long term flow capacities. Figures 5.26 to 5.28 compare the available flow capacities of geosynthetics to natural materials for various gradients after applying a factor of safety for creep and intrusion for the geosynthetics (see equation 9). The flow rate of the natural materials are calculated using equation 6 (assumes Darcy's law is valid i.e. laminar flow) based on a minimum 0.75 m thickness as outlined by the B.C. regulations. The geosynthetic comparisons are done using a moderate pressure of 200 kPa with all four geonets and with stiff and semi-stiff geomembranes.

Figure 5.26 compares the flow rates of the 5.1 mm HDPE geonet with those of the granular materials. The two geomembrane combinations shown are the 60 mil HDPE and the 40 mil LDPE which typically represent the fastest and the slowest flow rates of the materials tested for creep. The hydraulic conductivity of the granular soils range from 0.00001 m/s to 0.1 m/s;

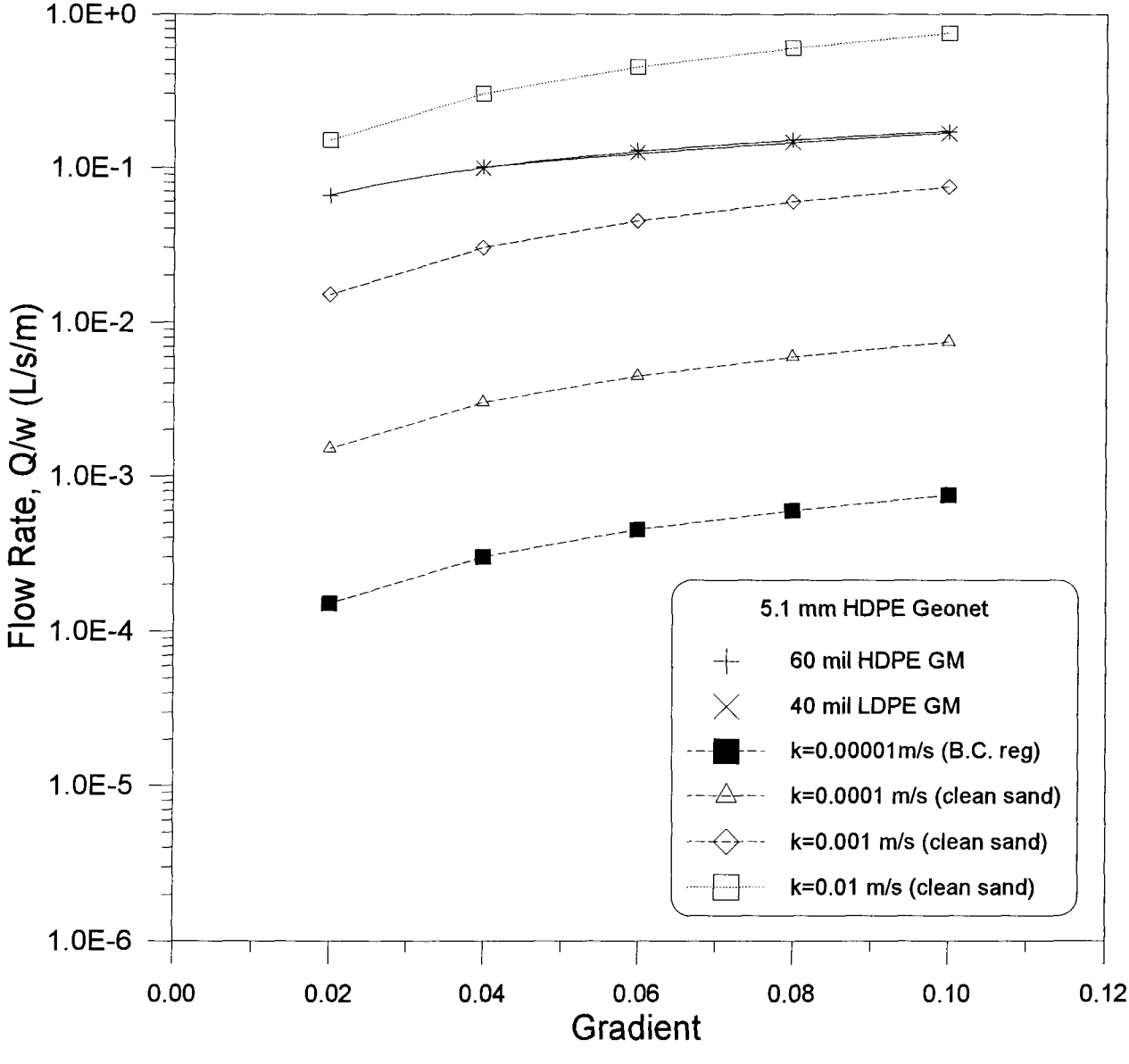

Figure 5.26 5.1 mm HDPE Geonet vs. Granular Soil Flow Capacity (geosynthetic flow rates at 200 kPa and 28.5 years)

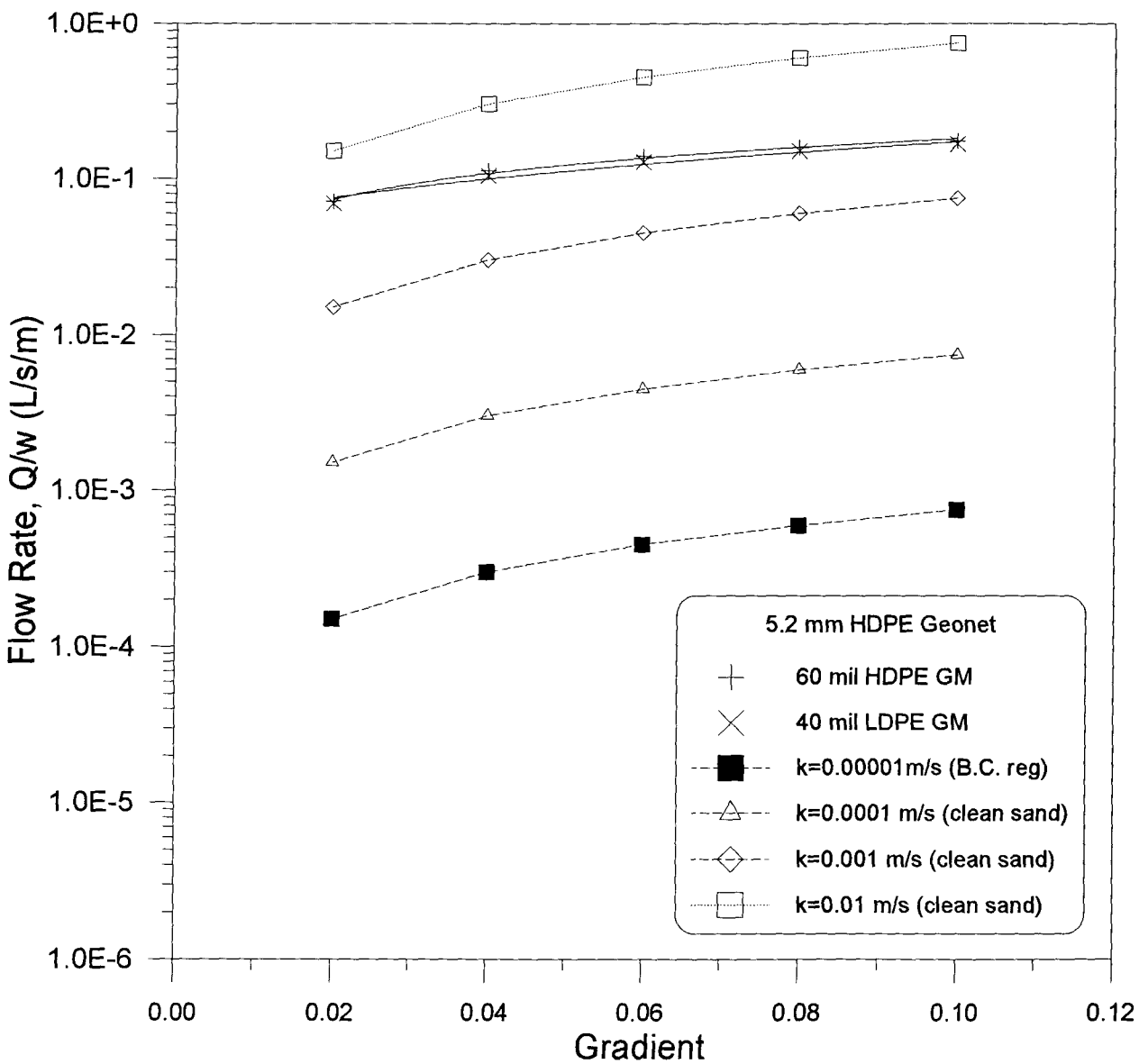

Figure 5.27 5.2 mm HDPE Geonet vs. Granular Soil Flow Capacity (geosynthetic flow rates at 200 kPa and 28.5 years)

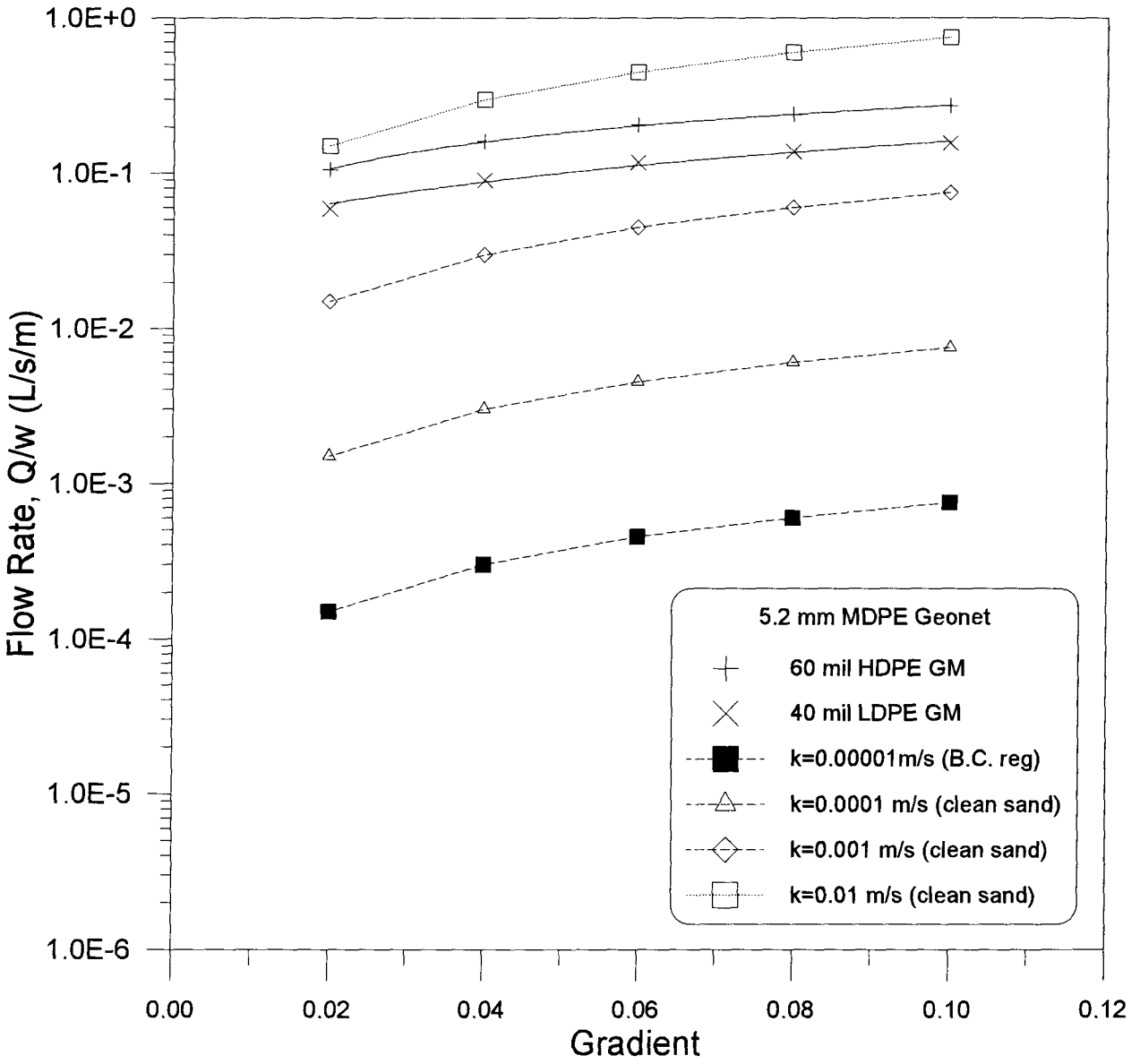

Figure 5.28 5.2 mm MDPE Geonet vs. Granular Soil Flow Capacity (geosynthetic flow rates at 200 kPa and 28.5 years)

this range of k values is representative of B.C. regulations minimum standard for leachate collection and clean sands (Freeze and Cherry, 1979). The granular flow capacities are not linear with the gradient because of the logarithmic vertical scale. Notice the wide range in flow capacities of the natural materials compared to the geosynthetics; the natural materials span several orders of magnitude, whereas the geosynthetics only vary slightly. From the comparison, it is apparent that the geosynthetics are approximately equivalent to a natural material having a hydraulic conductivity of about 0.04-0.06 m/s depending on the gradient. The other geonets shown on Figures 5.27 to 5.28 have similar flow capacities. This indicates that the choice of geonet (HDPE or MDPE) does not matter when compared to the flow capacity of granular soils at 200 kPa and 28.5 years. It appears that the choice of geonet (HDPE or MDPE) does not alter the long term flow capacity, whereas the geomembrane alters the long term flow capacity by a factor of about 2 (see Fig 5.28). This variation in flow rate among the geosynthetics tested (200 kPa, 28.5 years) is very small compared to the several orders of magnitude for the granular soils. However, the variation in flow rate would be larger if the PVC geomembrane or the LDPE geonet were used. At the moderate confining stress of 200 kPa and at 28.5 years, the PVC has a lower flow rate than the others shown by a factor of about 2; the LDPE geonet has similar flow rates as those shown. However, if the pressure were increased, both these materials would show a flow capacity that would eventually decrease to zero. Therefore, long-term flow capacity of geosynthetics (extrapolated) can be several times that of granular materials provided the proper material combinations are chosen for the design normal stress.

5.3 SUMMARY OF INTERPRETATIONS

Any interpretation of the test results has been made with respect to the influence of gradient and pressure on the flow capacity of a geomembrane and geonet system. These interpretations are summarized below with comments for the implications for design practice.

5.3.1 Influence of Hydraulic Gradient

The series W tests were performed at hydraulic gradients of 0.02, 0.04, 0.06, 0.08, and 0.10 for all geonet and geomembrane combinations. Results indicate that, while higher gradients

produce higher flow rates, the relationship between flow rate and gradient is non-linear, implying that flow is non-Darcian. Analysis of the data using Reynolds number and the method described by Cedergren (1989) showed that the flow regime was semiturbulent to turbulent for all geonet and geomembrane combinations. Interpretation of the data suggests the relative permeability of the geosynthetics is equivalent to that of a 1/2 inch to 3/4 inch gravel.

5.3.2 Influence of Confining Stress

The immediate application of a confining stress causes the geomembrane and geonet to bind together over a length of time referred to as the seating period; during this time, the flow capacity of the system decreases. After the seating period, the continued confining stress on the geomembrane and geonet system causes intrusion and creep. Intrusion describes movement of the geomembrane (or adjacent construction material) into the openings of the geonet which reduces the cross-sectional area for flow and leads to a decrease of available flow capacity. Creep occurs over long time periods and describes plastic or permanent deformation at constant load or stress. Creep of a geonet also results in a smaller cross-sectional area for flow and causes a decrease in the flow capacity of the system.

Results of the series W tests were examined to establish the combined effects of intrusion and creep. The flow rate at 24 hour intervals was plotted against time which was the same as confining stress since the stress was increased every 24 hours. Three characteristic responses were identified: concave-up, linear, and concave-down. A ranking system was developed for the response of the smooth geomembranes based on the slope of the curves which represented the rate of decrease of flow capacity with increasing pressure. The ranking system was independent of the shape of the curve: when the same geonet produced different shaped curves, concave-up was ranked higher than linear curves which were higher than concave-down curves. The order of the smooth geomembranes reflects the relative performance of each; the ranking from highest to lowest is: 60 mil HDPE, 62 mm PP, 40 mil HDPE, 60 mil LDPE, 40 mil LDPE, and finally 60 mil PVC. The results are consistent with the relative stiffness of the geomembranes and likely represent the amount of intrusion experienced by each geomembrane. The stiff geomembranes (HDPE and PP) had the smallest flow reduction, the semi-stiff geomembranes (LDPE) had

moderate flow reductions, and the flexible geomembrane (PVC) had a complete loss of flow.

The textured geomembrane combinations were examined separately and were not ranked with the smooth geomembranes because of their different behavior. This geomembrane exhibited concave-up shapes with three geonets and a linear relationship with the fourth geonet (5.6 m LDPE). This behavior is attributed to the textured surface of the geomembrane which does not allow proper seating against the geonet until a sufficient confining stress is applied at approximately 100 kPa.

Since the smooth geomembranes were ranked based on the rate of decrease of the flow capacity, it followed that the geonets can be ranked using the same criteria. In this case, the slope of the best fit lines of the geonets was compared for the same geomembrane. As with the geomembranes, the ranking was independent of the curve shape, but when the same geomembrane exhibited different shapes with the geonets, a linear behavior is ranked higher than a concave-down behavior (there was no concave-up shape). The ranking obtained for the geonets from highest to lowest flow is: 5.2 mm HDPE, 5.1 mm HDPE, 5.2 mm MDPE, and finally, 5.6 mm LDPE. This ranking is consistent with the density of the polymer, but more importantly, consistent with the compressive strength of the geonet. The two HDPE geonets showed little flow reduction with increasing confining stress, the MDPE geonet showed moderate flow reductions and the LDPE geonet showed a complete loss of flow.

The series W tests addressed the combined effects of intrusion and creep, but it was possible to separate these two effects using results of the tests with metal plates. In these tests, any reduction in flow is attributed to creep of the geonet only because the plates are rigid and cannot intrude into the openings of the geonet. The 5.1 mm HDPE experienced the smallest amount of creep followed by the 5.2 mm HDPE, 5.2 mm MDPE, and the 5.6 mm LDPE. Flow reductions caused by intrusion only were then obtained by subtracting the reductions caused by creep of the geonet from the overall flow reductions. The same ranking system for the geomembranes, described above, was verified from examination of the flow reductions due to intrusion. It is concluded that geomembrane stiffness is a major factor controlling the amount of

intrusion. From the geonet perspective, the width of the flow channels was also found to influence the amount of intrusion: narrower channels resulted in less intrusion.

The series WLC tests were performed under a constant confining stress of 300 kPa and hydraulic gradient of 0.02 for a period between 120 and 250 hours, and better indicate the long-term behavior with respect to creep. Since companion metal plate tests were not performed, these test have combined effects of intrusion and creep. Results of these tests were extrapolated by one log cycle (to 3.5 months) and three log cycles (28.5 years) to determine the long term effects of creep. Generally, predictions of behavior extrapolated over more than one log cycles should be interpreted with caution. The predicted total reduction in flow capacity at 3.5 months was between 18% and 52% of the initial measured flow rate depending on the geomembrane and geonet combination; the reduction in flow capacity at 28.5 years ranged from 30% to 67%. For the same geonet, the stiff geomembranes experienced less creep than the semi-stiff or flexible geomembranes. Based on these extrapolations, it is possible to determine a factor of safety for the reduction in flow capacity due to creep and intrusion. Since the three geonets did not exhibit the same flow reductions due to creep, each receives a separate factor of safety based on the upper limit from the extrapolated flow rate; they are 2.5, 1.75, and 3.0 for the 5.1 mm HDPE, 5.2 mm HDPE, and 5.2 MDPE geonets, respectively. The values are pertinent to the imposed test conditions, and will likely vary with applied confining stress, compressive strength of the geonet, and the stiffness of the adjacent geomembranes. For design purposes, the initial measured flow capacity of a geomembrane and geonet system would be divided by FS_{ci} to obtain the available flow capacity at 30 years under a design stress of 300 kPa. If no test data for a particular geonet (HDPE or MDPE) are available, then the upper limit of 3.0 could be used for the factor of safety for the same stress and performance period; however, this value should be verified by an appropriate creep test for the materials in question. An additional factor of safety should be applied for the uncertainty of extrapolating by three log cycles.

The introduction of a sediment into the flow illustrated the reductions encountered in the flow rate as a result of sediment clogging. A small amount of sediment decreased the flow capacity by up to 40%. Fortunately, the flow capacity could be recovered by simply flushing the

sediment; in these tests, the flushing was performed using a hydraulic gradient of 0.06 and 0.10. A gradient of 0.06 produced recovery ratios around 80% and a 0.10 gradient produced recovery ratios of around 93%. Hence, a relatively small driving force was successful in recovering flow capacity lost due to sediment clogging.

Finally, the flow capacities of the various geomembrane and geonet combinations were compared to granular materials which have been traditionally used for leachate collection. In order to compare the different materials, a factor of safety for creep was applied to the flow capacity of the composite test specimen to determine the long term flow capacity. Comparison reveals that the geosynthetic specimens are equivalent to a 0.75 m thick granular soil possessing a hydraulic conductivity of 0.05-0.01 m/s.

6 CONCLUSIONS AND RECOMMENDATIONS

Geosynthetics provide designers of landfills, surface impoundments, and heap leach pads alternative construction materials. When designed and constructed properly, geosynthetics can offer savings in terms of space and construction time which often mean economic savings as well. Unfortunately, available data on geosynthetics used for leak detection systems cannot be readily used for design purposes. Hence, the objectives of the research are:

- an evaluation of the material properties under simulated performance conditions;
- to establish a practical factor of safety to be applied to the in-plane flow capacity for long-term design;
- to provide recommendations for material testing and design of leak detection and removal systems based on the results of the research.

Conclusions from this study are presented, followed by recommendations for materials testing and design. Finally, the need for further research is discussed.

Materials Testing:

- From the series WLC tests, it was apparent that the seating period could last up to 24 hours; during that time, the flow capacity continued to decrease. Therefore, ***seating periods should be standardized before data is recorded.*** Clearly, if testing laboratories begin recording data after different seating periods, results between laboratories will never be consistent and it will be impossible to compare results. This holds true for tests on the same materials as well as different materials. A 24 hour seating period would appear to be sufficient, however, due to time restraints, a standardized seating period of 1 hour may be more reasonable.
- The ASTM test for transmissivity or flow capacity uses metal plate boundaries which are rigid and do not allow for intrusion into the geonet; therefore, geomembranes in contact with a geonet cannot be simulated with this test setup. From the test results presented here, geomembrane intrusion is a major factor in determining the available flow capacity and should not be discounted. In the series W tests, the rigid metal plates did not permit intrusion and had flow capacities approximately 60% higher than the average geomembrane/geonet composite. Therefore, ***boundaries should simulate field conditions.***

- The tests performed at a 0.02 gradient were very sensitive to small fluuctuations in gradient and variations in the flow capacity were common. It is perceived that testing at a lower gradient would result in greater fluctuation due to even greater sensitivity. Therefore, ***a 0.02 gradient should be the minimum hydraulic gradient used in testing***.

Design:

- The initial flow rate of geosynthetic leak detection systems tested in this study ranges from about 0.15 - 0.45 L/s/m (corresponding transmissivity of 0.0075 - 0.0045 m^2/s); the actual value depends on the material combinations, the confining pressure, and the hydraulic gradient. The flow rate or transmissivity decreases due to geomembrane intrusion, geonet compression and creep (geomembrane and geonet); the magnitude of the decrease also depends on the material combination, the confining stress, and the hydraulic gradient.
- From the response of the low density geonet, it is clear that the geonet compresses significantly even before its ultimate crush strength is reached. In fact, collapse of the rib structure occurred at about 80% of its compressive strength. The MDPE geonet also showed significant decreases in its flow capacity with increasing confining stress. Therefore, ***the geonet compressive strength should be a significantly larger than the design stresses***. In addition, ***air entrained geonets (5.6 mm LDPE) should only be used under relatively low confining stresses e.g. cover systems***.
- The test results indicate that stiffer geomembranes intrude less and as a result, have higher flow capacity. ***Optimizing the flow capacity for a geomembrane/geonet composite requires choosing a stiff geomembrane***. Note that the series WLC creep tests indicated little difference in the percentage reduction in the long-term, the stiffer geomembrane typically had higher initial flow rates than semi-stiff geomembranes, therefore, higher long-term flow capacity. In contrast to the stiff geomembranes, the PVC geomembrane has a great tendency to intrude into the geonet openings at high stress levels which greatly reduces its flow capacity. Therefore, ***PVC geomembranes should only be used in conjunction with geonets under low stresses e.g. cover systems***.

- High compressive strength is desirable to limit flow reductions due to geonet compression as shown somewhat by the MDPE geonet and dramatically by the LDPE geonet. Also, narrower flow channels were shown to allow less geomembrane intrusion. Therefore, ***optimizing the flow capacity involves choosing a geonet with a high compressive strength and large flow channels for maximum flow, but not large enough to allow intrusion***.
- The data from the series WLC tests were extrapolated to 28.5 years and showed a flow reduction ranging from 30% to 67% from the initial measured flow rate. Hence, a ***factor of safety (FS_{ci}) for reduction in flow capacity due to creep and intrusion should be approximately 1.75-3.0 depending on the geonet for a performance period of 28.5 years at 300 kPa.*** The initial measured flow capacity is divided by FS_{ci} to obtain the available flow capacity at 30 years. The factor of safety for creep (FS_c) estimated by Koerner (1990) ranges from 1.4 to 2.0 and 1.5 to 2.0 for intrusion (FS_i); $FS_{ci} = FS_c \times FS_i$. The FS_{ci} values presented should have an additional FS added for the uncertainty of extrapolation over three log cycles.
- The testing with sediments showed good success in restoring the flow capacity up to about 95% of its original value by flushing under a small hydraulic gradient. While not addressed in this study, there is potential for additional decreases in flow capacity as a result of chemical precipitation and biological clogging. Therefore, ***a means of restoring the flow capacity, which may be reduced as a result of sediment or biological clogging and chemical precipitation, should be implemented.***

Further Studies:

A wide and representative range of material combinations and testing conditions were addressed in this program of research. However, additional tests with other textured geomembranes are needed to verify the behavior of textured geomembranes. Also, scrim-reinforced geomembranes are perceived to intrude less than non-reinforced geomembranes, but tests are required for verification

The creep tests performed were of short duration, being less than 300 hours, but they provide a reasonable estimate for the behavior over the long term. However, the test should

really be performed for a period between 3-5 years so that the extrapolation only extends for one log cycle (30-50 years). In addition, several different magnitudes of confining stresses should be applied to check if there is any variation with the factor of safety with confining stress.

The sedimentation testing showed that reduced flow capacity due to sediment clogging can be recovered by flushing. However, these tests were only performed with one sediment and should be done with a wide range of sediments to verify the overall success of flushing.

Full-scale field tests should be performed to eliminate any possible scale effects that may influence laboratory test results. The small sample size used in the laboratory makes the orientation of the flow channels an important issue; the magnitude of the flow rate depends very much on the orientation. Also, the sediments introduced into the flow and then flushed, tended to follow the flow channels, but were stopped by the wall of the test device when the flow channel ended.

REFERENCES

ASTM Subcommittee D 35.03, "Standard Test Method for Constant Head Hydraulic Transmissivity (In-Plane Flow) of Geotextiles and Geotextile Related Products." 1993 Annual Book of ASTM Standards , Volume 04.08 Soil and Rock; Dimension Stone; Geosynthetics. ASTM, Philidelphia, 1993. 1033-36.

Barr, Roger, editor, "1992 Specifier's Guide.", Geotechnical Fabrics Report 9 December 1991.

Canadian Council of Ministers of the Environment (CCME). National Guidelines for the Landfilling of Hazardous Waste. 1991.

Canadian Geotechnical Society, Technical Comittee on Foundations. Canadian Foundation Engineering Manual. 3rd ed. Richmond, 1992.

Caterpillar Inc., "Caterpillar Performance Handbook Edition 19." Peoria, 1988. 881.

Cincilla, W. A., and G. A. Zagorski. "Application of Geosynthetics in the Design of Fully-Drained Mineral Waste Storage Facilities." Geosynthetics'91 Conference Proceedings 1 Altanta 1991. 61-76.

Eith, A. W., and R. M. Koerner, "Field Evaluation of Geonet Flow Rate (Transmissivity) under Increasing Load." Geotextiles and Geomembranes 11 (1992): 489-501.

Environmental Protection Agency (EPA). Lining of Waste Containment and Other Impoundment Facilities. Cincinnati, 1988.

Environmental Protection Agency (EPA). Requirements for Hazardous Waste Landfill Design, Construction, and Closure. Cincinnati, 1989.

Fannin, J. F. "Geosynthetics for Waste of Special Waste." Proceedings of 5th Annual Vancouver Geotechnical Society . Vancouver, 1990.

Feeney, M.T., and A.E. Maxson, "Field Performance of Double-Liner Systems in Landfills." Geosynthetics'93 Conference Proceedings 3 Vancouver 1993. 1373-87.

Freeze, R. Allen, and John A. Cherry, "Groundwater." Englewood Cliffs, 1979.

Halse, Yick H., Arthur E; Lord Jr. and Robert M. Koerner, "Effect of Dissolved Oxygen (and Bubbles) on the Measured Permittivity of Geotextiles." Geotechnical Testing Journal 11, June (1988): 158-60.

Hutwelker, Jan, Thomas Pullar, and Francis Taylor. "The Evolution of Geosynthetics in a Landfill System." Geosynthetics'91 Conference Proceedings 1 Altanta 1991. 31-60.

Hwu, Bao-Lin, Robert M. Koerner and C.Joel Sprague, "Geotextile Intrusion into Geonets." Proceedings of the 4th International Conference on Geotextiles Geomembranes and Related Products 2, The Hague, Netherlands 1990. 493-98.

Koerner, Robert M. "Designing With Geosynthetics." Englewood Cliffs, 1990.

REFERENCES (cont.)

Koerner, Robert M. "Preservation of the Environment Via Geosynthetic Containment Systems." Geotechnical Fabrics Report September/October, 1990, 18-22.

Koerner, Robert M., "Preservation of the Environment Via Geosynthetic Containment Systems." Geotechnical Fabrics Report November 1990, 31-45.

Koerner, Robert M., and John A. Bove, "In-Plane Hydraulic Properties of Geotextiles." Geotechnical Testing Journal, 6, December 1983, 190-95.

Koerner, Robert M., and Gregory N. Richardson. "Design of Geosynthetic Sytems for Waste Disposal." Geotechnical Practice for Waste Disposal '87 . Ed. Richard D. Woods. Geotechnical Special Publication No. 13. New York: American Society of Civil Engineers, Geotechnical Engineering Division, 1987. 65-86.

Kolbasuk, G.M., L.D. Lydick, and L.S. Reed, "Effect of Test Procedures on Geonet Transmissivity Results." Geotextiles and Geomembranes 11 (1992): 479-88.

Landreth, Robert E., "Concerns and Opportunities Involving Geosynthetics and Waste Containment." Geotechnical Fabrics Report September/October 1990, 24-34.

Ministry of the Environment, Parks and Lands. Waste Managemment Act - SpecialWaste Regulations. 1988.

Parker, Roger J., and Mike a. Salier. "Geomembrane Applications in Austalia." Geosynthetics'91 ConferenceProceedings 1 Altanta 1991. 77-86.

Reades, Denys W. et al., "Detailed Case History of Clay Liner Performance." Waste Containment Systems: Construction, Regulation, and Performance. American Society of Civil Engineering (ASCE) Special Geotechnical Publication, 1990. 156-74.

Vaid, YP., and R.G. Campanella, "Making Rubber Membranes." Geotechnical Testing Journal 10, (1978): 644-65.

APPENDIX A

SERIES W TEST RESULTS

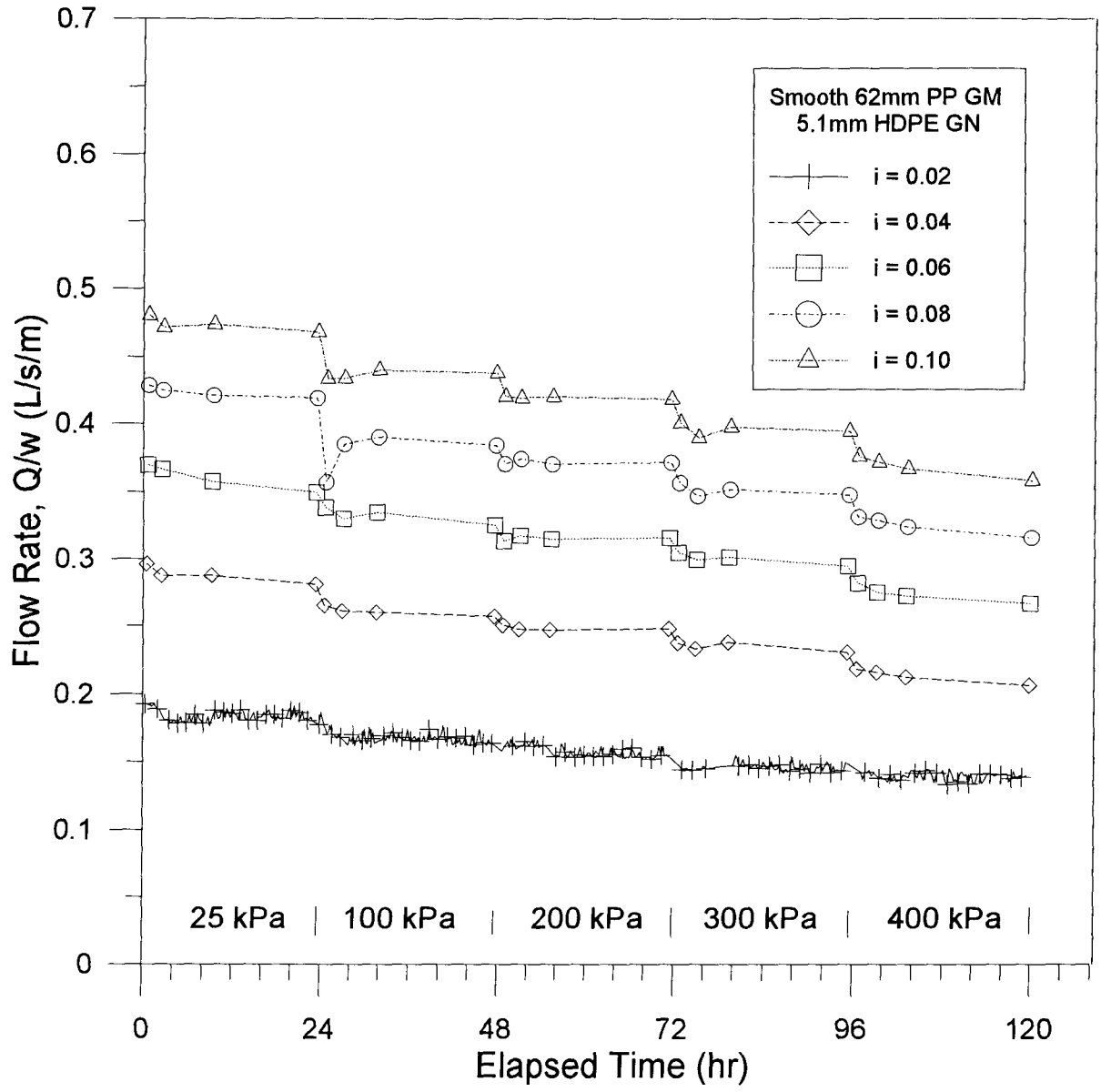
Smooth 62mm PP GM
5.1mm HDPE GN
i = 0.02
i = 0.04
i = 0.06
i = 0.08
i = 0.10
Flow Rate, Q/w (L/s/m)
0.7
0.6
0.5
0.4
0.3
0.2
0.1
0
25 kPa
100 kPa
200 kPa
300 kPa
400 kPa
0
24
48
72
96
120
Elapsed Time (hr)

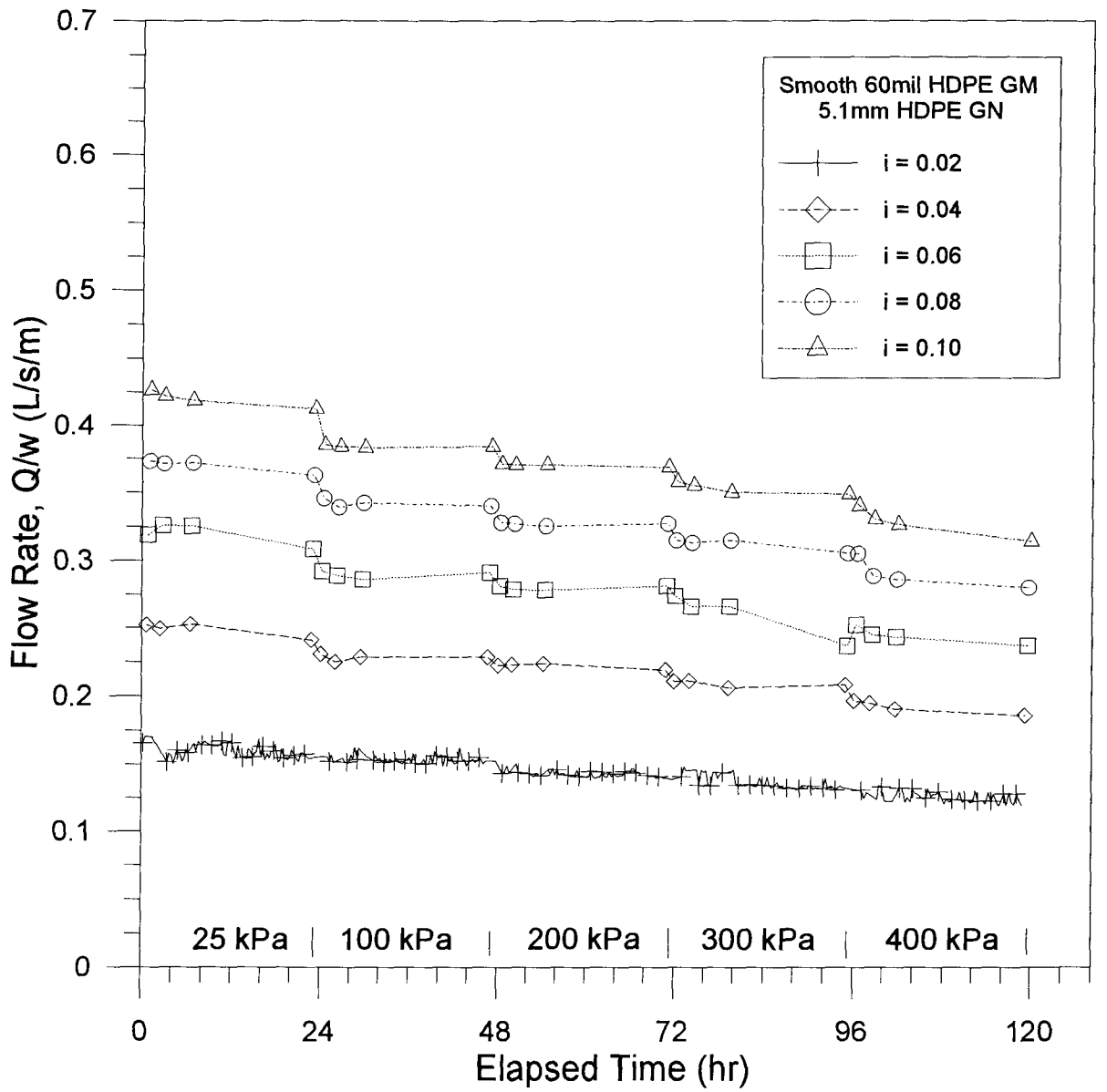
Smooth 60mil HDPE GM
5.1mm HDPE GN
i = 0.02
i = 0.04
i = 0.06
i = 0.08
i = 0.10
Flow Rate, Q/w (L/s/m)
0.7
0.6
0.5
0.4
0.3
0.2
0.1
0
25 kPa
100 kPa
200 kPa
300 kPa
400 kPa
0
24
48
72
96
120
Elapsed Time (hr)

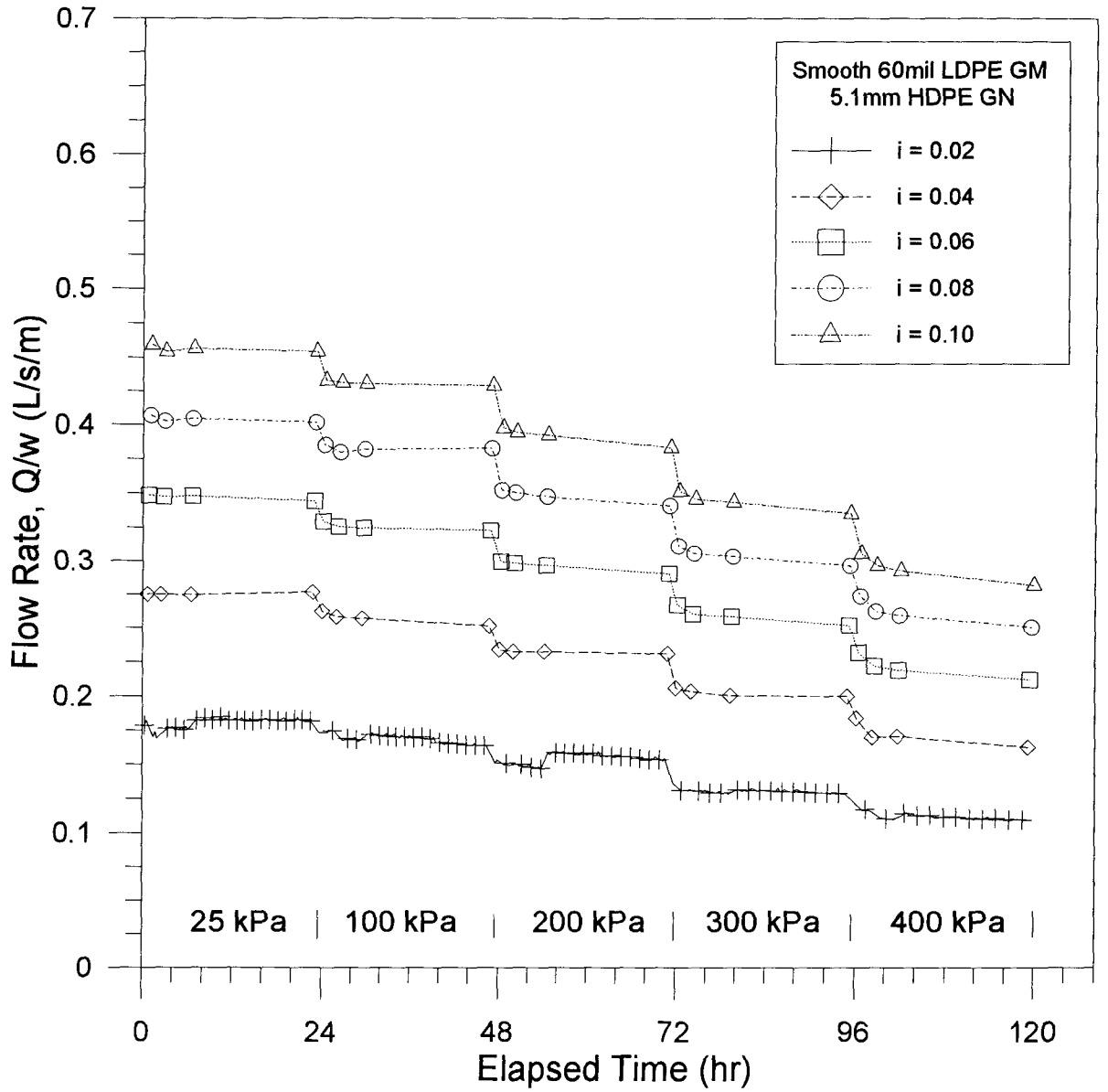
Smooth 60mil LDPE GM
5.1mm HDPE GN
i = 0.02
i = 0.04
i = 0.06
i = 0.08
i = 0.10
Flow Rate, Q/w (L/s/m)
0.7
0.6
0.5
0.4
0.3
0.2
0.1
0
25 kPa
100 kPa
200 kPa
300 kPa
400 kPa
0
24
48
72
96
120
Elapsed Time (hr)

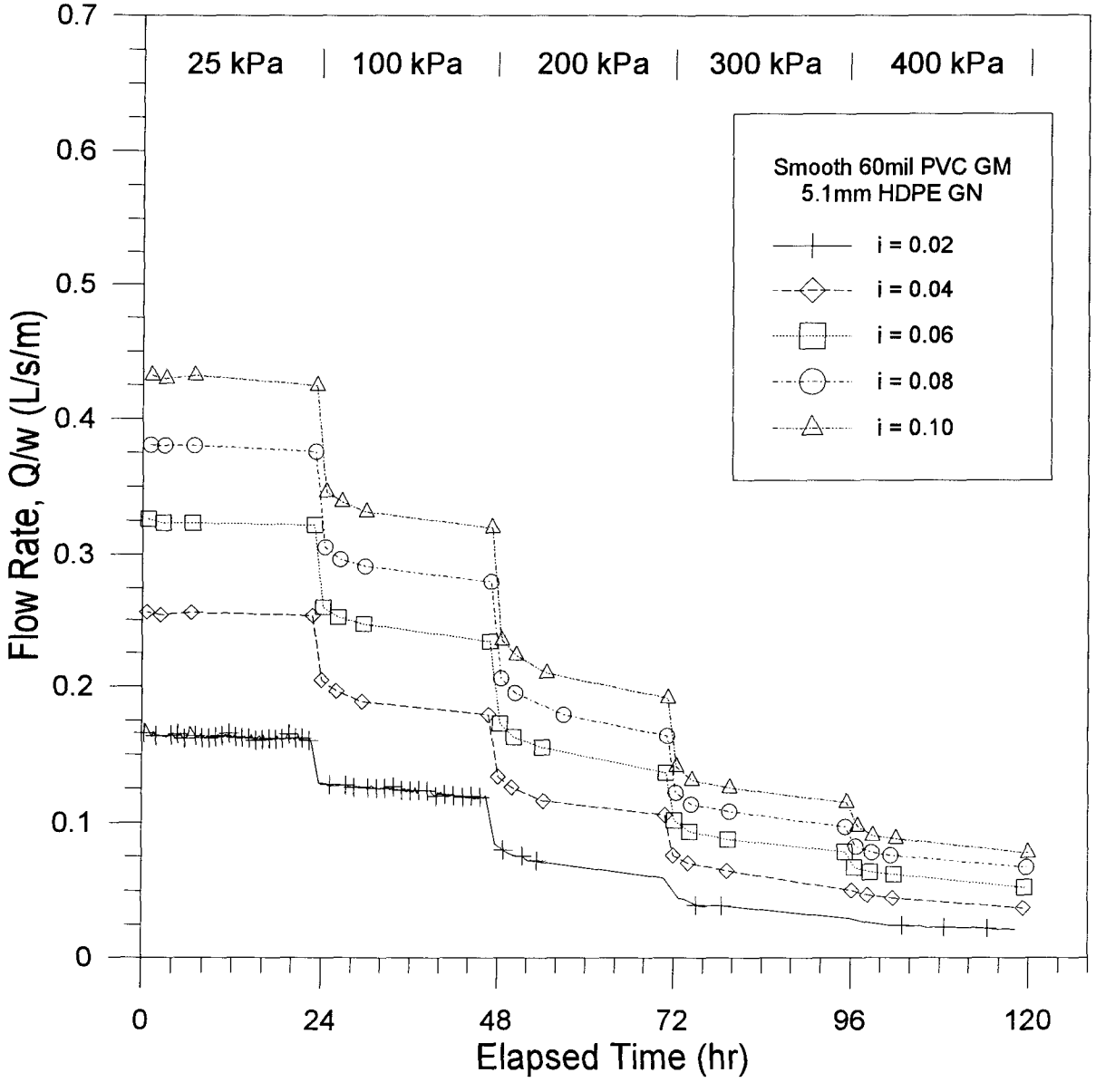
25 kPa
100 kPa
200 kPa
300 kPa
400 kPa
Smooth 60mil PVC GM
5.1mm HDPE GN
i = 0.02
i = 0.04
i = 0.06
i = 0.08
i = 0.10
Flow Rate, Q/w (L/s/m)
0.7
0.6
0.5
0.4
0.3
0.2
0.1
0
0
24
48
72
96
120
Elapsed Time (hr)

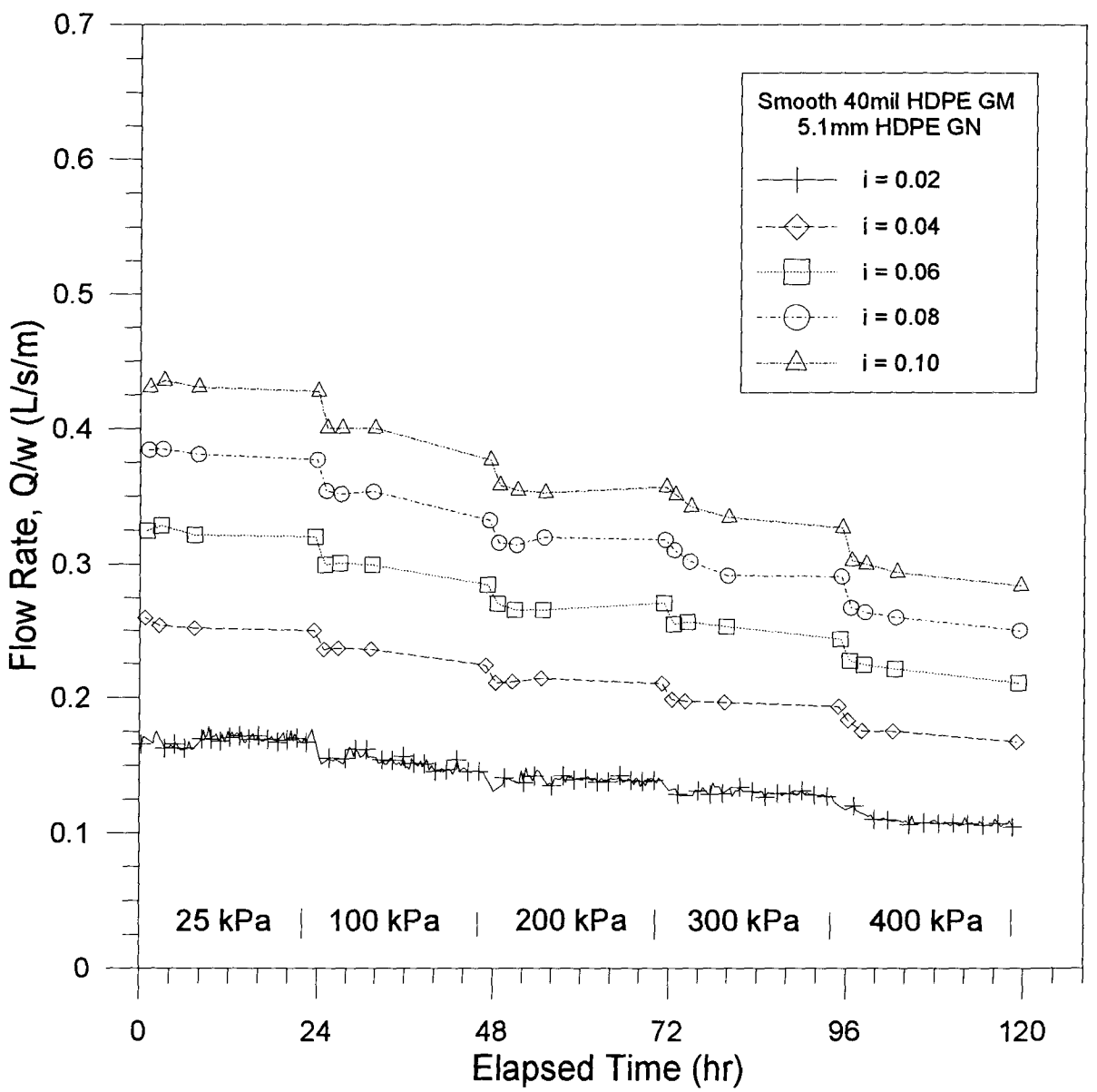
Smooth 40mil HDPE GM
5.1mm HDPE GN
i = 0.02
i = 0.04
i = 0.06
i = 0.08
i = 0.10
25 kPa
100 kPa
200 kPa
300 kPa
400 kPa
Flow Rate, Q/w (L/s/m)
Elapsed Time (hr)
0
0.1
0.2
0.3
0.4
0.5
0.6
0.7
0
24
48
72
96
120

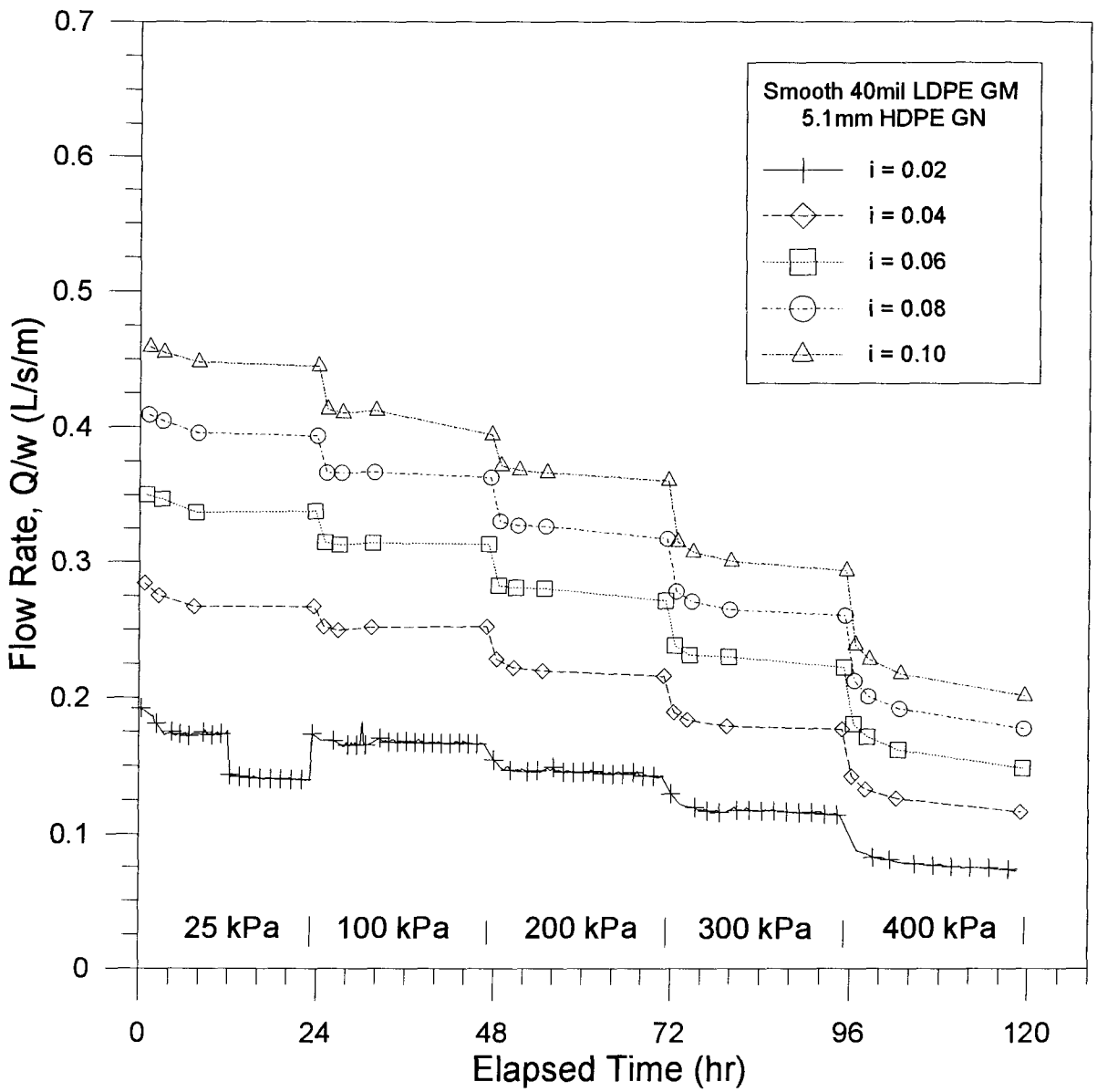
Smooth 40mil LDPE GM
5.1mm HDPE GN
i = 0.02
i = 0.04
i = 0.06
i = 0.08
i = 0.10
25 kPa
100 kPa
200 kPa
300 kPa
400 kPa
Flow Rate, Q/w (L/s/m)
Elapsed Time (hr)
0
0.1
0.2
0.3
0.4
0.5
0.6
0.7
0
24
48
72
96
120

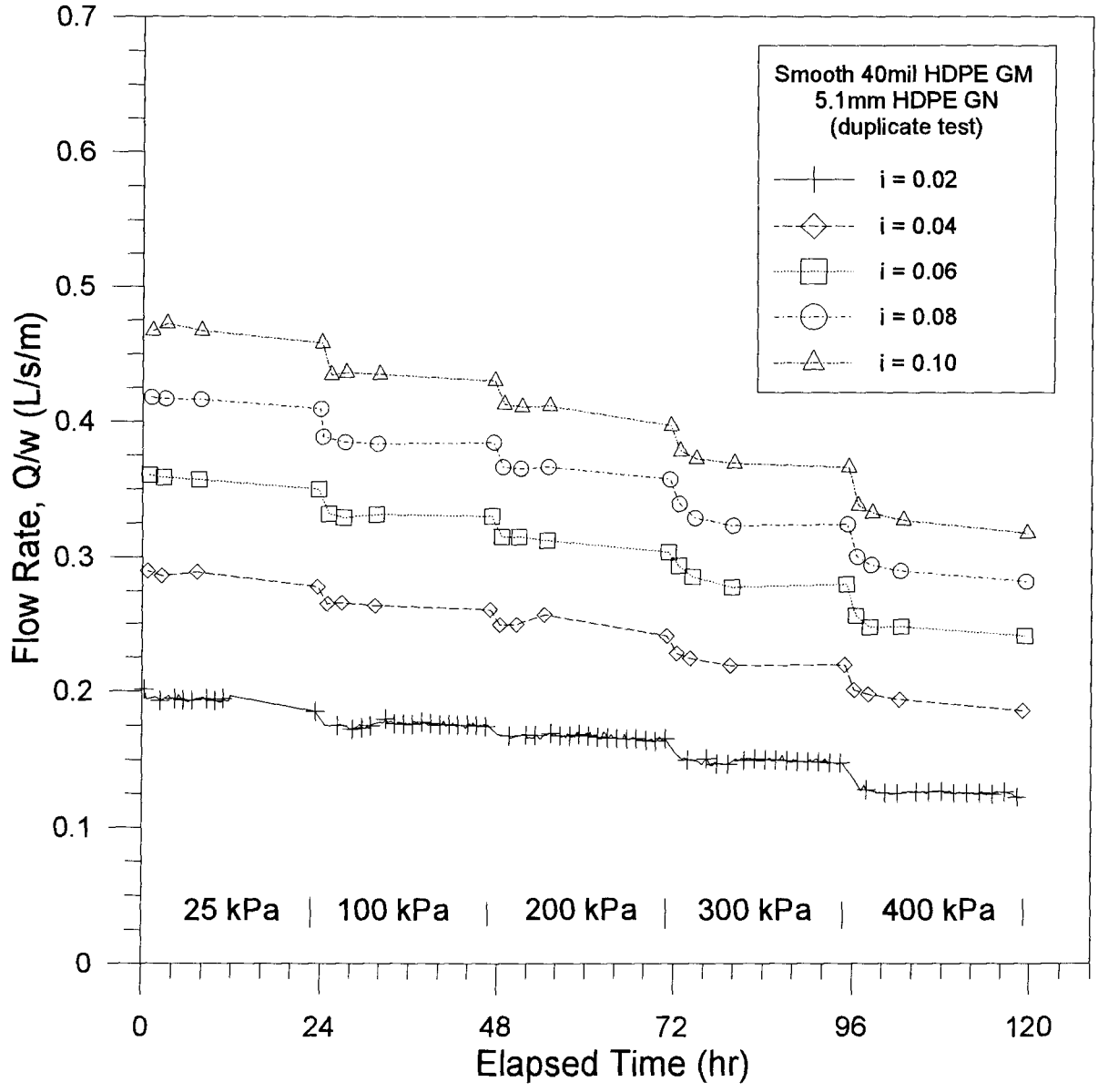
Smooth 40mil HDPE GM
5.1mm HDPE GN
(duplicate test)
i = 0.02
i = 0.04
i = 0.06
i = 0.08
i = 0.10
25 kPa
100 kPa
200 kPa
300 kPa
400 kPa
Flow Rate, Q/w (L/s/m)
Elapsed Time (hr)
0
0.1
0.2
0.3
0.4
0.5
0.6
0.7
0
24
48
72
96
120

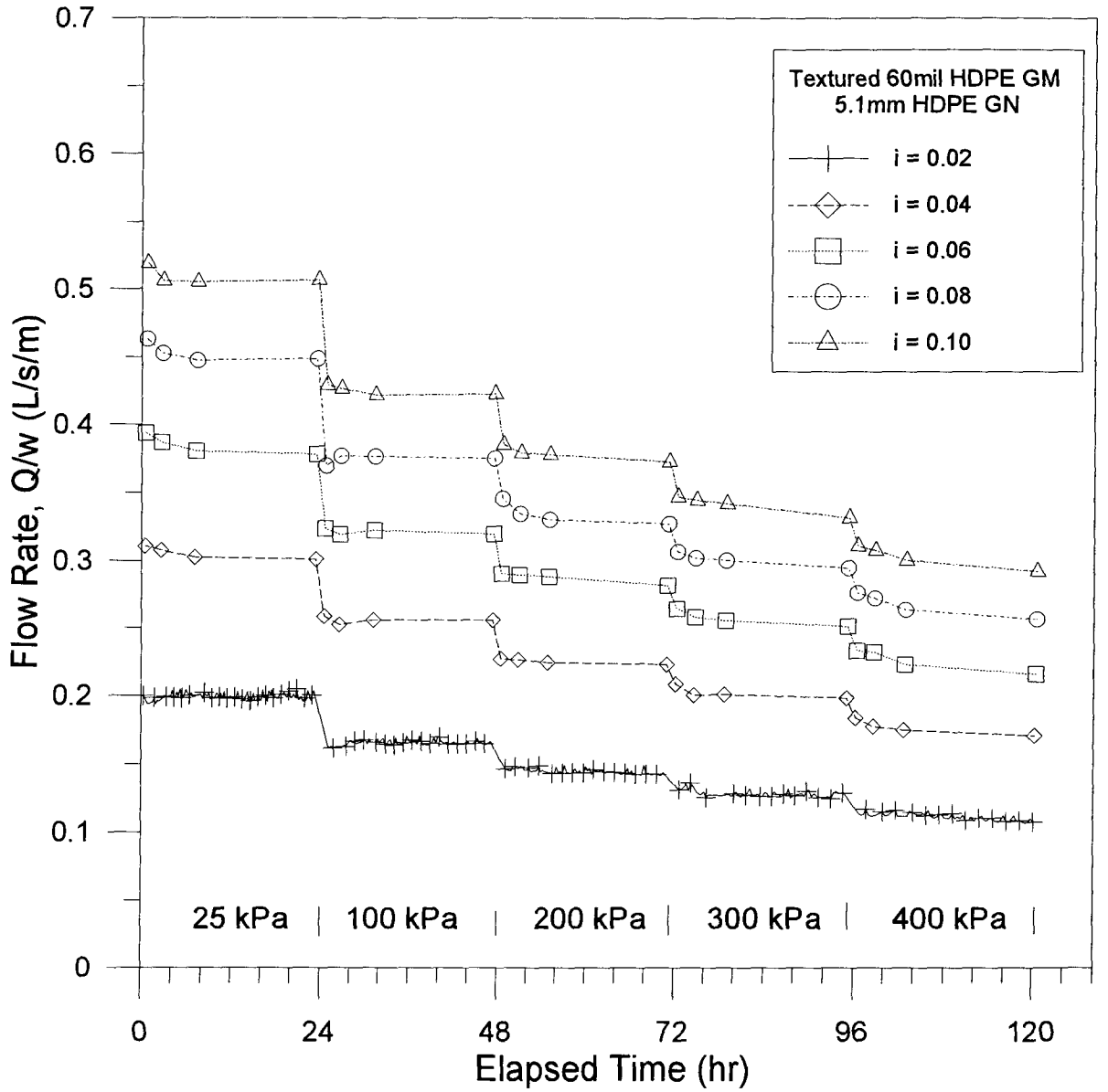
Textured 60mil HDPE GM
5.1mm HDPE GN
i = 0.02
i = 0.04
i = 0.06
i = 0.08
i = 0.10
Flow Rate, Q/w (L/s/m)
0.7
0.6
0.5
0.4
0.3
0.2
0.1
0
25 kPa
100 kPa
200 kPa
300 kPa
400 kPa
0
24
48
72
96
120
Elapsed Time (hr)

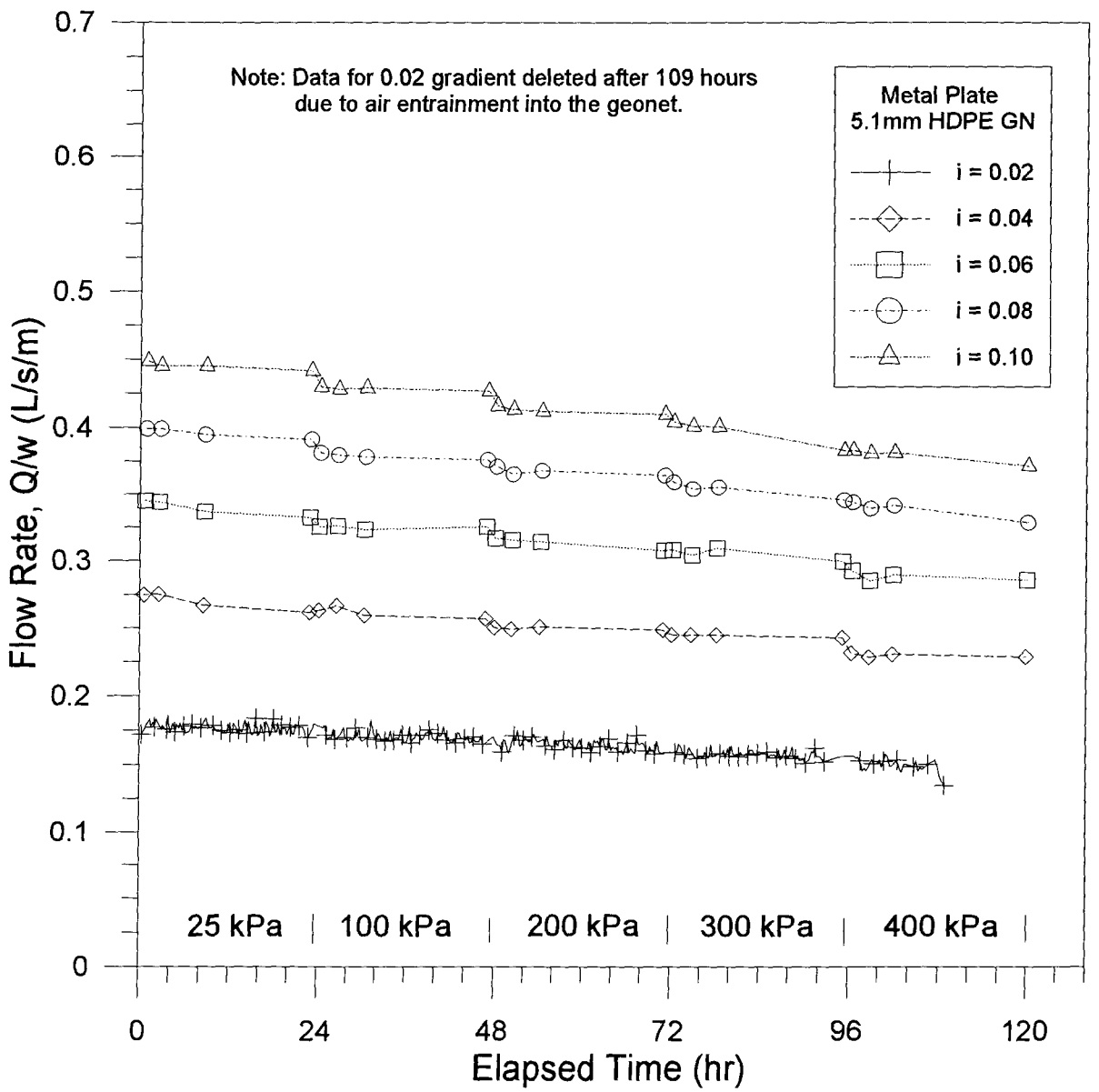
Note: Data for 0.02 gradient deleted after 109 hours due to air entrainment into the geonet.
Metal Plate
5.1mm HDPE GN
i = 0.02
i = 0.04
i = 0.06
i = 0.08
i = 0.10
Flow Rate, Q/w (L/s/m)
0.7
0.6
0.5
0.4
0.3
0.2
0.1
0
25 kPa
100 kPa
200 kPa
300 kPa
400 kPa
0
24
48
72
96
120
Elapsed Time (hr)

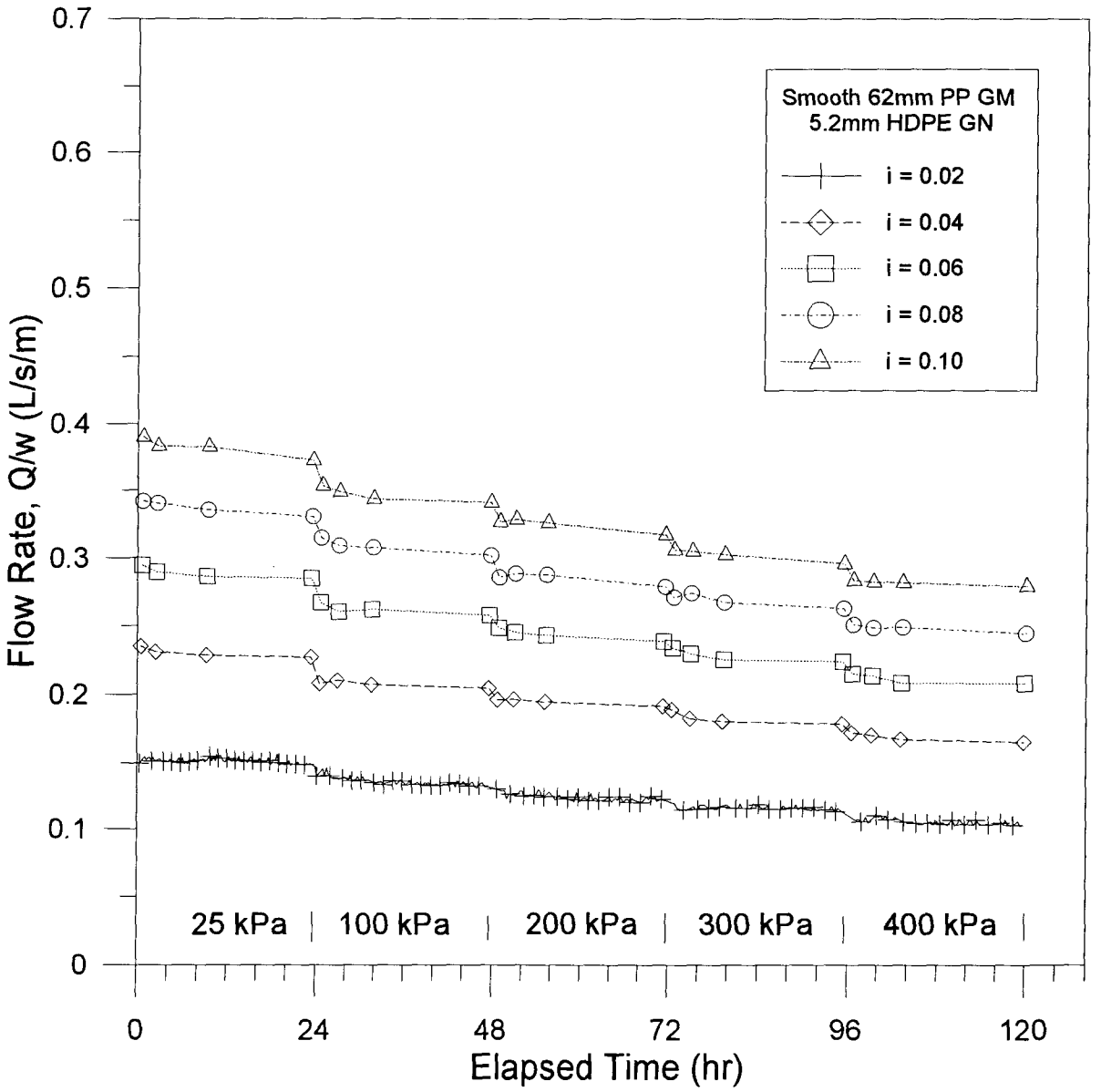
Smooth 62mm PP GM
5.2mm HDPE GN
i = 0.02
i = 0.04
i = 0.06
i = 0.08
i = 0.10
Flow Rate, Q/w (L/s/m)
0.7
0.6
0.5
0.4
0.3
0.2
0.1
0
25 kPa
100 kPa
200 kPa
300 kPa
400 kPa
0
24
48
72
96
120
Elapsed Time (hr)

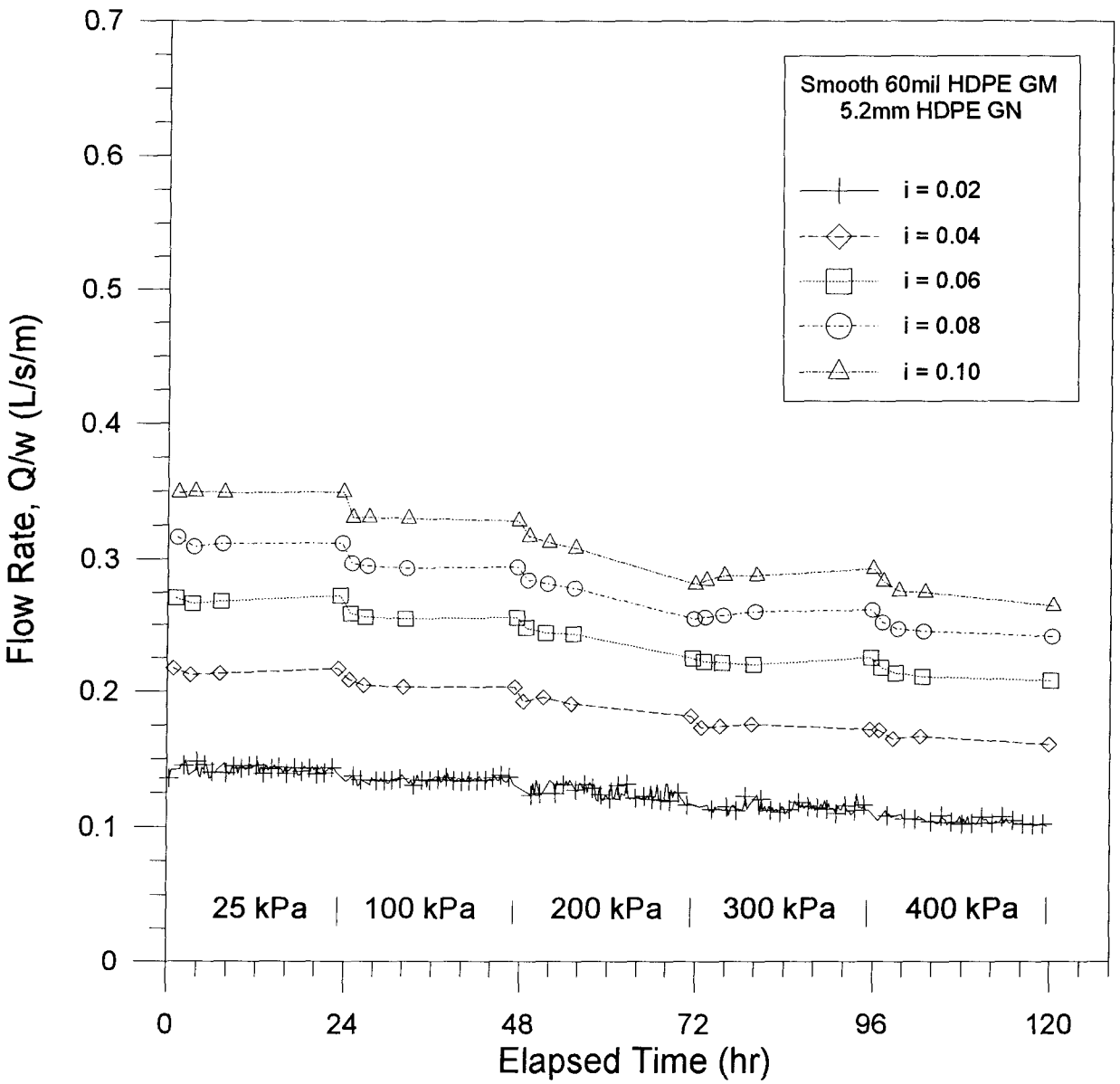
Smooth 60mil HDPE GM
5.2mm HDPE GN
i = 0.02
i = 0.04
i = 0.06
i = 0.08
i = 0.10
25 kPa
100 kPa
200 kPa
300 kPa
400 kPa
Flow Rate, Q/w (L/s/m)
Elapsed Time (hr)
0
0.1
0.2
0.3
0.4
0.5
0.6
0.7
0
24
48
72
96
120

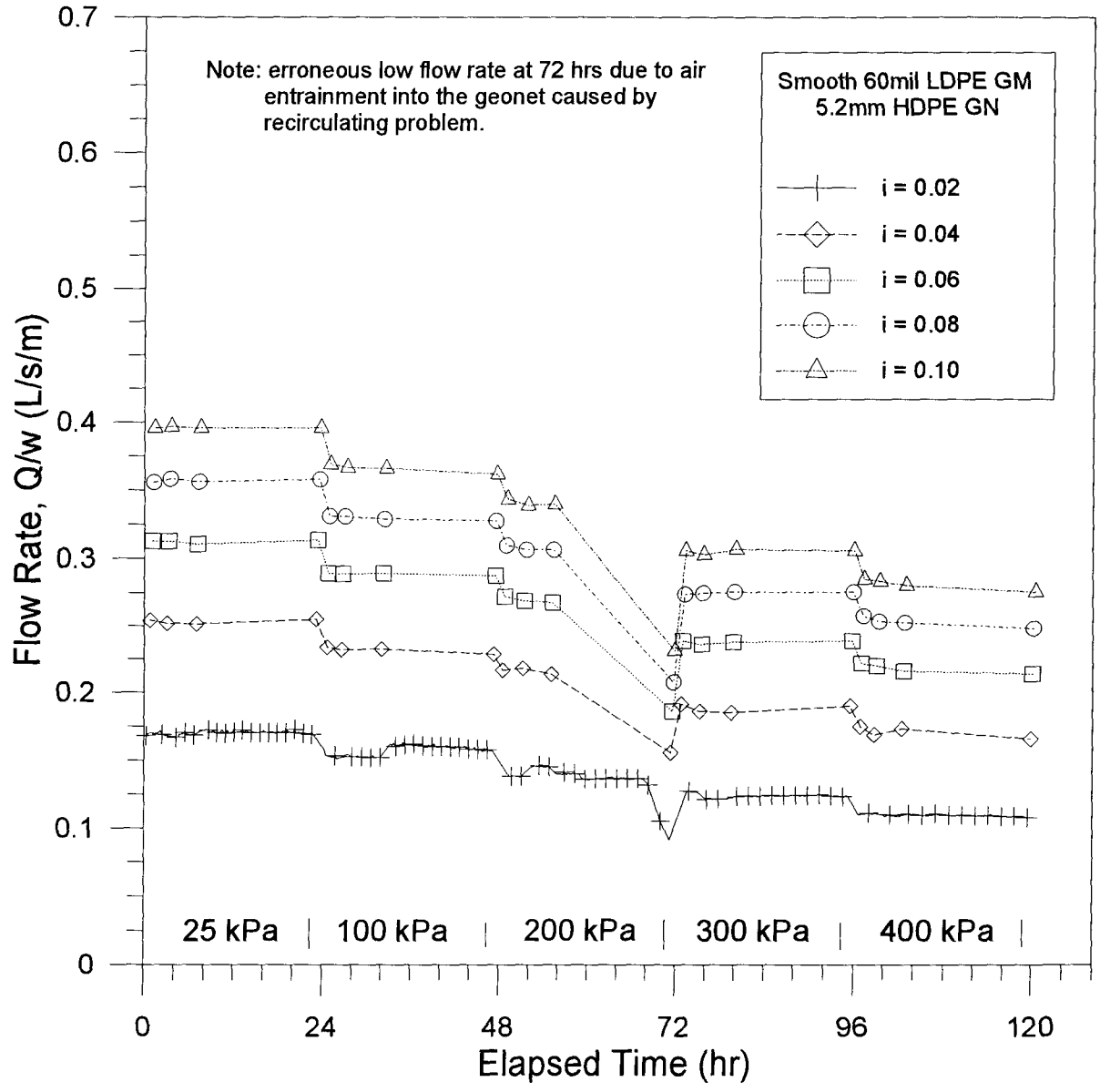
Note: erroneous low flow rate at 72 hrs due to air entrainment into the geonet caused by recirculating problem.
Smooth 60mil LDPE GM
5.2mm HDPE GN
i = 0.02
i = 0.04
i = 0.06
i = 0.08
i = 0.10
Flow Rate, Q/w (L/s/m)
0.7
0.6
0.5
0.4
0.3
0.2
0.1
0
25 kPa
100 kPa
200 kPa
300 kPa
400 kPa
0
24
48
72
96
120
Elapsed Time (hr)

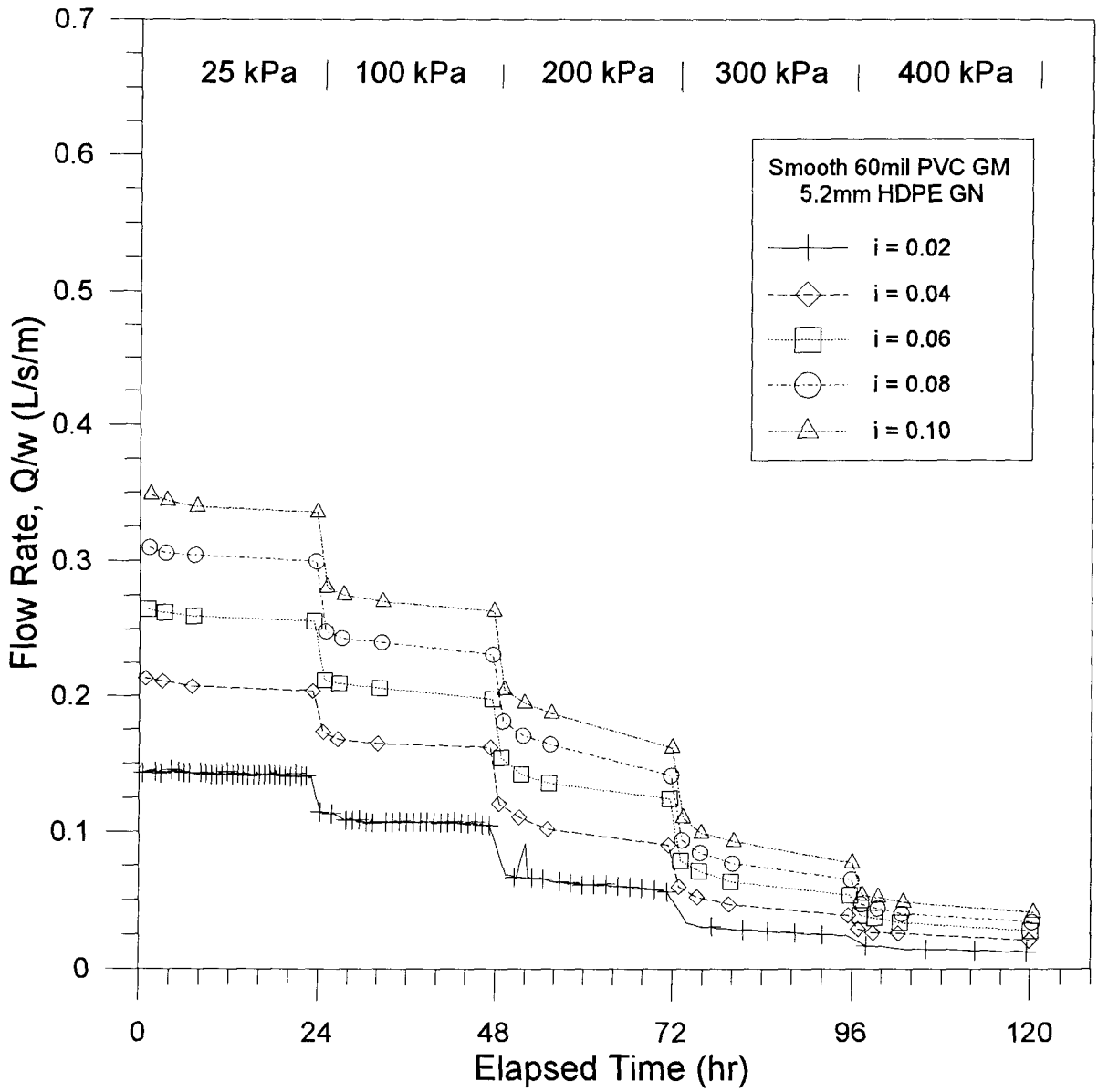
25 kPa | 100 kPa | 200 kPa | 300 kPa | 400 kPa |
Smooth 60mil PVC GM
5.2mm HDPE GN
i = 0.02
i = 0.04
i = 0.06
i = 0.08
i = 0.10
Flow Rate, Q/w (L/s/m)
0.7
0.6
0.5
0.4
0.3
0.2
0.1
0
0
24
48
72
96
120
Elapsed Time (hr)

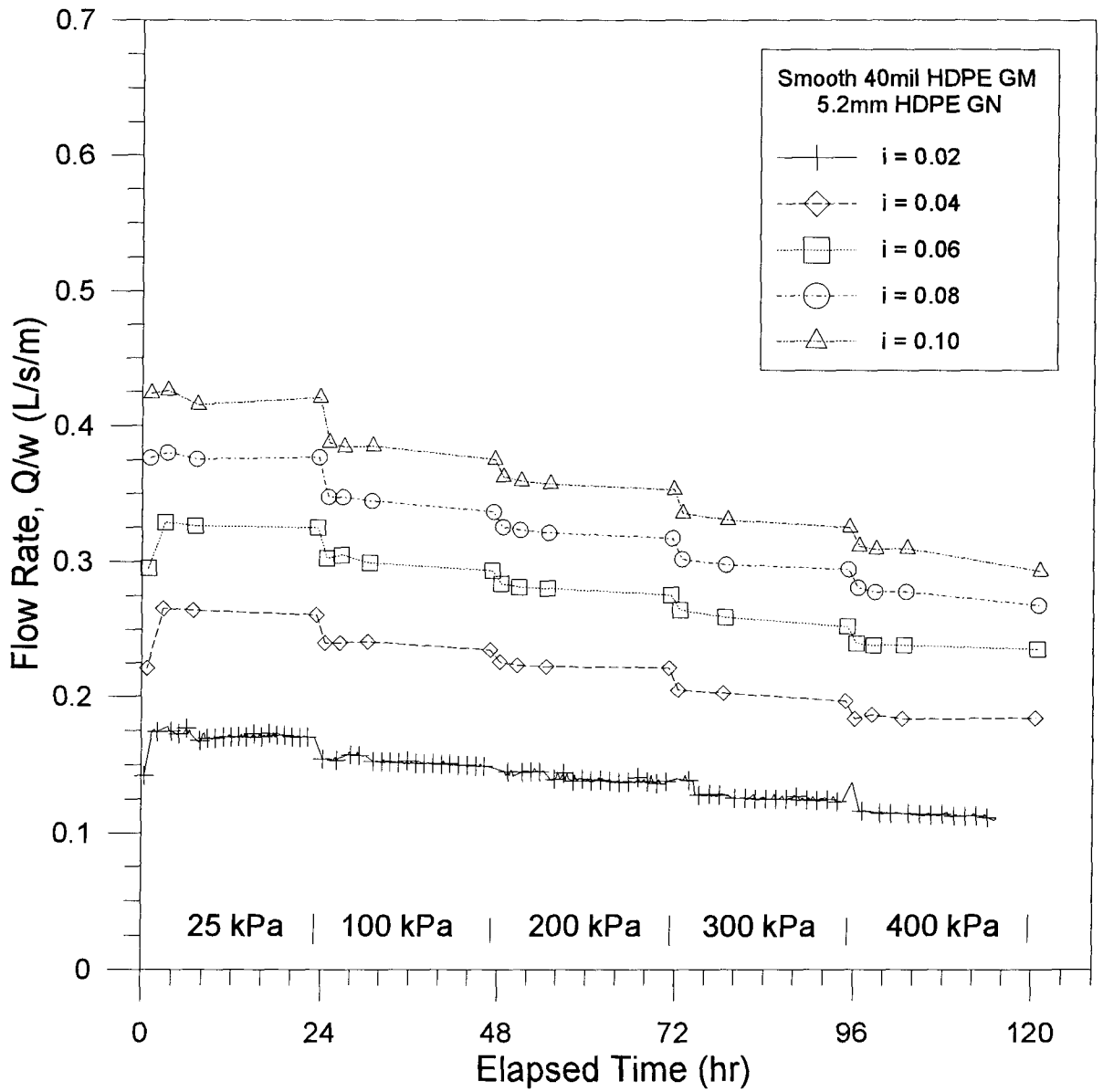
Smooth 40mil HDPE GM
5.2mm HDPE GN
i = 0.02
i = 0.04
i = 0.06
i = 0.08
i = 0.10
25 kPa
100 kPa
200 kPa
300 kPa
400 kPa
Flow Rate, Q/w (L/s/m)
Elapsed Time (hr)
0
0.1
0.2
0.3
0.4
0.5
0.6
0.7
0
24
48
72
96
120

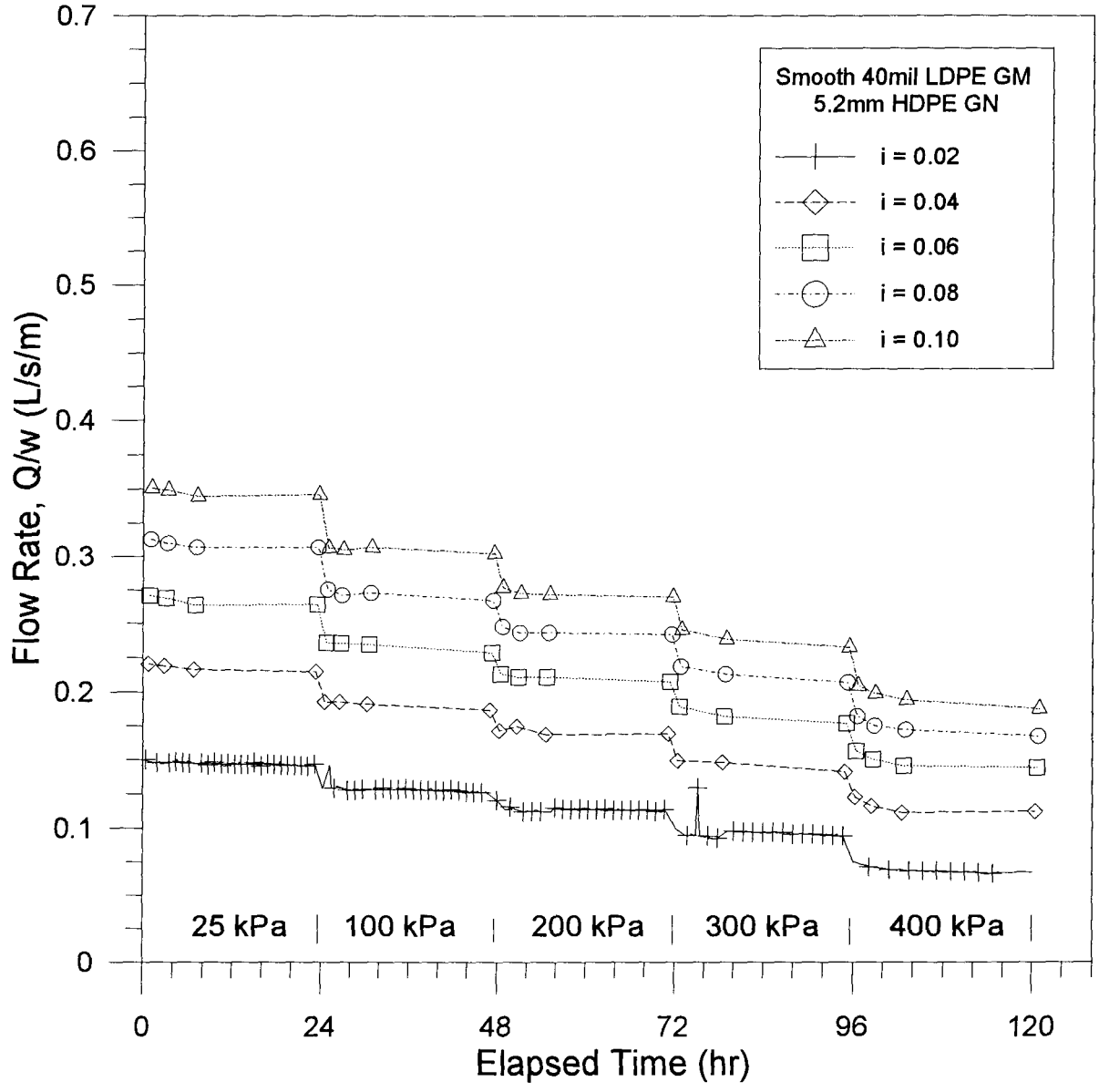
Smooth 40mil LDPE GM
5.2mm HDPE GN
i = 0.02
i = 0.04
i = 0.06
i = 0.08
i = 0.10
Flow Rate, Q/w (L/s/m)
0.7
0.6
0.5
0.4
0.3
0.2
0.1
0
25 kPa
100 kPa
200 kPa
300 kPa
400 kPa
0
24
48
72
96
120
Elapsed Time (hr)

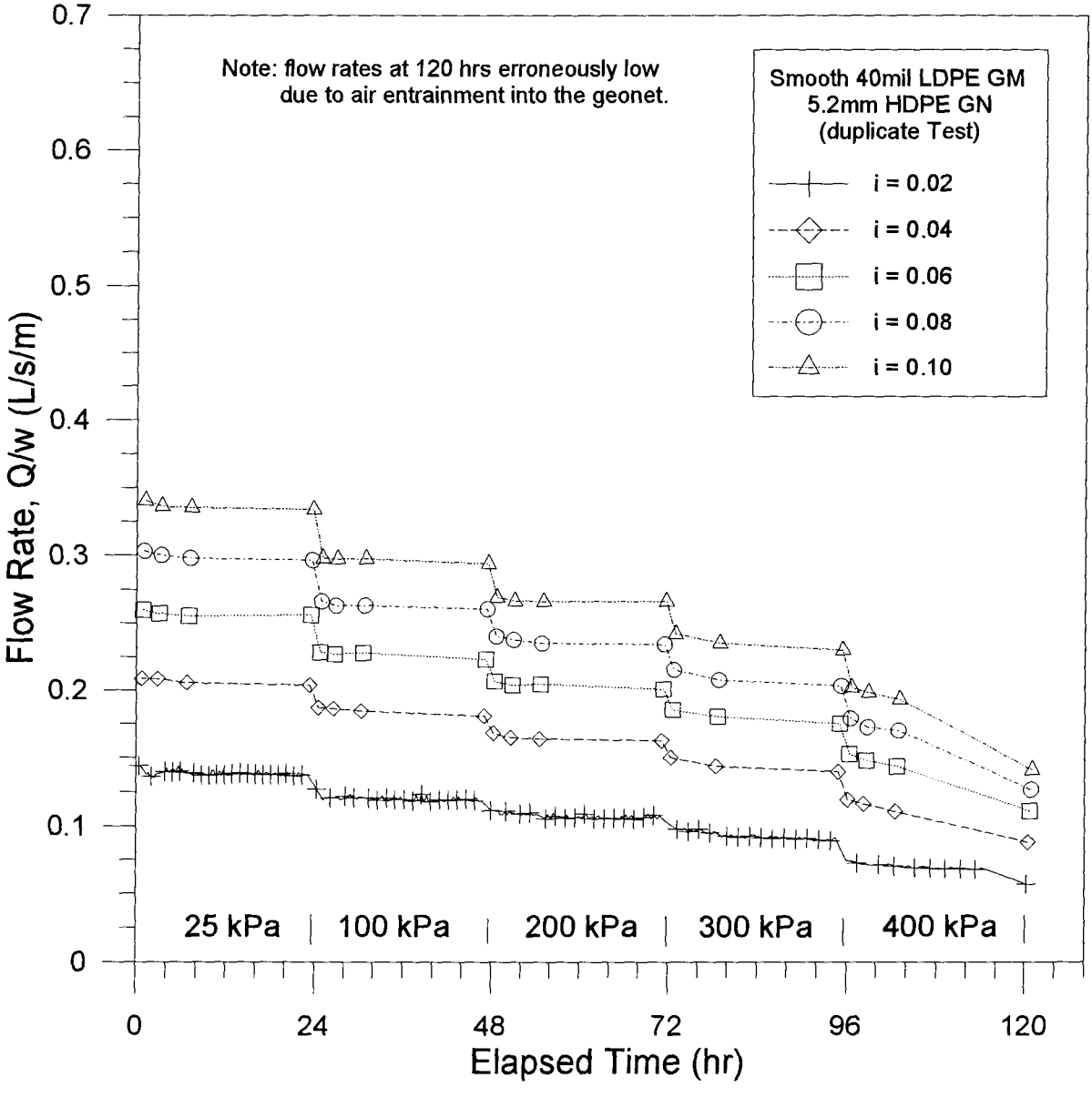
Note: flow rates at 120 hrs erroneously low due to air entrainment into the geonet.
Smooth 40mil LDPE GM
5.2mm HDPE GN
(duplicate Test)
i = 0.02
i = 0.04
i = 0.06
i = 0.08
i = 0.10
Flow Rate, Q/w (L/s/m)
0.7
0.6
0.5
0.4
0.3
0.2
0.1
0
25 kPa
100 kPa
200 kPa
300 kPa
400 kPa
0
24
48
72
96
120
Elapsed Time (hr)

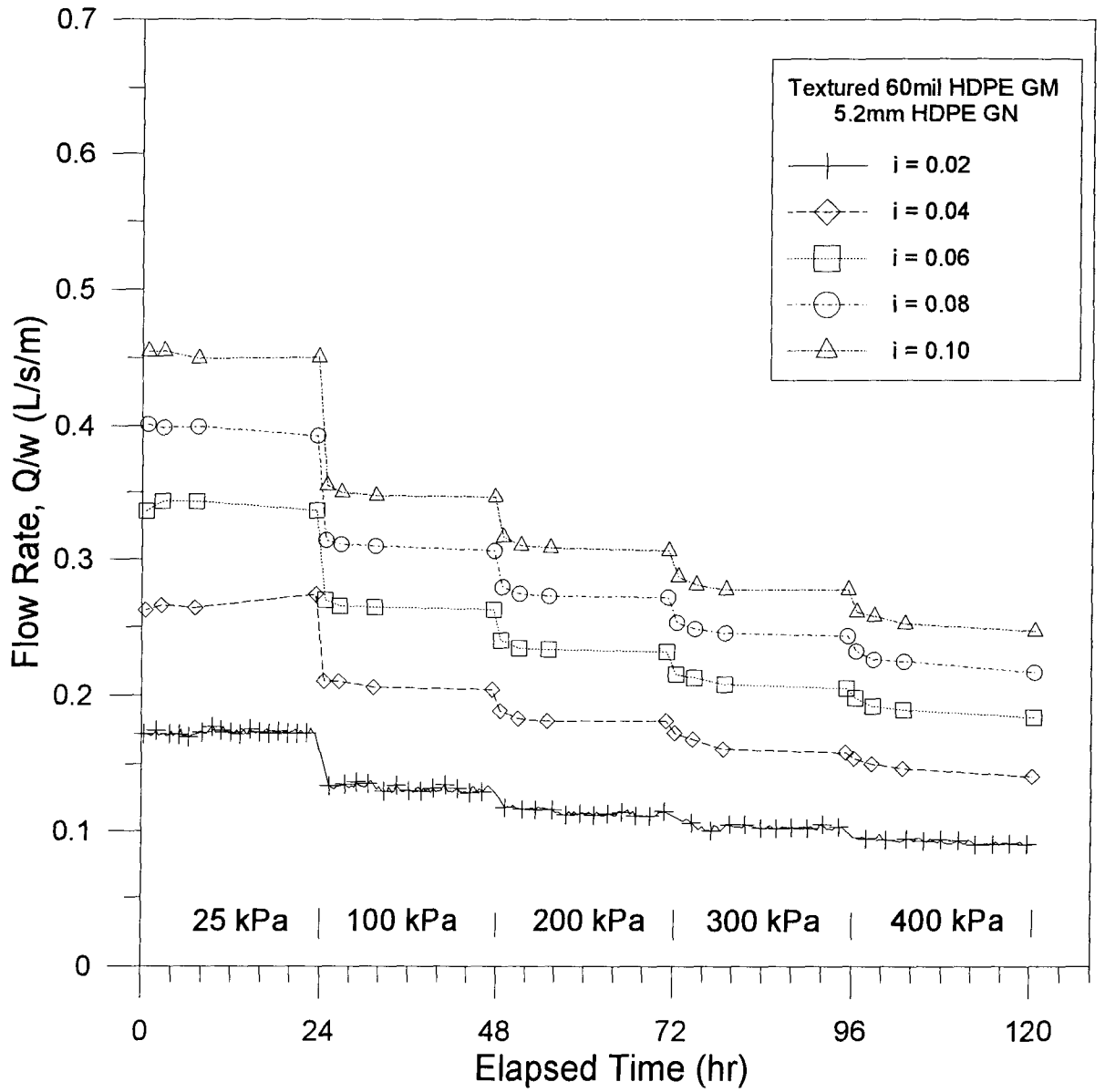
Textured 60mil HDPE GM
5.2mm HDPE GN
i = 0.02
i = 0.04
i = 0.06
i = 0.08
i = 0.10
Flow Rate, Q/w (L/s/m)
0.7
0.6
0.5
0.4
0.3
0.2
0.1
0
25 kPa
100 kPa
200 kPa
300 kPa
400 kPa
0
24
48
72
96
120
Elapsed Time (hr)

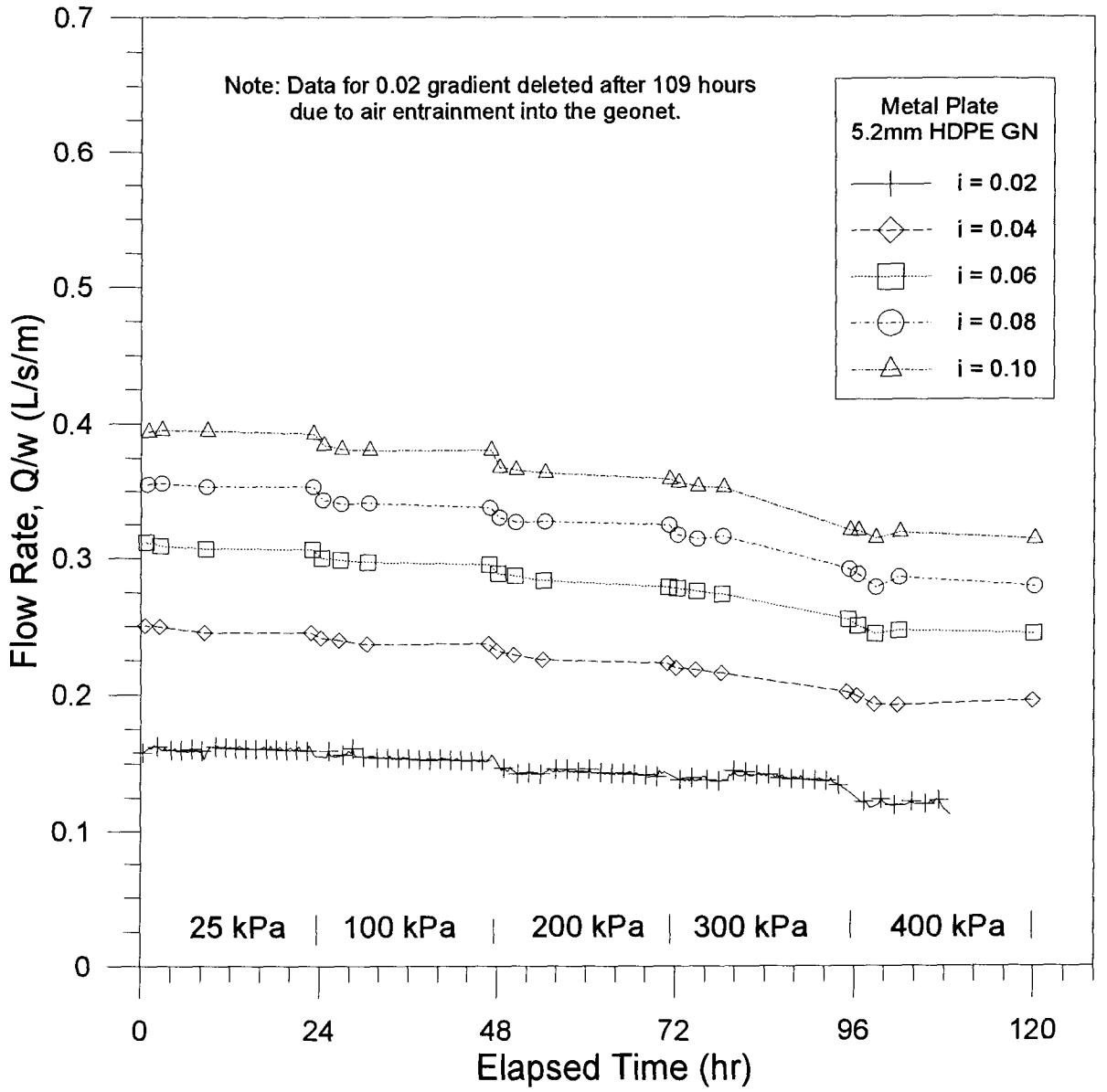
Note: Data for 0.02 gradient deleted after 109 hours
due to air entrainment into the geonet.
Metal Plate
5.2mm HDPE GN
i = 0.02
i = 0.04
i = 0.06
i = 0.08
i = 0.10
25 kPa
100 kPa
200 kPa
300 kPa
400 kPa
Flow Rate, Q/w (L/s/m)
0.7
0.6
0.5
0.4
0.3
0.2
0.1
0
0
24
48
72
96
120
Elapsed Time (hr)

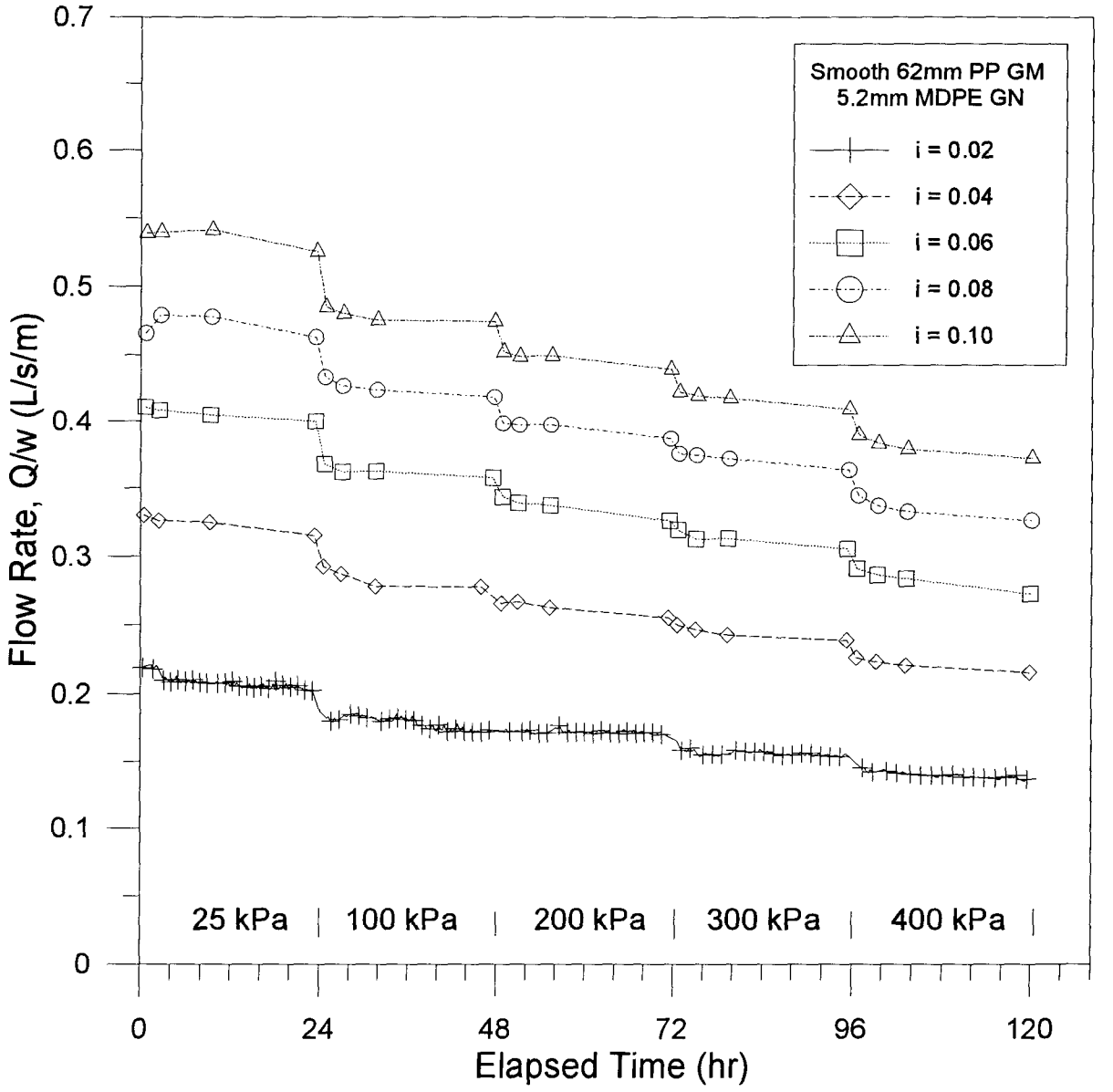
Smooth 62mm PP GM
5.2mm MDPE GN
i = 0.02
i = 0.04
i = 0.06
i = 0.08
i = 0.10
25 kPa
100 kPa
200 kPa
300 kPa
400 kPa
Flow Rate, Q/w (L/s/m)
Elapsed Time (hr)
0
0.1
0.2
0.3
0.4
0.5
0.6
0.7
0
24
48
72
96
120

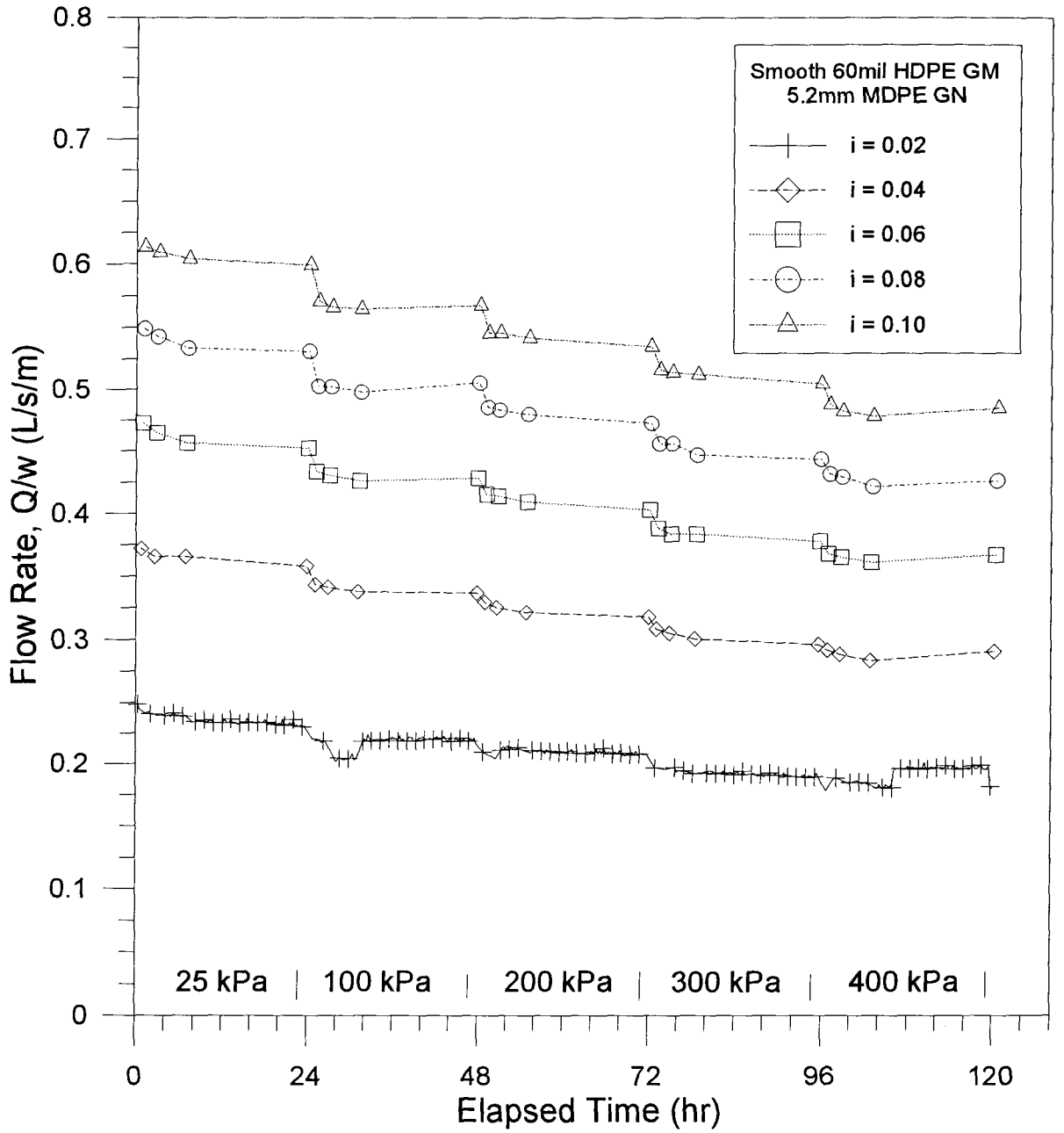
Smooth 60mil HDPE GM
5.2mm MDPE GN
i = 0.02
i = 0.04
i = 0.06
i = 0.08
i = 0.10
Flow Rate, Q/w (L/s/m)
0.8
0.7
0.6
0.5
0.4
0.3
0.2
0.1
0
25 kPa
100 kPa
200 kPa
300 kPa
400 kPa
0
24
48
72
96
120
Elapsed Time (hr)

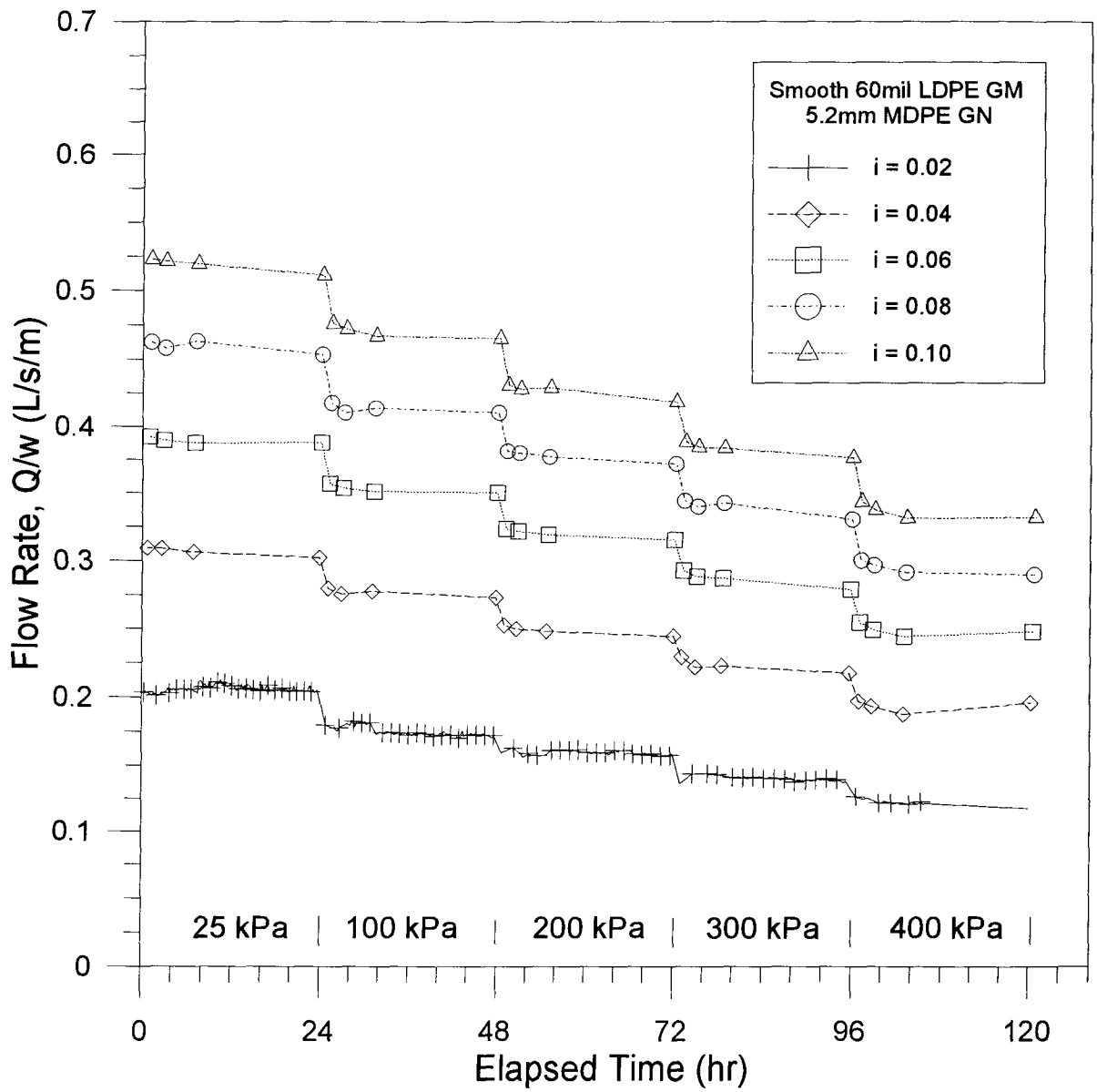
Smooth 60mil LDPE GM
5.2mm MDPE GN
i = 0.02
i = 0.04
i = 0.06
i = 0.08
i = 0.10
25 kPa
100 kPa
200 kPa
300 kPa
400 kPa
Flow Rate, Q/w (L/s/m)
Elapsed Time (hr)
0
0.1
0.2
0.3
0.4
0.5
0.6
0.7
0
24
48
72
96
120

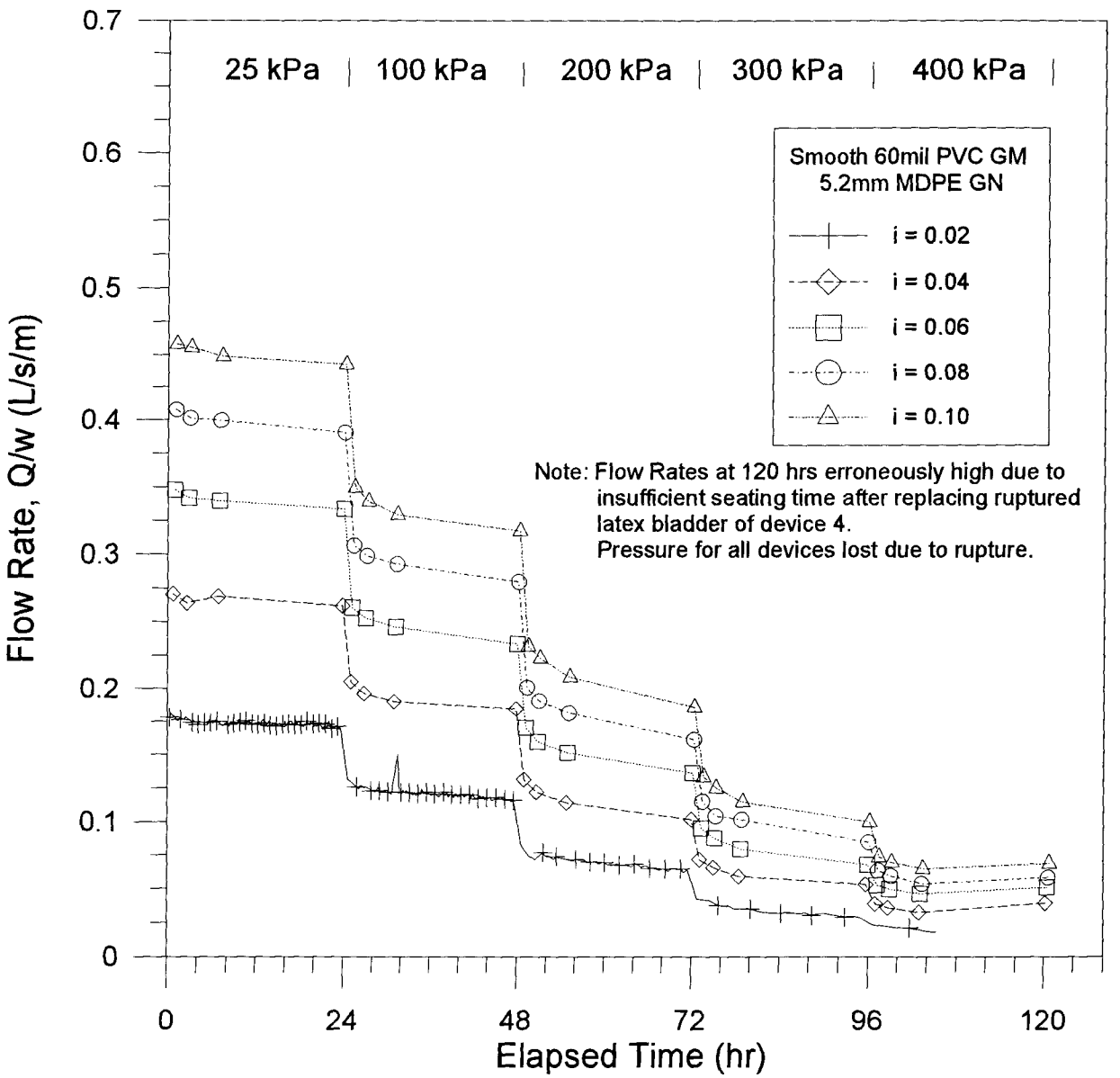
25 kPa
100 kPa
200 kPa
300 kPa
400 kPa
Smooth 60mil PVC GM
5.2mm MDPE GN
i = 0.02
i = 0.04
i = 0.06
i = 0.08
i = 0.10
Note: Flow Rates at 120 hrs erroneously high due to insufficient seating time after replacing ruptured latex bladder of device 4.
Pressure for all devices lost due to rupture.
Flow Rate, Q/w (L/s/m)
0.7
0.6
0.5
0.4
0.3
0.2
0.1
0
0
24
48
72
96
120
Elapsed Time (hr)

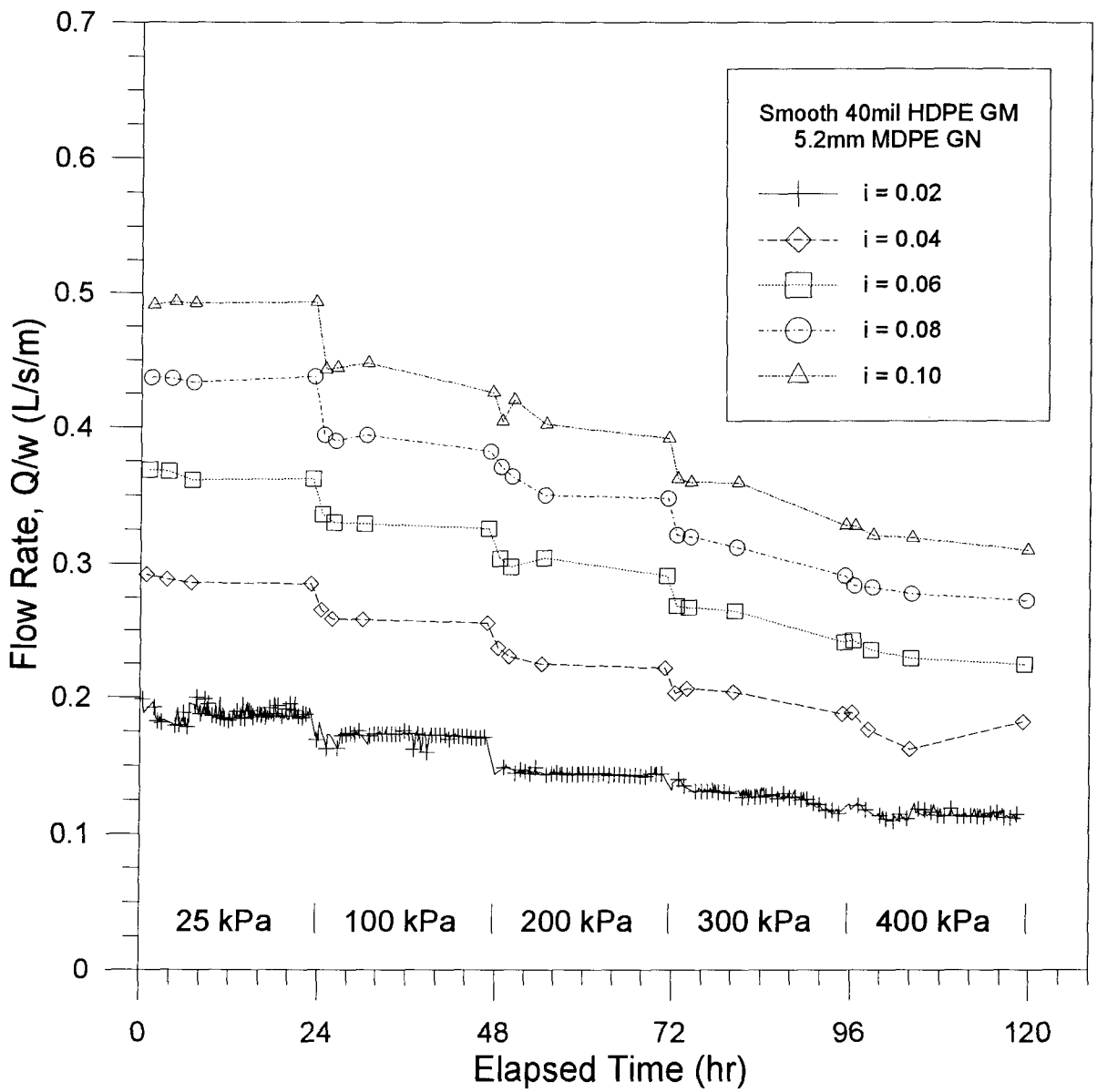
Smooth 40mil HDPE GM
5.2mm MDPE GN
i = 0.02
i = 0.04
i = 0.06
i = 0.08
i = 0.10
25 kPa
100 kPa
200 kPa
300 kPa
400 kPa
Flow Rate, Q/w (L/s/m)
Elapsed Time (hr)
0
0.1
0.2
0.3
0.4
0.5
0.6
0.7
0
24
48
72
96
120

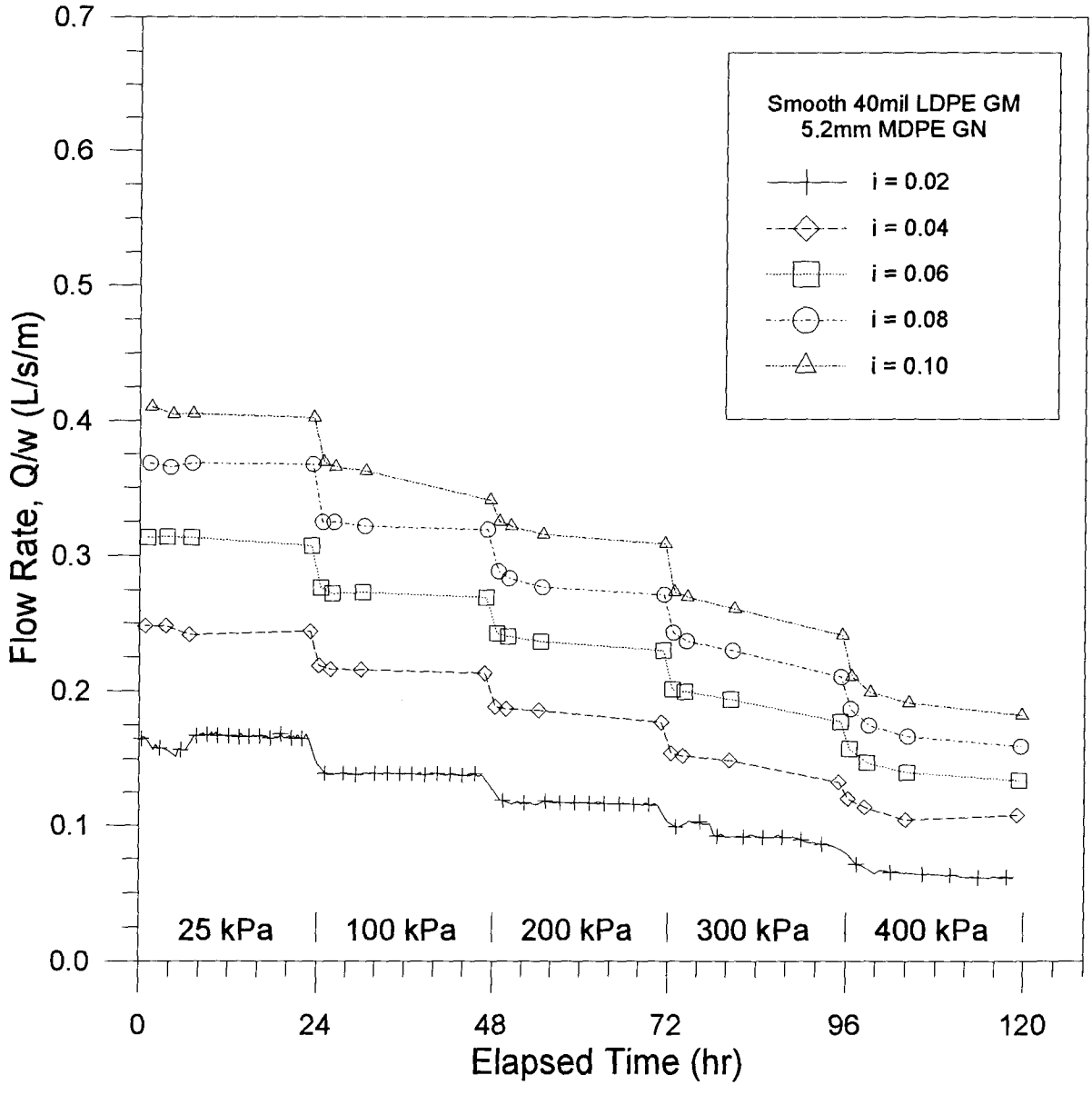
Smooth 40mil LDPE GM
5.2mm MDPE GN
i = 0.02
i = 0.04
i = 0.06
i = 0.08
i = 0.10
25 kPa
100 kPa
200 kPa
300 kPa
400 kPa
Flow Rate, Q/w (L/s/m)
0.0
0.1
0.2
0.3
0.4
0.5
0.6
0.7
0
24
48
72
96
120
Elapsed Time (hr)

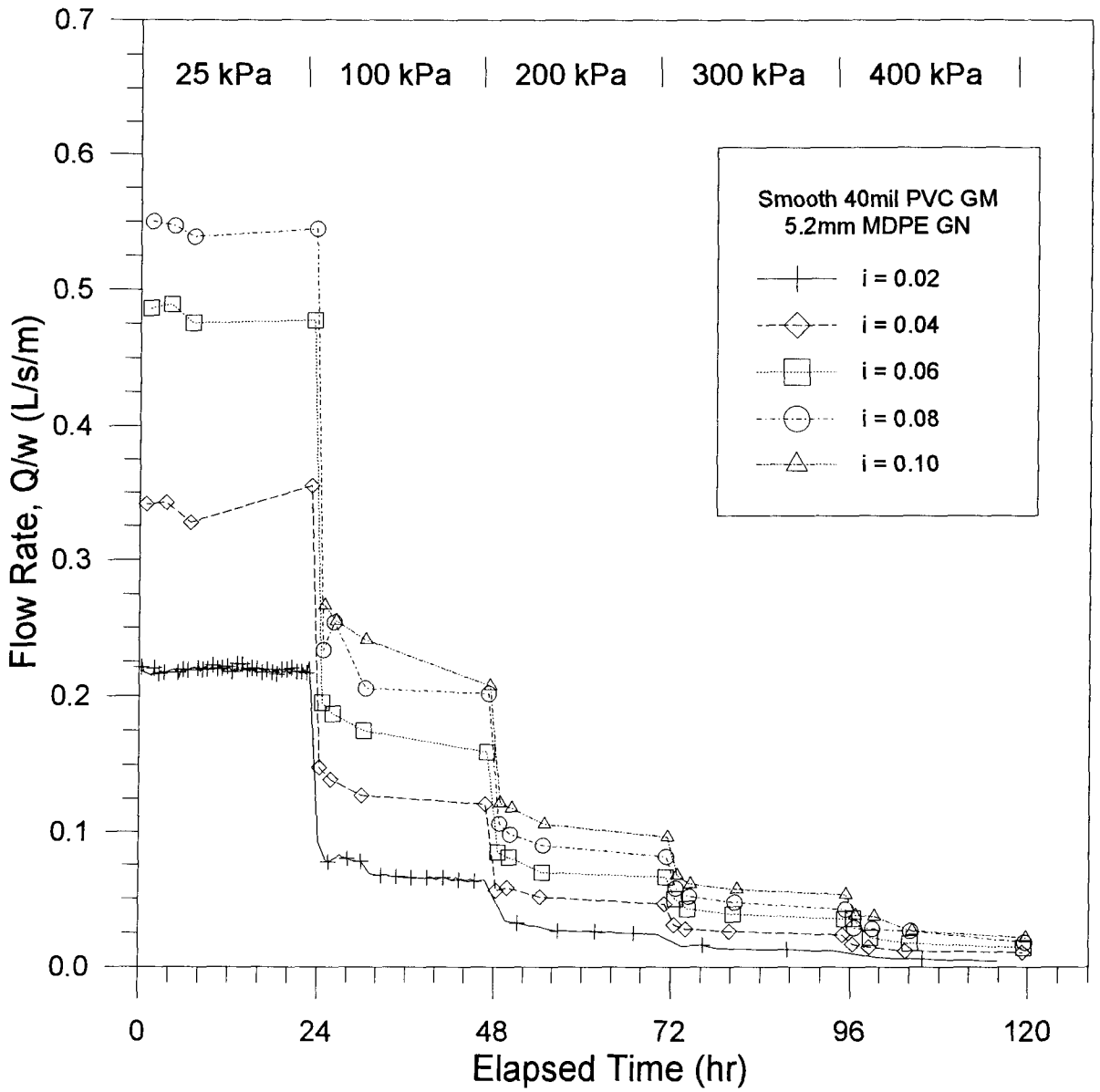
25 kPa
100 kPa
200 kPa
300 kPa
400 kPa
Smooth 40mil PVC GM
5.2mm MDPE GN
i = 0.02
i = 0.04
i = 0.06
i = 0.08
i = 0.10
Flow Rate, Q/w (L/s/m)
0.0
0.1
0.2
0.3
0.4
0.5
0.6
0.7
0
24
48
72
96
120
Elapsed Time (hr)

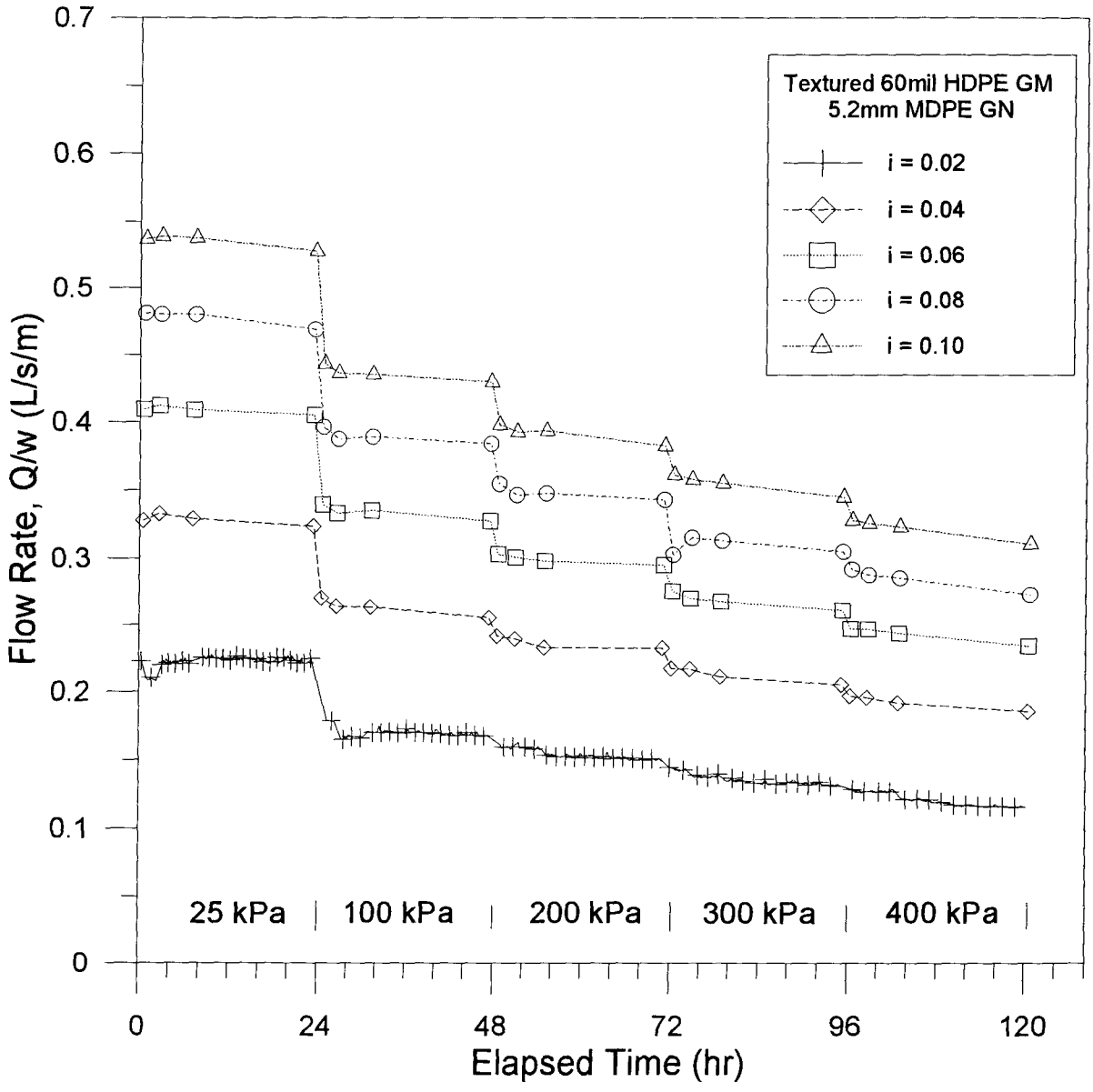
Textured 60mil HDPE GM
5.2mm MDPE GN
i = 0.02
i = 0.04
i = 0.06
i = 0.08
i = 0.10
25 kPa
100 kPa
200 kPa
300 kPa
400 kPa
Flow Rate, Q/w (L/s/m)
Elapsed Time (hr)
0
0.1
0.2
0.3
0.4
0.5
0.6
0.7
0
24
48
72
96
120

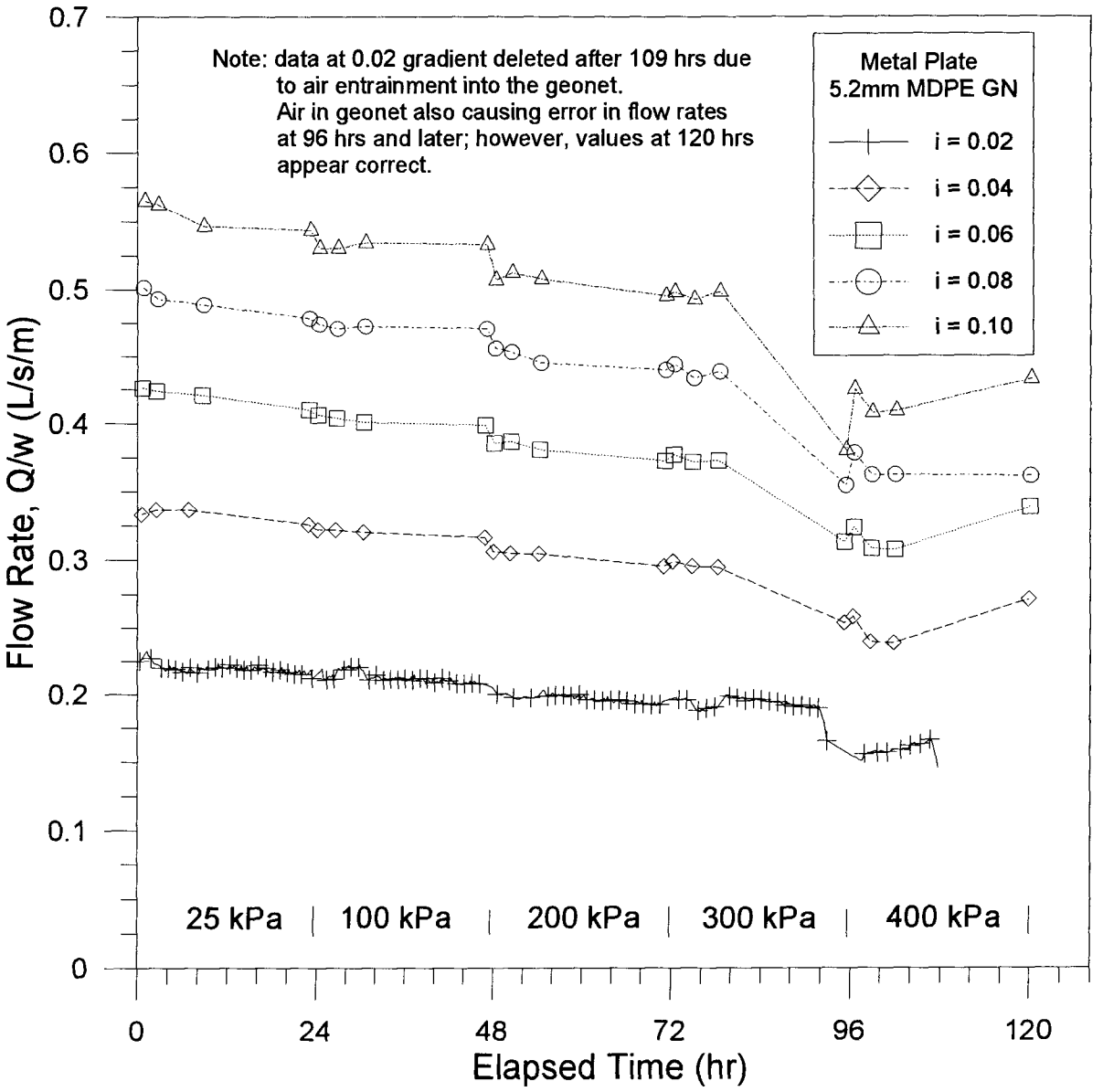
Note: data at 0.02 gradient deleted after 109 hrs due to air entrainment into the geonet.
Air in geonet also causing error in flow rates at 96 hrs and later; however, values at 120 hrs appear correct.
Metal Plate
5.2mm MDPE GN
i = 0.02
i = 0.04
i = 0.06
i = 0.08
i = 0.10
25 kPa
100 kPa
200 kPa
300 kPa
400 kPa
Flow Rate, Q/w (L/s/m)
Elapsed Time (hr)
0
0.1
0.2
0.3
0.4
0.5
0.6
0.7
0
24
48
72
96
120

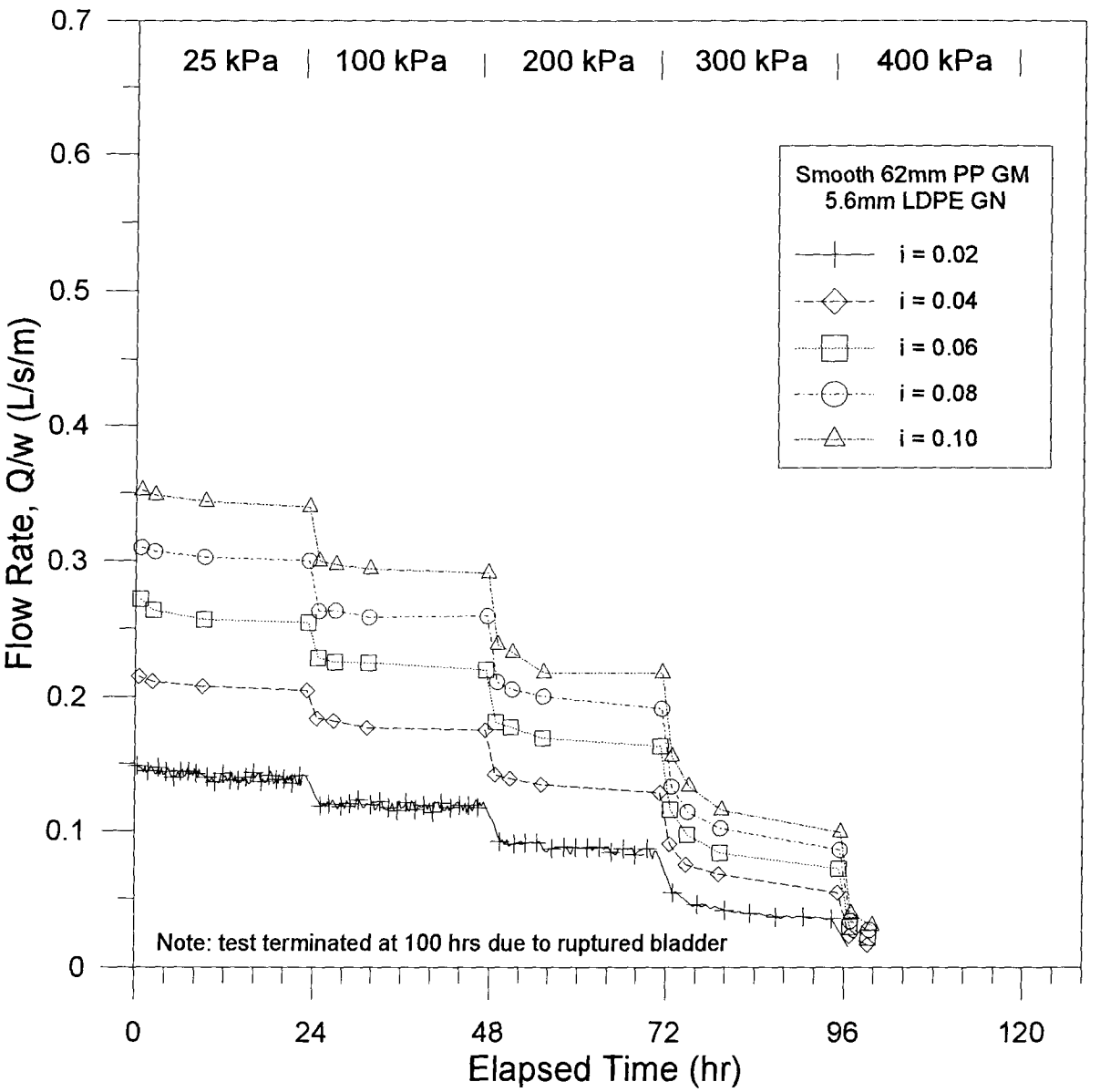
25 kPa
100 kPa
200 kPa
300 kPa
400 kPa
Smooth 62mm PP GM
5.6mm LDPE GN
i = 0.02
i = 0.04
i = 0.06
i = 0.08
i = 0.10
Note: test terminated at 100 hrs due to ruptured bladder
Flow Rate, Q/w (L/s/m)
Elapsed Time (hr)
0.7
0.6
0.5
0.4
0.3
0.2
0.1
0
0
24
48
72
96
120

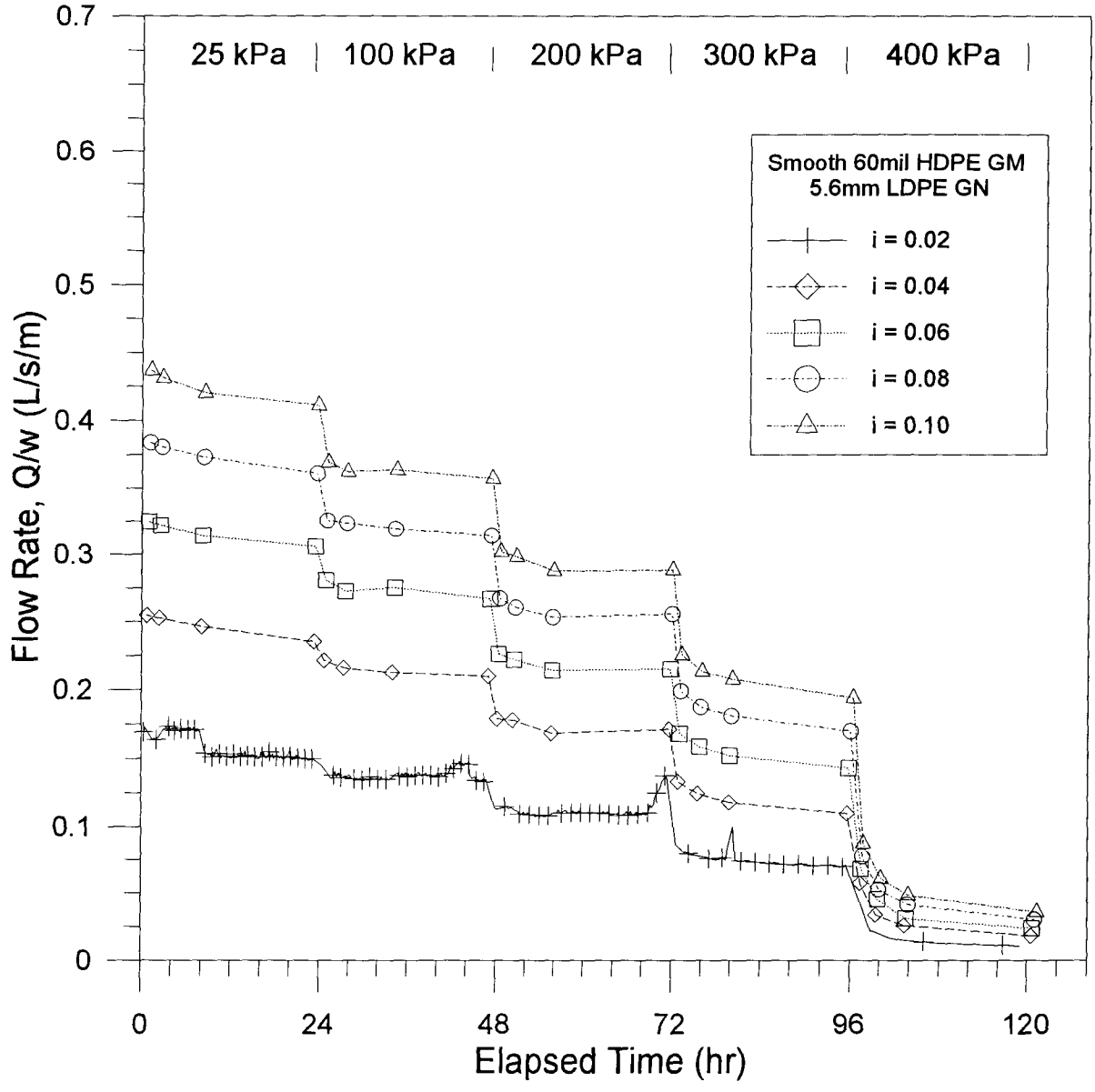
25 kPa
100 kPa
200 kPa
300 kPa
400 kPa
Smooth 60mil HDPE GM
5.6mm LDPE GN
i = 0.02
i = 0.04
i = 0.06
i = 0.08
i = 0.10
Flow Rate, Q/w (L/s/m)
0.7
0.6
0.5
0.4
0.3
0.2
0.1
0
0
24
48
72
96
120
Elapsed Time (hr)

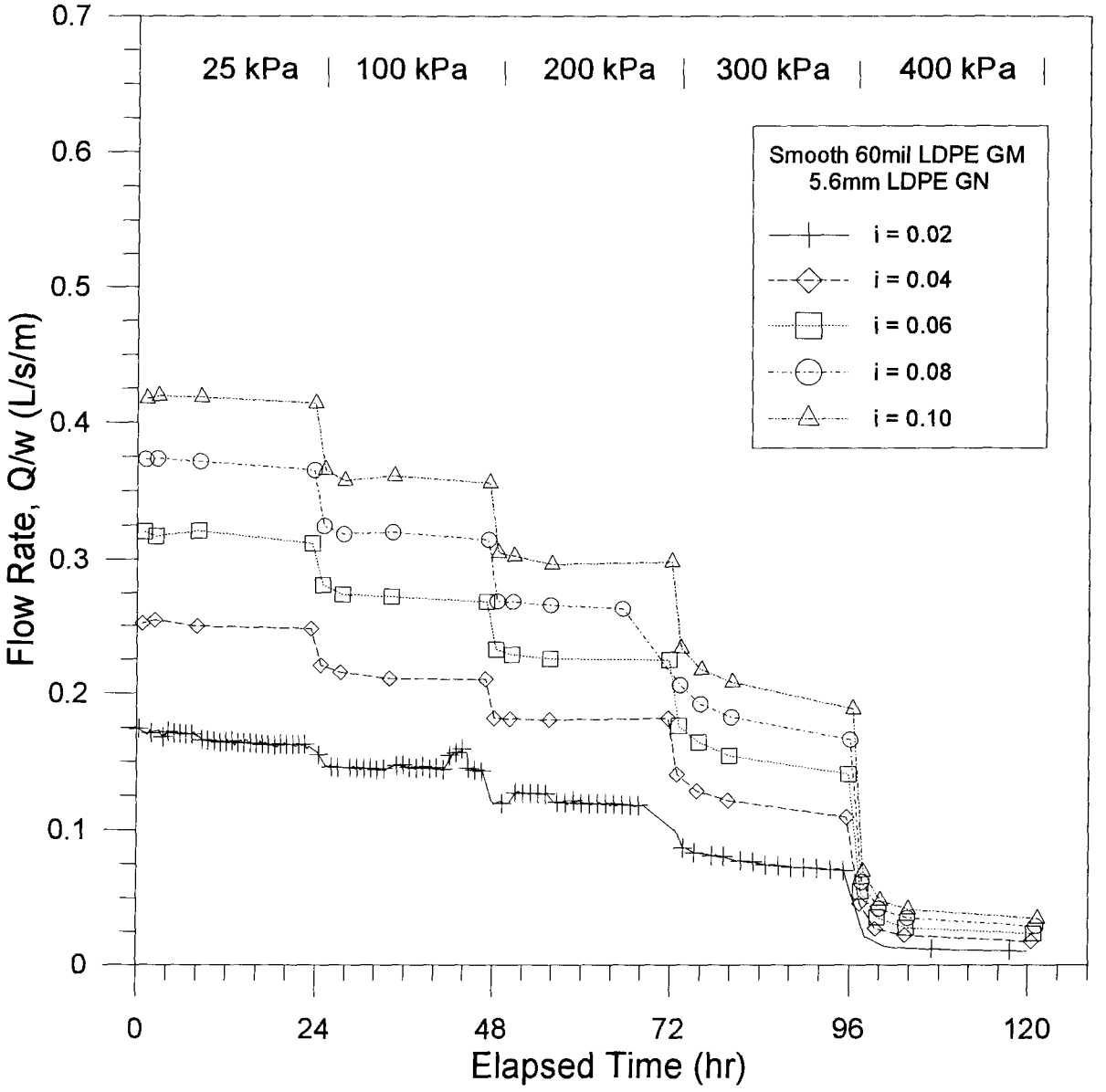
25 kPa
100 kPa
200 kPa
300 kPa
400 kPa
Smooth 60mil LDPE GM
5.6mm LDPE GN
i = 0.02
i = 0.04
i = 0.06
i = 0.08
i = 0.10
Flow Rate, Q/w (L/s/m)
0.7
0.6
0.5
0.4
0.3
0.2
0.1
0
0
24
48
72
96
120
Elapsed Time (hr)

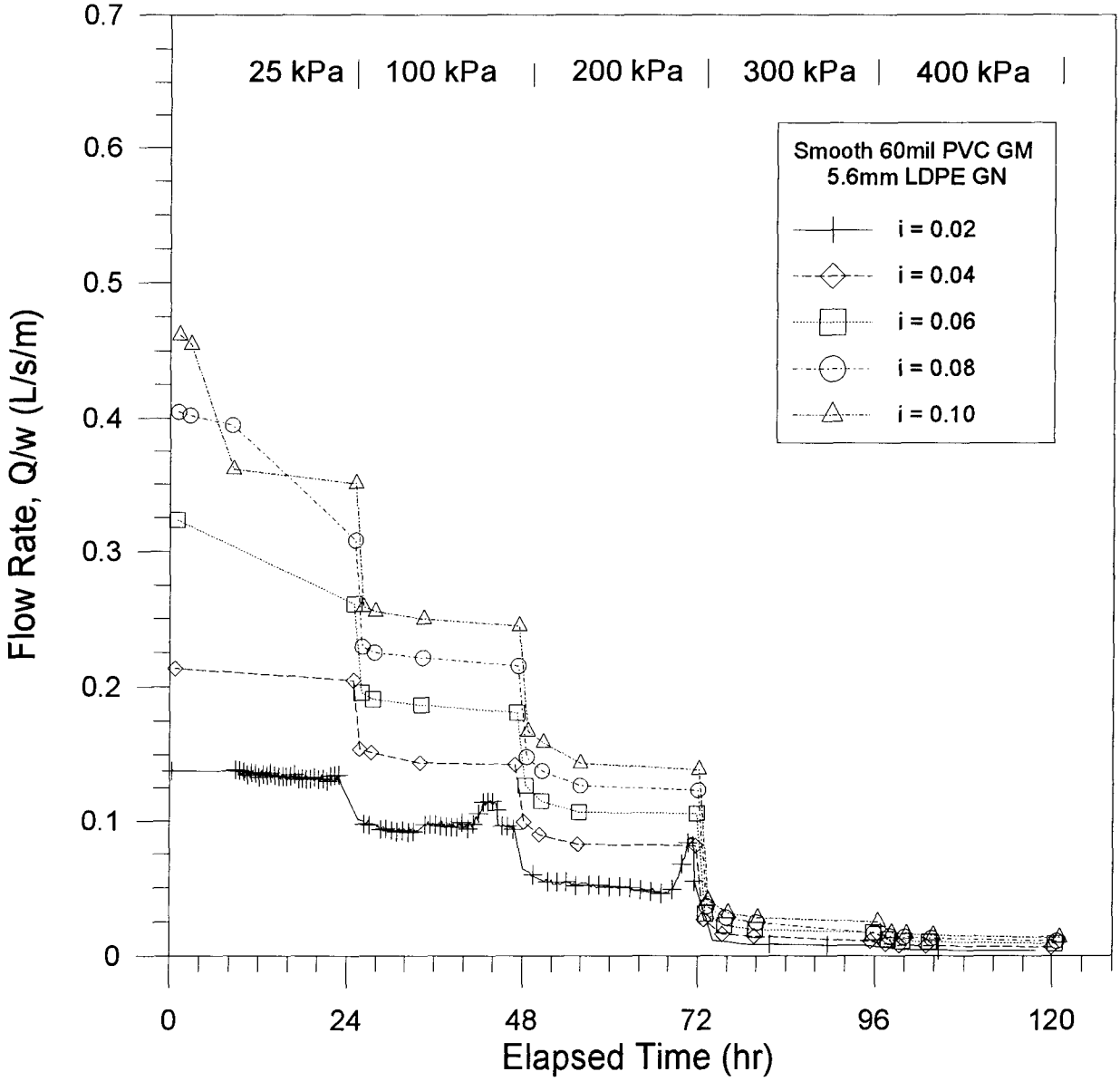
25 kPa
100 kPa
200 kPa
300 kPa
400 kPa
Smooth 60mil PVC GM
5.6mm LDPE GN
i = 0.02
i = 0.04
i = 0.06
i = 0.08
i = 0.10
Flow Rate, Q/w (L/s/m)
0.7
0.6
0.5
0.4
0.3
0.2
0.1
0
0
24
48
72
96
120
Elapsed Time (hr)

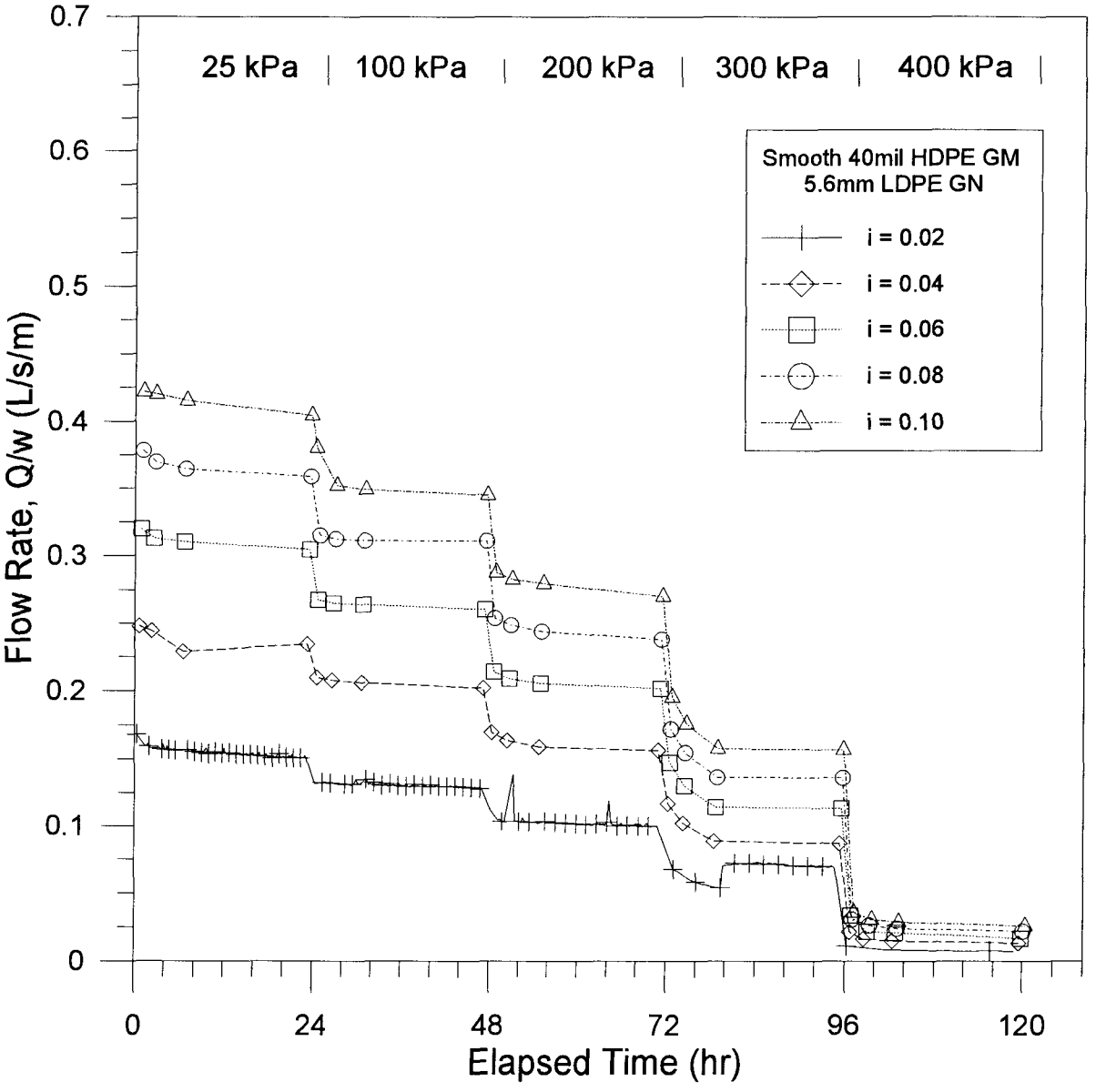
25 kPa
100 kPa
200 kPa
300 kPa
400 kPa
Smooth 40mil HDPE GM
5.6mm LDPE GN
i = 0.02
i = 0.04
i = 0.06
i = 0.08
i = 0.10
Flow Rate, Q/w (L/s/m)
0.7
0.6
0.5
0.4
0.3
0.2
0.1
0
0
24
48
72
96
120
Elapsed Time (hr)

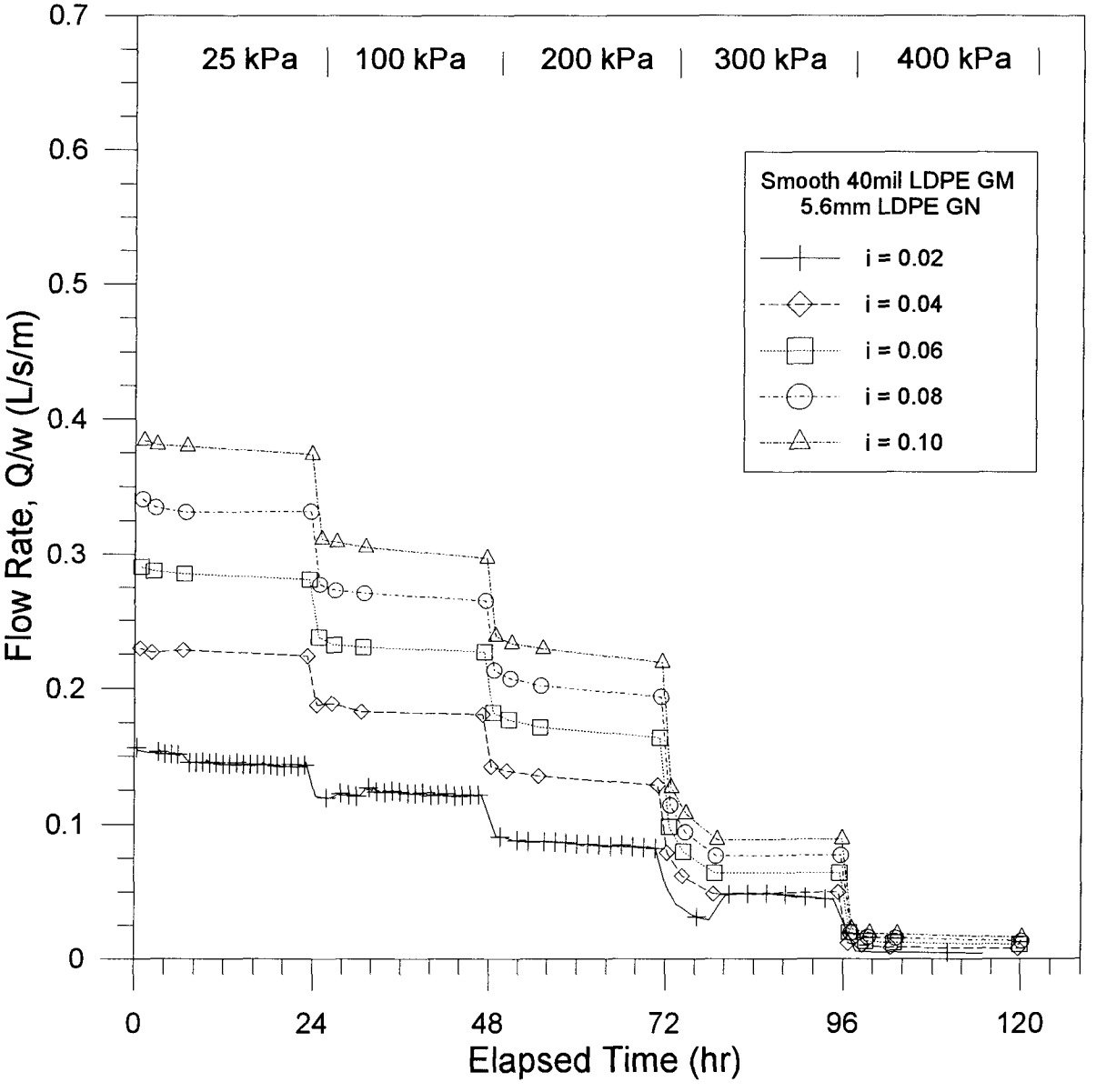
25 kPa
100 kPa
200 kPa
300 kPa
400 kPa
Smooth 40mil LDPE GM
5.6mm LDPE GN
i = 0.02
i = 0.04
i = 0.06
i = 0.08
i = 0.10
Flow Rate, Q/w (L/s/m)
0.7
0.6
0.5
0.4
0.3
0.2
0.1
0
0
24
48
72
96
120
Elapsed Time (hr)

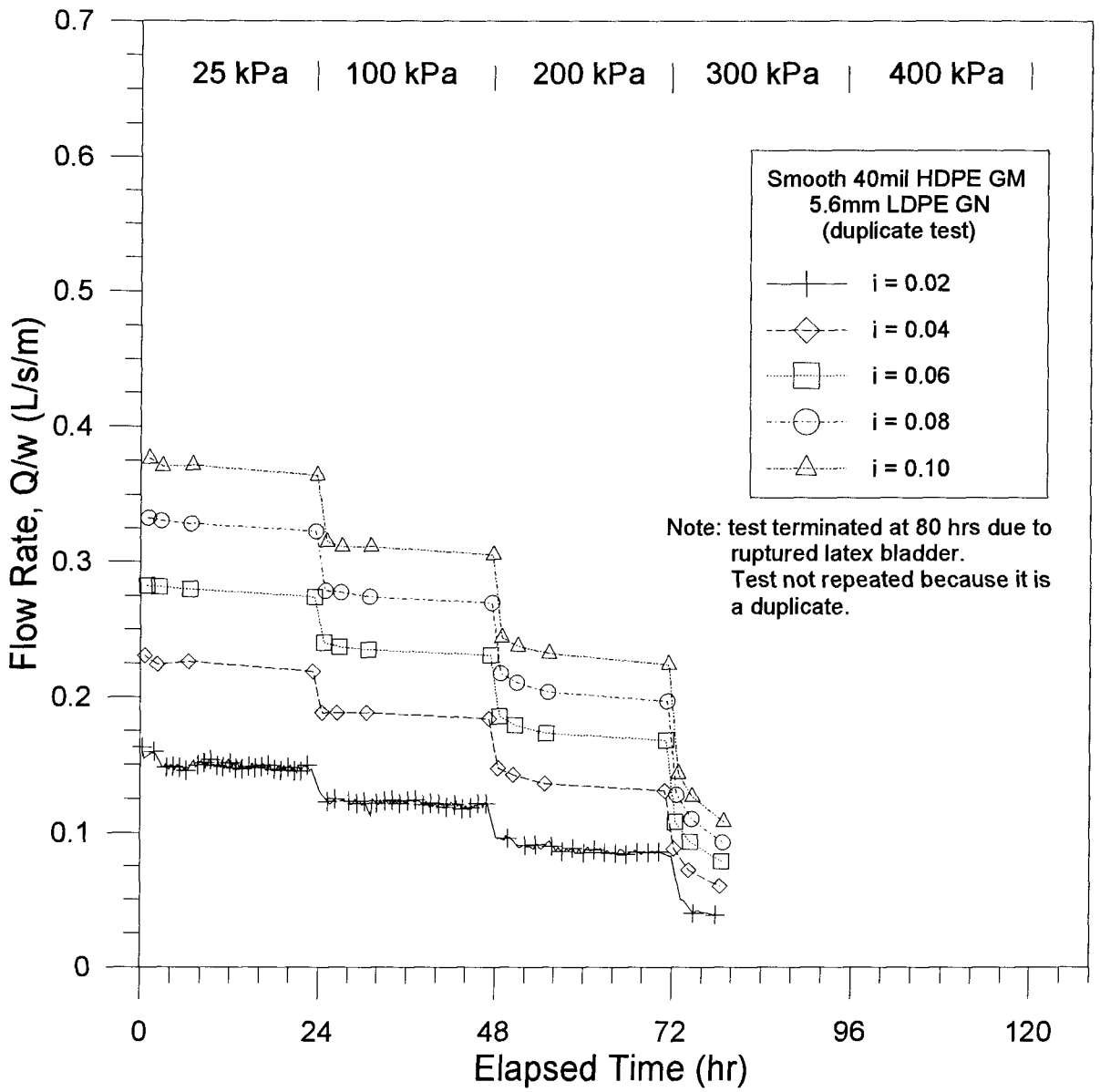
25 kPa
100 kPa
200 kPa
300 kPa
400 kPa
Smooth 40mil HDPE GM
5.6mm LDPE GN
(duplicate test)
i = 0.02
i = 0.04
i = 0.06
i = 0.08
i = 0.10
Note: test terminated at 80 hrs due to ruptured latex bladder.
Test not repeated because it is a duplicate.
Flow Rate, Q/w (L/s/m)
0.7
0.6
0.5
0.4
0.3
0.2
0.1
0
0
24
48
72
96
120
Elapsed Time (hr)

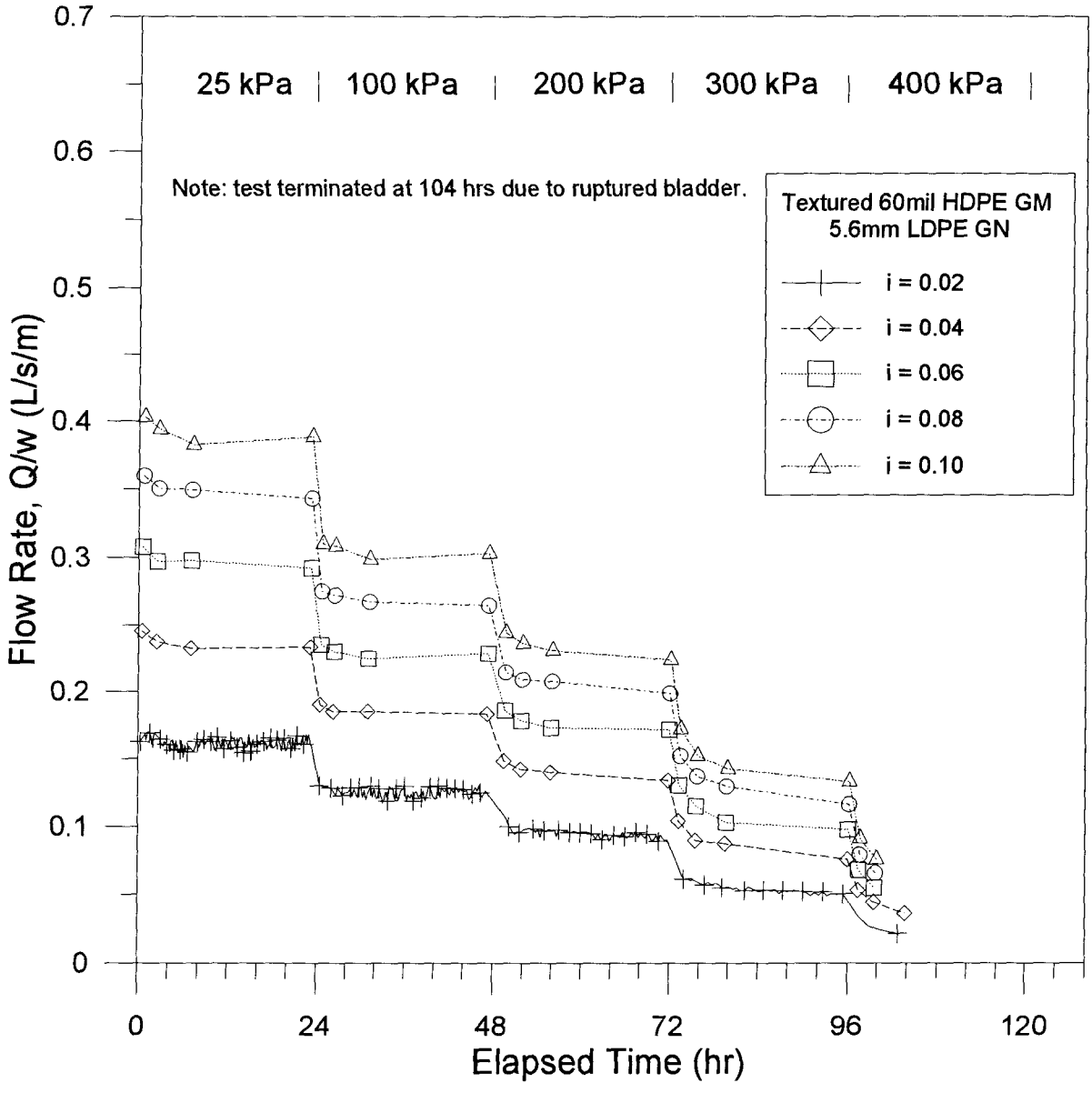
25 kPa
100 kPa
200 kPa
300 kPa
400 kPa
Note: test terminated at 104 hrs due to ruptured bladder.
Textured 60mil HDPE GM
5.6mm LDPE GN
i = 0.02
i = 0.04
i = 0.06
i = 0.08
i = 0.10
Flow Rate, Q/w (L/s/m)
0.7
0.6
0.5
0.4
0.3
0.2
0.1
0
0
24
48
72
96
120
Elapsed Time (hr)

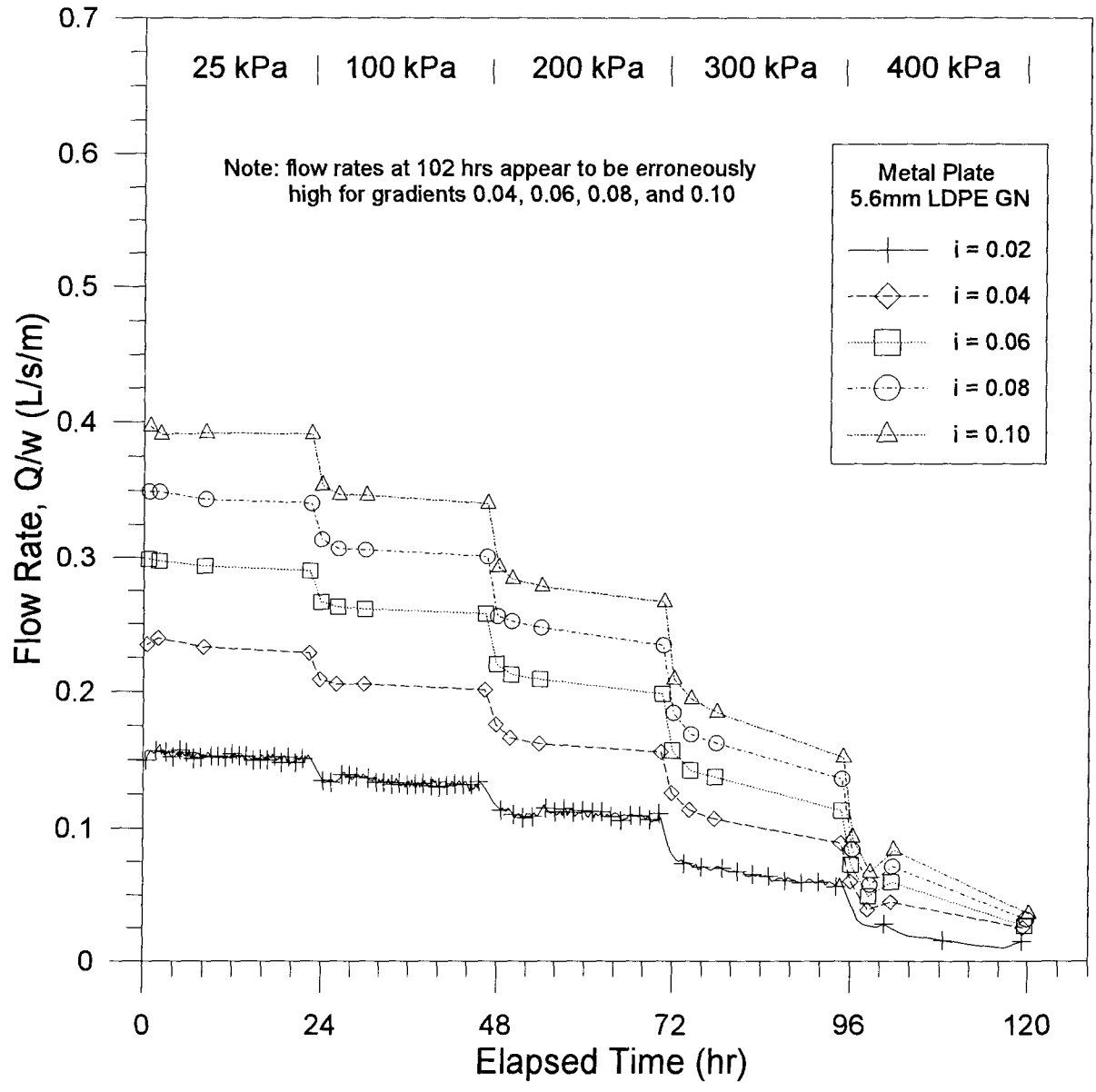
25 kPa
100 kPa
200 kPa
300 kPa
400 kPa
Note: flow rates at 102 hrs appear to be erroneously high for gradients 0.04, 0.06, 0.08, and 0.10
Metal Plate
5.6mm LDPE GN
i = 0.02
i = 0.04
i = 0.06
i = 0.08
i = 0.10
Flow Rate, Q/w (L/s/m)
0.7
0.6
0.5
0.4
0.3
0.2
0.1
0
0
24
48
72
96
120
Elapsed Time (hr)

APPENDIX B

SERIES WLC TEST RESULTS

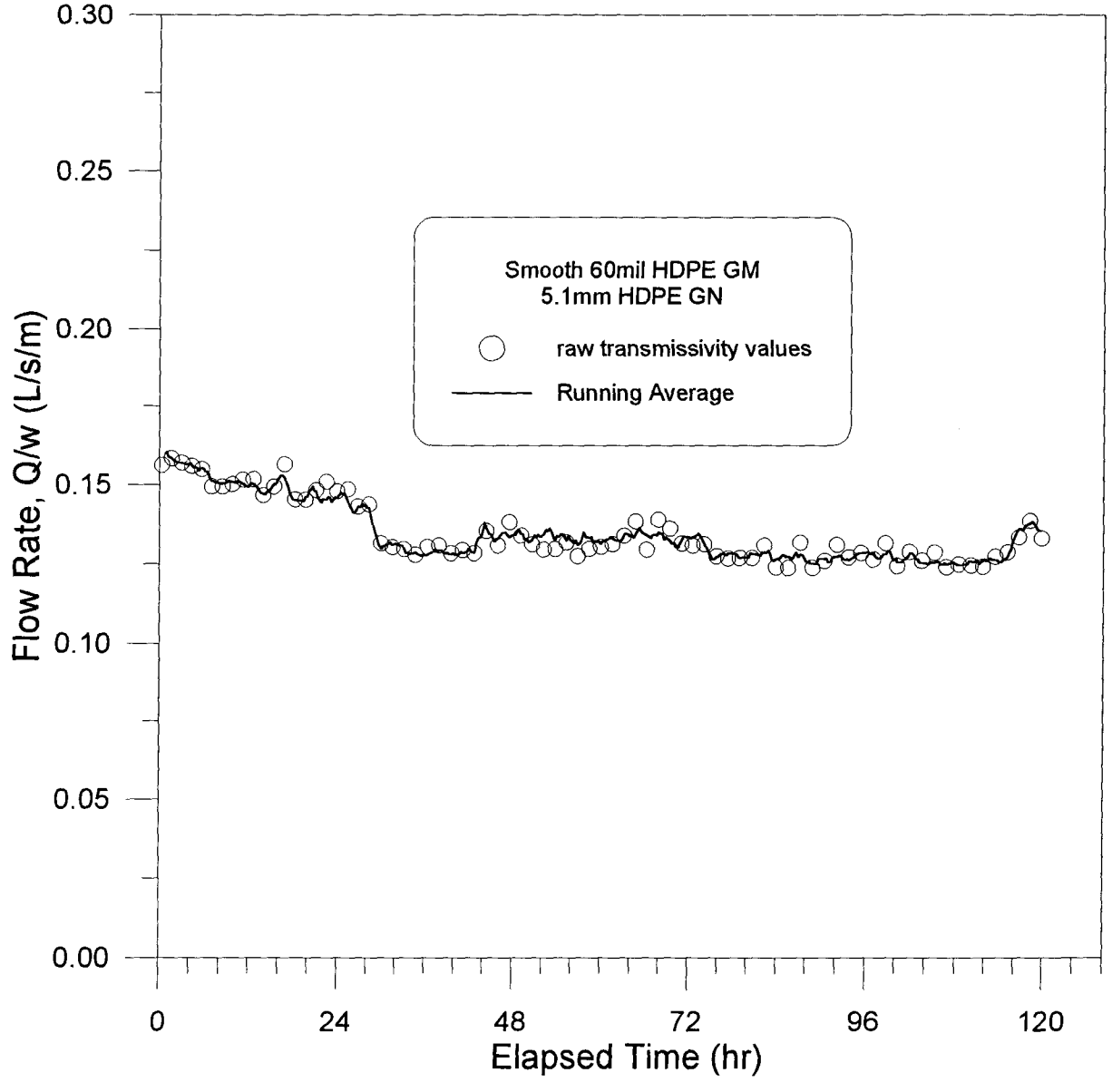
0.30
0.25
0.20
0.15
0.10
0.05
0.00
Flow Rate, Q/w (L/s/m)
0
24
48
72
96
120
Elapsed Time (hr)
Smooth 60mil HDPE GM
5.1mm HDPE GN
raw transmissivity values
Running Average

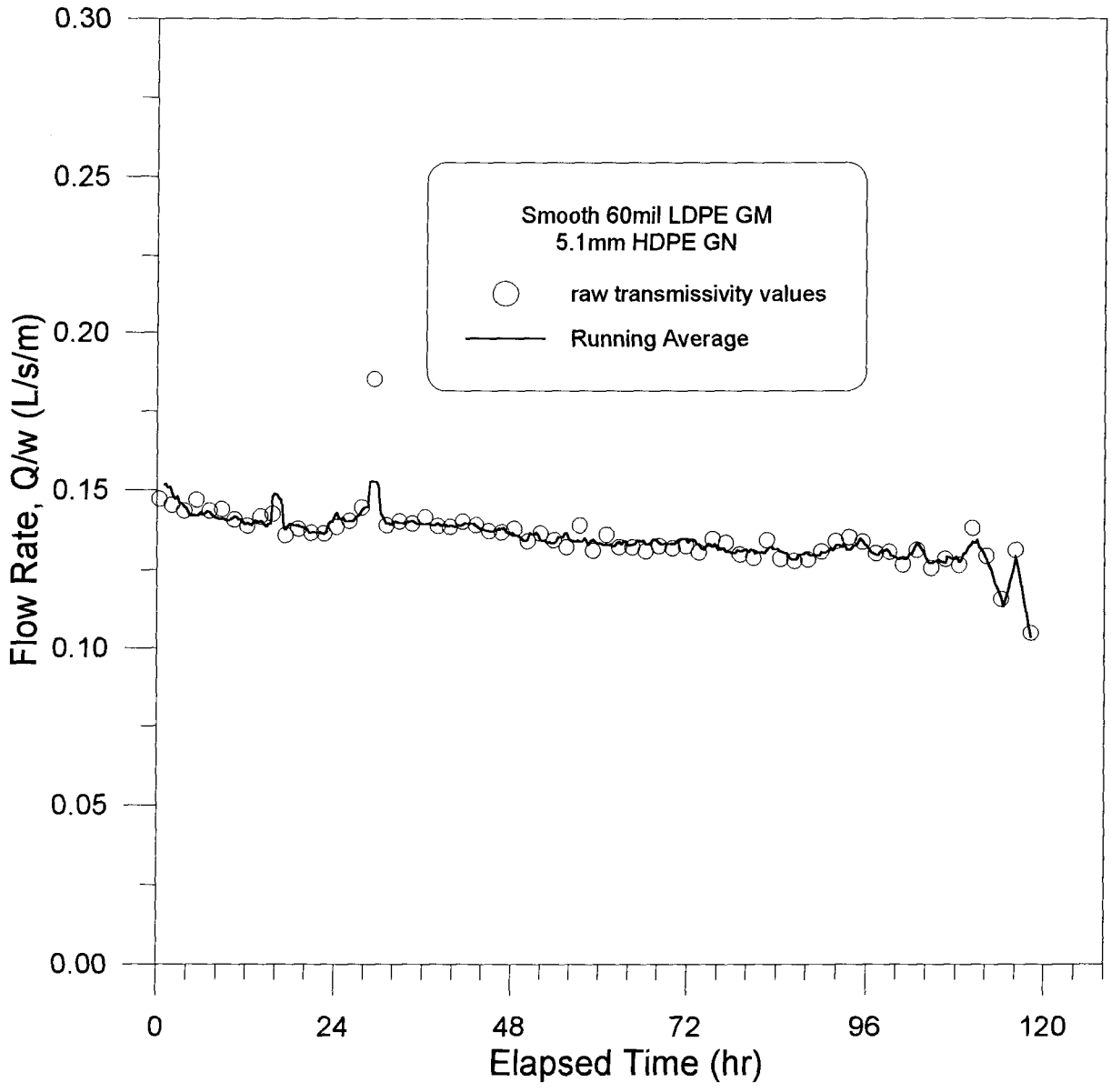
0.30
0.25
0.20
0.15
0.10
0.05
0.00
Flow Rate, Q/w (L/s/m)
0
24
48
72
96
120
Elapsed Time (hr)
Smooth 60mil LDPE GM
5.1mm HDPE GN
raw transmissivity values
Running Average

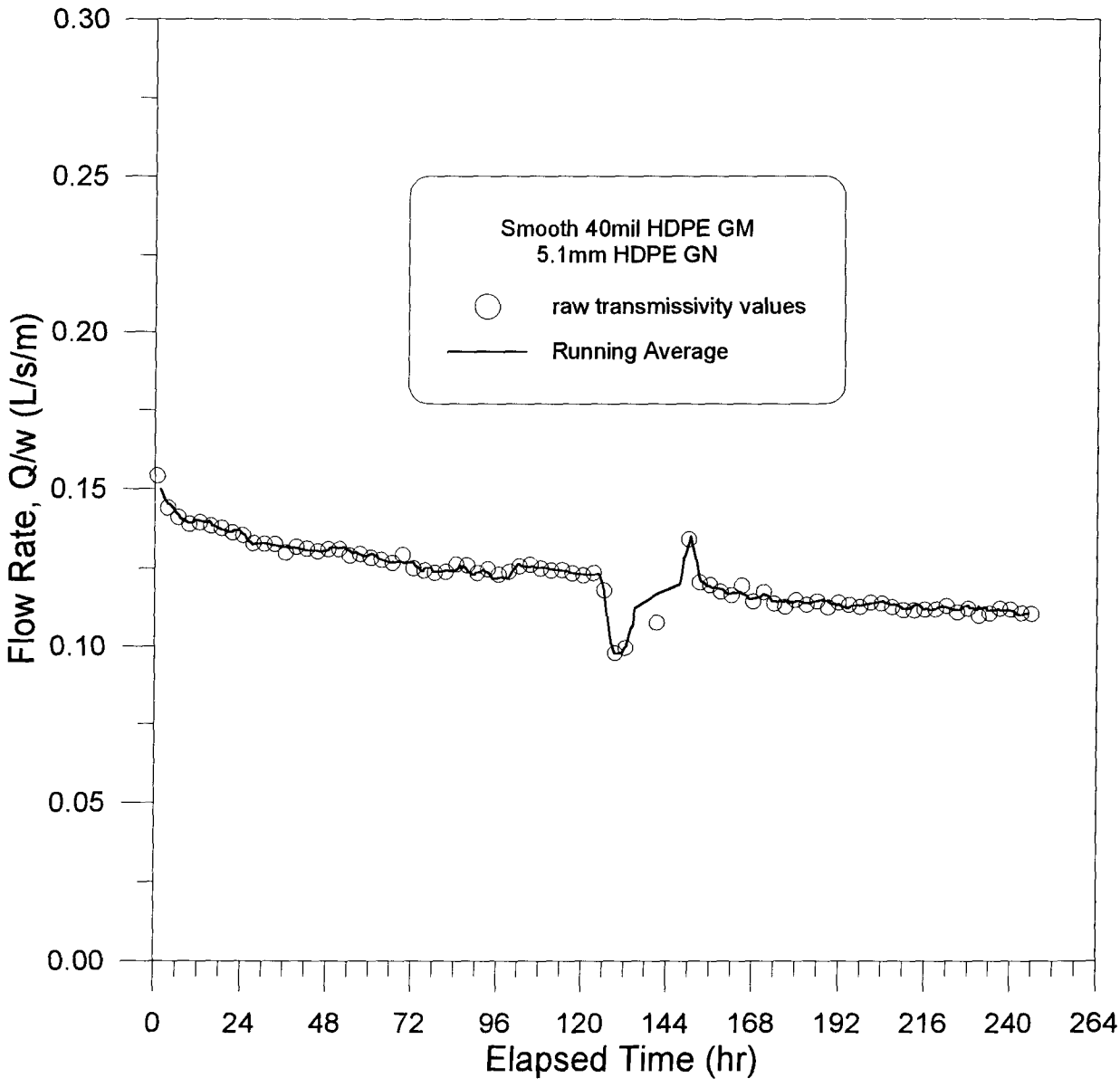
Smooth 40mil HDPE GM
5.1mm HDPE GN
raw transmissivity values
Running Average
Flow Rate, Q/w (L/s/m)
0.30
0.25
0.20
0.15
0.10
0.05
0.00
0
24
48
72
96
120
144
168
192
216
240
264
Elapsed Time (hr)

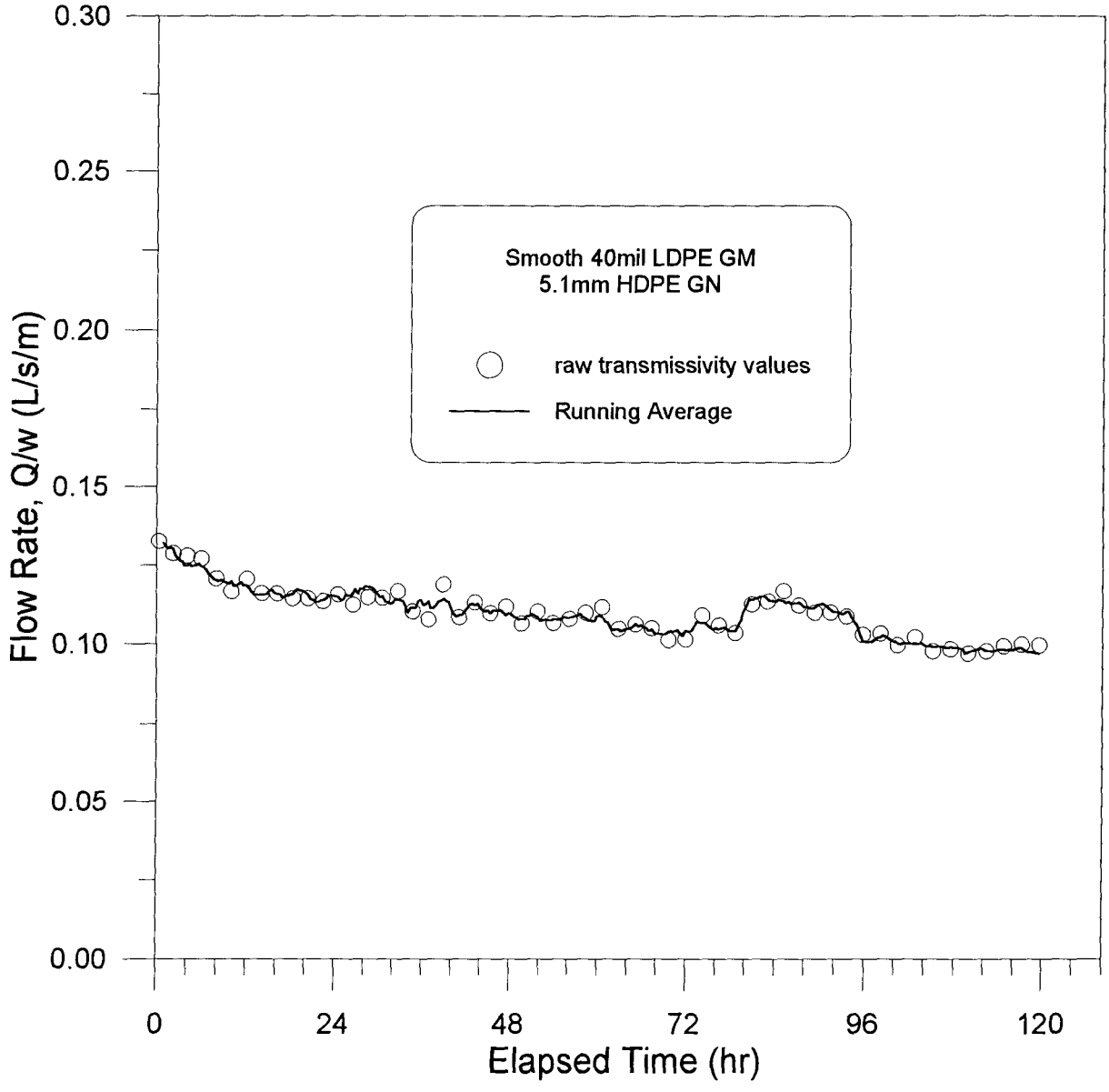
Smooth 40mil LDPE GM
5.1mm HDPE GN
raw transmissivity values
Running Average
Flow Rate, Q/w (L/s/m)
0.30
0.25
0.20
0.15
0.10
0.05
0.00
0
24
48
72
96
120
Elapsed Time (hr)

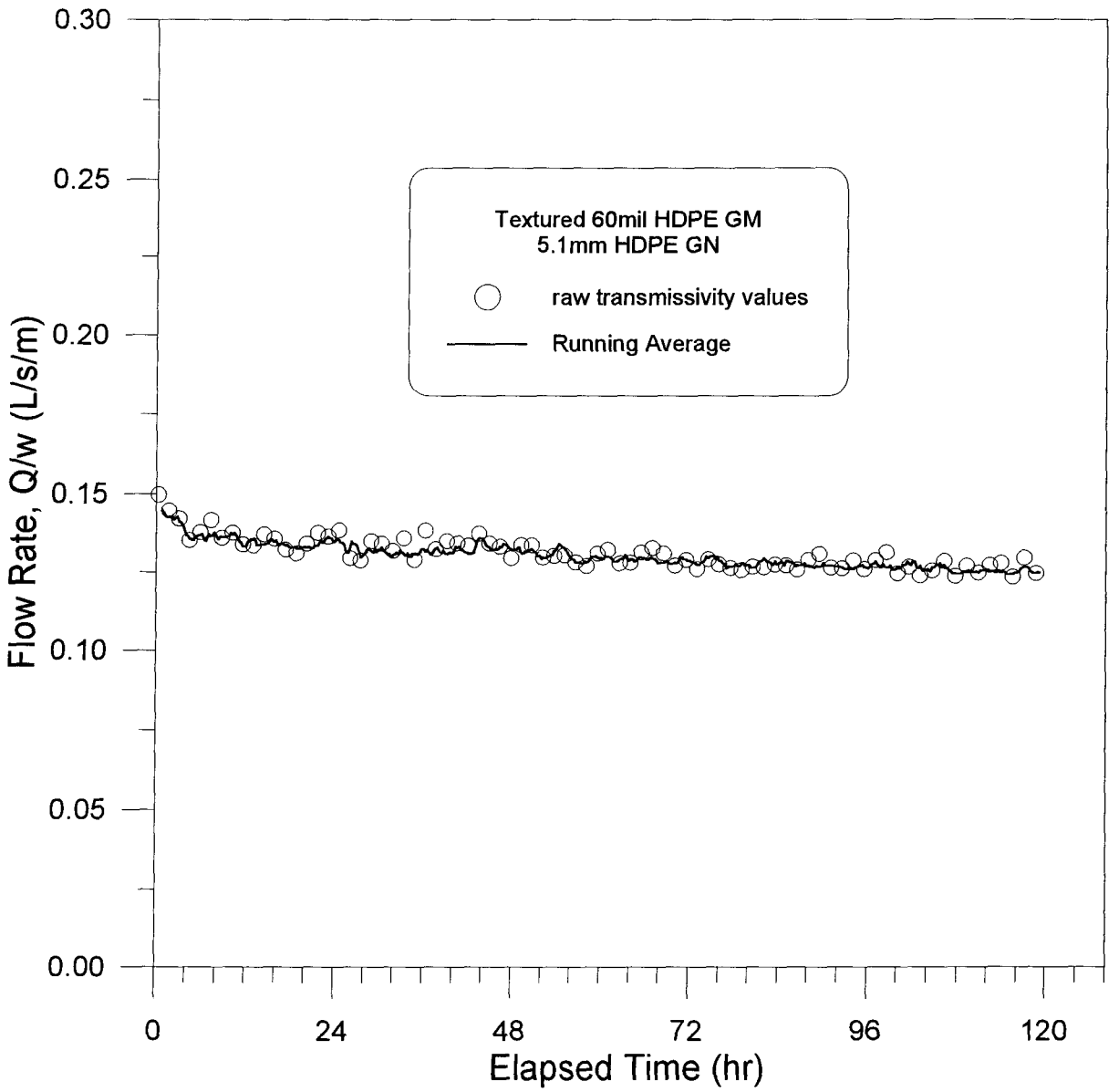
0.30
0.25
0.20
0.15
0.10
0.05
0.00
Flow Rate, Q/w (L/s/m)
0
24
48
72
96
120
Elapsed Time (hr)
Textured 60mil HDPE GM
5.1mm HDPE GN
raw transmissivity values
Running Average

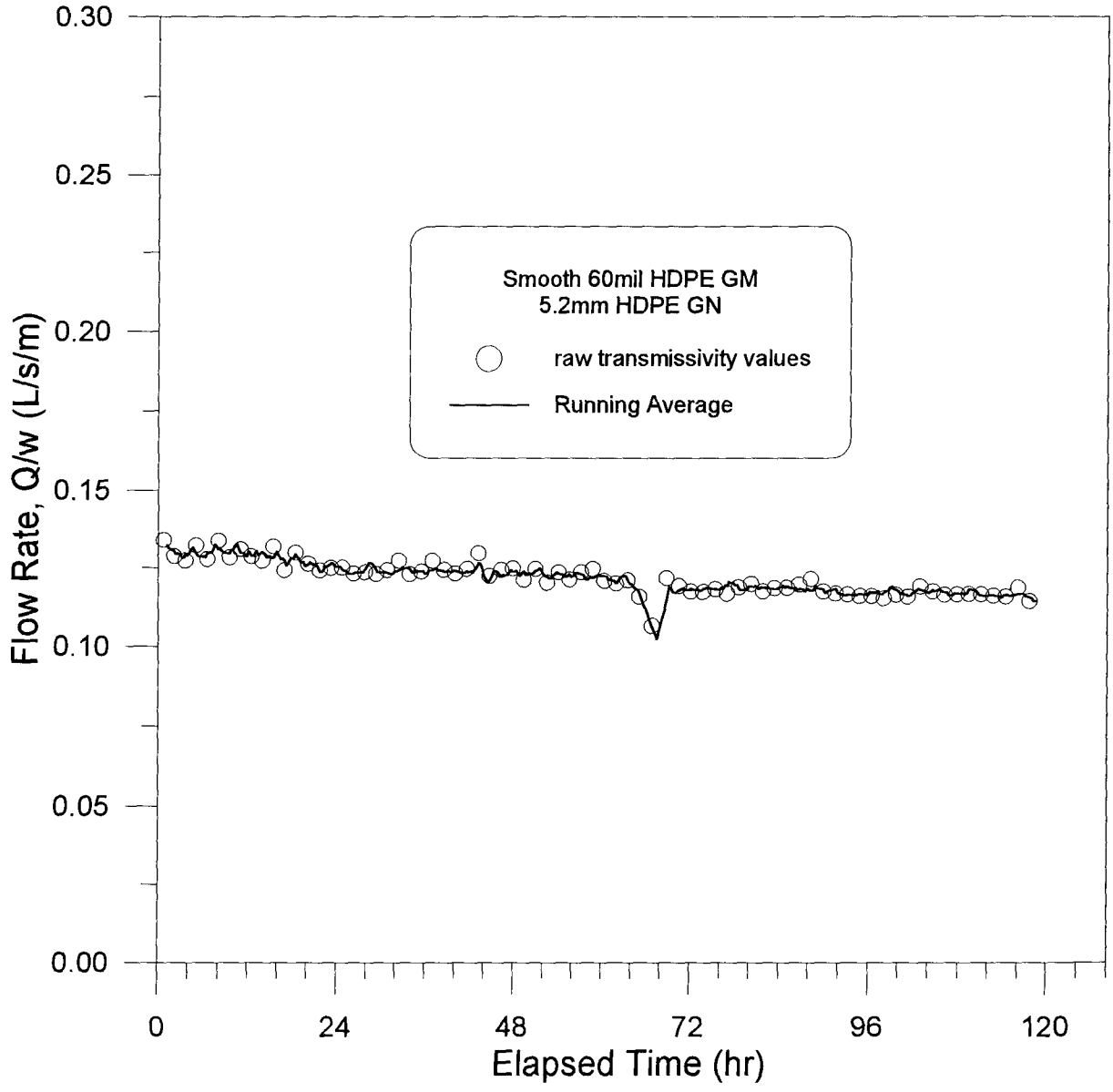
0.30
0.25
0.20
0.15
0.10
0.05
0.00
Flow Rate, Q/w (L/s/m)
0
24
48
72
96
120
Elapsed Time (hr)
Smooth 60mil HDPE GM
5.2mm HDPE GN
raw transmissivity values
Running Average

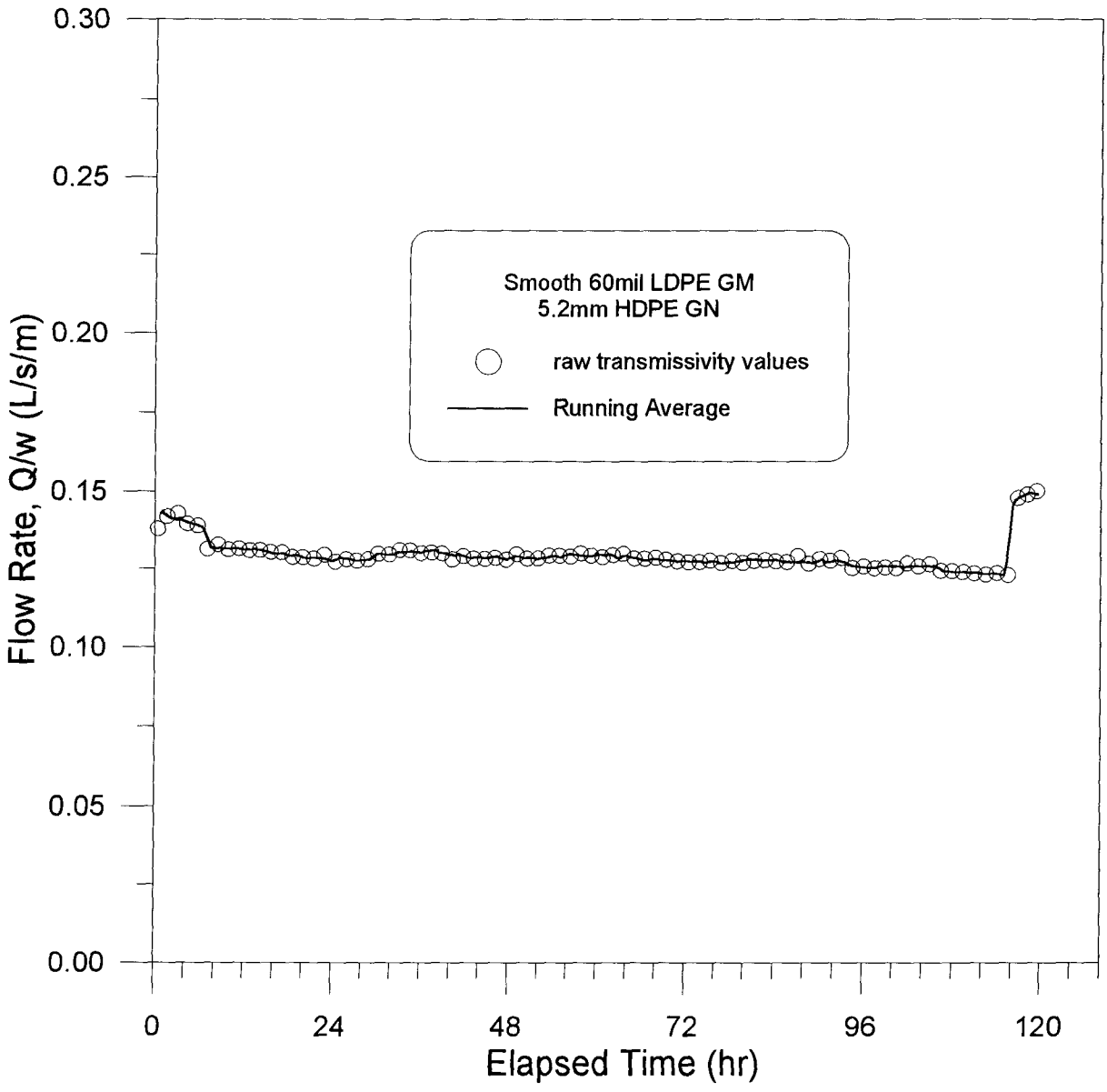
0.30
0.25
0.20
0.15
0.10
0.05
0.00
Flow Rate, Q/w (L/s/m)
Smooth 60mil LDPE GM
5.2mm HDPE GN
raw transmissivity values
Running Average
0
24
48
72
96
120
Elapsed Time (hr)

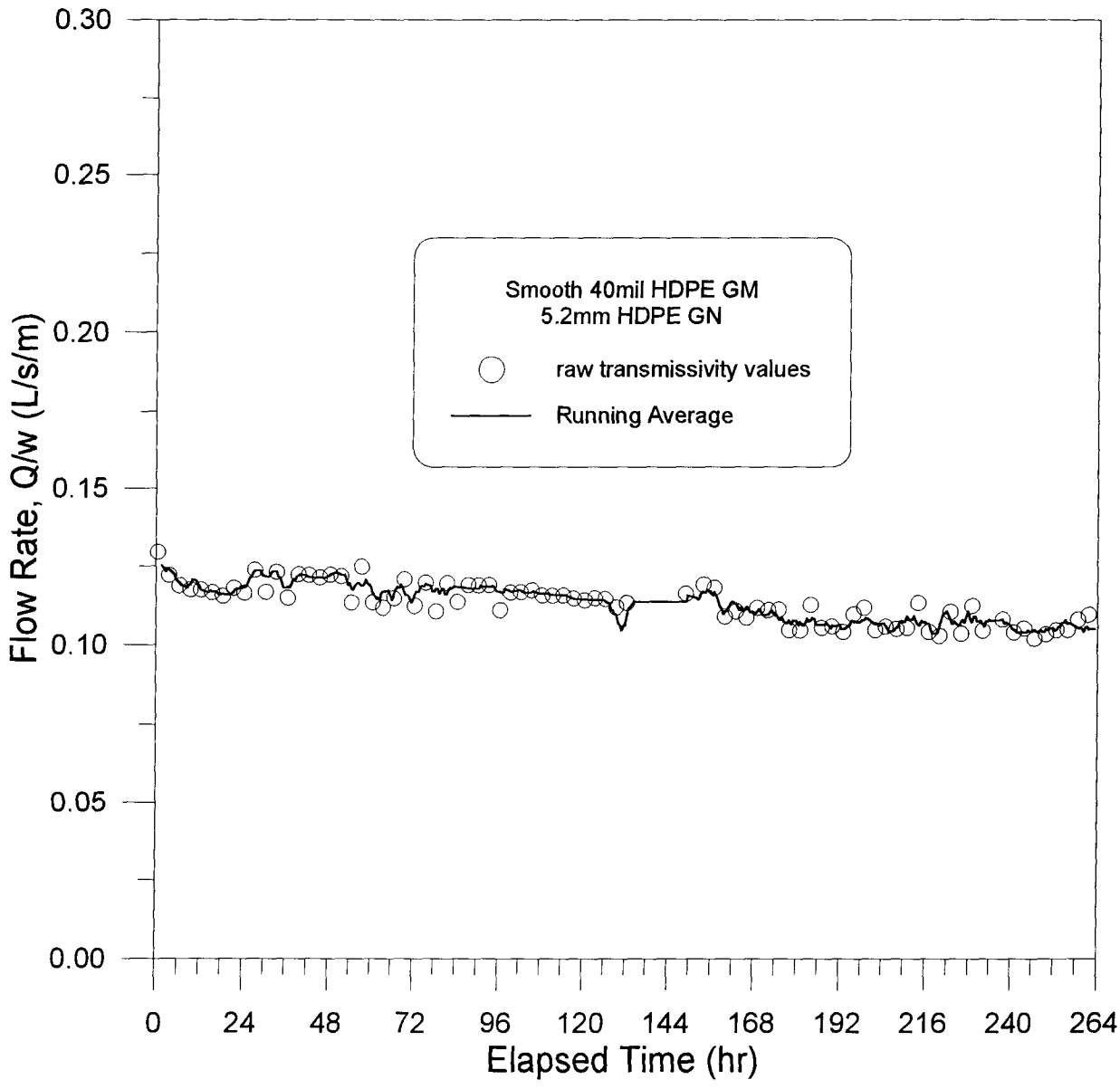
0.30
0.25
0.20
0.15
0.10
0.05
0.00
Flow Rate, Q/w (L/s/m)
Smooth 40mil HDPE GM
5.2mm HDPE GN
raw transmissivity values
Running Average
0
24
48
72
96
120
144
168
192
216
240
264
Elapsed Time (hr)

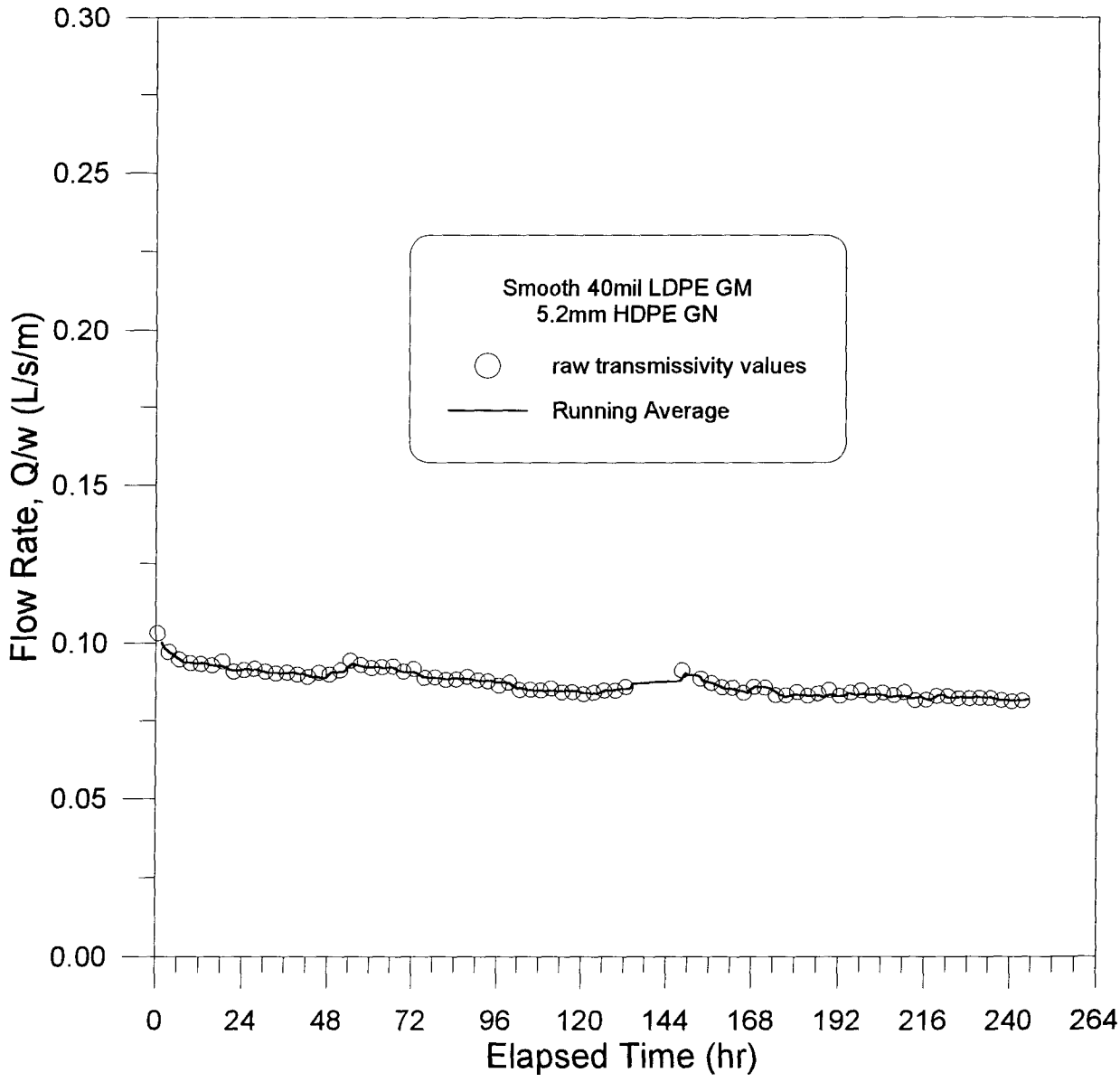
Smooth 40mil LDPE GM
5.2mm HDPE GN
raw transmissivity values
Running Average
Flow Rate, Q/w (L/s/m)
0.30
0.25
0.20
0.15
0.10
0.05
0.00
0
24
48
72
96
120
144
168
192
216
240
264
Elapsed Time (hr)

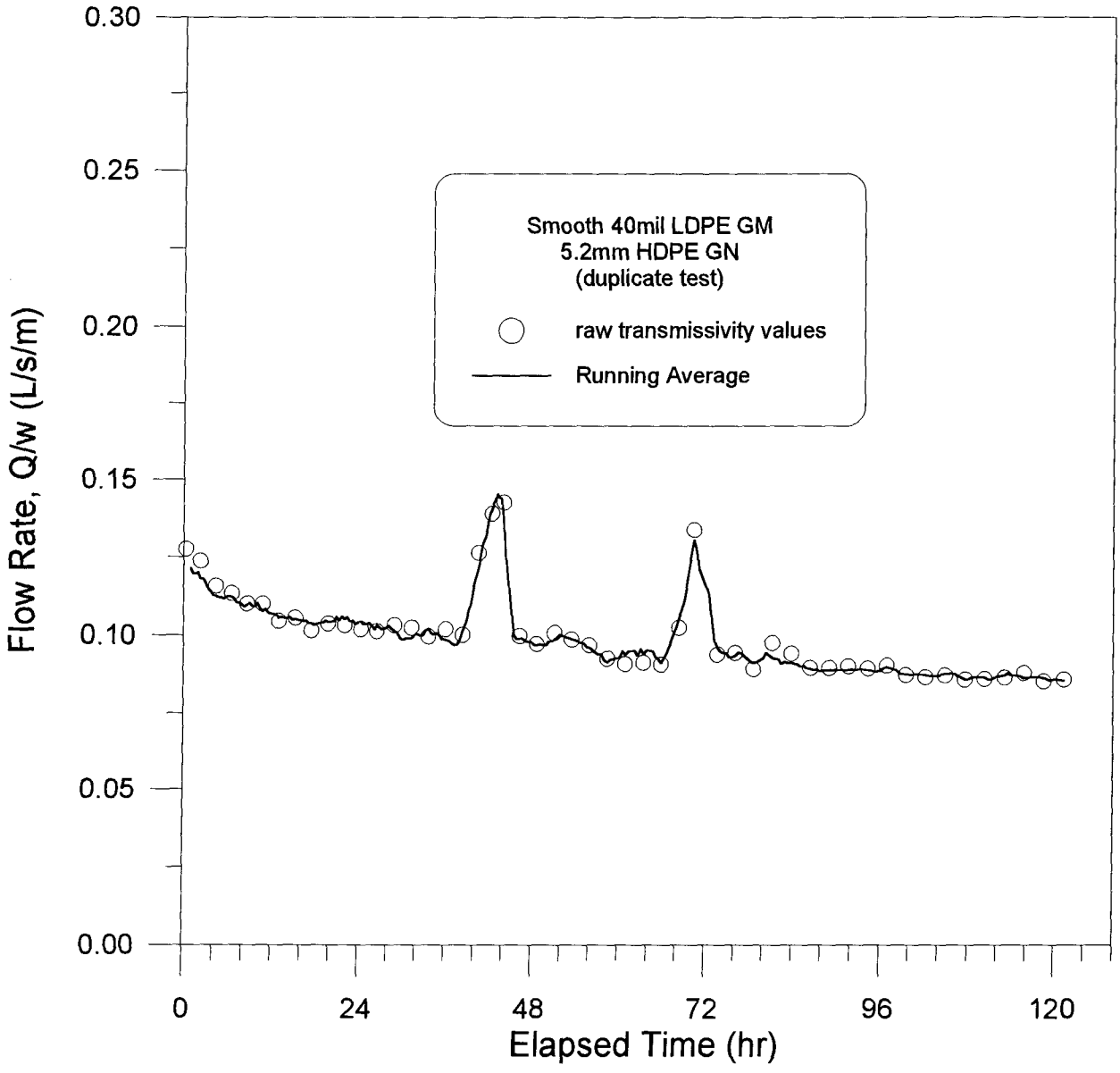
Smooth 40mil LDPE GM
5.2mm HDPE GN
(duplicate test)
raw transmissivity values
Running Average
Flow Rate, Q/w (L/s/m)
0.30
0.25
0.20
0.15
0.10
0.05
0.00
0
24
48
72
96
120
Elapsed Time (hr)

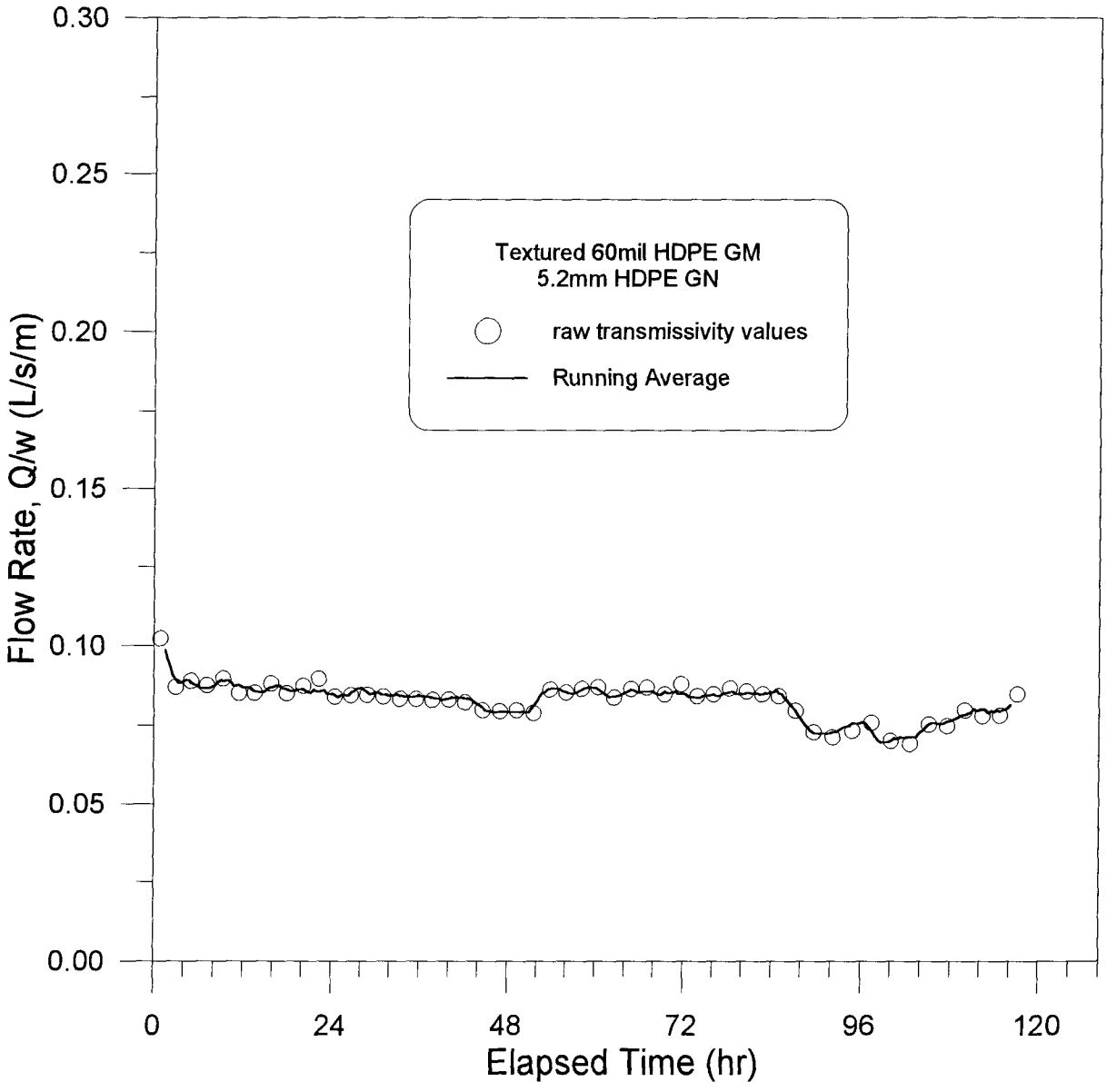
0.30
0.25
0.20
0.15
0.10
0.05
0.00
Flow Rate, Q/w (L/s/m)
Textured 60mil HDPE GM
5.2mm HDPE GN
raw transmissivity values
Running Average
0
24
48
72
96
120
Elapsed Time (hr)

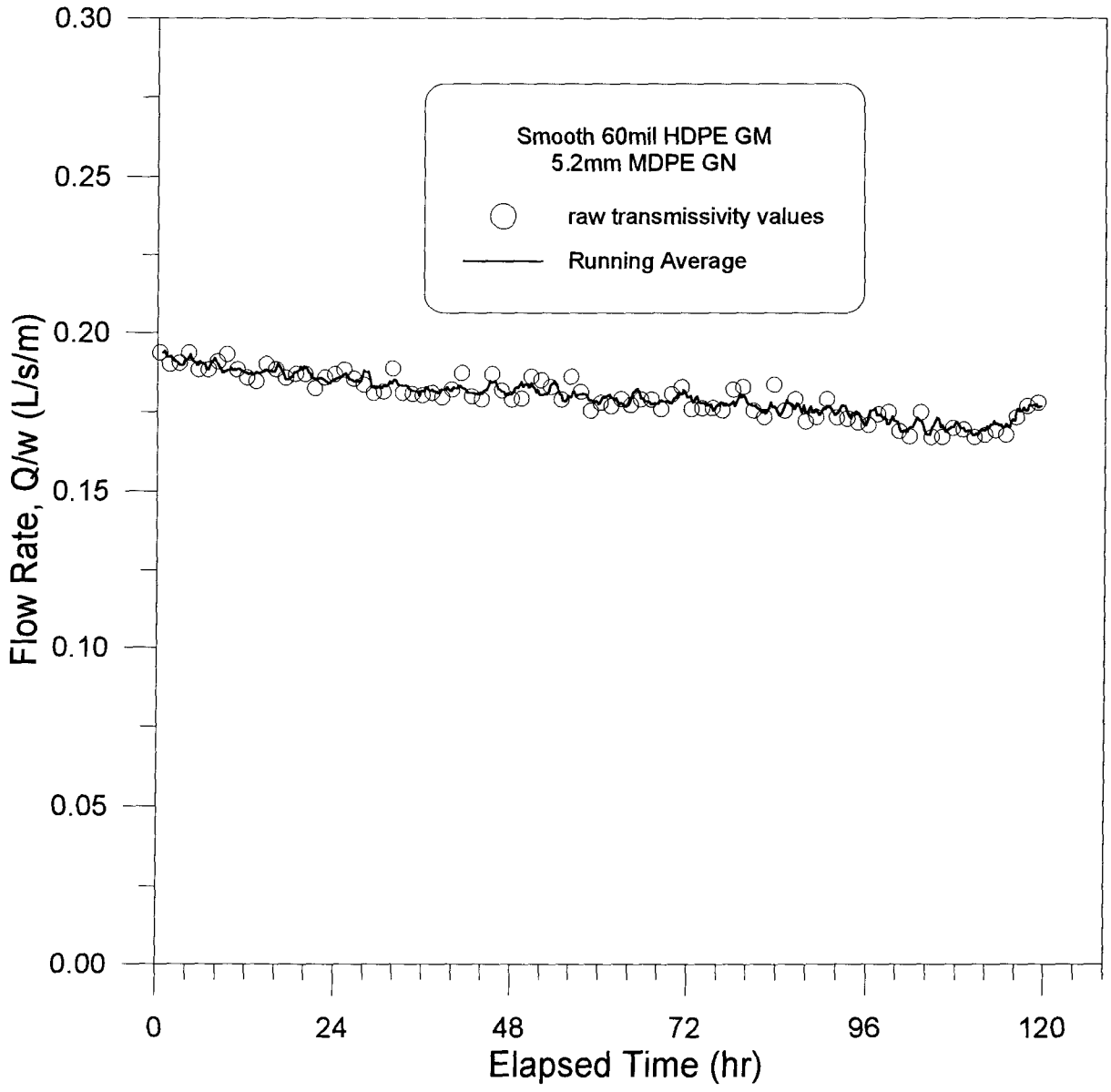
Smooth 60mil HDPE GM
5.2mm MDPE GN
raw transmissivity values
Running Average
Flow Rate, Q/w (L/s/m)
0.30
0.25
0.20
0.15
0.10
0.05
0.00
0
24
48
72
96
120
Elapsed Time (hr)

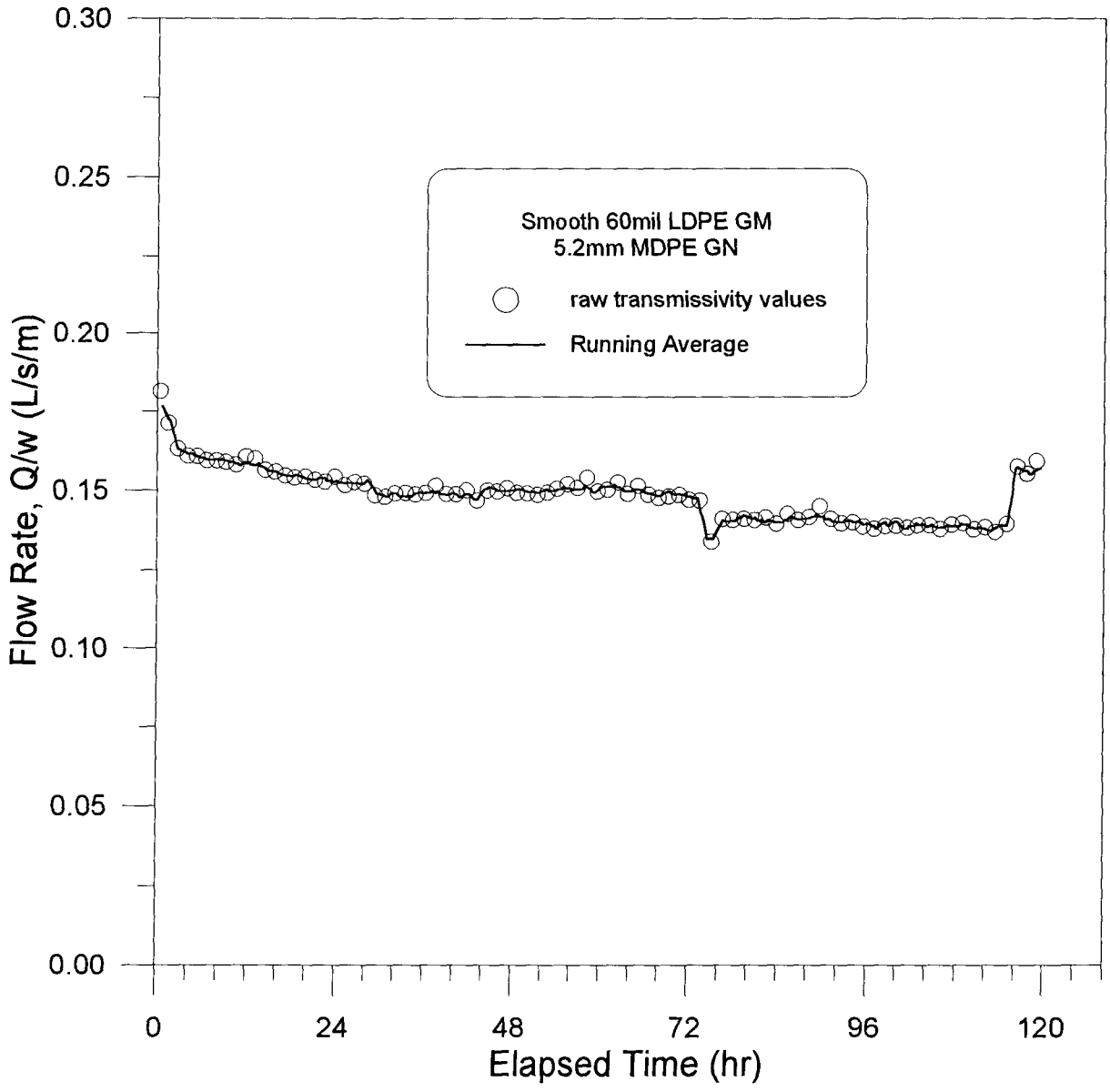
Smooth 60mil LDPE GM
5.2mm MDPE GN
raw transmissivity values
Running Average
Flow Rate, Q/w (L/s/m)
0.30
0.25
0.20
0.15
0.10
0.05
0.00
0
24
48
72
96
120
Elapsed Time (hr)

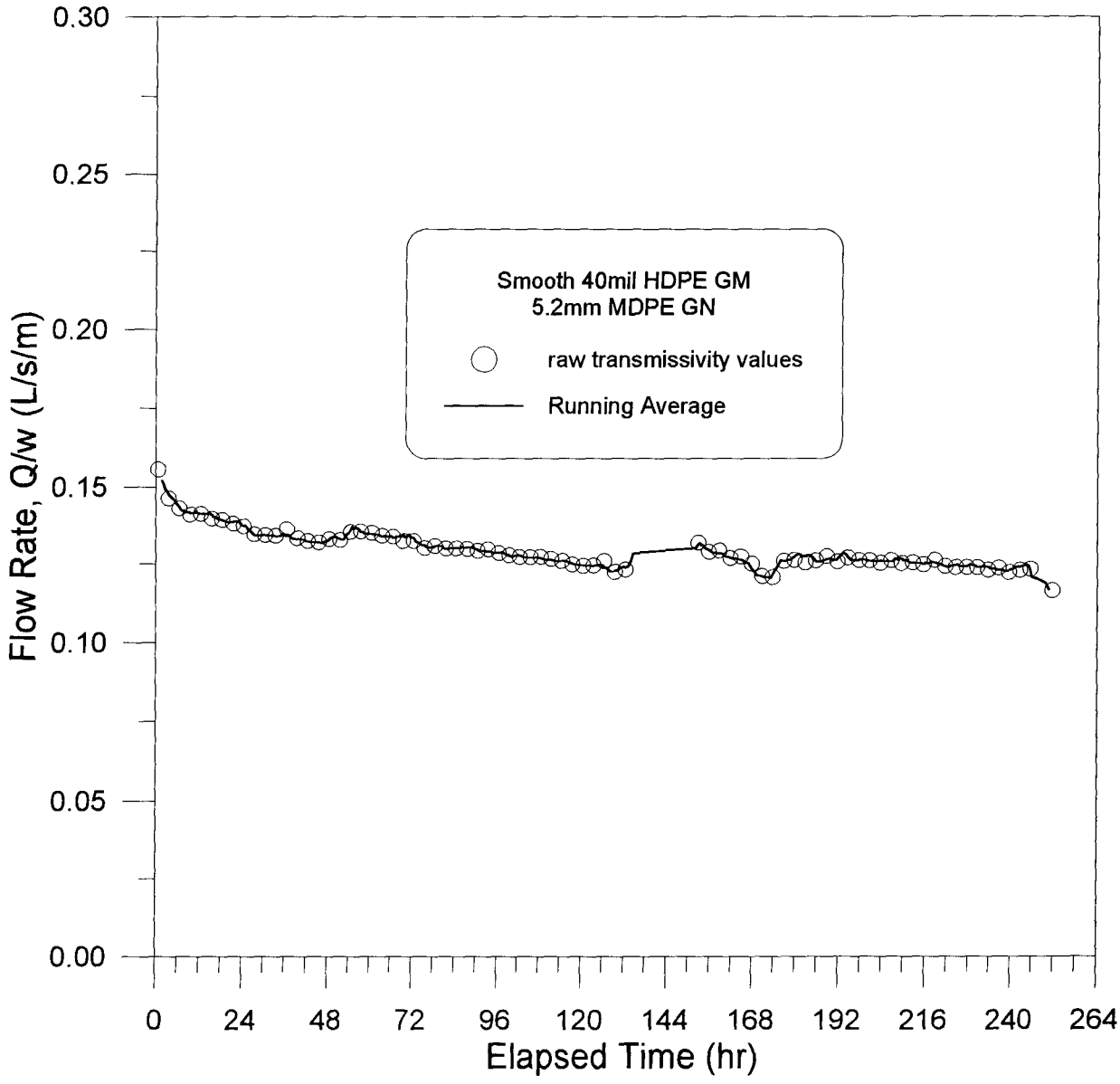
0.30
0.25
0.20
0.15
0.10
0.05
0.00
Flow Rate, Q/w (L/s/m)
Smooth 40mil HDPE GM
5.2mm MDPE GN
raw transmissivity values
Running Average
0
24
48
72
96
120
144
168
192
216
240
264
Elapsed Time (hr)

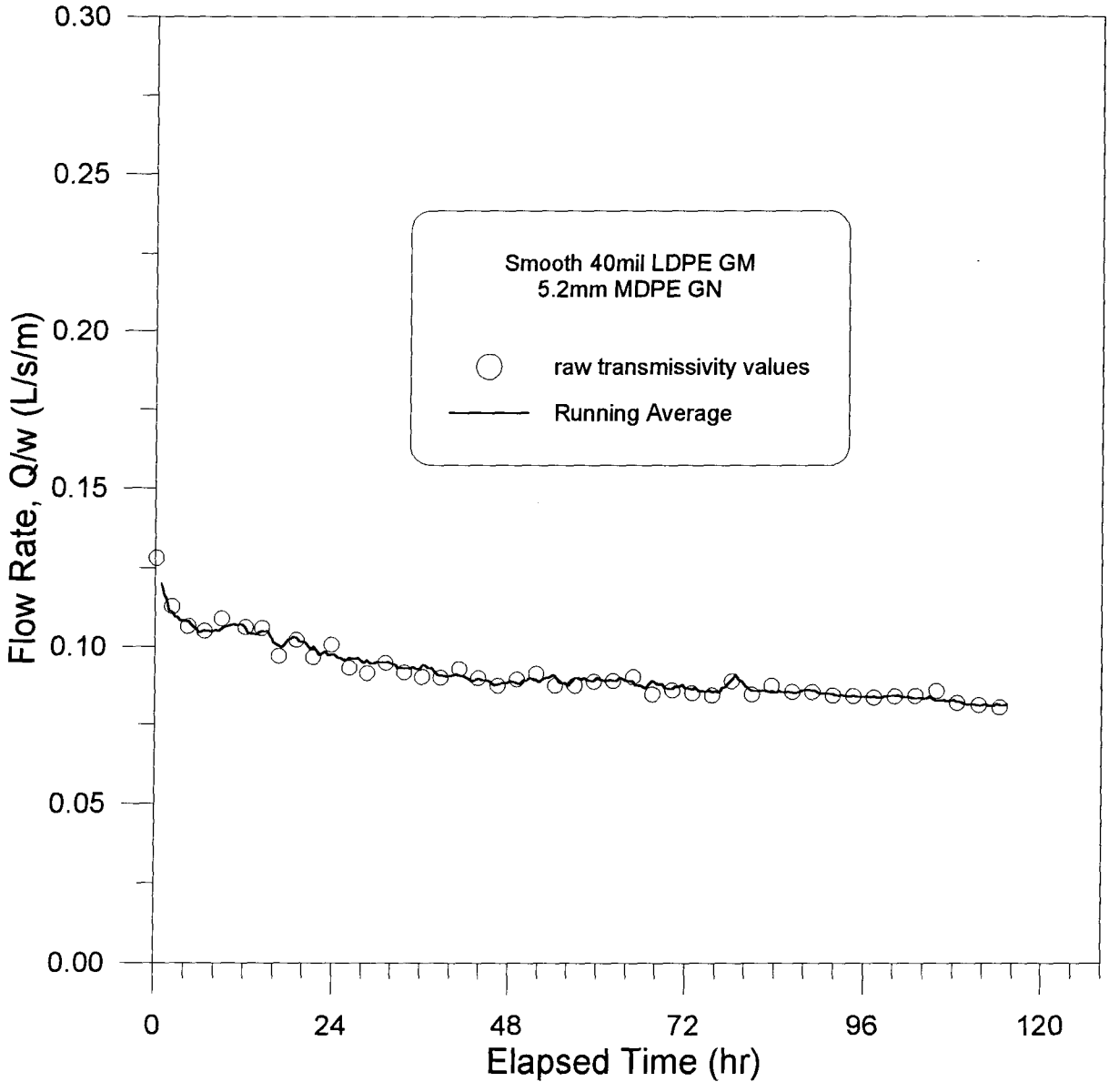
0.30
0.25
0.20
0.15
0.10
0.05
0.00
Flow Rate, Q/w (L/s/m)
Smooth 40mil LDPE GM
5.2mm MDPE GN
raw transmissivity values
Running Average
0
24
48
72
96
120
Elapsed Time (hr)

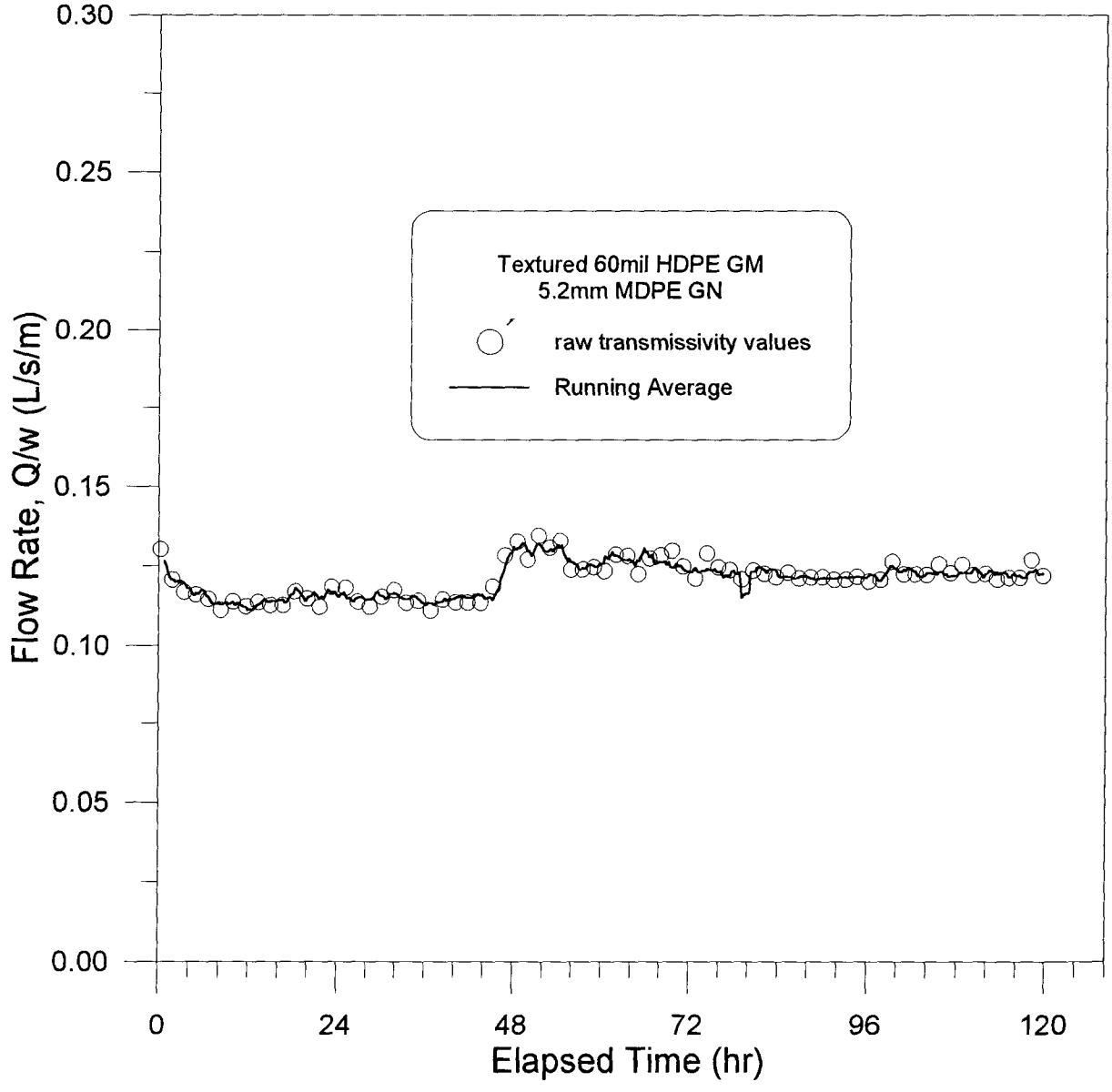
Textured 60mil HDPE GM
5.2mm MDPE GN
raw transmissivity values
Running Average
Flow Rate, Q/w (L/s/m)
0.30
0.25
0.20
0.15
0.10
0.05
0.00
0
24
48
72
96
120
Elapsed Time (hr)